

N O T I C E

THIS DOCUMENT HAS BEEN REPRODUCED FROM
MICROFICHE. ALTHOUGH IT IS RECOGNIZED THAT
CERTAIN PORTIONS ARE ILLEGIBLE, IT IS BEING RELEASED
IN THE INTEREST OF MAKING AVAILABLE AS MUCH
INFORMATION AS POSSIBLE

2A
NASA CR-

160748

SPACE CONSTRUCTION SYSTEM ANALYSIS

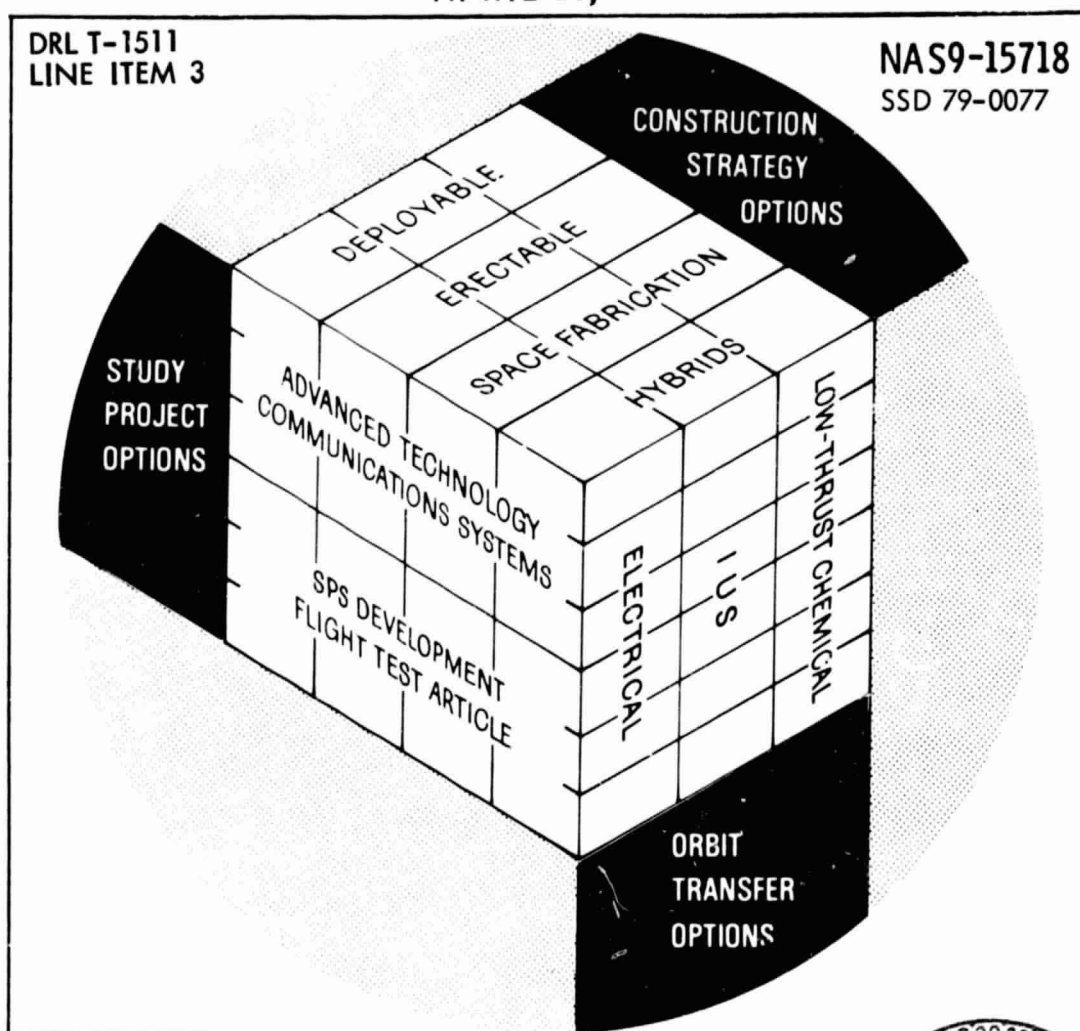
PROJECT SYSTEMS AND MISSION DESCRIPTIONS

TASK 1 FINAL REPORT

APRIL 26, 1979

DRL T-1511
LINE ITEM 3

NAS9-15718
SSD 79-0077



N80-27400

Unclas
24464

(NASA-CR-160748) SPACE CONSTRUCTION SYSTEM
ANALYSIS STUDY: PROJECT SYSTEMS AND
MISSIONS DESCRIPTIONS Final Report
(Rockwell International Corp., Downey,
Calif.) 301 p HC A14/MF A01
CSCL 22A G3/12



Rockwell International

Satellite Systems Division
Space Systems Group
12214 Lakewood Boulevard
Downey, CA 90241



Satellite Systems Division
Space Systems Group



SSD 79-0077

SPACE CONSTRUCTION SYSTEMS ANALYSIS STUDY
PROJECT SYSTEMS AND MISSIONS DESCRIPTIONS

Task 1 Final Report

Contract No. NAS9-15718
DRL T-1511
Line Item 3

April 26, 1979

Approved by


Ellis Katz



Rockwell International

Satellite Systems Division
Space Systems Group
12214 Lakewood Boulevard
Downey, CA 90241

FOREWORD

This report provides engineering definition of three potential large space construction project systems suitable for the period 1985-1990. The document is a study product of Task 1 - Project Systems Description, Contract NAS9-15718, Space Construction System Analysis Study, which was conducted by the Satellite Systems Division, Space Systems Group of Rockwell International Corporation for the National Aeronautics and Space Administration (NASA), Johnson Space Center (JSC).

The study was conducted under the direction of Ellis Katz, Study Manager. The following persons made significant contributions toward completion of the systems described herein.

P. Buck
R. E. Cook
R. D. Donavan
Dr. E. P. French
W. Fredericks
H. S. Greenberg
R. Hart
K. E. Kunz
Dr. A. W. Love
C. K. McBaine
H. L. Myers
R. C. Quartararo
J. A. Roebuck
A. J. Stefan
R. R. Thompson

CONTENTS

<u>Section</u>	<u>Page</u>
1.0 INTRODUCTION	1-1
2.0 DEFINITION OF SPS FLIGHT TEST ARTICLE	2-1
2.1 SPS Test Article Project Scenario	2-2
2.1.1 General	2-2
2.1.2 Operating Scenario	2-2
2.1.3 Flight Modes	2-4
2.1.4 Servicing and Growth	2-7
2.2 Configuration Description - SPS Test Article	2-11
2.2.1 General Configuration Description	2-12
2.2.2 Microwave Antenna Description	2-15
2.3 Subsystems Definition	2-17
2.3.1 Structure Subsystem Definition - SPS Test Article	2-18
2.3.2 Electrical Power Generation, Distribution and Control Subsystem Definition	2-31
2.3.3 Microwave Subsystem Definition	2-45
2.3.4 Propulsion Subsystems Definition	2-59
2.3.5 Attitude and Velocity Control Subsystem	2-67
2.3.6 Tracking, Telemetry and Command Subsystem Definition	2-79
2.3.7 Thermal Analysis and Thermal Control Subsystem Definition	2-83
2.4 Mass Properties - SPS Test Article	2-88
2.5 Construction Requirements - SPS Test Article	2-91
2.5.1 Overall Strategy	2-91
2.5.2 Component Inventory	2-92
2.5.3 General Construction Sequence Guidelines	2-92
2.5.4 General Tolerances	2-92
3.0 DEFINITION OF ADVANCED TECHNOLOGY COMMUNICATIONS PLATFORMS	3-1



<u>Section</u>	<u>Page</u>
3.1 Advanced Communications Platform Scenario	3-3
3.1.1 General	3-3
3.1.2 Platform Concept Approach	3-3
3.1.3 Operating Scenario	3-5
3.1.4 Servicing and Growth	3-7
3.2 Configuration Descriptions - Advanced Communi- cations Platforms	3-11
3.2.1 Configuration Description - Erectable Communications Platform	3-11
3.2.2 Configuration Description - Tri-Beam Space Fabricated Platform	3-16
3.3 Subsystems Definition	3-19
3.3.1 Space - Erectable Truss Structure Defini- tion	3-20
3.3.2 Space Fabricated Tri-Beam Structure Definition	3-30
3.3.3 Electrical Power Generation, Distribution and Control Subsystem Definition	3-41
3.3.4 Microwave Subsystem Definition	3-54
3.3.5 Thermal Analysis and Thermal Control Subsystem Definition	3-72
3.3.6 Propulsion Subsystem Definition	3-88
3.3.7 Attitude and Velocity Control Subsystem	3-97
3.3.8 Tracking, Telemetry and Control Subsystem	3-106
3.4 Mass Properties	3-109
3.5 Construction Requirements - Advanced Communica- tions Platforms	3-112
3.5.1 Erectable Advanced Communications Platform	3-112
3.5.2 Space Fabricated Advanced Communications Platform	3-113
3.5.3 Construction Process Requirements Related to Common Features of Antenna Platform Configurations	3-122

APPENDIXES

A.	PROJECT DEFINITION DRAWINGS	A-1
B.	CONSTRUCTION TOLERANCES	B-1

ILLUSTRATIONS

<u>Figure</u>		<u>Page</u>
2.0-1	Key Features of the Solar Power Satellite Flight Test Article Construction Project	
2.1-1	SPS Test Article Scenario	2-3
2.1-2	Mission Profile for SPS Test Article	2-5
2.2-1	SPS Test Article General Arrangement LEO Configuration	2-11
2.2-2	SPS Test Article GEO Configuration	2-11
2.2-3	Microwave Antenna Configuration	2-13
2.3.1-1	Baseline Beam Structural Characteristics	2-19
2.3.1-2	Lap Joint Design Features	2-20
2.3.1-3	Euler Column Loading Diagram	2-24
2.3.1-4	Diagonal Cord Configuration	2-26
2.3.1-5	RCS Thruster Loading Diagram	2-26
2.3.1-6	Solar Blanket Tension Cable Loading	2-29
2.3.1-7	SPS Ladder - First Modal Frequency	2-29
2.3.2-1	Electrical Power Distribution Subsystem Assembly	2-32
2.3.2-2	SPS Flight Test Article - Efficiency Chain	2-34
2.3.2-3	Solar Array (20m x 200m)	2-35
2.3.2-4	SPS Flight Test Article Typical Element (10F25)	2-36
2.3.2-5	Nickel-Hydrogen Battery Cells	2-40
2.3.2-6	SPS Flight Test Article EPDS Simplified Block Diagram	2-42
2.3.2-7	SPS Flight Test Article - Simplified Ion Propulsion System	2-43
2.3.3-1	SPS Test Article Antenna	2-46
2.3.3-2	Transverse Feeder Guide for Slot Array	2-48
2.3.3-3	Resonant Array Design Basis	2-49
2.3.3-4	SPS Antenna Tolerance	2-52
2.3.3-5	1 kW Klystron	2-54
2.3.3-6	50 kW Klystron	2-55
2.3.3-7	Solar Power Experiment	2-56
2.3.4-1	Reaction Control System (RCS) Module	2-60
2.3.4-2	Solar Electric Propulsion System (SEPS) Module	2-64
2.3.5-1	AVCS Summary, SPS Test Article	2-68
2.3.5-2	Attitude Control Requirements for the Microwave Transmission Experiment	2-69
2.3.5-3	Environmental Disturbances, SPS Test Article	2-70
2.3.5-4	CMG's for SPS Test Article Attitude Control	2-72
2.3.5-5	Sensors for SPS Test Article Attitude Control	2-74
2.3.5-6	Antenna Pointing Control Frequency Requirements, SPS Test Article	2-78
2.3.6-1	Communication Links for SPS Flight Test Article	2-80
2.3.7-1	Klystron Panel Configurations	2-84
2.4-1	Mass Summary - SPS Flight Test Article	2-89
3.0-1	Advanced Technology Communications Platforms	3-1
3.1-1	Advanced Communications Platform Scenario	3-4
3.1-2	Mission Profile, Advanced Communications Platform	3-6

ILLUSTRATIONS
(Continued)

<u>Figure</u>		<u>Page</u>
3.2-1	Erectable Communications Platform	3-12
3.2-2	Space Fabricated Communications Platform	3-12
3.2-1.1	Solar Array Location Concepts	3-15
3.3.1-1	Antenna Mounting to Pentahedral Truss	3-21
3.3.1-2	Pentahedral Truss Elements Configurations	3-22
3.3.1-3	Pentahedral Truss NASTRAN Model - Operational Configuration	3-28
3.3.1-4	First Mode Shape - Solar Panel Array	3-28
3.3.2-1	Thrust Structure Configuration	3-31
3.3.2-2	Tri-Beam Column Loading - Orbit Transfer Thrust	3-33
3.3.2-3	Beam-to-Beam Load Considerations	3-35
3.3.2-4	Tri-Beam Orbit Transfer First Bending Mode	3-37
3.3.2-5	Antenna Structure Stick Model	3-37
3.3.2-6	First Mode - Operational Configuration	3-40
3.3.3-1	Electrical Power Distribution System Assembly	3-42
3.3.3-2	Efficiency Chain for Advanced Communication Platform System	3-45
3.3.3-3	Solar Array	3-46
3.3.3-4	Advanced Communication Platform System Typical Solar Array Blanket Schematic (10F8)	3-48
3.3.3-5	Advanced Technology Communications Platform Simplified Schematic	3-49
3.3.3-6	Rotary Joint Schematic	3-51
3.3.4-1	Advanced Communications System Platform	3-55
3.3.4-2	Perspective View of an Individual Offset - Fed Parabolic Reflector Antenna	3-56
3.3.4-3	Continuous, Interleaved Footprints with Three Antennas	3-58
3.3.4-4	Offset Reflector Without Blocking	3-59
3.3.4-5	73 Beam Offset Reflector Footprints	3-61
3.3.4-6	Dual Offset Cassegrain Reflector	3-63
3.3.4-7	Elevation View of Dual Offset Reflector and Feed Cluster	3-64
3.3.4-8	Autotrack Feed System	3-67
3.3.5-1	Thin-Walled Tube Thermal	3-73
3.3.5-2	Comparison of Eclipse Temperature Predictions	3-75
3.3.5-3	Large-Diameter Strut Temperatures - Uncoated	3-76
3.3.5-4	Large-Diameter Strut Temperatures - Selective Coating	3-76
3.3.5-5	Small-Diameter Strut Temperatures - Uncoated	3-77
3.3.5-6	Small-Diameter Strut Temperatures - Selective Coating	3-78
3.3.5-7	Strut Temperature Gradients During Equinoctial Eclipse	3-80
3.3.5-8	Radiator Heat Rejection Performance	3-82
3.3.5-9	Typical PCM-Radiator Trade Analysis	3-83
3.3.5-10	Radiator for 7.5m Antenna Feed	3-85

ILLUSTRATIONS
(Continued)

<u>Figure</u>		<u>Page</u>
3.3.6-1	Reaction Control System (RCS) Module	3-89
3.3.6-2	Low Thrust Propulsion (LTP) Module	3-92
3.3.6-3	Delta-V Requirements Versus T/V	3-94
3.3.7-1	AVCS Summary, Advanced Communications Platform	3-98
3.3.7-2	Single-Axis CMG's for Attitude Control, Advanced Communications Platform	3-101
3.3.7-3	Orbit Transfer Accuracy, Advanced Communications Platform	3-104
3.3.8-1	Communication Links for Advanced Communications Platform	3-107

TABLES

<u>Table</u>		<u>Page</u>
2.1-1	SPS Test Article Project Requirements	2-9
2.3.1-1	SPS Ladder Structure-Requirements/Capability	2-21
2.3.1-2	Station Keeping and Attitude Control Loads	2-23
2.3.1-3	Torsional Modes for SPS Configuration	2-30
2.3.2-1	Electrical Power Generation, Distribution & Control Subsystem	2-31
2.3.2-2	Power Generation Subsystem	2-37
2.3.2-3	Comparison of Nickel-Hydrogen to Nickel Cadmium Batteries	2-38
2.3.2-4	Energy Storage System (Nickel-Hydrogen Battery)	2-39
2.3.2-5	Distribution Of Electrical Power	2-44
2.3.2-6	SPS Flight Test Article EPDS Weight Summary	2-44
2.3.4-1	RCS Summary	2-59
2.3.4-2	RCS Requirements	2-61
2.3.4-3	SEPS Summary	2-63
2.3.4-4	SEPS Characteristics	2-66
2.3.5-1	Antenna Pointing Drive Torque Requirement, SPS Test Article	2-75
2.3.5-2	Attitude Control Frequency Separation	2-76
2.3.6-1	SPS Flight Test Article Link Parameters	2-81
2.3.6-2	SPS Flight Test Article LRU Mass and Power Summary	2-82
2.3.7-1	16-Klystron Panel Heat Dissipation Requirements	2-85
2.4-1	Mass Summary - SPS Flight Test Article	2-89
2.5.2-1	Component Inventory - SPS Test Article	2-93
2.5.4-1	Critical Construction Tolerances - SPS Test Article	2-95
3.1-1	Advanced Communication Platform Project Requirements	3-9
3.3.1-1	Erectable Communications Platform Structure - Requirements/Capability	3-24
3.3.1-2	Pentahedral Truss Element Compression Loads and Sizes	3-25
3.3.1-3	Erectable Communication Antenna Platform Rotations	3-29
3.3.2-1	Space Fabricated Communication Platform Structure Requirements/Capability	3-32
3.3.2-2	Antenna Feed Column Structure Characteristics	3-39
3.3.3-1	Electrical Power Generation, Distribution and Control System	3-41
3.3.3-2	Power Generation Subsystem	3-44
3.3.3-3	Nickel-Hydrogen Battery Parameters	3-50
3.3.3-4	Electrical Power System Weight Summary	3-53
3.3.4-1	Reflector Tolerances	3-65
3.3.4-2	Solar Array Power for Satellite at Indicated Latitude	3-69
3.3.4-3	4 GHz Downlink Characteristics	3-70
3.3.4-4	12 GHz Downlink Characteristics	3-71
3.3.5-1	Representative Heat Dissipation Requirements for 112.5kW Communications Platform	3-81

<u>Table</u>		<u>Page</u>
3.3.5-2	Thermal Dissipation for High-Power Antenna (7.5 meter)	3-84
3.3.5-3	Thermal Dissipation From CMG Housing	3-86
3.3.6-1	RCS Summary	3-88
3.3.6-2	RCS Requirements	3-90
3.3.6-3	Orbit Transfer Propulsion Summary	3-91
3.3.6-4	LTP Maximum Propellant Load Conditions	3-96
3.3.6-5	Engine Performance Summary	3-96
3.3.7-1	Antenna Pointing Accuracy Error Budget	3-99
3.3.7-2	Momentum Build-up Due to Disturbance Torques	3-99
3.3.7-3	Structural Stiffness Requirements	3-105
3.3.8-1	S-Band and Ku-Band Link Capacity for Advanced Communication Platform at GEO	3-108
3.4-1	Mass Summary - Advanced Communications Platforms	3-110
3.5.1-1	Component Inventory - Erectable Advanced Communications Platform	3-114
3.5.1-2	Critical Construction Tolerances - Erectable Communica- tions Platform	3-117
3.5.2-1	Component Inventory - Space Fabricated Advanced Communications Platform	3-119
3.5.2-2	Critical Construction Tolerances - Space Fabricated Communications Platform	3-121
3.5.3-1	Construction Implications of Design Features, Antenna Platforms	3-123

1.0 INTRODUCTION

This report summarizes the three project system definitions developed as part of the overall Task 1.0 effort. The three systems are: (1) an SFS Development Flight Test Vehicle configured for space fabrication and compatible with solar electric propulsion orbit transfer; (2) an Advanced Communications Platform configured for space fabrication and compatible with low thrust chemical orbit transfer propulsion; and (3) the same Advanced Communications Platform, configured to be space erectable but still compatible with low thrust chemical orbit transfer propulsion. These project systems are intended to serve as configuration models for use in detailed analyses of space construction techniques and processes. They represent feasible concepts for "real" projects; real in the sense that they are realistic contenders on the list of candidate missions currently projected for the national space program. Thus, they represent reasonable configurations upon which to base these early studies of alternative space construction processes. Not only will we learn about some of the fundamental problems associated with space construction, but we will also begin to learn about some of the specific issues likely to occur in the initial applications of large area space systems.

The three project systems presented here represent the culmination of concept analysis and selection efforts started earlier in Task 1.0. Preliminary analyses of some 49 concept variations spanning three basic types of space projects were conducted to identify the main combinations of project options, configuration design approaches and orbit transfer propulsion modes. These concept variations were screened to select a manageable number of specific project systems which could then be used in detailed space construction analyses. The screening process considered the individual project characteristics, their legacy interactions with the space program, construction implications and drivers, and the exploitation of different orbit transfer propulsion modes. The concept variations and screening analyses are presented in Reference 1 (SSD 79-0025).^{*} Thus, the effort reported here begins with the three selected concepts identified above and expands them into complete system definitions covering all of their important design and configuration features.

Although these project systems represent relatively complete definitions, the main intent was to establish reasonable and typical subsystem sizing levels and interface characteristics rather than optimized designs. Since the main objective of the study is to analyze space construction, it was felt to be more important to have "reasonable" designs with good traceability of their principal features than to expend vital study resources on design optimizations. It is more important to know that the construction process must handle a given type of subsystem module with its particular installation constraints/considerations than it is to have the module size and features optimized to the nearest inch or pound. With good traceability through clearly documented rationale the configuration design drivers can easily be correlated with resulting construction issues. This will simplify the application of the construction analysis results of this study to future project systems. Thus, the main guidelines used in the development of the chosen project systems were:

^{*}References appear at the end of each section.

- (1) Utilize first order sizing analyses to produce feasible and practical configurations, not optimized designs.
- (2) Emphasize design characteristics which significantly affect space construction processes.
- (3) Provide good traceability through clear, succinct rationale.

The three project system definitions resulting from the application of these guidelines are presented in the following book sections. Section 2.0 presents the definition of the SPS Development Flight Test Vehicle project and Section 3.0 presents the definitions of two configurations for the Advanced Communications Platform project, a space fabricated design and an erectable design. The content of each section includes overall project requirements, a configuration concept summary, subsystem descriptions and a summary of construction requirements. The project requirements were developed through an abbreviated approach using a scenario technique. With this technique requirements are established more on the basis of judgemental logic rather than on rigorous design trades and cost benefits analyses, thereby leaving more study resources for analysis of space construction. The configuration summary describes the overall design concept along with the design drivers and key rationale. The subsystem descriptions briefly highlight the important features of each subsystem along with their main sizing rationale. The construction requirements translate the configuration design characteristics for each project system into specific rules and guidelines for construction including overall strategies, individual "piece parts" inventories and construction tolerance considerations.

The design definitions and construction requirements data presented here, then, make up the principal input data to Task 2.0 of the study (System Analysis of Space Construction).

Reference

1. Space Construction System Analysis Project System Review,
Rockwell International Corporation, Document No. SSD 79-0025,
Dated 12 December 1978.

2.0 DEFINITION OF SPS FLIGHT TEST ARTICLE

The following definition of the solar power satellite flight test article is complete and independent from the descriptions of antenna platforms which follow in Section 3.0. It begins with a project scenario and continues with overall configuration description and rationale for design, detail subsystem definitions, and a mass properties statement. Finally, there is a presentation of overall construction process requirements, which is limited to the given constraints, and suggested guidelines for construction inherent in the design concept. Key features of the project are introduced in Figure 2.0-1

ORIGINAL PAGE IS
OF POOR QUALITY

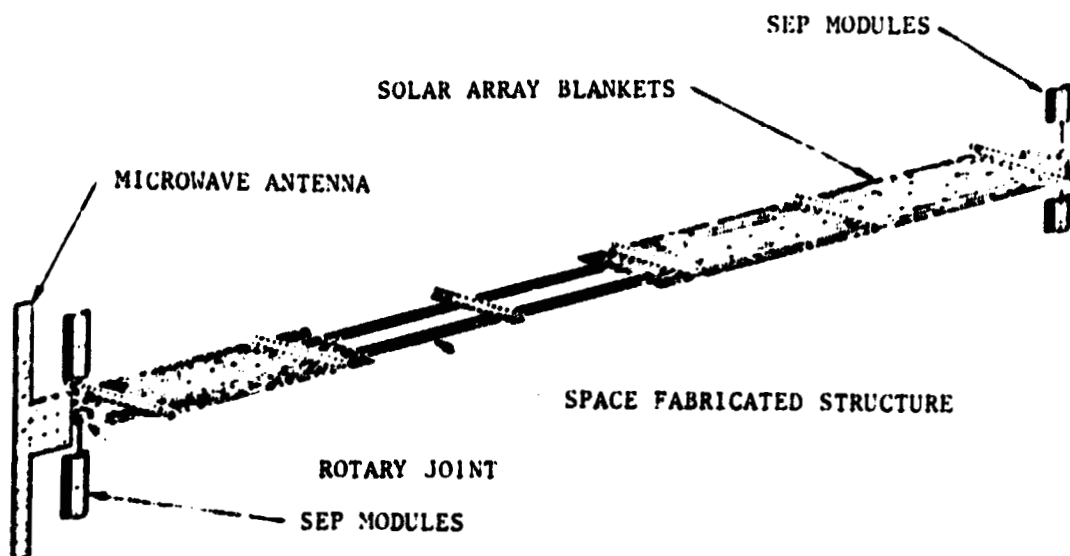


Figure 2.0-1 Key Features of the Solar Power Satellite Flight Test Article Construction Project.

2.1 SPS TEST ARTICLE PROJECT SCENARIO

The purpose of this section is to provide a "word picture" of the major factors likely to influence or shape the design concept for this project. It includes a brief summary of the overall motivating environment surrounding this project, general operating modes suited to the project objectives and servicing/growth considerations related to the scope and objectives of the project. It serves as an abbreviated approach in establishing the top level system requirements for use in the concept synthesis and design analyses.

2.1.1 General

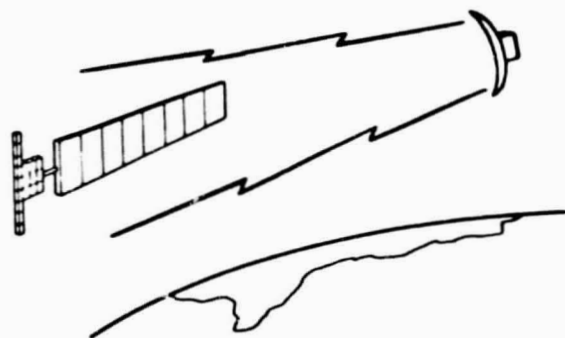
The scenario for the SPS Test Article is outlined in Figure 2.1.1. This scenario presumes the results of on-going NASA-DOE research activities will continue to show solar voltaic space power satellites to be a viable contender in satisfying future US and world needs for clean energy. Implied with this presumption is the execution of the basic plan outlined in the SPS "Red Book" (Reference 1) calling for continued research and analysis of vital issues and the introduction of key hardware/technology developments. Many details of this plan are unimportant to this scenario, but the general need for a major development test vehicle such as that depicted here for the SPS Project is presumed. This, then, sets the overall motivating environment for the analysis of the SPS Test Article Project.

Within this projected environment the SPS scenario specifies a 1985 time period for the flight vehicle IOC as currently planned in the SPS Red Book. The prime objective of this project is to perform space-to-space tests of the microwave power beam. These tests are centered on the verification of the retro-directive phase control concept for beam formation and beam focus/containment and the demonstration of heat rejection in the high thermal flux environment of the beam-forming electronics.

Other objectives, such as high-voltage photovoltaic power generation, large system construction tests and evaluation and behavior of light-weight space structures are also an integral part of the plan. Further, the significant investment represented by the flight vehicle along with its potentially high electrical power output suggests that extra versatility should be incorporated into its design so that it can serve as a multipurpose facility after the primary test objectives have been met. These considerations, then, set the timeframe and background of thinking which are applied to the operating, servicing and growth facets of the overall SPS Test Article Project scenario discussed below.

2.1.2 Operating Scenario

In addition to the operating scenario of Figure 2.1-1, a basic mission and the main flight modes required to perform the test operations are presented in Figure 2.1-2. An orbit altitude of 555 km (300 nmi) was selected for the microwave tests. This was deemed the lowest feasible altitude consistent with the large area, low W/CpA characteristics of the configuration. A higher orbit may prove to be required, but the lowest practical orbit was selected here in recognition of the payload performance/transportation costs



PROJECT SCOPE

1985 TIME PERIOD
 μ -WAVE TESTS (PRIME)
 VERSATILE, MULTI-USE FACILITY

OPERATING SCENARIO

ORBIT: ≈ 300 NMI, $i = 28.5^\circ$
 FLT MODES: ORBIT ADJUST/STATIONKEEP
 μ -WAVE ϕ CONTROL
 μ -WAVE THERMAL EFFECTS
 DAY - NIGHT OPS
 MISSION DURATION: SPS LEO TEST ≈ 6 MO

SERVICING SCENARIO

MANNED SERVICING AVAIL, LEO
 UNMANNED-REMOTE SERVICING ABOVE LEO
 RESUPPLY STATIONKEEPING PROPELLANT
 REPLACE FAILED/DEGRADED MODULES

GROWTH SCENARIO

ADV TECHNOLOGY ORBIT, ≈ 400 NMI
 REOUTFITTER: VARIETY OF POSSIBLE USES,
 INCREASED ENERGY STORAGE
 ADDED USER INTERFACE PROVISIONS
 ORBIT TRANSFER, UP TO GEO

CONFIGURATION/DESIGN IMPACTS

- SINGLE DOF SOLAR ARRAY
- "RELATIVE" STATIONKEEPING
- ALL MAIN MODULES ACCESSIBLE,
REVERSIBLE INSTALLATION
- "TEST BED" INSTRUMENTATION
- ENERGY STORAGE SIZED TO
HOUSEKEEPING
- PROVISIONS FOR ADDED ENERGY
STORAGE

Figure 2.1-1. SPS Test Article Scenario

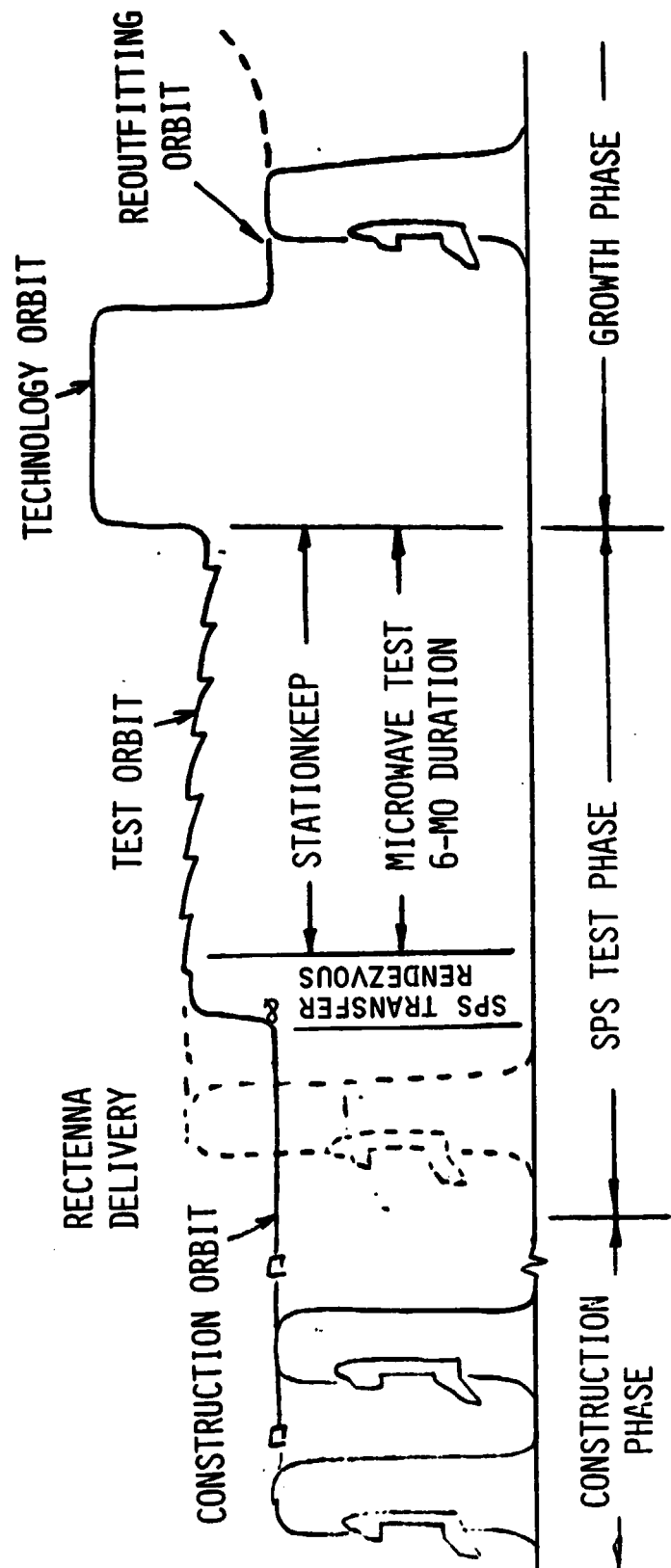


Figure 2.1-2. Mission Profile for SPS Test Article

associated with higher orbits.

A six month mission duration was estimated to be adequate for the performance of the planned microwave tests. This provides over 2700 orbit revs with nearly four full cycles of sun/orbit geometries. As a preliminary estimate, these multiple cycles of the space orbital environment should be adequate to meet the various test objectives including the microwave performance assessments, electrical power generation tests and measurements of structural behavior/response to both thermal cycling and thruster pulses. Future, more detailed planning may establish the need for a longer mission duration, but six months was felt to be sufficiently representative for use at this time to size system features for space construction analyses.

2.1.3 Flight Modes

The mission profile in Figure 2.1-2 identifies several main flight phases/modes. Also, several different orbit altitudes are depicted in recognition of the various influences shaping the project throughout the life of the test vehicle. Construction is shown to occur at a lower, more "Shuttle accessible" orbit, than the test mission orbit. An altitude of 460 km (250 nmi) was arbitrarily selected for space construction. Later, detailed analyses of the space construction process (Task 2.0) may require a change in construction orbit altitude, but for the preliminary requirements here, 460 km was selected.

A higher, 740 km (400 nmi), orbit is also shown after the microwave test mission is completed. This was introduced in recognition of the potential value of long duration (≥ 1 yr) advanced technology experimentation which could be conducted in the post microwave test phase. Experiments during this extended period could include solar electric propulsion, remote servicing, and many others. Following this period, the system could then be transferred to a lower, more Shuttle-accessible orbit for re-outfitting to a new mission configuration.

The above mission profile calls for the orbital delivery of a rectenna vehicle following construction and checkout of the SPS Test Article. The rectenna is the receiving element of the space-to-space microwave beam performance test and is a separate flight vehicle. Its delivery is depicted in dashed lines (Figure 2.1-2) to signify that the definition of this important element is outside the scope of the SPS Test Article definition reported herein. However, it is identified in order to clarify its mission interfaces.

Once the rectenna vehicle is suitably placed in the test orbit the SPS Test Article would be maneuvered to the same orbit with the appropriate stand-off distance. An "orbit adjustment" phase is included which is comprised of a series of small correction maneuvers to achieve the proper "co-orbital" accuracies between the two vehicles. These correction maneuvers are assumed to be provided by the SPS test vehicle rather than the rectenna system. This allows the rectenna vehicle which is a relatively special purpose device to be as simple and low cost as possible. Placing the maneuvering capability on the SPS test vehicle follows the design versatility criteria mentioned earlier. Versatility offers additional productivity from the facility investment after the microwave tests are completed.



For these same reasons, the stationkeeping maneuvers were also assumed to be performed by the SPS test vehicle. These maneuvers are needed to maintain the 16.5 km (8.9 nmi) separation distance between the SPS test vehicle and the rectenna. This separation distance is bounded by beam spreading/loss of side lobe capture on the high side, and near field effects on the low side. A stationkeeping "deadband" of ± 1 km was assumed. This could require maneuvers as frequent as three or four times per day, depending upon the drag/weight differences between the two vehicles. A wider deadband to reduce the maneuver frequency might be possible within the experiment requirements, but would not significantly affect the ΔV required. Hence, the 1 km deadband was selected as a representative value. Although excursions up to 1 km are allowed with this assumption, the actual separation distance must be measured within an accuracy of ± 80 m to properly correlate beam performance measurements.

In addition to stationkeeping, the flight mode for the microwave tests requires precision pointing of the antenna toward the rectenna receiving system. Further, the solar array area must be sun oriented. Thus, a rotary joint is needed between the antenna and the solar array to provide their respective viewing requirements. A single degree-of-freedom (d.o.f.) joint appears to be adequate for this function and would offer lower costs than a more complex two d.o.f. concept. With a Y-POP flight mode (Y is the long axis of the solar array area) rotated to maximize solar view factors, the array kW output is more than sufficient to power the microwave test, even for maximum sun out-of-plane angles ($\beta_{\max} = 52$ degrees).

It further appears that the microwave tests could be performed in a "daylight only" mode, that is, only during the illuminated portion of the orbit. The illuminated fraction of the orbit ranges from 60 to 70 minutes. This is approximately twice the 30 minute thermal response time constant estimated to exist for the high power Klystron installation and antenna assembly. Thus, two "time constants" would be available for generating the desired thermal response data and heat rejection performance trends. This would provide nearly the full range of thermal data up to steady-state conditions for good correlation with thermal models and would greatly reduce energy storage requirements. Thus, with a "daylight only" test mode for the microwave experiments, energy storage need only accommodate a power level of a few kW for basic housekeeping functions rather than the several hundred kW required for the microwave tests.

This results in an austere, but practical, concept for the SPS Test Article. Future, more detailed determinations of test requirements may indicate the need for longer test runs. These would involve additional energy storage capacity, but not necessarily sized to full time, continuous high power testing. High power test runs could be scheduled with several days between tests to allow longer battery charging periods. There is a wide range of possible combinations of test run durations, battery charging intervals and test runs with and without simultaneous battery charging. However, the austere "daylight only" approach was selected for this analysis as a practical concept sufficient to meet the system definition needs for space construction analyses.

2.1.4 Servicing and Growth

Servicing and growth considerations are also important elements in the overall project scenario. In keeping with the preliminary nature of the system definition presented here the scope of servicing considerations is necessarily limited. Trades between reliability, redundancy and level of servicing are inappropriate. Emphasis is on the assurance that the project design not preclude on-orbit servicing, thus, allowing these trades to be made in the future when the design definition reaches the appropriate level of detail.

Since the SPS Test Article will be constructed and operated within shuttle accessible orbits, the servicing scenario for this project would logically include man-in-the-loop approaches. Also, commensurate with the lesser detail available within this early conceptual design process, the servicing considerations treated here are focused on the changeout of major elements or modules (not their internal redundancies). These module type replacements are similar in nature to the equipment changeouts required in re-outfitting the test vehicle for growth missions.

The desirability of incorporating versatility into the SPS Test Article design to handle possible growth missions was indicated in the beginning paragraphs of the scenario discussion. This idea is expanded upon here. The relatively high power output of this vehicle suggests several growth mission options, each with its particular re-outfitting requirements. It could serve as an advanced technology platform in either LEO or GEO, or it could serve as a high power facility for an advanced applications program.

One interesting concept could be a solar electric propulsion (SEP) technology platform. This mission would likely not require large increases in energy storage capacity and would have several other useful features. It could be operated "up" and "down" through the Van Allen radiation belts to determine solar cell degradation characteristics, as well as demonstrating SEP performance envelopes. Different thruster modules and different solar array/solar cell/shielding configurations could be introduced through re-outfitting operations as part of the overall SEP technology program. Other technology programs could also be accommodated as growth missions. The servicing and growth scenario, then, leads to the need for consideration of modular type equipment installations which can be replaced with units of similar or different capacities for extending and/or changing over to a growth mission.

All of the above scenario conditions result in the top level system requirements summarized in Table 2.1-1. These requirements form the basic framework from which the individual subsystems requirements and concepts were derived.

Reference

1. Solar Power Satellite Concept Evaluation, Volume 2 Detailed Report, Johnson Space Center, Dated July 1977 ("Red Book").

Table 2.1-1. SPS Test Article Project Requirements

Mission Objectives

- Prime—Space-to-space microwave beam forming and containment test and klystron high thermal flux impacts and heat rejection performance
- Other—Demonstrate high-voltage solar voltaic power generation
Demonstrate space construction techniques
Measure behavior of lightweight space structure

Operational Time Period

- 1985-1987

Test Mission Orbit

- h = 555 km (300 nmi)
- i = 28.5 degrees

Test Mission Flight Operations

- Orientation: Y-POP, sun incidence varies with β -angle
Microwave antenna tracks co-orbiting rectenna
- Test article stationkeeps w.r.t rectenna
- Microwave test operations only during "daylight" side of orbit
- Housekeeping and structural behavior tests continue on dark side

Orbital Maneuvers

- Construction orbit to test orbit, 460 to 555 km (250 to 300 nmi)
- Orbit adjust to rectenna standoff distance
- Stationkeep w.r.t. rectenna
- Test orbit to advanced technology orbit, 555 to 740 km
(300 to 400 nmi)
- Advanced technology orbit to reoutfitting orbit, 740 to 460 km
(400 to 250 nmi)

Servicing

- Consider man-in-the-loop and/or teleoperator available

Growth

- Consider versatility in design to permit adaptability to multi-use facility after SPS test

2.2 CONFIGURATION DESCRIPTION - SPS TEST ARTICLE

The general arrangement of the SPS Test Article is illustrated in Figure 2.2-1. This figure also lists the subsystems and the major component/descriptions of each of the subsystems that make up the project system as required to implement the project scenario discussed in Section 2.1. The configuration shown represents the LEO operational configuration. Figure 2.2-2 illustrates the orbit transfer and GEO operating configuration, showing the installation of the SEP modules used for orbit transfer. Drawing 42662-27 defines the SPS Test Article concept (Appendix A).

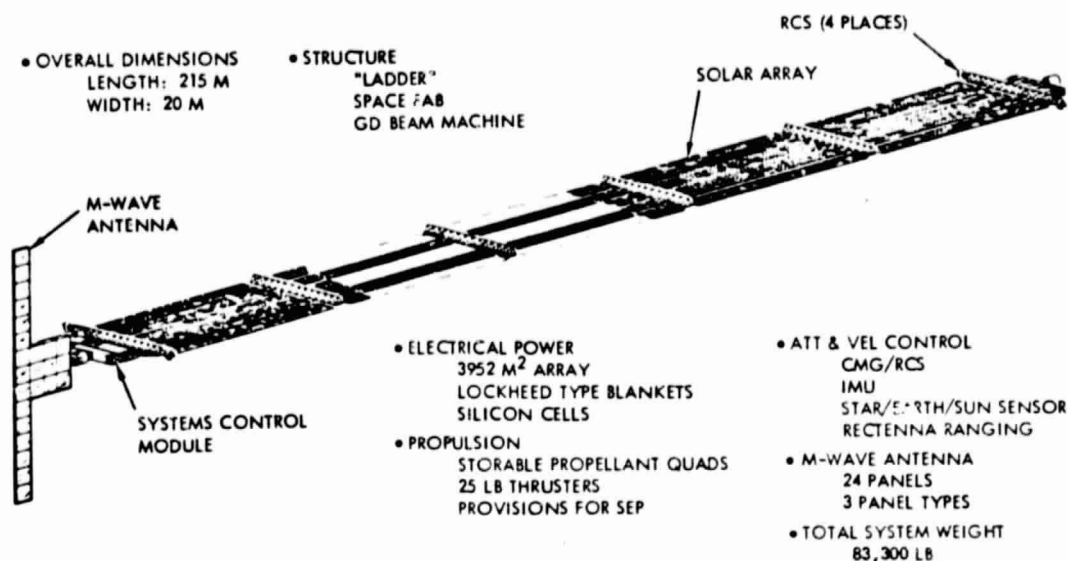


Figure 2.2-1 SPS Test Article
General Arrangement
LEO Configuration

ORIGINAL PAGE IS
OF POOR QUALITY

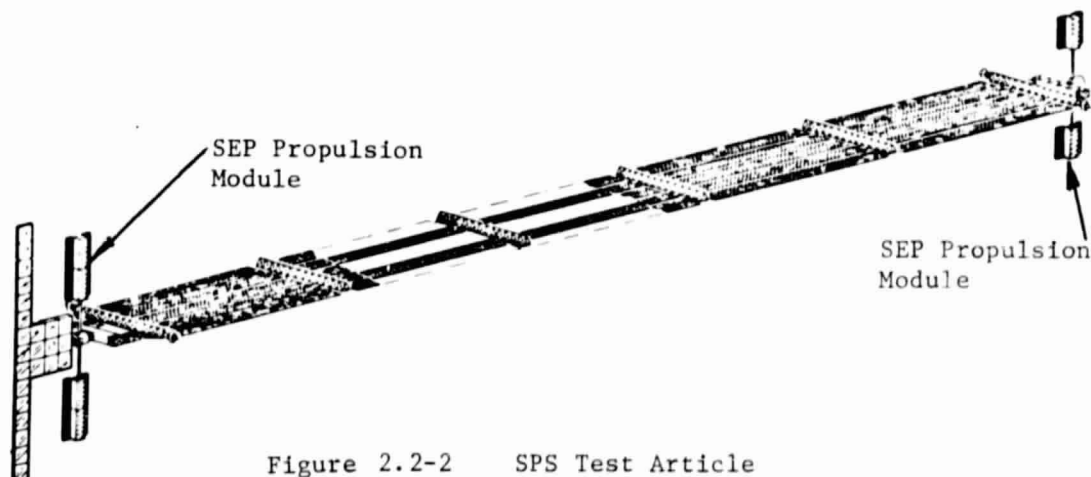


Figure 2.2-2 SPS Test Article
GEO Configuration

The microwave antenna is illustrated in Figure 2.2-3 in its folded configuration for Shuttle Orbiter delivery as well as in its operational configuration. The microwave antenna is attached to the rotary joint. The rotary joint is the interface for the microwave antenna and for other payloads that may be selected. A drawing defining the microwave antenna concept, Drawing 42662-20, is contained in Appendix A.

The SPS Test Article has a linear type of configuration in contrast to equidimensional, planar type arrangements that have been associated with previous large space structures projects. This linear arrangement is also characteristic of the Advanced Communications Platform projects developed for this study. This shape is particularly compatible with automatic space fabrication concepts. It utilizes the beam builder's capability to generate long uninterrupted members. The ladder structural arrangement of the SPS microwave test article and the tri-beam structural arrangement of the advanced communications antenna platform are representative of efficient, automatic space fabrication concepts. The erectable type of structure utilizing struts and unions is equally capable of being constructed into linear or planar arrangements. However, the linear arrangement represented by the erectable advanced communications antenna platform was selected to provide a more direct comparison with the space fabrication concept of construction techniques as well as a comparison of structural characteristics such as stiffness, natural frequencies, modal shapes, etc.

The linear configurations represent relatively flexible structures as compared to a planar configuration. However, the stiffness requirements desired for the mission operations of the study projects can be met. Torsional stiffness is recognized as being the designing driver for the linear configurations, particularly during orbit transfer. Consequently, additional analysis is necessary to determine the locations of concentrated masses, such as antenna packages, in order to minimize torsional moments.

In summary, the linear configurations sensitivities have been considered, and analyzed. The results indicate such project systems configurations can be designed to meet the requirements for control and orientation. Consequently, the project systems configurations selected represent viable configurations for the construction analysis and comparison tasks.

2.2.1 General Configuration Description

The SPS microwave test article project consists of "ladder" type structural arrangement utilizing space fabricated beam members to which 25 solar blankets are attached. A control moment gyro/reaction control system (CMG/RCS) attitude control stationkeeping concept is incorporated. A system housing contains the CMG's, Tracking, Telemetry and Control (TT&C), and power storage batteries with thermal control provided by a radiator and external insulation. Micro meteoroid protection is also incorporated. A rotary joint provides the connection between the solar array power generation system and the microwave test antenna. The microwave test antenna can be replaced with other test articles if so desired.

ORIGINAL PAGE IS
OF POOR QUALITY

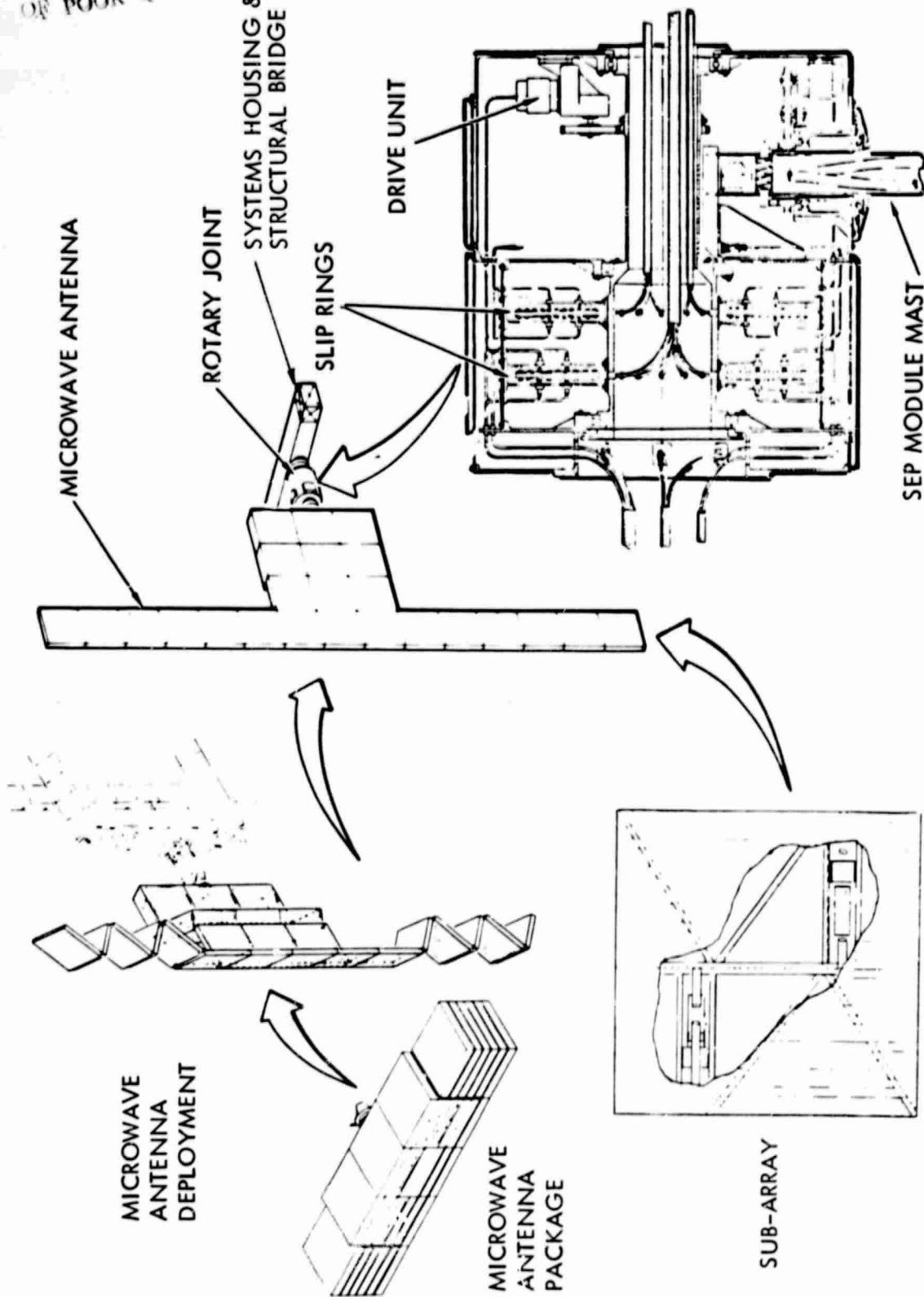


Figure 2.2-3. Microwave Antenna Configuration

For orbit transfer, solar electric modules are installed on both ends of the solar array structure. The SEP modules are installed on rotary joints. Consequently, another rotary joint is required at the end of the solar array structure opposite from the microwave antenna in order to accept the SEP modules at this location. This represents the system configuration in GEO.

The ladder structure is an assembly of beams fabricated by a single beam builder in orbit. The beam configuration is that developed by the General Dynamics SCAFE study with modifications as required, such as increased cap gages and diagonal cord diameters. The structure configuration is dictated by the requirement for approximately 4000m² of solar array, and by the stiffness required for attitude control during operations in LEO and during orbit transfer. Consideration of the assembly fixture size and packaging concept also influenced the width of the configuration. The 20m width selected is compatible with the solar blanket width of 4m, thus permitting a 5-blanket wide arrangement.

All of the larger modular items such as the RCS modules, and the systems housing are attached to the structure via berthing ports. The berthing port concept is the three-petal, neuter concept, baselined for the Shuttle Orbiter. Because all of the berthing activities are accomplished by using the orbiter Remote Manipulator System (RMS), no velocity attenuation system is required. Structural latches are provided only on the mating module. This permits a final checkout of the active latching system on the ground and immediately before assembly in orbit. A utilities interface is provided at each berthing port and each interface will be unique to its particular utilities requirements.

Smaller units such as the electrical junction boxes and the solar blanket switching boxes will be secured to the structure with clamp type devices that are compatible with the structural beam configuration and load capability. The clamping devices that secure the solar array switching boxes also provide the attachments for the individual solar array blankets.

Electrical lines are secured to the structure with special clips. The clips may require pre-punched holes in the post members of the fabricated beams.

The systems housing which contains the electrical power storage batteries and controls, the CMG's, the TT&C equipment, and the heat rejection radiator is also the structural bridge that provides the structural interface between the solar array structure and the rotary joint to which the microwave antenna is attached (see Figure 2.2-3). The housing will also be provided with thermal control insulation and meteoroid protection. A similar structural bridge at the opposite end of the solar array structure provides the support for the rotary joint and solar electric propulsion modules used for orbit transfer. No other system components are included in this bridge structure.

The solar array consists of 25 solar blankets. Each blanket is attached to the transverse beams of the structure. The attachment is provided with clamp type fittings to which the solar blankets are attached at three places along the 4m width of the blanket. Power leads will plug into individual switching boxes. From each of the switch gear boxes power lines will run along the longitudinal beams to interface with the systems housing and continue on to the power slip ring of the rotary joint. This arrangement provides voltage control to each of the 25 blankets.

The rotary joint provides one degree of freedom rotation between the solar array and the microwave antenna. It also provides the support for the Solar Electric Propulsion (SEP) modules. A slip ring assembly within the rotary joint provides the electrical power transfer across the rotary joint and a second slip ring assembly provides for the transfer of data and control signals. The rotary joint as a unit is attached to the systems housing via a berthing port. An electrical power and data/control signal interface is established at this port. A berthing port also is provided on the other end of the rotary joint unit to accept the microwave test antenna or other test articles if desired.

When GEO operations are desired, as discussed in the project scenario of Section 2.1, then, and only then, will the SEP modules be installed. Each module consists of 12 engines and their controls and propellant. Each of four modules contains a mounting post which is designed to plug into the rotary joints making the structural attachment as well as the electrical power and data/control connections. Two additional modules are mounted to two of the module/post configurations to make two 24 engine clusters which are required at the microwave antenna end of the SPS microwave test article. The rotary joint required at the other end of the solar array structure will also only be installed when the orbit transfer mode is desired.

The estimated weight of the SPS microwave test article in the LEO operational configuration is 37,800 kg (83,160 lb). The orbit transfer configuration estimated weight is 49,200 kg (108,250 lb).

2.2.2 Microwave Antenna Description

The microwave antenna is considered as the initial payload item for the SPS Flight Test Article. It would probably be replaced by another payload for subsequent operations at GEO after the initial microwave testing effort.

The microwave test antenna is composed of 24 subarray panels. Each panel is approximately 3m square, but their internal arrangement differs depending on their test function.

The 15 "A" panels constitute the phase control function of the test. The panel is approximately 3m square by .4m deep. It contains two 1 kW Klystrons which excite 16 wave guides on one half and 17 on the other half of the subarray. The wave guides are soft mounted to the panel frame to minimize thermal expansion effects. Two receiving elements which receive signals from the trailing antenna are located along one edge of the subarray panel. The heat rejection radiator is located on the surface opposite the microwave radiating wave guides.

The 8 "B" panels are configured for the thermal phase of the test. Sixteen (16) Klystrons are utilized in this panel for the purpose of thermal testing and are arranged as shown in Drawing 42662-20. Five of the panels require the additional structure shown for packaging purposes which will be discussed later.

The center panel, (C) of the thermal test portion of the antenna is configured to obtain a heat flux comparable to that anticipated for the SPS transmitting antenna. This panel contains 121 1-kW Klystrons within the same three-meter-square panel. The depth of the panel is 1.1m which is sized to accommodate the Klystrons. Additional heat rejection radiator surface may be required for this unique panel.

The total antenna assembly is folded for transport to the LEO operating altitude. The total package is installed on a berthing port located on the end of the rotary joint of the solar array assembly. The antenna is deployed into the using configuration only after the antenna has been secured to the rotary joint.

The estimated weight of the antenna assembly is 9,140 kg (20,110 lbs).

2.3 SUBSYSTEMS DEFINITION

Detailed descriptions of the subsystems for the SPS Flight Test Article project are presented in the following sections. In each subsystem discussion there is an introductory summary description which includes design requirements, a detail description and a discussion of rationale or analytical effort accomplished to support the design of the subsystem. The structure is described first, then the power generation, distribution and control subsystem. Following these are the descriptions of microwave subsystem, propulsion, guidance and TT&C subsystems. A discussion of thermal control devices and effects concludes the series.

2.3.1 Structure Subsystem Definition—SPS Test Article

Objectives

The objectives of the structural engineering reviews and analyses conducted in this space construction study were:

- To ensure construction system study realism by representing structural configurations that are suitable for the total spectrum of mission requirements.
- To ensure that all the particular requirements for structural integrity, that significantly impact construction, are understood and identified.
- To support the total systems weight analysis through definition of major component structural sizes.

SPS Flight Test Structural Configuration Description

The configuration of the SPS flight test article is pictorially described on Drawing 42662-27 (Appendix A). The structural configuration is that of a "ladder," which is extremely simple to construct, yet is structurally suitable since it is fabricated in the benign environment of space, and then subjected only to the low levels of loading described herein.

The ladder is comprised of two longitudinal beams (215 m long) spaced 10 meters apart and interconnected by a total of eight lateral beams. The two longitudinal and six of the lateral beams shown are the baseline machine-made beams currently being developed by General Dynamics under Contract NAS9-15310 (Figure 2.3.1-1) except that the diameter of the diagonal cords (1 mm) has been increased to two millimeters (.080 inch). Also, the cord pretension has been appropriately increased from 45 to 180 newtons (40 lb) to maintain the same cord pretension unit stress. Discussion with General Dynamics has confirmed the suitability of these modifications. The two additional laterals at the **extremities** of the ladder, while provided for mounting of the electrical propulsion panels, antenna, and housing of the control moment gyros, batteries, and TT&C equipment are bending and torsional strongbacks to increase the configuration stiffness. The strongback bending stiffness significantly supplements the in-plane Vierendahl behavior of the ladder achieved by welding the **laterals** to longitudinal members at the four corners of each lap joint (Figure 2.3.1-2). The strongback torsional stiffness significantly enhances the configuration overall stiffness.

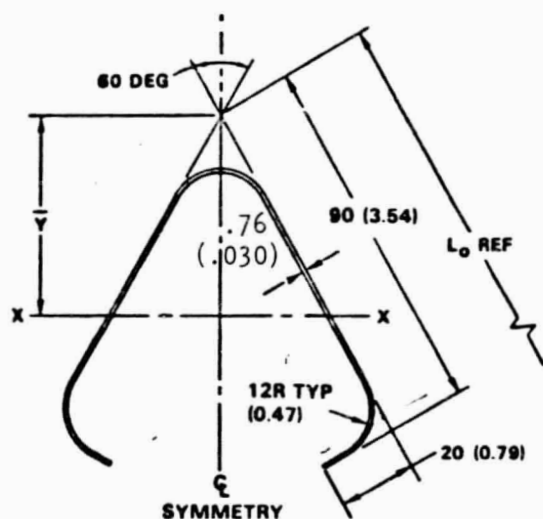
The solar blanket panels are stretched to 26.2 N/m (0.15 lb/in.) limit tension, between the six laterals spaced 41.6 m apart and are attached as shown, on the drawing, in Section B-B. The six laterals with two overhangs of 5 m and a center span of 10 m provide the minimum shear-induced lateral deflection due to blanket tensioning. The four RCS modules are mounted to the **extremities** of the end bay 20-m laterals. The struts shown are provided to limit lateral deflection, during RCS longitudinally directed thruster loads, to values compatible with the solar array blanket tension system design.

Technical drawing of a truss structure. Dimensions and labels include:

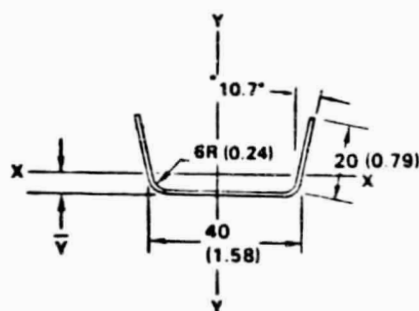
- CUTOFF: 0.300 (11.81 IN.)
- BAY: 1.434m (56.46 IN.)
- 1.180m (46.44 IN.)
- $L_0 = 1.362m$ (53.62 IN.)
- Labels: CAP B, CAP A, CAP A, CAP, DIAGONAL CORD, CROSS MEMBER.

A	$4.43 \times 10^{-4} \text{ m}^2$ (0.687 in. ²)
I	$1.205 \times 10^{-4} \text{ m}^4$ (289.7 in. ⁴)
AE	$63.41 \times 10^6 \text{ N}$ ($14.26 \times 10^6 \text{ lb}$)
EI	$17.25 \times 10^6 \text{ Nm}^2$ ($6.014 \times 10^9 \text{ lb-in}^2$)
GJ	$11.1 \times 10^3 \text{ Nm}^2$ ($3.87 \times 10^6 \text{ lb-in}^2$)

Typical Beam



Cap Section



Cross-Member
Section

2-19

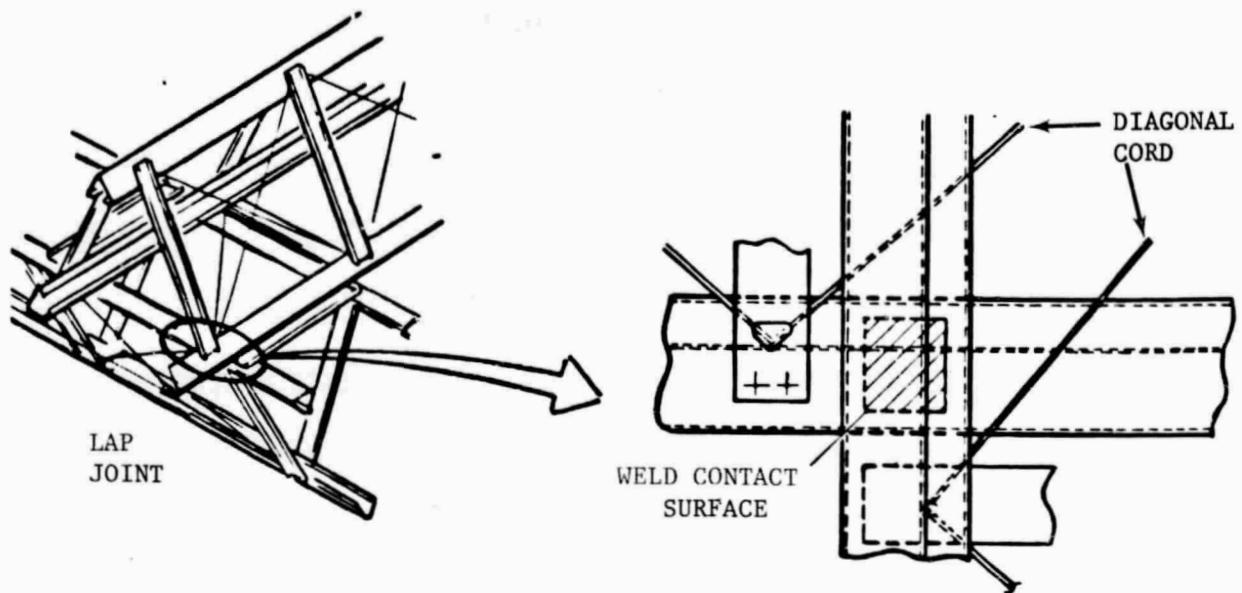


Figure 2.3.1-2. Lap Joint Design Features

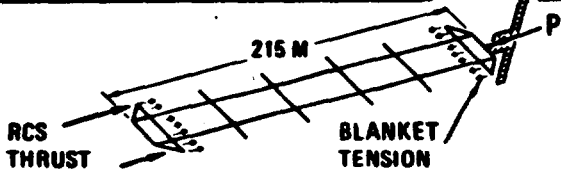
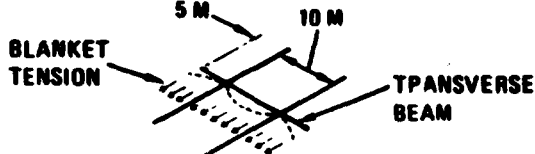


The detailed structural requirements and analyses that directed the structural design of this SPS configuration are described herein. However, for review convenience, a summary of the most significant requirements and design capability are shown in Table 2.3.1-1.

Structural Requirements

This SPS configuration has been reviewed and analyzed in order to assure that the basic concept is suitable for the SPS flight test article mission. To ascertain its suitability at this stage of maturity of the concept and mission requirements, the structural requirements delineated below were established. All of these requirements are regarded to be hard except the requirements evolving from the interplay between stationkeeping, attitude control, and structure loading and, hence, will be reconsidered during the course of the study. However, it is felt that the requirements shown are sufficiently realistic to be the basis of determining the suitability of the basic concept.

Solar Array Blanket Tension Loading. The structure must have sufficient rigidity to maintain a minimum limit solar array blanket pretension loading of 17.5 N/m (0.10 lb/in.) in each of the 4m wide blankets that comprise the 20m wide array. The ladder structure, therefore, allowing for thermal effects, must be capable of sustaining the resulting compression due to a peak limit blanket pretension loading of 26.2 N/m (0.15 lb/in.) across each 4m blanket as discretely imposed during construction and in the final constructed state. The initial diagonal cord pretension-induced compression of the basic beam is, for convenience, included in this requirement. The pretension is 180 N (40 lb) for each cord.

Table 2.3.1-1 SPS Ladder Structure - Requirements/Capability

REQUIREMENT		DESIGN CONCERN/IMPACT	DESIGN CAPABILITY
SOLAR BLANKET TENSION -15 LB/IN. STATION KEEPING THRUST - 100 LBS		LONG COLUMN BEHAVIOR - ARRAY LENGTH < 300 M	ULTIMATE AXIAL LOAD 480 LBS CAPABILITY = 850 LBS
SOLAR BLANKET TENSION		MINIMUM DEFLECTION WITH WITH LONGITUDINAL @ 10 M	RELATIVE DEFLECTION BETWEEN SPRINGS -.20 IN.
MODAL FREQUENCY > .0040 HZ		TORSIONAL MODE - BEAM DIAGONAL CORD DIA .080 IN. SYSTEM SUPPORT HOUSING TORSIONAL STRONGBACK	FIRST MODE (TORSION) = .010 HZ 2ND MODE (BENDING) = .025 HZ (BLANKET ON RIGID SUPPORT = .045 HZ
ATTITUDE CONTROL & STATION KEEPING		LATERAL BENDING BEHAVIOR ARRAY LENGTH < 225 M	THRUST MAGNITUDE + 4% THRUST BUILDUP < .050 SEC
DIMENSIONAL STABILITY SOLAR ARRAY WITHIN 9° (1% POWER REDUCTION)		ANGLE OF TWIST - RCS THRUST TOLERANCES	< 9°
DIMENSIONAL STABILITY MICROWAVE ANTENNA < 6 MIN		THERMAL/INERTIAL DEFORMATION	EXPECTED TO BE < 6 MINUTES

ORIGINAL PAGE IS
OF POOR QUALITY

2-21

Satellite Systems Division
Space Systems Group

Rockwell
International

Thermal Gradients. The structure must sustain the loads resulting from the thermal gradients throughout the structure with the resulting deflections. For this concept feasibility analysis, the peak thermal gradients between the beam caps is 28°K (50°F) and the peak change in temperature from that of the "as built" condition is ±111°K (200°F).

Stationkeeping and Attitude Control Loads. The structure must be capable of sustaining the stationkeeping and attitude control loads delineated in Table 2.3.1-2. Presently (to be reconsidered at a later date), the thrusters have a rise time substantially less than the structure's first modal frequency period; hence, an amplification factor of 2 is applied to the limit load.

Control System Requirements. The structural stiffness of the configuration must be compatible with the control system design. The design of the control system has torsionally decoupled the solar array configuration from that of the antenna. The minimum modal frequencies of the solar blanket array and microwave antenna structures must be respectively greater than 0.0040 and 0.022 Hz.

Miscellaneous Loads. The load sources contained herein for completeness have been reviewed and/or analyzed and found to be non-critical, and for reporting convenience are contained herein. A "soft dock" concept utilizing the RMS will be employed. Prior analyses for this concept (ATL/LSS program) indicate the loads will be less than the amplified thruster loads shown in Table 2.3.1-2.

For transfer to synchronous orbit, the SEP system imposes loads that are negligible. Gravity gradient, solar pressure, and atmospheric drag loads acting upon the structure directly are not significant.

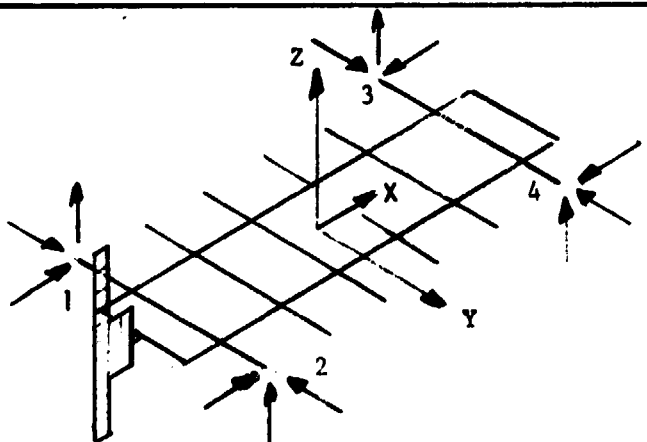
Dimensional Stability. The solar array blankets must be positioned within 9 degrees of the sun. By inspection, this is not a critical requirement.

The total accuracy of the antenna must be maintained within 13 minutes. The portion allocated to structural deflection is 6 minutes.

Structural Analyses

The structural analyses performed to support design definition and verify the suitability of the structural configuration to satisfy the foregoing requirements are delineated herein. All these analyses utilize a safety factor of 1.5 applied to limit load. As stated previously, a load amplification factor of 2 is applied to the rigid body calculated RCS thruster-induced loads.

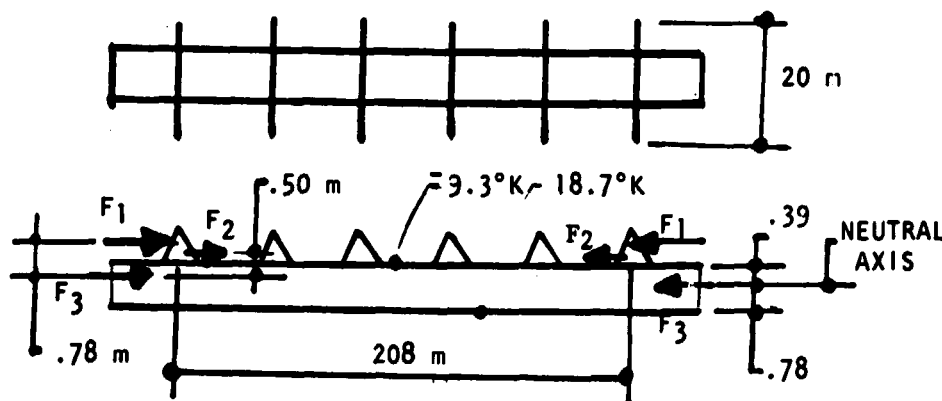
Table 2.3.1-2. Stationkeeping and Attitude Control Loads

CASE LOAD	LOAD CONDITIONS (NEWTONS)											
	STATIONKEEPING								ATTITUDE			
	1	2	3	4	5	6	7	8	9	10	11	12
1 _x	222											
1 _y			111							111		
1 _z							22		-22			22
2 _x	222											
2 _y				111							111	
2 _z							22		-22			-22
3 _x		222										
3 _y					111						111	
3 _z								22	22			+22
4 _x		222										
4 _y						111				111		
4 _z								22	22			-22
<p>TIME DELAY BETWEEN FIRST AND LAST LOAD NOT TO EXCEED .15 SECOND, PEAK DIFFERENCE IN LOAD MAGNITUDE NOT TO EXCEED 4%.</p> <p>AMPLITUDE FACTOR OF 2.0 TO BE APPLIED TO RIGID BODY ANALYSIS LOADS.</p>												
												

Since the baseline beam being developed by General Dynamics is used (except for the diagonal cord modifications discussed previously), Figure 2.3.1-1 is included to present the basic beam structural characteristics. For this design, the GJ value is four times that shown. The analysis presumes, pending a static test of the prototype beam, that the individual cap ultimate load capability is 6583 N (1480 lb), i.e., the value quoted in Reference 1. It is pertinent to note the feasibility of the concept is not dependent on that value since the basic cap can be significantly strengthened, if necessary, by increasing the basic effective cap gauge from 0.75 mm (0.030 in.) to 1.25 mm (0.050 in.). The associated structure weight increase of 225 kg (500 lb) with the 1.25 mm gauge would represent approximately 0.60% of the total low earth orbit SPS weight.

Euler Column Analysis. The total limit compression loading on each beam due to the combined limit pretension of 26.2 N/m (0.15 lb/in.), the diagonal cord pretension of 180 N per cord (40 lb), and an RCS total thrust of 444 N (100 lb) per beam (Case 2, Table 2.3.1-2) is shown on Figure 2.3.1-3. While the inertial reaction to the RCS thrust is primarily distributed over the array length; the total reaction is shown at the extreme end for convenience (and conservatism). The total limit compression, due to pretension of the six diagonal cords per bay, of 748 N (168 lb) is included only for local cap stability. It does not affect Euler column capability or produce deflection magnification since it is an internal load with each bay a closed force system. The compression load from blanket tension (267 N) cannot produce deflection magnification, but its effect on Euler stability is questionable; hence, it is included in the analysis.

The Euler column capability, per longitudinal, is determined from Reference 2, which includes the effect of shear deflection.



F_1 is RCS thrust load = 444 N (100 lb)
 F_2 is solar array tension load = 267 N (60 lb)
 F_3 is diagonal cord tension load = 748 N (168 lb)

Temperatures quoted are relative to neutral axis.

Figure 2.3.1-3. Euler Column Loading Diagram

$$P_{cr} = \frac{\pi^2 EI}{\ell^2} \frac{1}{1 + \frac{\pi^2 EI}{\ell^2} \frac{1}{A_d E \sin \phi \cos^2 \phi}}$$

where $\frac{\pi^2 EI}{\ell^2} = \frac{\pi^2 (17.25 \times 10^6)}{(208)^2} = 3935 \text{ N (884 lb)}$

$$P_{cr} = 3935 \frac{1}{1 + \frac{3935}{4(71,200)(.35)}} = 3785 \text{ N (850 lb)}$$

To assure no significant magnification of load and deflection, the permissible ultimate axial load is limited to one half of the determined value; hence, for the total configuration this value is 3785 N (850 lb), and is greater than the total ultimate applied load of 2136 N (480 lb).

The combination of loads and thermal gradients is analyzed more rigorously as follows.

Referring to Figure 2.3.1-3, and Reference 2, the peak deflection y at the center of a beam column is determined from

$$y = \frac{M_T \ell^2}{8EI} \frac{2(1 - \cos u)}{u^2 \cos u}$$

where $u = \frac{\ell}{2} \sqrt{\frac{P}{EI}}$

hence $u = \frac{208}{2} \sqrt{\frac{712 \times 1.5}{17.25 \times 10^6}} = .818$

Accounting for shear stiffness affects, $u = .834$; hence, $y = .000439 M_T$, where M_T is the total equivalent end moment due to the offset loads shown and the existing thermal gradient. For this condition $M_T = 875 \text{ NM (7747 LB in.)}$, for which the peak deflection is .38 m (15 in.). The maximum ultimate moment of 1126 N·m, in conjunction with the total ultimate axial load of 2190 N, induces a peak cap load of 1209 N (272 lb) on cap "A" (Figure 2.3.1-1) which is well below the design capability. The effects of a fabrication deviation of .100 m will not be deleterious.

Cord Pretension Considerations. The intent of this section is to demonstrate the suitability of the selected diagonal cord pretension of 180 N, insofar as maintenance of pretension. The worst possible case visualized is a cord temperature increase of 111°K (200°F) concurrent with compression in the cap and vertical shear across the element (Figure 2.3.1-4). Although the peak 6583 N (1480 lb) compression will not occur at the same station as the peak shear, the analysis conservatively assumes that to occur.

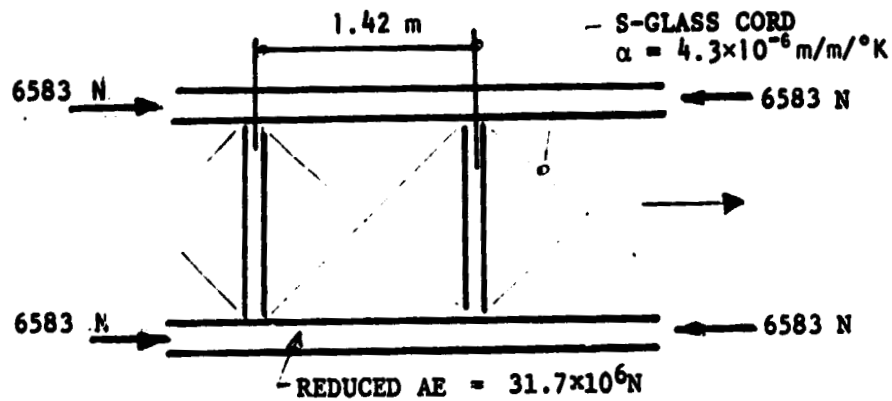
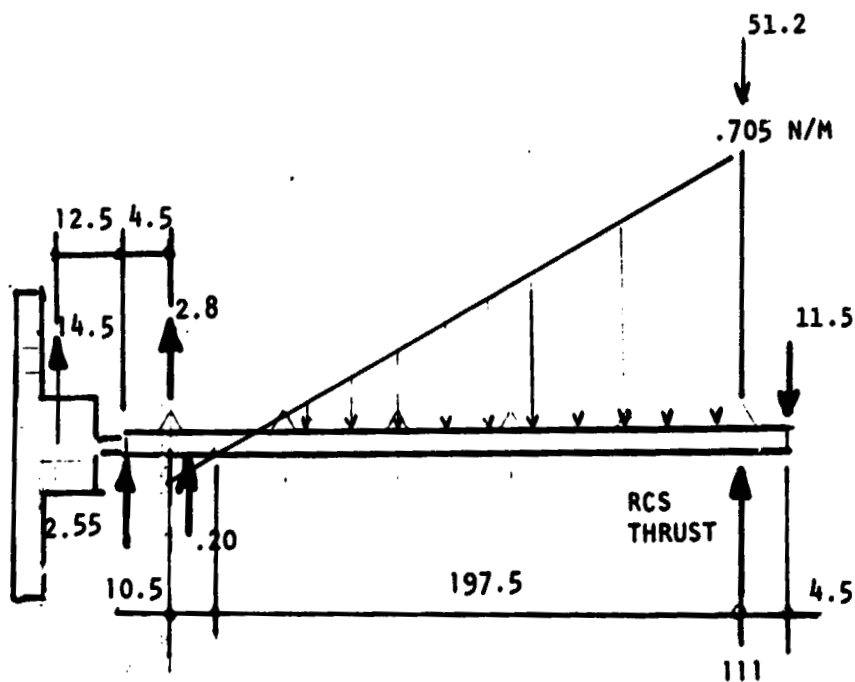


Figure 2.3.1-4. Diagonal Cord Configuration



All forces in newtons
All dimensions in meters

Figure 2.3.1-5. RCS Thruster Loading Diagram

- The cap shortening (6583 N compression) = 0.889 mm
- Cord thermal-induced length change
along X-axis = 0.584
- Cord shear-induced length change
along X-axis = 0.889
- Peak relative length change = 2.36 mm
- Initial diagonal cord elongation
along X-axis = 3.10 mm
- Remaining elongation = 0.74 mm

The initial pretension appears adequate since creep is not expected to be significant for the stress level in the glass which is approximately 3% of ultimate.

RCS Thruster Loads. Referring to Table 2.3.1-2, the suitability of Cases 1 or 2 concurrent with the loads discussed previously has been demonstrated.

The suitability of Case 5 is illustrated as follows. Refer to Figure 2.3.1-5 which is the balanced rigid body loading on one longitudinal beam due to a 111-N (25 lb) thruster force as shown.

The peak limit moment due to this loading only is 1875 NM (16,600 lb in.) which imposes an ultimate load on cap "A" (Figure 2.3.1-1) of 2230 N (502 lb). The total axial compression load due to blanket and diagonal cord pretension induces an additional ultimate cap load of 507 N (114 lb). The total cap ultimate load is 2737 N (616 lb). As stated previously, neither of the pretension loads will produce any deflection magnification since they are both closed-force systems. Both load systems also are attached to the beam and move with the beam. The predicted lateral deflection, due to this loading, is 0.30 m (12 in.).

The capability of Cases 4 and 6 through 12 can be demonstrated through the same type of analysis.

Attention is directed to the requirement of Table 2.3.1-1 relating to the peak thruster forces not varying by more than 4%. This could conceivably result in a 0.90 N (0.20 lb) difference in thruster forces, producing an applied torque of 18 N/m (159 lb/in.). The resulting relative angle of twist across the 208 m structure end to end would be approximately 1.2 degrees, and is not deleterious.

Solar Array Blanket Structure—Strain Compatibility. The design of the spring tension system to comply with the differences in strain between the solar array blanket and the longitudinal beams is beyond the present stage of study scope. However, the performed conceptual evaluation efforts are discussed as follows.

It is reasonable to assume the blanket expansion over half of the 40 m bay is $18.50 \times 10^{-6} \times 111 \times 20 = 0.041$ m (1.60 in.). The shortening of the beams due to thermal variation and/or compression loading is negligible by comparison. For each 4 m width containing three tension springs each, each spring is initially loaded to 35 N (7.9 lb). Using a spring constant of 297 N/m (1.7 lb/in.), the initial stretch = 0.118 m (4.65 in.). The remaining tension equals

$$\frac{0.118 - 0.041}{0.118} \times 26.2 = 17 \text{ N/m (0.10 lb/in.)}$$

During a peak g-load, normal to the array, of 0.001 (conservative), the solar array blanket static response would be as follows:

Referring to Figure 2.3.1-6, a basic membrane calculation indicates a deflection of 0.116 m (4.6 in.). This is considered to be reasonable. Incidentally, the basic blanket natural frequency with the minimum tension is 0.045 Hz.

Along the same lines, it is very desirable for the lateral beams to be quite stiff to preclude tuning problems during blanket installation. An analysis of the lateral deflections (shear deformation predominates) of the beam indicated the following lateral deflection due to a limit tension of 26.2 N/m (0.15 lb/in.).

- Maximum cantilever tip deflection = 1.8 cm (0.70 in.)
- Maximum center span deflection = 1.8 cm (0.70 in.)
- Maximum deflection between 1.4-m support points = 0.51 cm (0.20 in.)

Modal Analyses. A modal analysis performed on NASTRAN to the current SPS weight distribution indicated the minimum modal frequency to be 0.010 Hz (Case 6, Table 2.3.1-3). The associated mode is torsion (see Figure 2.3.1-7). The second mode is bending with a frequency of 0.029 Hz.

The lowest mode is above the minimum requirement of 0.0040 Hz. It is pertinent to note the value of 0.010 Hz could be increased to 0.016 Hz with placement of the RCS tankage modules on the SPS centerline rather than 10 meters outboard as presently shown. The new requirement for propellant lines is appreciated.

The present design having a natural frequency of 0.010 Hz evolved from consideration of several alternate designs for which the minimum torsional modal frequencies are shown in Table 2.3.1-3. While the trades were performed upon a configuration weighing 25,000 kg, the trends are valid. It is apparent that additional laterals was not an effective means of increasing the frequency and that the most effective increase came from increasing the torsional stiffness of the strongbacks at the extremity of the structure and increasing the diameter of the diagonal chords to 2 mm.

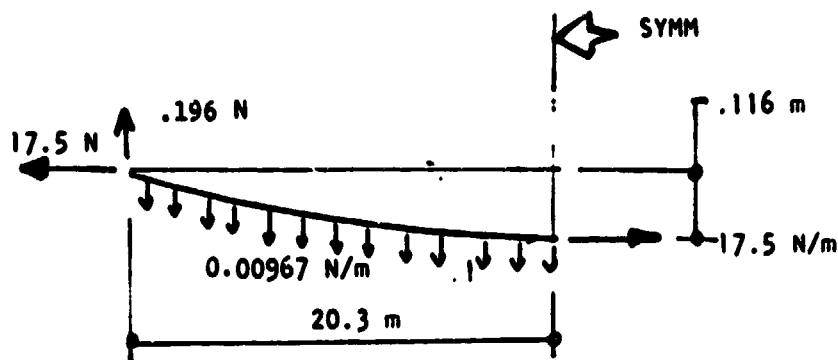


Figure 2.3.1-6. Solar Blanket Array
Tension Loading

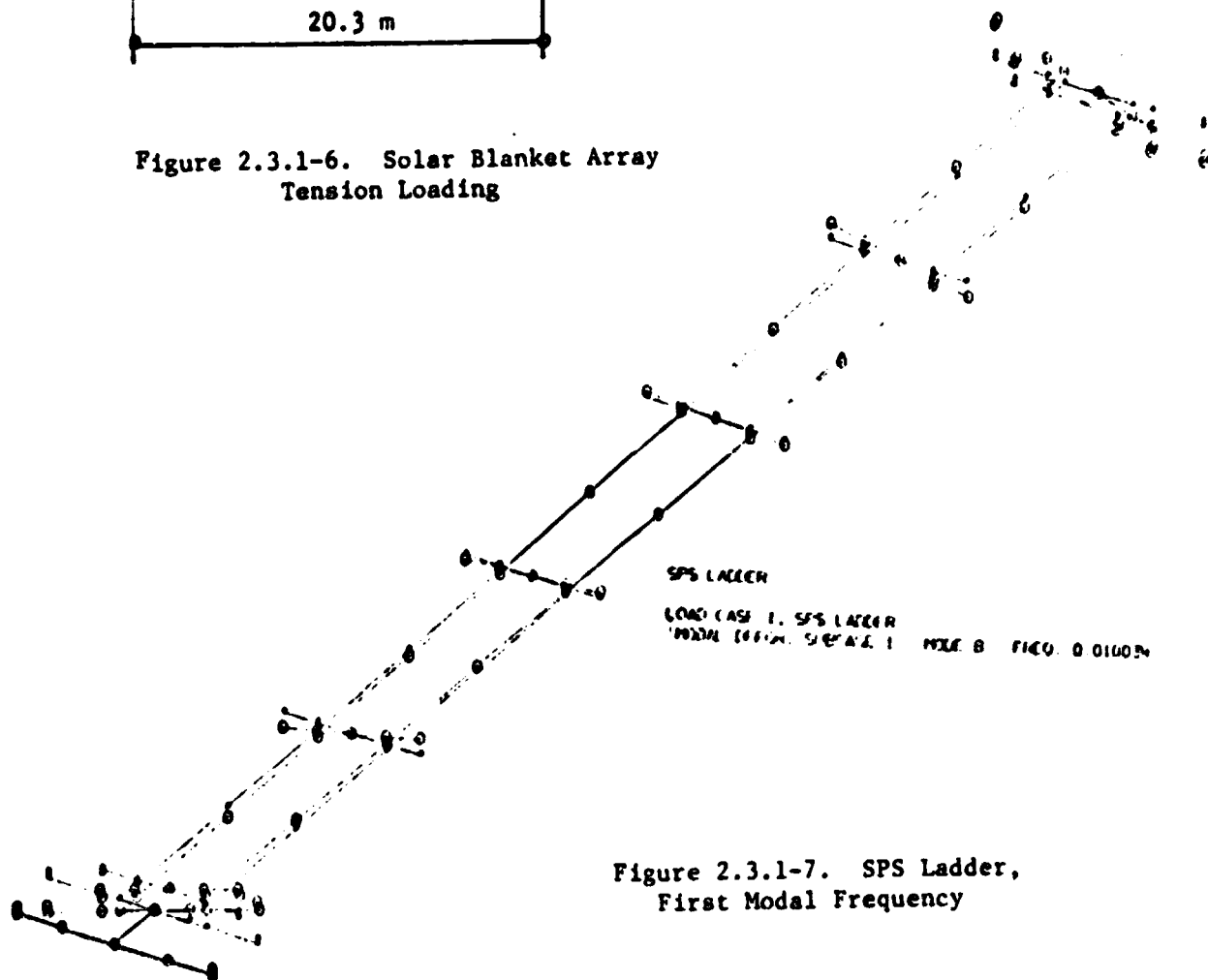


Figure 2.3.1-7. SPS Ladder,
First Modal Frequency

ORIGINAL PAGE IS
OF POOR QUALITY

Table 2.3.1-3. Torsional Modes for SPS Configuration

CASE	SPS WEIGHT (KG)	NUMBER OF LONGITUDINAL BEAMS	NUMBER OF LATERAL BEAMS	DIAGONAL CORD DIA. (MM)	STRONGBACK GJ INCREASE	1ST TORSIONAL FREQUENCY (Hz)
1	25,000	2	6	1	NO	0.00652
2	25,110	2	11	1	NO	0.00740
3	25,570	4	11	1	NO	0.0105
4	25,600	2	6	1	YES	0.0134
5	25,600	2	6	2	YES	0.0170
6	38,180	2	6	2	YES	0.010*

*2nd Modal Frequency = 0.029 Hz (Bending)

Antenna Dimensional Stability. While a structural analysis to determine the antenna thermal and mechanical deflections has not been performed, the allocation of six minutes is expected to be achievable.

Reference 1 - Space Construction Automated Fabrication Experiment Definition Study (SCAFEDS) - Convair Division, General Dynamics, CASD ASP77-017 (26 May, 1978)

Reference 2 - S. Timoshenko, Theory of Elastic Stability, New York, McGraw-Hill Inc.

2.3.2 Electrical Power Generation, Distribution & Control Subsystem Definition

Description Summary

The characteristics of the major components of the electrical power subsystem are summarized in Table 2.3.2-1. Figure 2.3.2-1 schematically summarizes the power distribution system assembly.

Table 2.3.2-1
Electrical Power Generation, Distribution & Control Subsystem

Item	Characteristic
Power Generation	4000m ² Solar Array 130 Watts/m ² End-of-Life Output High Efficiency Hybrid Solar Cell 20 Year Life
Electrical Power Distribution	520 kW Power @ 200 Volts dc 5% Regulation Transmission Efficiency = 94%
Energy Storage	Nickel-Hydrogen Batteries 37 kW Hours
Rotary Joint	Slip Rings Transfer 488.8 kW @ 204.7V
Test Article	279 Klystrons
Microwave Antenna	dc-dc Converter/Klystron Interface 334.05 kW @ 204V dc
Telemetry, Tracking & Command (TT&C)	5 kW @ 28 V dc and 200 V dc

The electrical power distribution system (EPDS) receives power from the power generation subsystem, and provides the regulation and switching required to deliver the power for distribution to the various satellite loads or to the storage batteries. Figure 2.3.2-1 illustrates the major assemblies comprising the EPDS system. The subsystem consists of main feeders, secondary feeders, tie bars, summing buses, regulators, voltage converters switch gear, remote power contactors, slip rings, brushes and subsystem cabling. Batteries and battery chargers are included for eclipse periods.

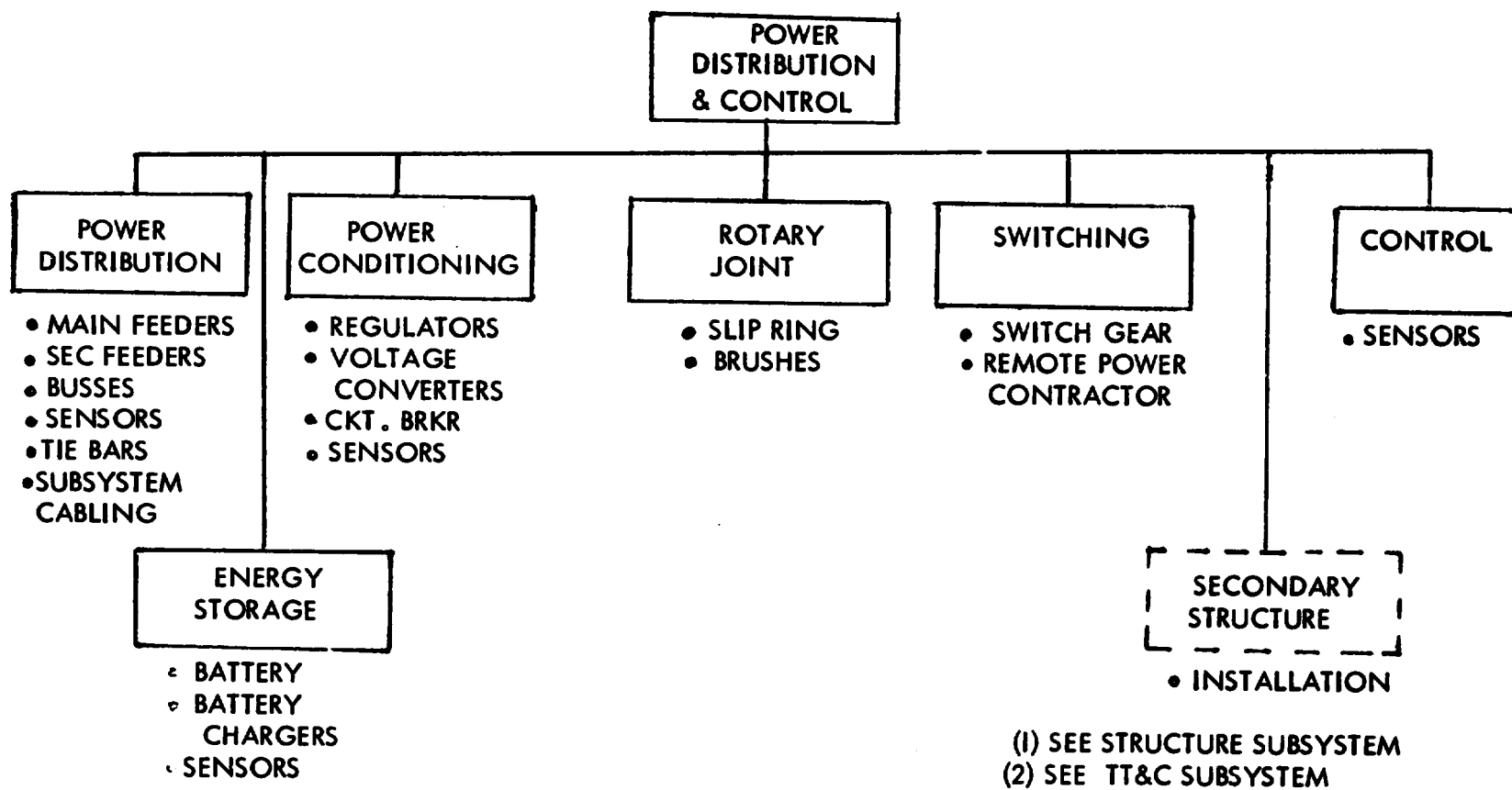


Figure 2.3.2-1 Electrical Power Distribution Subsystem Assembly

The major requirements are to deliver power at specific voltages and levels on a continuous basis throughout the solar seasons for a duration of 20 years. The solar array will deliver 520 kW of electrical power through a distribution system with a transmission efficiency of 94%. Electrical power at a level of 489 kW is transferred across the rotary joint, through slip rings to the flight test article. The distribution will transmit the electrical power to the flight test article with a transmission efficiency of 98%. Power at a level of 448 kW at 200 volts will be delivered to the dc/dc converter/Klystron interface (SPS Flight Test Article). Figure 2.3.2-2 illustrates the efficiency chain of the electrical power distribution system.

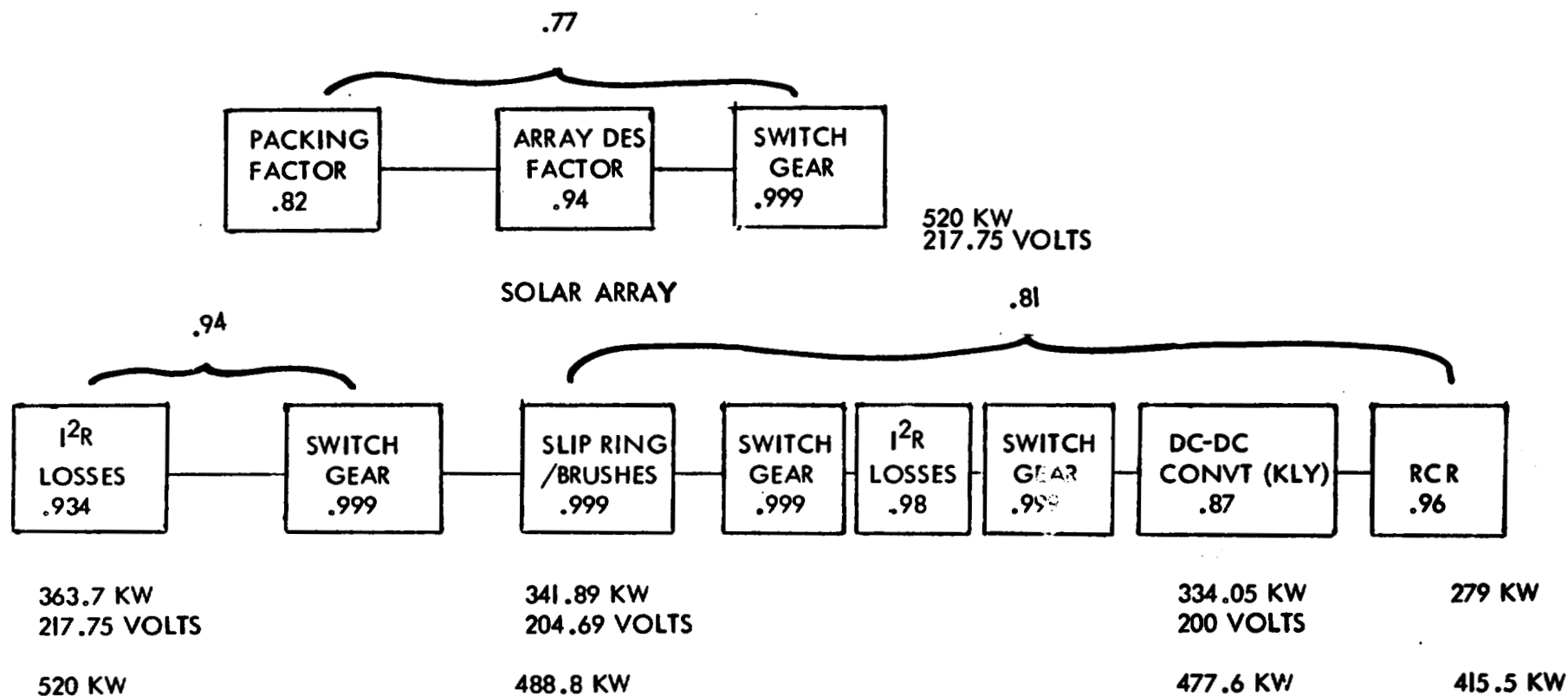
Power Generation

Figure 2.3.2-3 and Table 2.3.2-2 summarize the physical format for the solar array. The solar photovoltaic power system follows the direction within Section IX.B of the NASA "Red Book," Solar Power Satellite Concept. Power output per square meter of solar cell blanket is calculated to be 130 W/m². Thus, the total dc power generated for a 4000m² solar array would be 520 kW.

The 4000 square meters is implemented as a 20 meter x 200 meter solar array. The array is divided into five bays approximately 20 meters x 40 meters. Each bay has five solar blankets which are 4 meters x 40 meters. A solar blanket is comprised of 52 solar panels, of dimensions 0.756 meters x 4 meters. There are two electrical modules per panel. Based on the technology from the PEP solar array, there are 1530 solar cells per electrical module.

Utilizing the PEP design concept, the array harness will be a flat cable conductor mounted on the back of the solar array blanket at the two long edges of the blanket. The harness folds up in the same manner as the array panels for retraction and storage. The flat cable conductor insulation is 1 mil thick Kapton film. Two sheets of Kapton film, bonded together with a thin film of high temperature polyester adhesive, are used to encapsulate the 1mm copper conductors. Conductor pairs from six panels will be routed to form a cable which will terminate in a connector at the base of the blanket. Figure 2.3.2-4 shows a schematic of a typical solar array blanket. The connectors, capable of remote manipulator handling, will be engaged into an Electrical Power Distribution Switch Box located at the base of each blanket. The number of these connectors will be minimized to augment the remote fabrication operations in space. Feeder cables from the EPD switch boxes are routed to two electrical power distribution panels, located at the base of the array to form a split bus of equal power. Individual blankets feed power from their respective EPD switch boxes through feeders to the electrical power distribution panel. Switchgear isolate each blanket from the summing bus. As each switchgear is closed, its respective blankets output is connected to the summing bus.

Voltage and power output and excess power at the beginning of life will be controlled by the isolation switch gear through the data management system within the TT&C system. Voltages, currents and bus temperatures will be monitored by TT&C system to detect any shorts throughout the solar array. Controlled emergency disconnects can occur under the TT&C data management system or be effected by breaker control to avoid catastrophic effects. The design is such that no single point failure may cause a total loss of the SPS function.



SATELLITE POWER DISTRIBUTION (INCLUDING SPS TEST ARTICLE)

SPS TEST ARTICLE, 279 KW

Figure 2.3.2-2 SPS Flight Test Article Efficiency Chain

ORIGINAL PAGE IS
OF POOR QUALITY

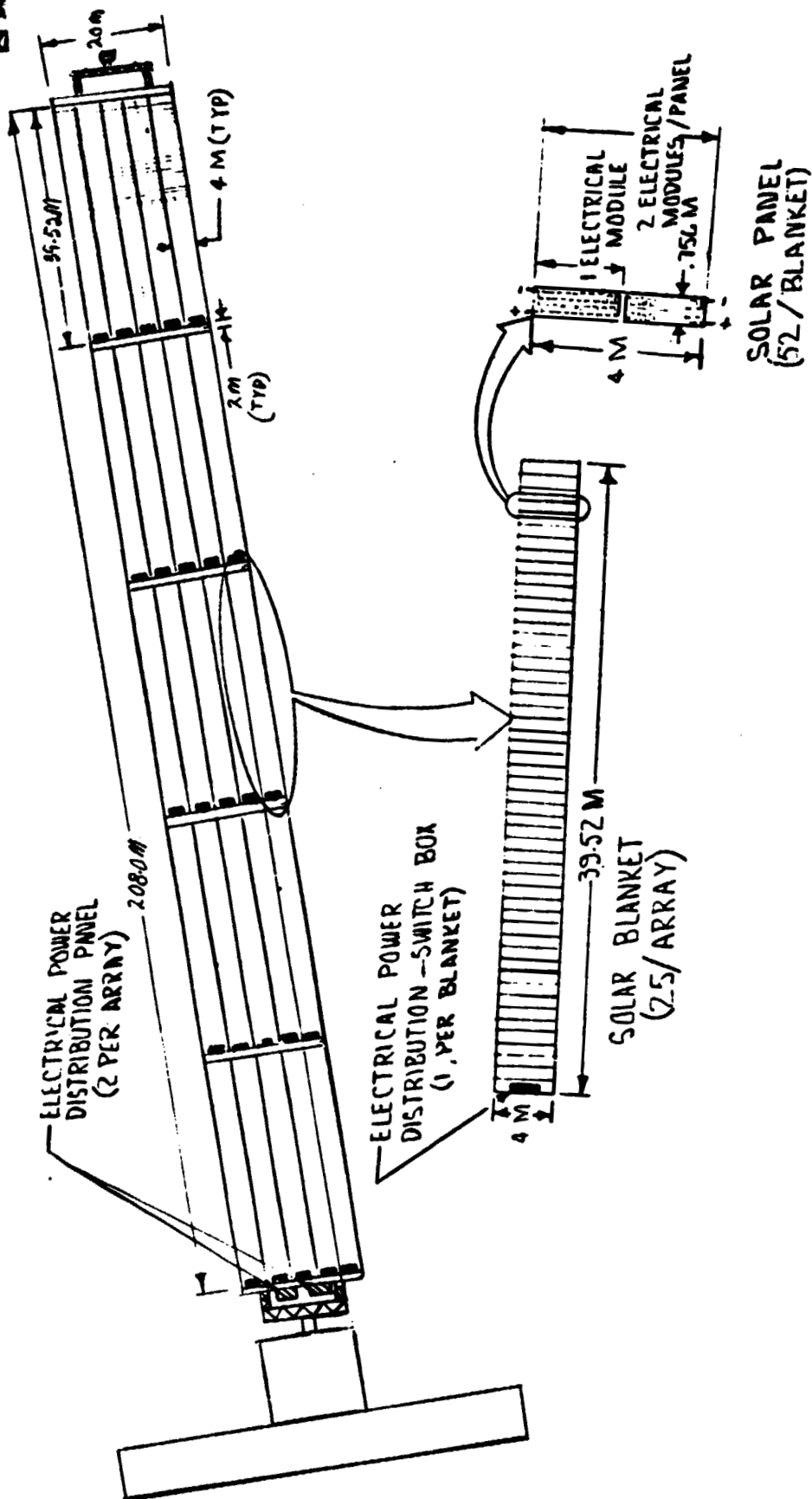


Figure 2.3.2-3 Solar Array (20M X 200M)

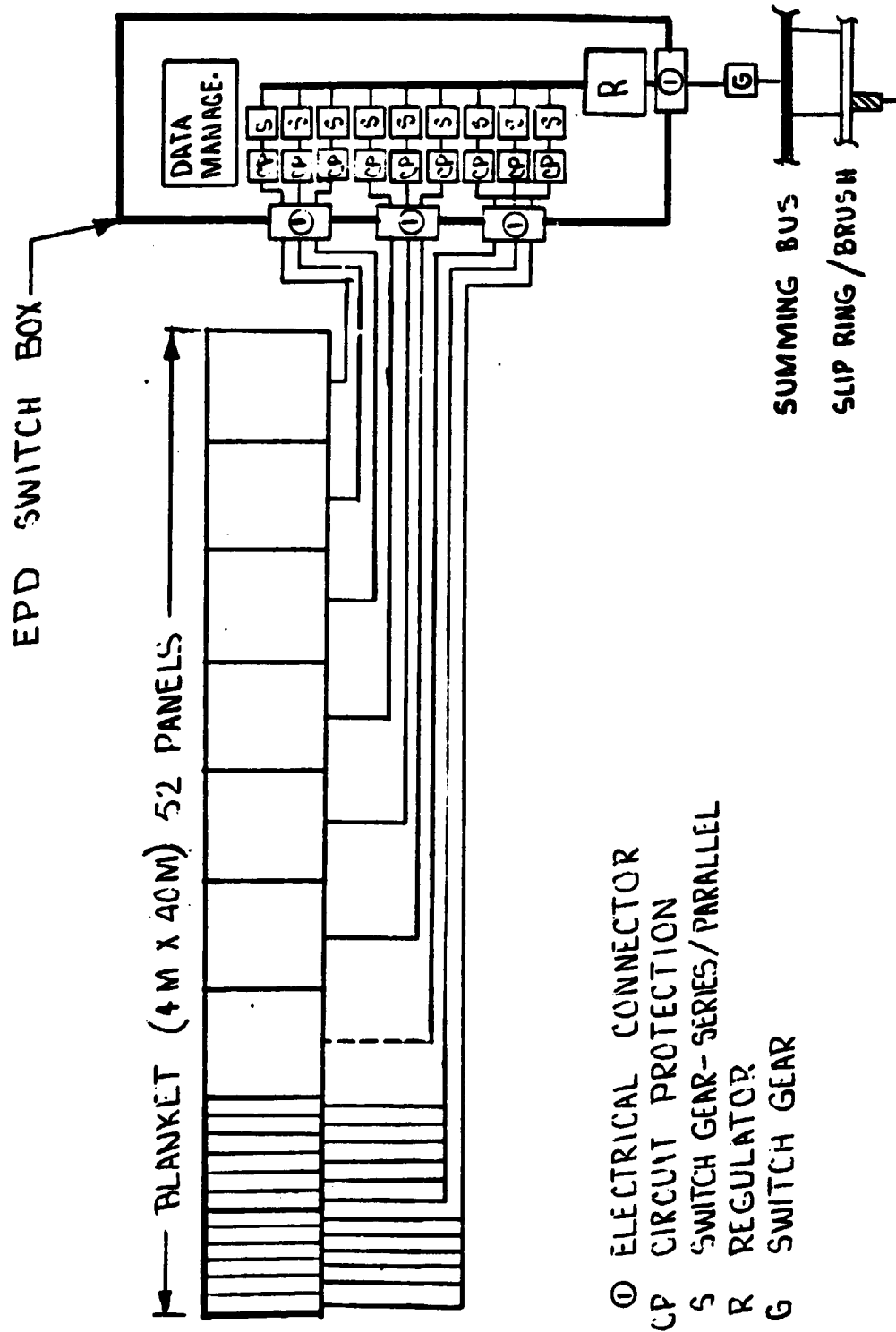


Figure 2.3.2-4 SPS Flight Test Article Typical Blanket Element (1 of 25)

Table 2.3.2-2
Power Generation Subsystem

Item	Characteristics
Solar Array	4000 Square Meters (20m x 200m) 25 Solar Blankets (4m x 40m) Solar Cell Output EOL 130 W/m ² Power Output 520 kW
Solar Cell Blanket	160 Square Meters (4m x 40m) 52 Solar Panels (4m x .7564m) 104 Electrical Modules
Solar Panel	3.0256 Square Meters (.7564m x 4m) 2 Electrical Modules/Panel
Electrical Module	1.512 Square Meters (.7564m x 2m)

Energy Storage

An energy storage system will be utilized during the eclipse periods to provide approximately 37 kW-hours of electrical power. Batteries and a regenerative fuel cell system have been reviewed as candidate energy storage subsystems. The regenerative fuel cell system was not selected at this time due to the long, costly development program required for the electrolysis unit. Nickel-hydrogen and nickel-cadmium batteries were evaluated as candidates for the energy storage system. Table 2.3.2-3 provides comparative data which led to the selection of the nickel-hydrogen battery to be used for the energy storage system. Operationally, Ni-H₂ and Ni-Cd batteries are similar. However, Ni-H₂ cell voltage is 3mV higher than the Ni-Cd. Also, inherent overcharge and over discharge capabilities of the Ni-H₂ battery simplifies cell protection requirements. The Ni-Cd battery requires reconditioning periodically, prior to each eclipse period, due to its memory effect. This is not

Table 2.3.2-3. Comparison of Nickel-Hydrogen to Nickel-Cadmium Batteries

AMP-HOUR EFFICIENCY	SIMILAR, 75 TO 80%
CELL VOLTAGE	NI-H ₂ 3.5% HIGHER
SELF DISCHARGE	NI-H ₂ SLIGHTLY HIGHER
OVERCHARGE CAPABILITY	NI-H ₂ 0.5C, NI-CD 0.1C
OVER DISCHARGE (CELL REVERSAL)	NI-H ₂ SUPERIOR, STABLE @ 0.5C
CHARGE CONTROL METHODS	SIMILAR
RECONDITIONING	NOT REQUIRED FOR NI-H ₂
OPERATING TEMPERATURE	NI-H ₂ 0-20 ° C, 10 ° C DESIRABLE NI-CD 5-20 ° C DESIRABLE 30 ° C SHORTENED LIFE
WEIGHT	NI-H ₂ 50% GREATER POWER/POUND
VOLUME	NI-H ₂ 2 TIMES GREATER
DEPTH OF DISCHARGE	NI-H ₂ @ 80% 2 TIMES LIFE OF NI-CD
POTENTIAL LIFE, PERFORMANCE & COST	NI-H ₂ HAS ADVANTAGE

a problem with the Ni-H₂ battery. The Ni-H₂ battery may be operated at a higher temperature without impacting its potential life. The Ni-H₂ battery system weight has a significant advantage over the Ni-Cd, whereas the Ni-Cd battery system has the volume advantage. Nickel-hydrogen batteries may be discharged to a greater depth than the Ni-Cd. The charge/discharge cycle has no apparent flaking effect of the plates in the Ni-H₂ as it has in the Ni-Cd. Costs of the two batteries are comparable. Considering the weight of the Ni-Cd battery, its transportation cost per kilowatt-hour to orbit is greater than that of the Ni-H₂ battery.

Nickel-Hydrogen Battery. The parameters for the nickel-hydrogen battery are listed on Table 2.3.2-4. The current nickel-hydrogen cell, as developed, has a capacity of 50 ampere-hours. The cell is approximately 9 cm (3.5 inches) in diameter and 23 cm (9 inches) long. Figure 2.3.2-5 is a picture of seven nickel-hydrogen cells in a series connection. The energy storage system will utilize 122 of these cells in series to form a battery and two batteries will be required. A new cell plate in the stack would be increased. Current technology would be applied along with some test verification.

Table 2.3.2-4
Energy Storage System (Nickel-Hydrogen Battery)

Item	Characteristic
Power Requirement	
@ LEO	15,280 Watt-Hours
@ GEO	31,900 Watt-Hours
Capacity	27,093 Watt-Hours
Charging	1.6 Volts
Discharging	1.25 Volts
Charging Rate	C/10
Weight Factor	8.18 Watt-Hours/kg
Depth of Discharge	80%
Cell Size	125 Ampere-Hour
Number Cells/Battery	122
Battery Weight	942.8 kg

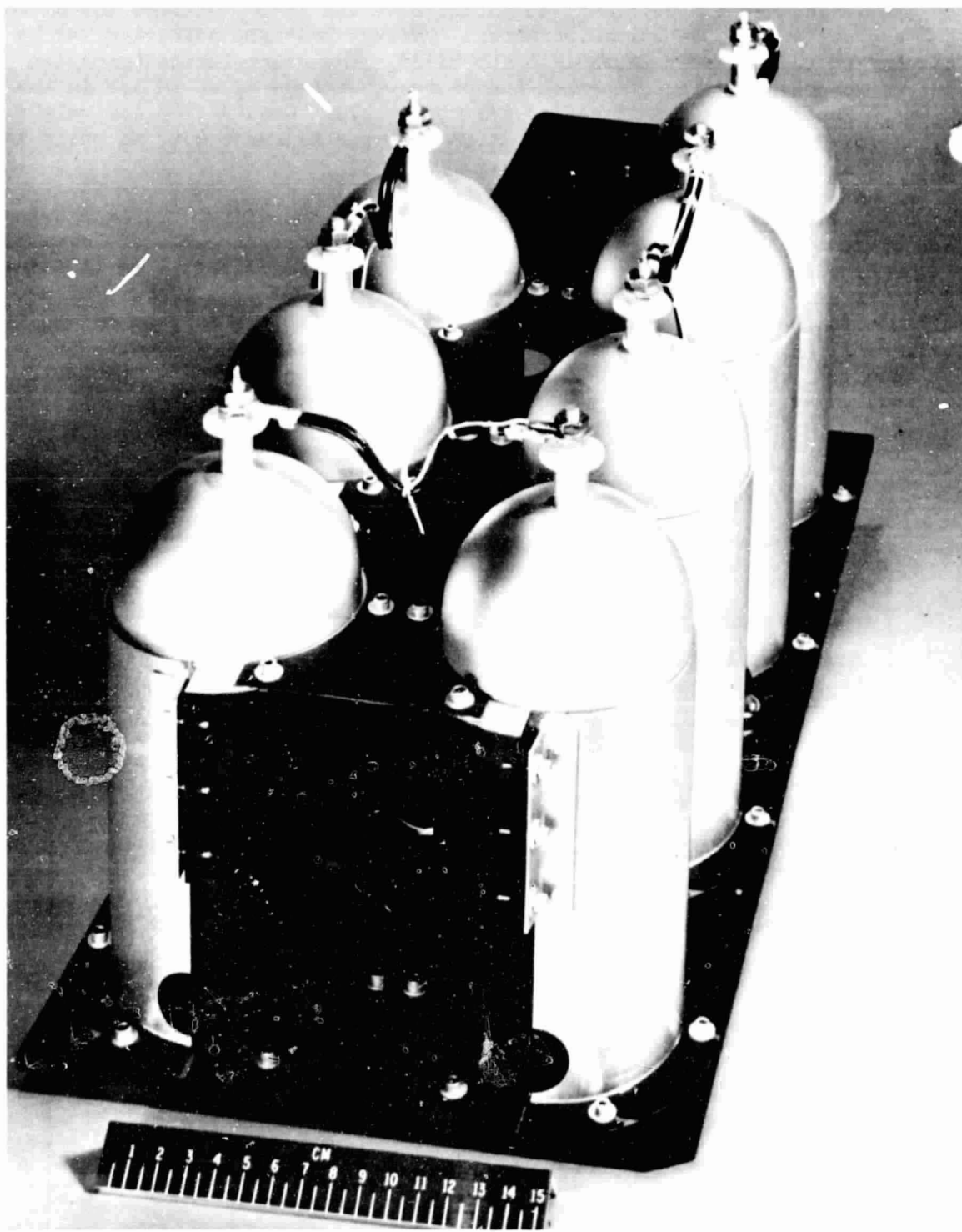


Figure 2.3.2-5. Nickel-Hydrogen Battery Cells

The battery switch gear and bus tie contactors are located within the Electrical Power Distribution Panels shown in Figure 2.3.2-3. Sensing circuits of the data management system will monitor orbit times and will control when the battery will be connected and disconnected to the busses. As the battery power is connected, sensing circuits will disconnect loads not requiring electrical power during the eclipse periods. Battery power will be switched off in the same manner when sun energy illuminates the photovoltaic subsystem. The energy storage subsystem will have its energy resupplied by the solar array through the charging system.

Electrical Power Distribution

Figure 2.3.2-6 shows a simplified block diagram for the electrical power distribution system for the SPS Flight Test Article - Solar Powered Microwave Antenna. Main power feeders are routed from each solar blanket and are summed and divided into two busses. The split bus offers protection from losing all electrical power and provides some redundancy in event of a catastrophic event to the solar array. Bus ties from each summing bus of the Electrical Power Distribution Panel will interconnect to the power slip rings. The slip rings will transmit the electrical power across the rotary joint and maintain the split bus concept. Risers from each brush of the power slip rings will be tied to a summing bus. Feeders routed through switch gear will connect to dc/dc converters which are located on the microwave test antenna structure. These switch gear isolate each converter for maintenance and are controlled by the data management system for controlled emergency disconnects that may be required in the event short circuits occur within the feeder loop. These switch gear, monitored through the data management system may be used to control the microwave test.

The electrical propulsion system will be powered through the electrical power distribution panel. Switch gear will be located within the panel for isolation of the propulsion system from the summing busses. Power feeders will be routed through the rotary joint, with a loop, to a switch box located on each propulsion mast at the base of the ion thrusters stack. Switchgear and circuit protection devices are provided for isolation and maintenance purposes. The data management system will monitor each ion thruster through data-command signals. The Attitude-Velocity Control and TT&C systems will have complete control of powering each individual ion thruster and RCS unit as required. The battery system has been sized to maintain electrical power on the ion thrusters for a stand-by status and to apply discharge power 12 minutes prior to the climax of the eclipse period. This action will be controlled by the data management system. A simplified block diagram and schematic is shown in Figure 2.3.2-7. Table 2.3.2-5 shows the distribution of electrical power to the various subsystems.

Electrical power, up to a level of 5 kW, will be supplied to the TT&C system for the housekeeping tasks this system performs. The battery system has been sized to maintain power for all required functions during the eclipse periods. Power will be supplied from the housekeeping bus to each of its loads, such as telemetry, rendezvous beacon, attitude and velocity control system, RCS, TT&C system, etc.. Each of these will be monitored by sensors and controlled thru the data management system of the TT&C unit.

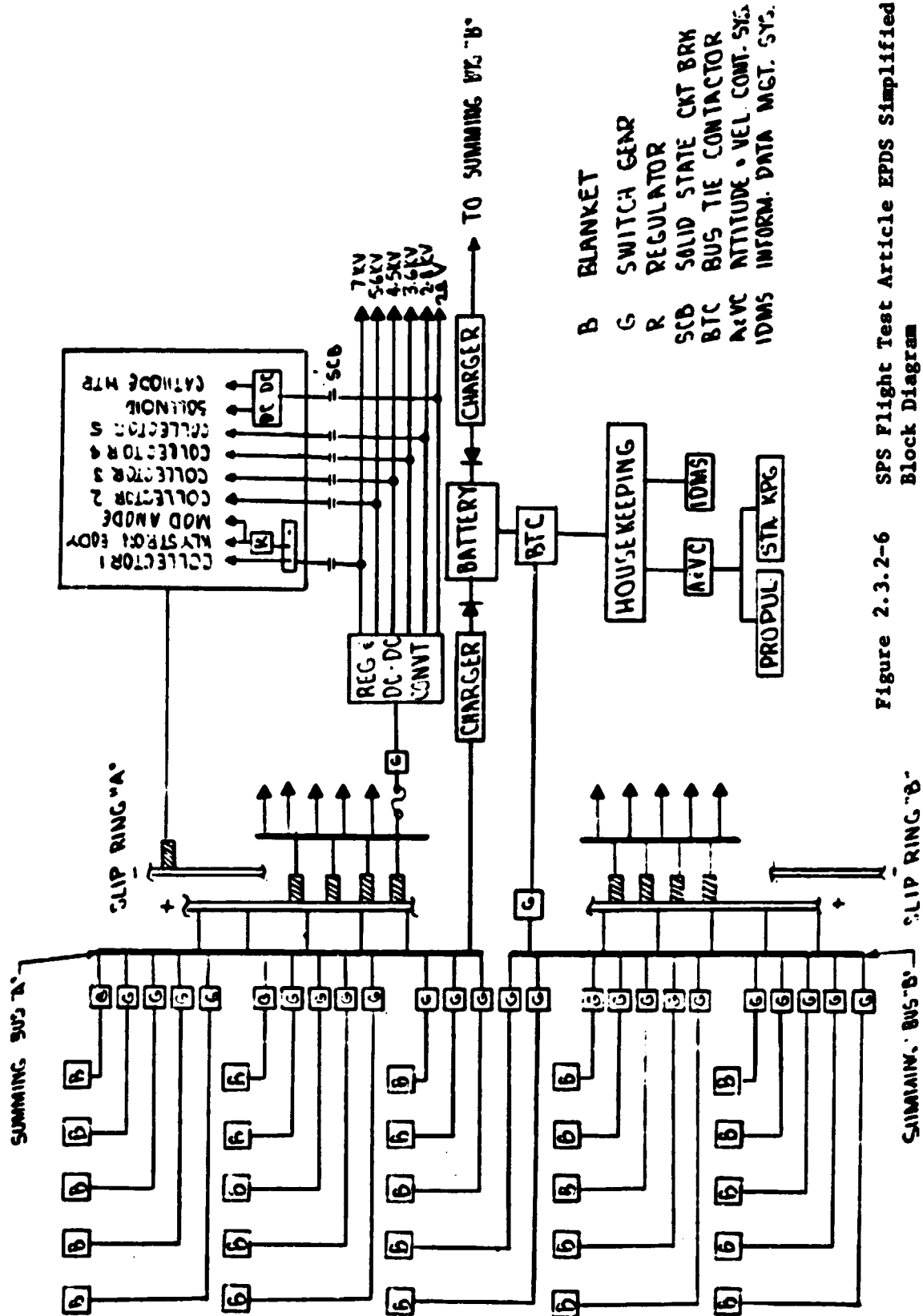


Figure 2.3.2-6 SPS Flight Test Article EPDS Simplified Block Diagram

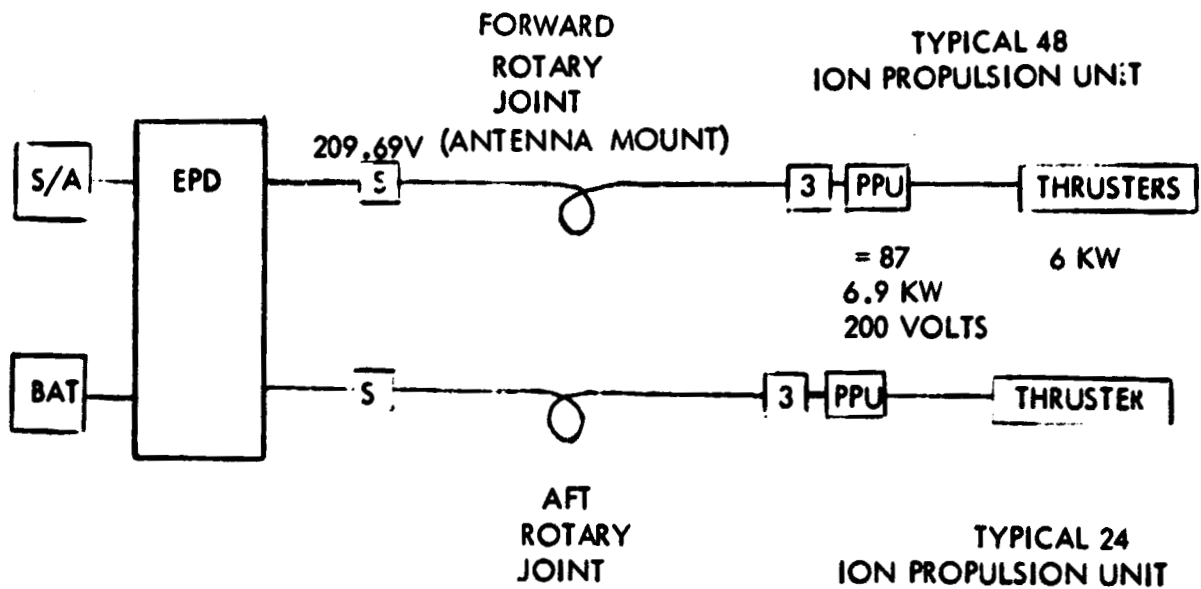
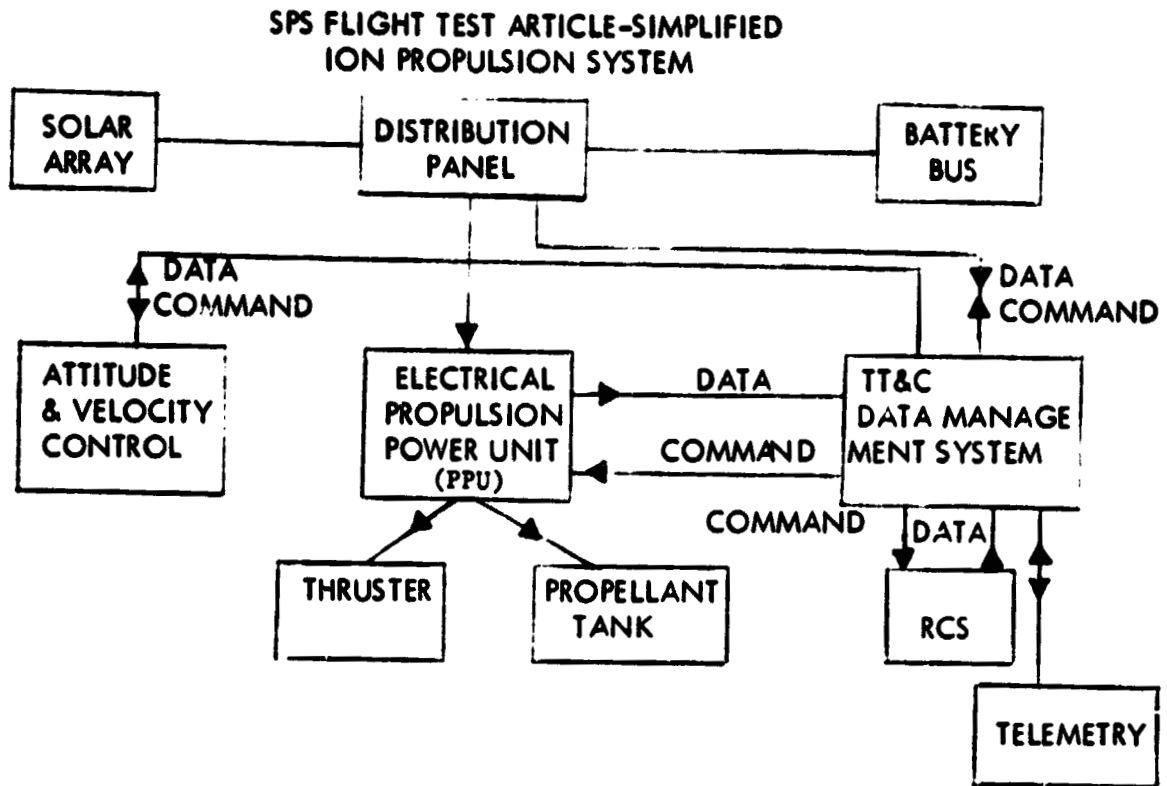


Figure 2.3.2-7

SPS Flight Test Article-Simplified Ion
Propulsion System



Table 2.3.2-5
Distribution of Electrical Power

Item	Power/Energy Generated or Required
Solar Array	520 kW
Battery	37.1 kW-H
Test Article	342 Kw
Telemetry Tracking & Control	5 kW
Attitude & Velocity Control	5 kW
Propulsion	
Orbit Transfer	520 kW
RCS	500 W

A weight summary of the Electrical Power Distribution System for the SPS Flight Test Article is shown in Table 2.3.2-6.

Table 2.3.2-6
*SPS Flight Test Article EPDS Weight Summary

Solar Array	4,091.1
EPD Wire Harness	1,503.1
Blanket Switch Box (25)	892.5
Electrical Power Distribution Panel (2)	962.4
Battery Systems	
Batteries	942.8
Chargers	103.2
Wire Harness & Control	88.23
Ion Propulsion EPD System	
Wire Harness	1,798.29
Propulsion Switch Boxes	584.4
Antenna System	1,472.52
Secondary Structure	1,243.85
	<hr/> 13,682.39 kg

*Does not include cooling, TT&C or attitude and velocity control system weights.

2.3.3 Microwave Subsystem Definition

Summary

The microwave subsystem which consists of an antenna complex and supporting electrical/electronic system components is contained in a modular unit, attached to one end of the spacecraft. Functionally, it is divided into two major sections. One includes a slotted waveguide array which radiates a high power beam (250 kW). The second, operating at a lower power level, consists of a long, narrow waveguide array which radiates a fan beam toward a rectenna. Figure 2.3.3-1 provides key dimensions and configuration information.

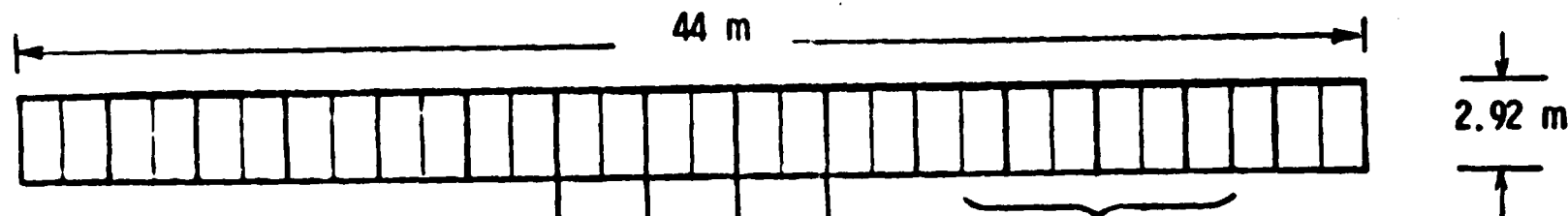
Subsystem Description

The design of the microwave subsystem reflects the two primary operational requirements for accomplishing the test functions. These requirements are listed as follows:

- The microwave subsystem shall be capable of simulating two types of Satellite Power System (SPS) transmission conditions. One is a beam quality test and the other is a maximum power test which demonstrates thermal effects expected to exist at the center of the actual SPS transmitting antenna.
- The antennas shall be pointed at a rectenna orbiting the earth in approximately the same plane and altitude as the spacecraft, and situated at a distance of approximately 16.5 km (at the edge of the far field of the transmitter).

The SPS test article antenna, shown in Figure 2.3.3-1, consists of two contiguous but independent parts. The thermal test portion is comprised of 9 sub-arrays, each 2.92 meters square and made up of 33 waveguides each having 33 radiating slots. The central sub-array radiates 121 kW, produced by 2450 MHz Klystron tubes mounted on its rear surface. Each Klystron has a nominal rating of 1 kW RF output and 121 such tubes are arrayed in an 11 x 11 matrix. It is emphasized that this slotted waveguide sub-array could equally well be excited by four 50 kW tubes in a 2 x 2 matrix without requiring any major changes. The central sub-array is surrounded by eight identical 2.92 meter square sub-arrays, but these are each excited by 16 1-kW Klystrons in a 4 x 4 matrix. Total RF power input to the 9 element array is therefore $16 \times 8 + 121 = 249$ kW.

The phase control test portion is a linear array 2.92 meters wide and about 44 meters long consisting of 30 sub-arrays each 2.92m x 1.46m. Two of these sub-arrays adjacent to each other make up a unit that is identical to one of the 33 x 33 slot subarrays used in the thermal test array. However, each of these 2.92m x 1.46m subarrays is fed by only a single 1 kW Klystron tube so that total RF power into the array is 30 kW. Each Klystron, and therefore each of the 30 elements in the linear array, is subject to phase control for the purpose of beam formation and pointing control. Each sub-array receives a pilot tone emanating from the rectenna. The phases of all



THERMAL TEST ARRAY

- 9 SUB-ARRAYS, EACH 2.92 x 2.92 m. WITH 33 x 33 SLOTS.
- 8 OUTER SUB-ARRAYS HAVE 16 KLYSTRONS EACH 1 kW OUTPUT
- CENTRAL SUB-ARRAY HAS 121 ONE kW TUBES
- TOTAL RF POWER
 $16 \times 8 + 121 = 249 \text{ kW}$
- ALUMINUM WAVEGUIDE .05 cm (.020 in) WALL: TOTAL MASS 970 kg.

PHASE CONTROL TEST ARRAY

- 30 ELEMENTS EA. 2.92 x 1.46 m.
- EACH ELEMENT - ONE HALF OF BASIC 33 x 33 SLOT SUB-ARRAY HAVING EITHER 33 x 16 OR 33 x 17 SLOTS (ALTERNATING).
- SINGLE 1 kW KLYSTRON PER ELEMENT. TOTAL RADIATED RF POWER 30 kW.

Figure 2.3.3-1 SPS Test Article Antenna

the received pilot tone signals are sensed and the necessary control signals are applied to each Klystron tube input in such a way that every subarray radiates its 1 kW signal in phase conjugation with respect to the pilot tone signal received by it. This active, retrodirective, control system ensures that the beam from the 30 element array is correctly formed and steered toward the rectenna. Steering, however, occurs only in one dimension. The detailed design for such a retrodirective control system is not part of this study, nor is the design of the rectenna which receives and samples the transmitted beam. The rectenna is a co-orbiting, but independent, free flying vehicle. It is expected that the pilot tone will be received by each of the slotted waveguide subarrays themselves. Thus the weak pilot tone signals must be separated from the strong transmitted signals by means of duplexers, which poses a difficult design problem. As an alternative, separate receiving antennas for the pilot tone might be used at each subarray. These should be cross-polarized relative to the high power transmitted signal so that they pick up only a very small leakage signal. If such separate pilot tone receiving antennas are used it is important that they do not cause any significant increase in spacing between adjacent subarrays in order to prevent the formation of grating lobes.

Concept Definition and Rationale

Each sub-array is an assemblage of slotted waveguide radiators each of which is of the standing wave, resonant slot type. The array is excited by one or more slot coupled transverse feeder guides placed on the back (i.e., non-radiating) side of the subarray. The arrangement is shown in Figure 2.3.3-2 wherein only a single transverse feeder guide is shown for simplicity. The design basis for this array can be explained with the aid of Figure 2.3.3-3. The radiating and feeder guides have the same dimensions, the height "b" being one half of the width "a", as is customary for rectangular guide. The crosses indicate the locations of the slot centers for both the radiating and the coupling slots.

A standing wave slot radiator requires that the spacing between adjacent slots be equal to $\lambda_g/2$ where λ_g is the guide wavelength. The slotted guide then radiates a broadside beam normal to the plane containing the slots. Several such guides are arranged parallel to one another to form a square subarray that radiates a symmetrical beam normal to its face. The spacing between adjacent guides is denoted by δ and is assumed to include the thickness of the waveguide walls. Thus, the spacing between neighboring coupling slots in the feeder guide is $a + \delta$.

In all cases alternate slots must have π radians phase shift which is obtained by the use of staggered longitudinal shunt slots in the radiating guides, and oppositely inclined series slots in the feeder guide. All slots are cut to resonant length ($\sim \lambda/2$) so that slot admittance is simply $g + j0$. Each slot is either displaced from, or inclined to, the guide centerline just enough to make its conductance g equal to $1/N$ where N is the total number of slots in the guide. When the guide is short-circuited at one end, at a distance $\lambda_g/4$ from the center of the last slot, all slots appear in parallel. Hence, the admittance looking in at the other end is $gN = 1$ and the guide is matched.

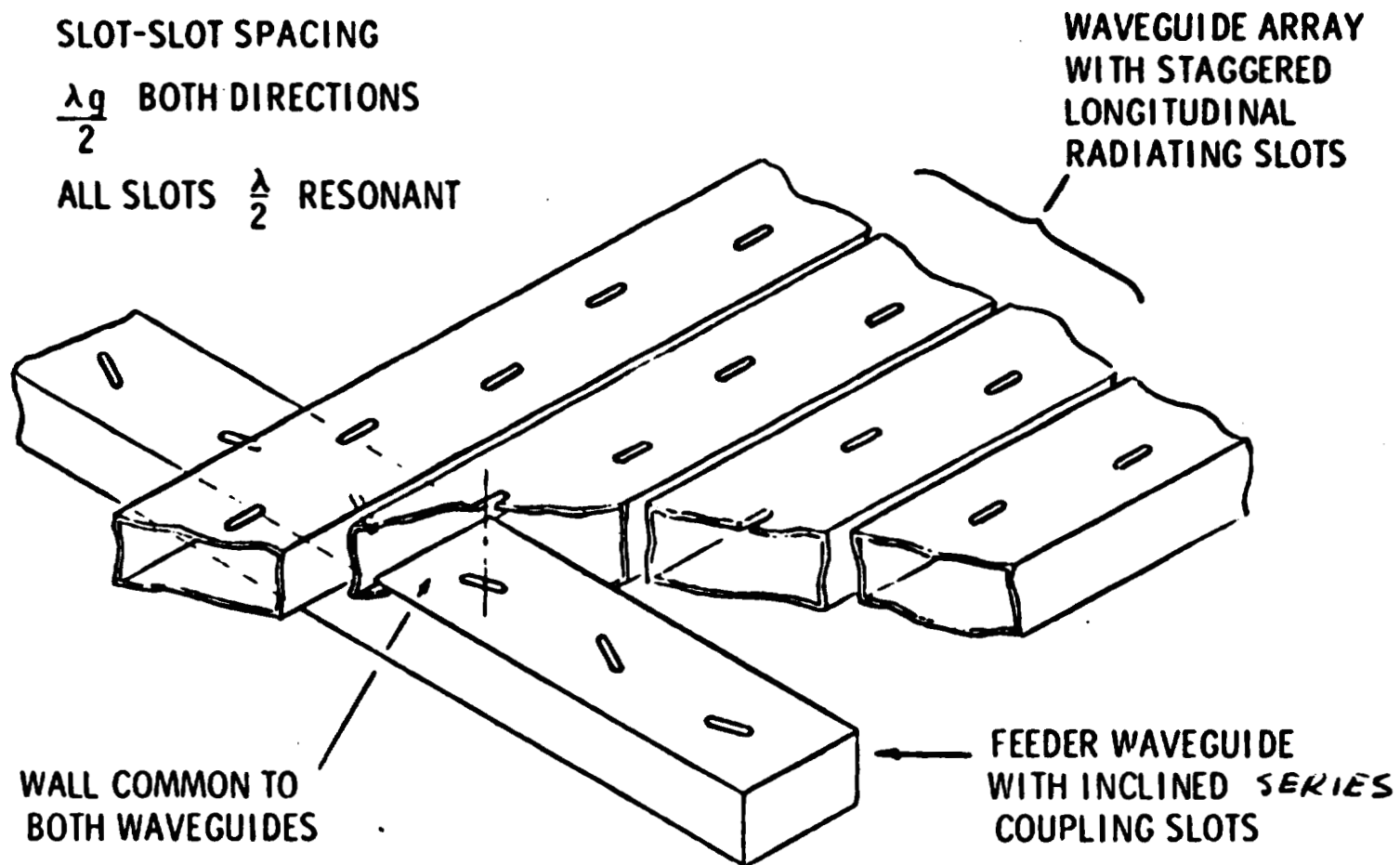


Figure 2.3.3-2 Transverse Feeder Guide for Slot Array

ORIGINAL PAGE IS
OF POOR QUALITY

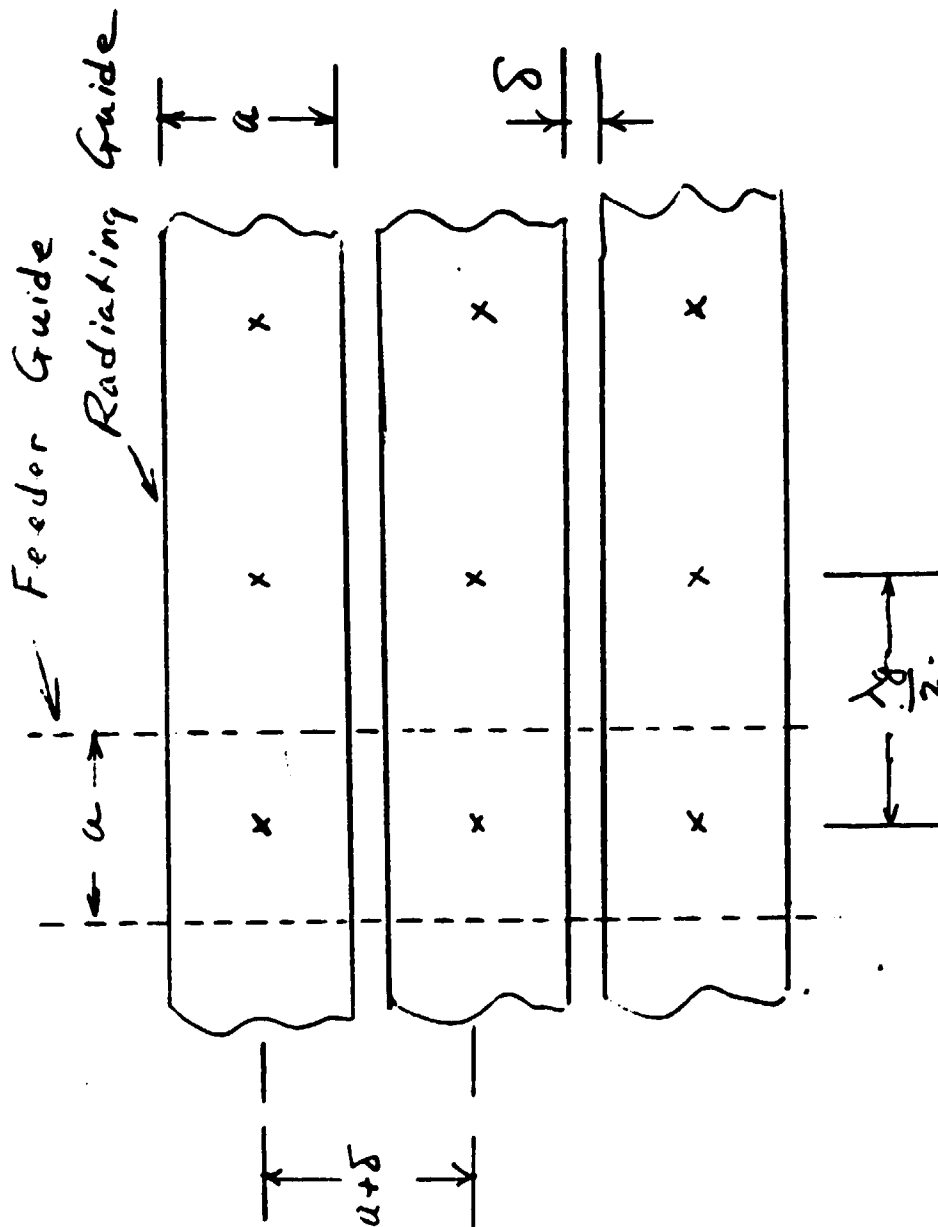


Figure 2.3.3-3 Resonant Array Design Basis

The guide can be shorted at both ends, in which case it may be excited by a probe or a slot in the wall opposite to the radiating face. This probe or slot must be located at one of the loops in the "standing wave" pattern in the guide, i.e., at a distance equal to an odd number of quarter guide wavelengths from either end. One, or any number of such excitation points, may be used providing they are located in the above manner.

In order to ensure suppression of grating lobes the spacing between adjacent slots must be less than one free space wavelength. Thus

$$\frac{\lambda_g}{2} < \lambda \text{ in the radiating guide and}$$

$$a + \delta < \lambda \text{ in the feeder guide.}$$

Noting that $a = \frac{\lambda_c}{2}$, where λ_c is the guide cutoff wavelength, it is clear that values of λ/λ_g and λ/λ_c in the neighborhood of $1/\sqrt{2}$ are satisfactory as long as δ is small. The feeder guide is also a standing wave resonant slot structure that radiatively couples into the radiating guides. Therefore, the spacing between its coupling slots must be equal to one-half the wavelength in the feeder guide. Choosing identical dimensions for all guides then requires that

$$a + \delta = \frac{\lambda_g}{2}$$

and leads to a symmetrical array with identical spacing in both planes. The above condition, along with the usual waveguide relation

$$\frac{1}{\lambda_g^2} + \frac{1}{\lambda_c^2} = \frac{1}{\lambda^2},$$

has a unique solution which can be expressed as

$$\frac{\lambda}{\lambda_g} = \cos\left(\frac{\pi}{4} + \Delta\right), \quad \frac{\lambda}{\lambda_c} = \sin\left(\frac{\pi}{4} + \Delta\right)$$

where, for small δ , $\Delta \approx \sin \Delta \approx \frac{\delta}{\lambda \sqrt{2}}$.

Choosing $\delta = 0.4$ cm with $\lambda = 12.24$ cm (2450 MHz) then gives

$$\frac{\lambda}{\lambda_g} = .6906, \quad \frac{\lambda}{\lambda_c} = .7232$$

so that $\frac{\lambda_g}{2} = 8.86$ cm and $a = 8.46$ cm.

Every subarray in the thermal test portion has 33 parallel waveguides each containing 33 radiating slots. The overall dimensions of this 33 x 33 slot array are 2.920 x 2.924 meters. The central subarray has 11 transverse feeder guides on its back face, each carrying 11 Klystron tubes (1 kW ea), that are probe coupled into the guide at loops in the standing wave pattern. The surrounding eight subarrays have only four feeder guides each being probe

fed by four Klystron tubes. This arrangement is changed slightly for the half-size subarrays in the phase control test portion. Here, the standard 2.92m square subarray described above carries two feeder guides. One of these guides couples to 16 adjacent radiating guides; the other one couples to the remaining 17 radiating guides. In this way the standard subarray is effectively split into two independent units. The units are not quite identical, however, since one has 16 x 33 slots while the other has 17 x 33 slots.

The radiation pattern function of a standard subarray is the product of a 33 element array factor and the slot pattern function. Although the slot pattern is different in the E and H planes it is very much broader than the array factor. Thus, the latter dominates and the resultant pattern is symmetrical and essentially that of a uniformly illuminated square aperture that is 2.92 meters per side. Hence, the half-power beamwidth will be 2.1° , the first nulls will occur at 2.4° from the array normal and the level of the first side lobes will be -13.2 dB. The phase control test array, which is 43.8 meters by 2.92 meters, will radiate a fan beam. In the plane normal to the linear array the beam characteristics are just those of the standard subarray given above. In the plane containing the linear array the pattern is much narrower, the half power width being 0.14 degrees with first nulls occurring at 0.16 degrees from the array normal. First side lobe levels are still -13.2 dB.

In order to perform successful testing in space of the phase control test array, certain tolerances must be placed on the dimensions and orientation of the array and its component subarrays. The most important tolerance requirements are those summarized in Figure 2.3.3-4. Proper operation of the retro-directive, active control system will compensate for small displacements between adjacent subarrays, providing they remain parallel to each other. Nevertheless, it appears prudent not to allow such displacements to exceed $\lambda/4$ or ± 3 cm. Any non-parallelism, i.e., tilt, between adjacent subarrays must be held to ± 13 minutes of arc. This is based on an allowable loss in boresight gain not exceeding 3% and is calculated from the loss relation

$$\left(\frac{\sin \Delta X}{\Delta X} \right)^2$$

$$\text{where } \Delta X = \frac{\pi D}{\lambda} \Delta \epsilon$$

$\Delta \epsilon$ is the differential tilt angle and $D = 2.92$ is the length of a standard subarray.

The radiating surface of each subarray must be flat with an rms deviation, σ , not exceeding 3.4mm. Again, this is based on an allowable loss of 3%, using the Ruze formula

$$e^{-\left(\frac{2\pi\sigma}{\lambda} \right)^2}$$

TILT ANGLE BETWEEN SUB ARRAYS	$\pm 13^\circ$
RMS SURFACE ROUGHNESS	3.4 mm
PARALLEL DISPLACEMENT BETWEEN SUB ARRAYS	± 3 cm
ARRAY ATTITUDE STABILITY	
X AXIS	$\pm 13^\circ$
Y AXIS	$\pm 3^\circ$
Z AXIS	$\pm 5^\circ$
(FOR $< 3\%$ GAIN LOSS)	
MAXIMUM ALLOWABLE GAP BETWEEN SUB-ARRAYS	~ 2 cm

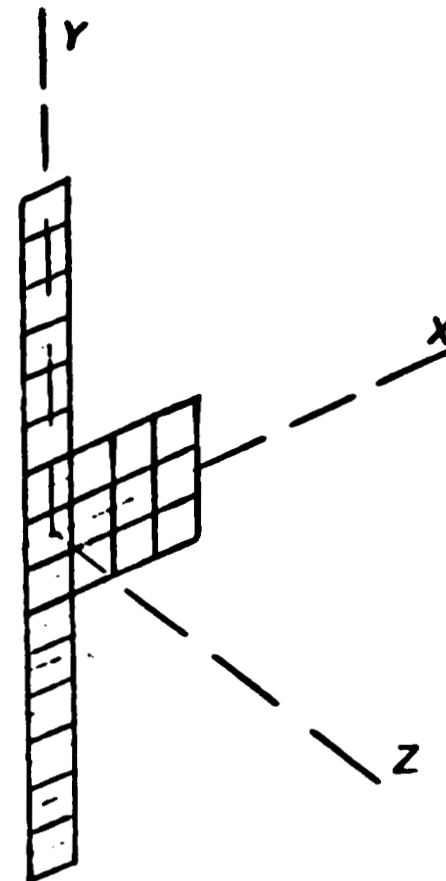


Figure 2.3.3-4 SPS Antenna Tolerances

Attitude stability requirements must be placed on the array orientation and are most stringent for rotation about the X-axis. This must be limited to ± 13 arc minutes in order to hold the loss to 3% or less. Much looser tolerances can be placed on rotation about either the Y or Z axis, viz $\pm 3^\circ$ and $\pm 5^\circ$ respectively, for the same 3% loss.

Adjacent subarrays must be closely spaced in order to avoid grating lobe formation. The maximum tolerance gap between subarrays is about 2 cm.

Substitution of Low-Power Klystrons

Because the high-efficiency (83%), high-power (50 kW), depressed-collector Klystron apparently will not be available for the 1985 Solar Power Experiment Mission, some changes have been made in the plan as originally set forth in the Red Book. The purpose of this section is to document these changes.

Klystrons (1 Kilowatt)

It has been suggested that the low-power 1 kW tubes developed for ground tests also be used in space until the high-power (50 kW) tubes are available (see Figures 2.3.3-5 and 2.3.3-6). This is to be our new baseline.

Another alternative is to use the 50 kW Klystron without a depressed collector for this experiment. Its efficiency will approximate that of the low-power tube (75%). At this time we will continue with the 1 kW Klystron.

The attached drawing (Figure 2.3.3-7) shows the placement of 279 tubes for the condition of thermal and phase-control tests. The thermal test will have the same heat generated per unit area as given in the Red Book (and full-scale SPS).

Taking the RF power density as 20.9 kW/m^2 (maximum), the RF power is:

$$20.9 \text{ kW/m}^2 \times 9\text{m}^2 = 188 \text{ kW}$$

Since

$$\text{Total tube power } P_T = \text{RF power } P_{RF} + \text{Power in Heat } P_H$$

$$P_T = \eta P_T + (1-\eta) P_T$$

where

$$\eta = \text{efficiency}$$

Then

$$P_T = P_{RF}/\eta = 188 \text{ kW}/.83 = 226.5 \text{ kW}$$

The heat generated is

$$\begin{aligned} P_H &= (1-\eta) P_T = .17 (226.5 \text{ kW}) \\ &= 38.5 \text{ kW} \end{aligned}$$

121 TUBES @ 0.96 KW = 116.5 KW

DC POWER = $\frac{116}{.75}$ = 155 KW

HEAT DISSIPATED = 38.5 KW

TUBE WEIGHT - 29 Kg

EFFICIENCY - 75%

ANODE VOLTS = 7 KV

(121 TUBES ON 9m²

SUB-ARRAY WITH

HEAT PIPES FOR

COLLECTOR COOLING;

BODY TEMPERATURE

195 - 250° C)

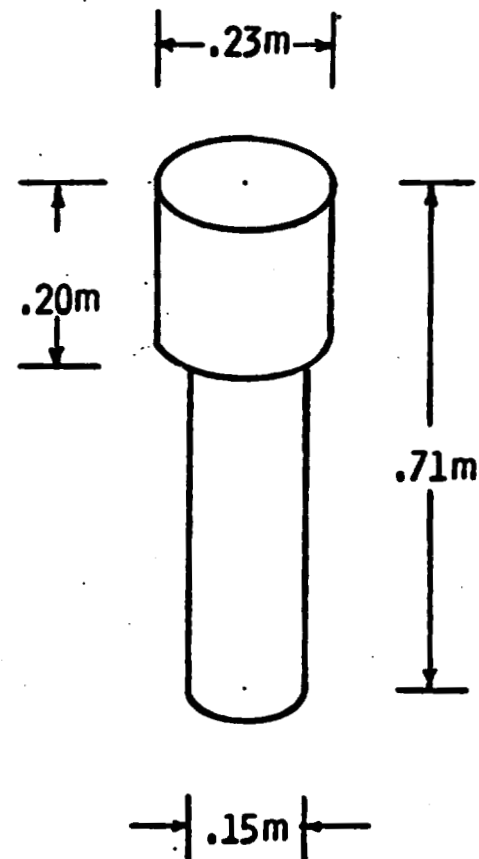


Figure 2.3.3-5 1 kW Klystron

4 KLYSTRONS @ 47 KW EA. = 188 KW

POWER DENSITY = $\frac{188 \text{ W}}{9 \text{ m}^2} = 20.9 \text{ KW/m}^2$

DC POWER = $\frac{188}{0.83} = 226.5 \text{ KW}$

HEAT DISSIPATION = 38.5 KW

TUBE WEIGHT = 69 Kg

EFFICIENCY = 83%

ANODE VOLTS = 33 KV

THERMAL T. C. = 35 MIN.

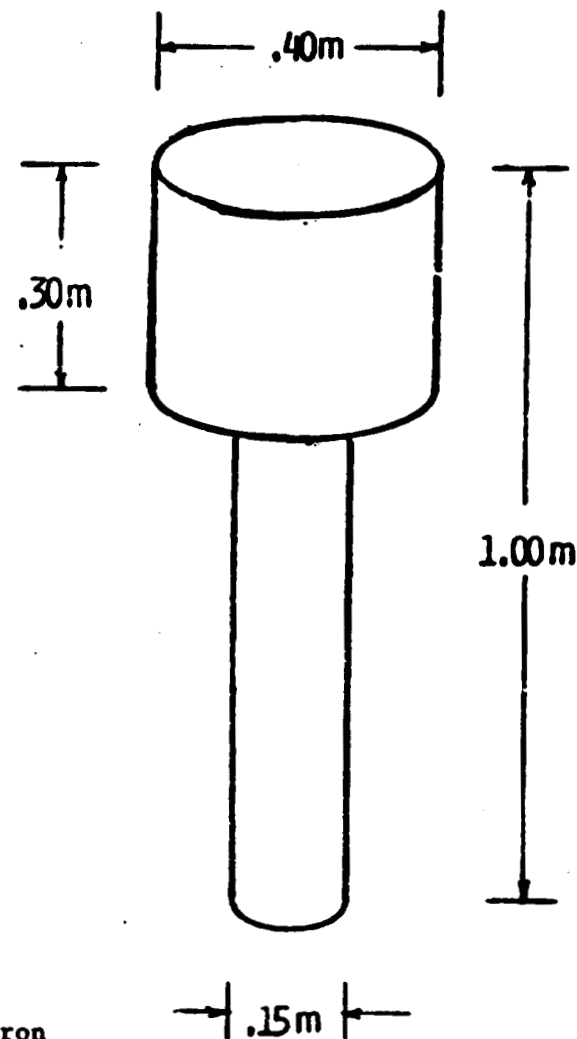


Figure 2.3.3-6 50 kW Klystron

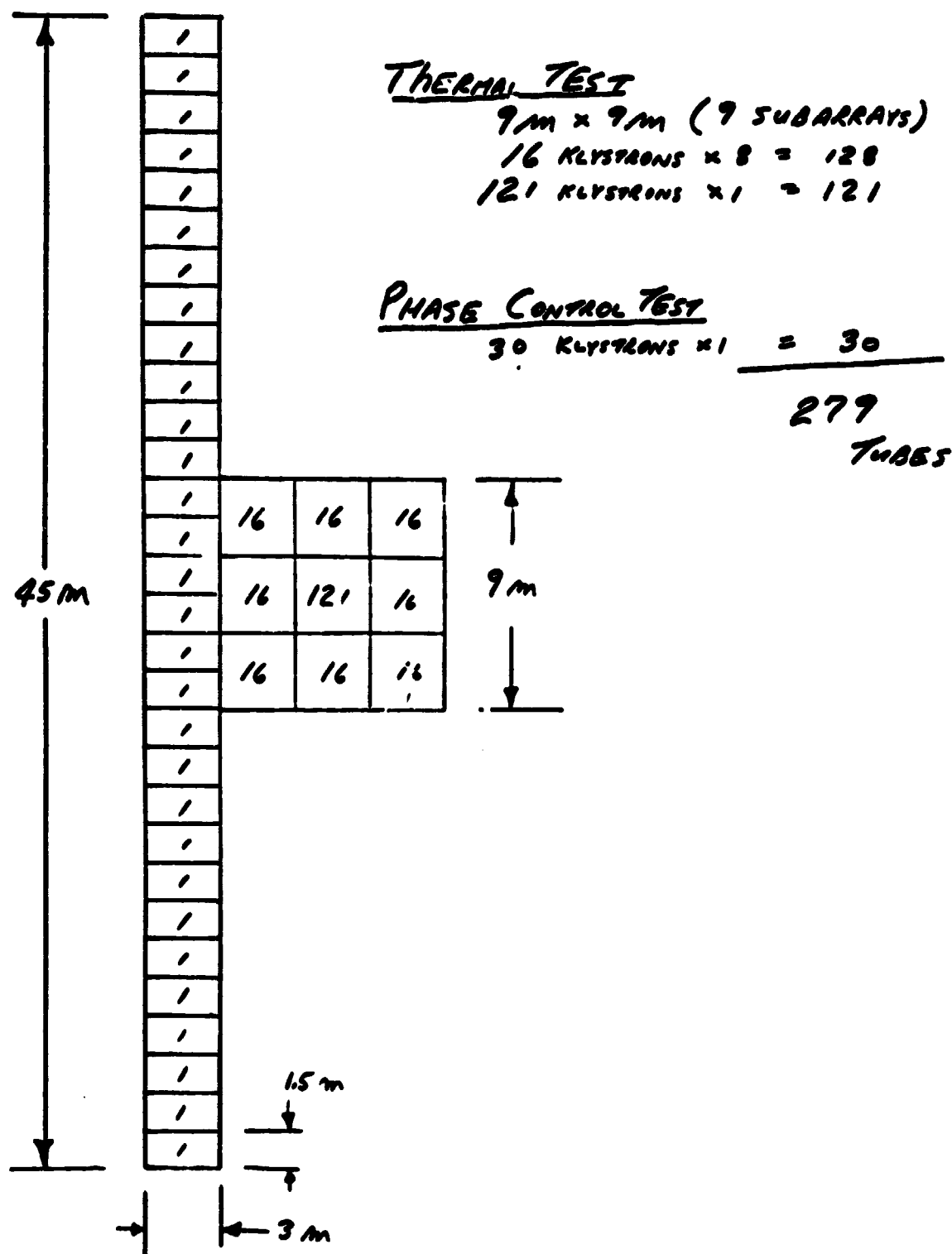


Figure 2.3.3-7 Solar Power Experiment

For the new configuration, we shall use the same thermal power (38.5 kW) and solve for the total tube power P_T in the center thermal square.

$$\begin{aligned} P_T &= P_H / (1 - \eta) = 38.5 \text{ kW} / .25 \\ &= 154 \text{ kW} \end{aligned}$$

The RF power is now

$$\begin{aligned} P_{RF} &= \eta P_T = .75 (154 \text{ kW}) \\ &= 116 \text{ kW} \end{aligned}$$

The power capability for each Klystron needs to be

$$P_{RF} = P_{RF/M} = 116 \text{ kW} / 121 = 960 \text{ Watts}$$

The 1 kW tubes will do very well.

The physical characteristics of the Klystron are given in Figure 2.3.3-5.

Antenna Array Mass

1. Thermal Test Array

(a) Central Subarray	
44 W/G's ea 2.924m long @ .36 kg/m	46.3 kg
Add 8% for fittings, etc.	<u>3.7 kg</u>
	50.0 kg

(b) Outer Subarrays (total of 8)	
37 W/G's ea 2.924m long	38.9 kg
Add 8%	<u>3.1 kg</u>
	42.0 kg

Mass, Thermal Test Array	
Center 1 @ 50 kg	50.0 kg
Outer 8 @ 42 kg	<u>336.0 kg</u>
	386.0 kg

2. 30 Element Phase Control Array

15 x 34 W/G's ea 2.92m @ .36 kg/m	536.8 kg
Add 8%	<u>42.9 kg</u>
	579.7 kg

3. Radiator Mass

Thermal Test Array	386.0 kg
Phase Control Test Array	<u>580.0 kg</u>
	966.0 kg

4. Tube Mass

279 Klystrons @ 29.3 kg 8,175 kg

5. Overall Antenna Mass 9,141 kg

Thermal Requirements

The worst thermal problem occurs in the center 3m x 3m subarray where 38.5 kW of heat is generated. The Red Book recommends that the temperature be held to 195°C or less for extended tube life. Although our mission is only six months or so, we should demonstrate a capability of approaching the 195°C to help prove out the SPS concept.

A preliminary analysis of the heat rejection of the 121 Klystron 3 x 3 meter panel gave the following results:

Klystron Surface Temperature	195°C (Design)
Top (Radiator) Peak Temperature	190°C
Bottom (Waveguide) Temperature	95°C
Total Heat Rejection	24.2 kW Thermal

This is less than the required 38.5 kW. It is estimated that the Klystron surface temperature must be raised to 250°C to reject 38.5 kW. Design approaches to lowering Klystron temperature are as follows:

1. Improve top radiator efficiency.
2. Improve Klystron-waveguide thermal coupling.

The dc/dc converters and phase control electronics packages must be held to 65°C or less to ensure proper operation of semiconductor elements.

Power Requirements

The heater and solenoid power required for each 1 kW Klystron is 130 watts. The beam voltage is 7 kW at 0.17 amperes, giving an efficiency of 75%.

Notes: 279 tubes x 1 kW = 279 kW RF

dc Power = 279 kW/.75 = 372 kW

Various efficiency factors as listed by Red Book:

.92 x .98 x .96 x .99 x .97 = .831

Solar Array Power = 372 kW/.831 = 448 kW

4,000m² gives 520 kW, giving a need margin for solar array not being normal to sun.

2.3.4 Propulsion Subsystem Definition

The propulsion subsystem for the SPS test article consists of a reaction control system (RCS) and an orbit transfer propulsion system.

Reaction Control System (RCS)

An RCS is provided for control of the SPS platform in low earth orbit (LEO) during a six month life, during which the microwave antenna is tested. The RCS provides control for both translation maneuvers and for attitude orientation control in conjunction with AVCS (attitude and velocity control subsystem).

Summary. The key features of the RCS are summarized in Table 2.3.4-1. The RCS module is illustrated in Figure 2.3.4-1.

Table 2.3.4-1 RCS Summary

Propellants	N ₂ O ₄ /MMH
Pressurization Gas	Helium
Total Impulse	15.1 x 10 ⁶ N-sec (3.4 x 10 ⁶ lb-sec)
Number of Modules	4
Number of Thrusters	20
Thrust, Each	
12 Thrusters	111 N (25 Lbf)
8 Thrusters	22 N (5 Lbf)
Total Weight	7,200 kg (15,900 Lbm)

Requirements. The translation functional requirements consist of (1) low altitude orbit transfer, (2) rendezvous with the rectenna, and (3) stationkeeping for six months. The RCS attitude control functional requirements consist of periodic thrusting for momentum dumping of the control moment gyros (CMG) about the pitch, yaw and roll axes. These requirements in terms of delta-V (velocity increment) and total impulse are shown in Table 2.3.4-2. The delta-V for the orbit transfer maneuvers include a 6% increase for low T/W (0.01 N/kg or 0.001 Lbf/Lbm) effects. The initial orbit transfer maneuver transports the platform from the construction orbit altitude (463 km or 250 nmi) up to operational test altitude (556 km or 300 nmi). After the microwave test, the platform is transported to a holding orbit (741 km or 400 nmi) where it is parked until required; then later, the platform is returned to the construction altitude (463 km or 250 nmi) for re-outfitting, refurbishment, and re-supply in preparation for a subsequent mission in GEO.

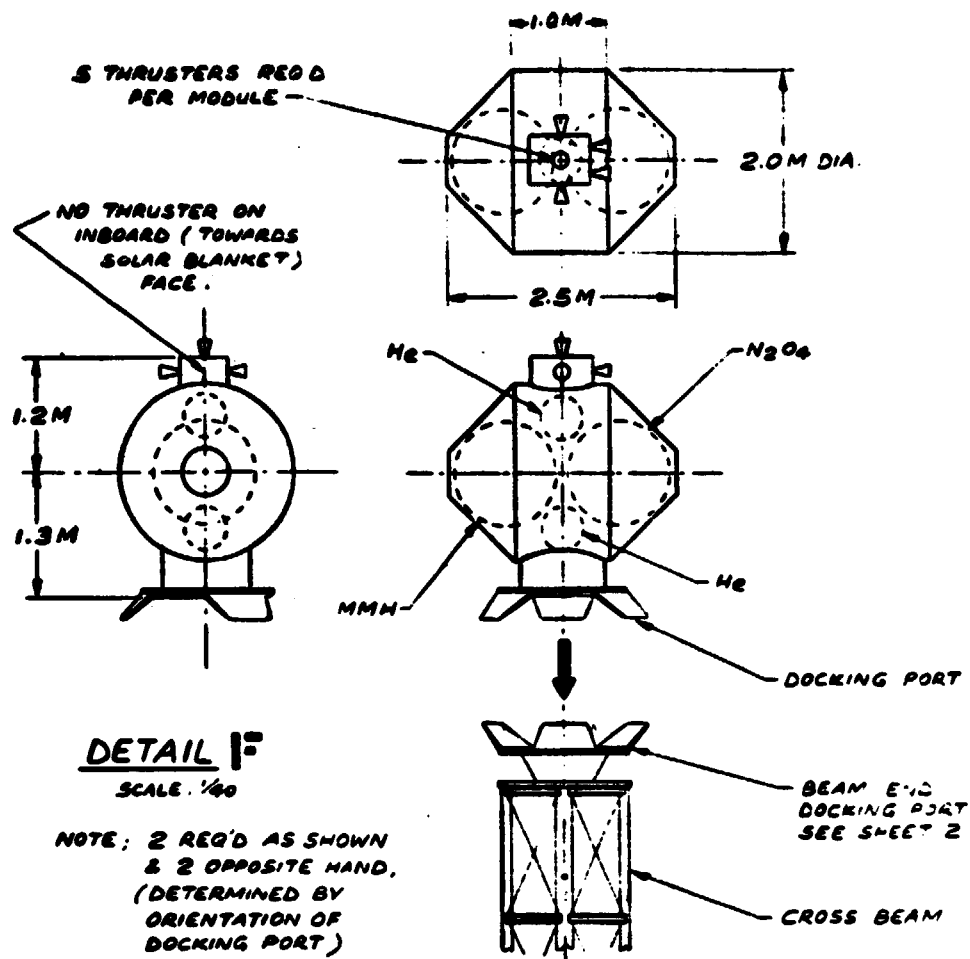


Figure 2.3.4-1 Reaction Control System (RCS) Module

ORIGINAL PAGE IS
OF POOR QUALITY

Table 2.3.4-2 RCS Requirements

Function	Requirement	
	<u>Delta-V</u>	
	M/Sec	(Ft/Sec)
1. Translation Maneuvers		
a. Orbit Transfer, 463 km to 556 km (250 to 300 nmi)	54.7	(180)
b. Rendezvous W/Rectenna	30.5	(100)
c. Stationkeeping 6 Months, 556 km (300 nmi)	45.7	(150)
d. Orbit Transfer, 544 to 741 km (294 to 400 nmi)	116.4	(382)
e. Orbit Transfer, 741 km to 463 km (400 to 250 nmi)	<u>164.9</u>	<u>(541)</u>
TOTAL TRANSLATION	412.2	(1,353)
2. Attitude Control CMG Momentum Dump (6 Months)		
	<u>Total Impulse</u>	
	N-Sec	(Lb-Sec)
a. Roll	36,862	(8,287)
b. Yaw	336,646	(75,681)
c. Pitch	<u>2,633</u>	<u>(592)</u>
TOTAL MOMENTUM DUMP	376,141	(84,560)

Description. A 20-thruster configuration, grouped in four modules with propellants, and located at the four corners of the rectangular shaped platform, provides an RCS that meets the mission and functional requirements. This configuration is shown on Sheet No. 1 of the drawing 42662-27 (see Appendix A). The corner locations were selected to provide maximum length moment arms and to avoid thruster exhaust impingement on the vehicle structure and components.

Figure 2.3.4-1 illustrates a typical RCS module each of which contains an oxidizer tank, a fuel tank and helium pressurization tanks located within a structural shell that acts as a micro-meteoroid shield and provides for thermal control. On one side of the RCS module, an assembly of five thrusters are located, with a docking port on the opposite side for mating and attachment to the platform structure.

The assembly of five thrusters (per module) consists of three 111 N (25 lbf) thrusters and two opposing 22 N (5 lbf) thrusters. Operation of the four module RCS consists of firing four 111 N (25 lbf) thrusters at a time for low altitude orbit transfer, two 111 N (25 lbf) thrusters at a time for yaw-axis CMG momentum dump and stationkeeping, and two or four 22 N (5 lbf) thrusters for pitch and roll CMG momentum dump.

Storable propellants (N_2O_4/MMH) were selected for the RCS to be compatible with long duration propellant storage for the six month mission and still provide reasonable performance. Bi-propellant RCS thrusters, such as those being developed by Aerojet, 2 N (0.5 lbf), 22 N (5 lbf) and 445 N (100 lbf), provide a steady state specific impulse of 2,750 N-sec/kg (280 sec) to 2,890 N-sec/kg (295 sec). These performance values were used in sizing propellant quantities since relatively long pulse durations are required, with 90% of this propellant required for translation.

RCS propellant requirements were based on a platform weight of 31,300 kg (69,000 lb), without RCS, and with RCS a platform weight of 38,600 kg (85,000 lb). Each RCS module contains 1,320 kg (2,900 lb) propellant and has an initial gross weight of 1,800 kg (3,975 lb). The total gross weight of the four RCS modules is 7,200 kg (15,900 lb).

Orbit Transfer Propulsion System

A solar electric propulsion system (SEPS) is provided for transporting the SPS test article solar array from the construction and test altitude in LEO up to an operational altitude at GEO, on a "growth" mission subsequent to the LEO microwave antenna test mission.

Summary. The key features of the SEPS are summarized in Table 2.3.4-3. The module is illustrated in Figure 2.3.4-2.

Requirements. The requirements for the SEPS are summarized as follows:

- (1) A delta-V velocity increment 6,000 m/s (19,700 ft/sec) is required for transporting the SPS test article from an $28\frac{1}{2}$ degree inclined low earth orbit to GEO.

- (2) An SPS vehicle weight of 38,500 kg (84,900 lb), not including orbit transfer propulsion, is required to be transported from LEO to GEO.
- (3) DC electrical power of 520 kW from a 4,000m² (43,000 ft²) silicon solar cell array is available for the maximum power source at beginning of life (BOL). End of life (EOL) power available is based on 50% solar cell degradation from the radiation effects of passage through the Van Allen Belt at low accelerations, corresponding to transit times in excess of 100 days.
- (4) Trip time should be minimized for economic reasons to expedite the return on investment. With a fixed electrical power level available and a given spacecraft weight, the prime area for decreasing trip time lies in using the electric propulsion type that provides the highest thrust-to-power ratio, and a solar cell array with the highest power-to-weight ratio.
- (5) The specifics of a required GEO mission objective are undefined and remain an open issue. Therefore, the required operational time period for the GEO mission is undefined, but would occur sometime after the microwave test in LEO, or in the post-1985 time period.
- (6) Thrust Vector Control (TVC) is required (relative to the sun-oriented solar array platform) to provide both in-plane and out-of-plane deflection of the thrust vector.
- (7) Earth shadowing effects should be considered in causing intermittent operation of an otherwise constant thrusting mode. Therefore, electrical power storage is required to provide low power or initial warm-up to re-start mercury ion thrusters after each shadow period.

Table 2.3.4-3 SEPS Summary

Propellant	Mercury
Total Impulse	279 x 10 ⁶ N-sec (63 x 10 ⁶ lb-sec)
Power Input	520 kW
Number of Modules	6
Number of Tanks	18
Number of Thrusters	72
Beam Diameter	30 cm (1 ft)
Thrust, Each	0.205 N (0.046 lbf)
T/W, Initial	3 x 10 ⁻⁴ N/kg (3 x 10 ⁻⁵ lbf/lbm)
Weight	10,650 kg (23,500 lb)

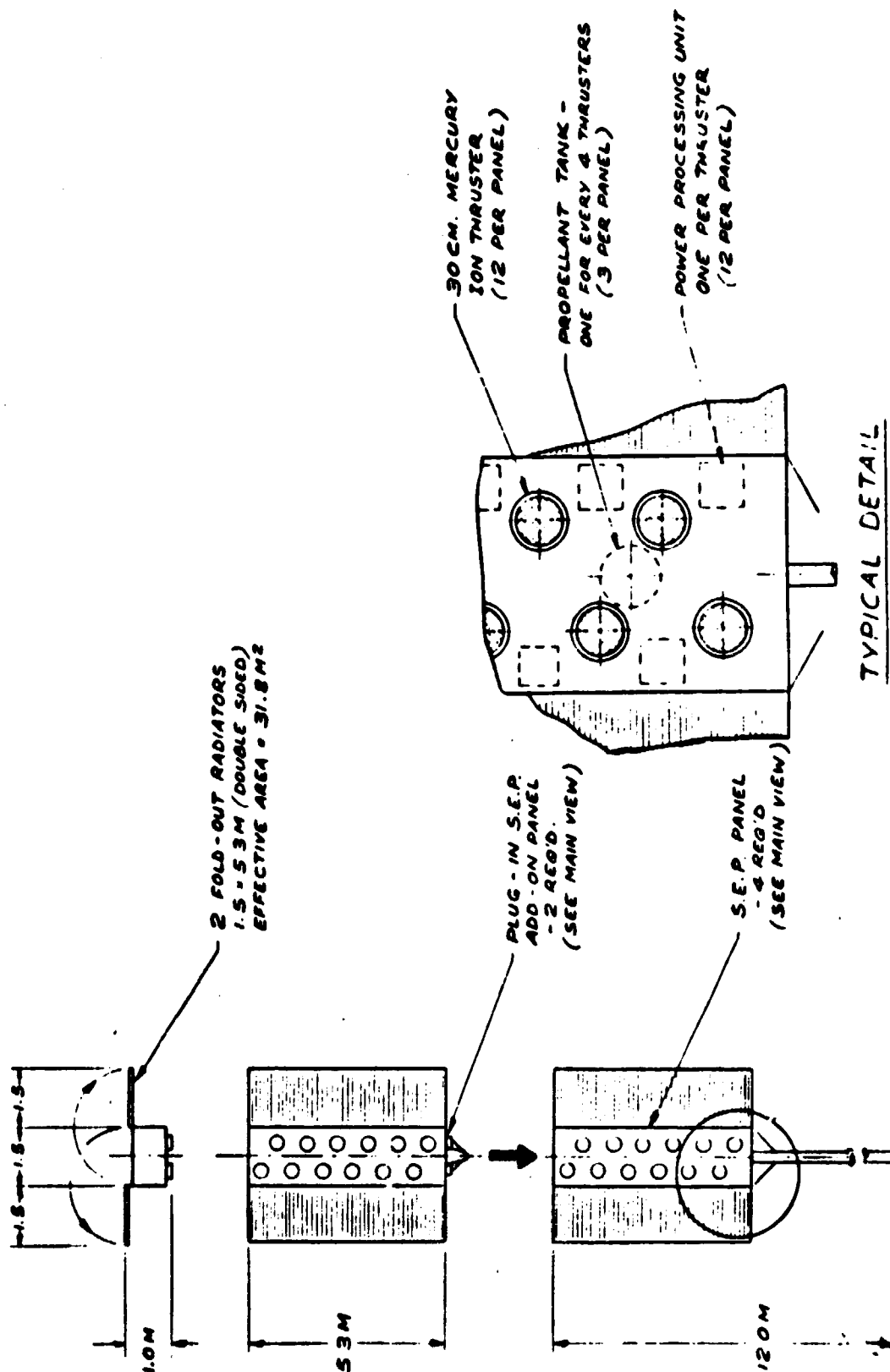


Figure 2.3.4-2 Solar Electric Propulsion System Module

Description. An electric propulsion system using 72 mercury ion thrusters is provided for orbit transfer of the SPS solar array platform. This configuration is shown on Sheet No. 1 of drawing 42662-27 (see Appendix A). Electric thrusters are located at both ends of the platform and are mounted on rotatable and nodable panels to allow solar array sun-pointing and separate thrust vector pointing for orbit transfer, including orbital plane change. The total number of thrusters are distributed between the two end installations according to the vehicle C.G. location between the ends. The asymmetrical C.G. location shown, located approximately one-third the platform length from the cargo end (microwave test antenna shown), results in the 48 and 24-thruster groupings at either end.

A basic 12-thruster module is used in multiples to obtain the 48 and 24 thruster groupings (six modules total). The modules are mounted on masts which are attached to the rotary joint. Slip rings in the rotary joint provide for electric power transmission; further details of the rotary joint may be found in the section on Mechanical/Electrical.

In addition to the thrusters, the basic module contains the power processing units (PPU, one per thruster), propellant tanks (one per 4 thrusters), and radiators for heat dissipation (see Figure 2.3.4-2). The performance of the 30 cm mercury ion thruster is summarized in Table 2.3.4-4, which also includes characteristics of the PPU and mercury tanks.

The 520 kW solar array power available is adequate for 75 thrusters at BOL after power processing by the PPU. The selected 72 thruster system was chosen for the aforementioned C.G., geometry, and modular design considerations. Each PPU provides processing in bringing the required multi-voltage dc power to each thruster. The PPU concept assumed also has the capability of maintaining control of operating performance of each thruster during the start-up and shutdown transients and steady-state operation.

Two fold-out radiators are provided on each module primarily for heat dissipation of 0.9 kW from each PPU. An allowance of 2.5m^2 (27ft^2) of radiation surface area per PPU is provided by the double-sided radiators, used with variable conductance heat pipes (VCHP).

Three mercury propellant tanks are located in each module; each tank feeding four thrusters. Two of the four thrusters, fed by each tank, will be shutdown as the power degrades through radiation, so that a total of 36 thrusters are firing upon reaching GEO. This selective shutdown allows the multiple tankage to be utilized fully. The pressurizing gas (GN_2 or Freon 113) is stored integral with the mercury propellant in the tank at 414 kilo-pasquals (60 psia), a relatively low pressure tank. A positive expulsion device provides a constant force for feeding propellant under the low acceleration conditions. Each 45 cm (17.6 inch) diameter tank provides capacity for 315 kg (696.7 lb) of mercury propellant (50% of tank volume) and the pressurizing gas. The eighteen propellant tanks provide storage for the 5,681 kg (12,524 lb) of mercury propellant which represents 53% of the total SEP system.

The resulting trip time is 324 days (10.7 months). This is based on transporting the 38,500 kg (84,900 lb) platform from LEO to GEO using the average of 54 thrusters firing continuously, allowing 10% time for earth shadow (non-thrusting) effects.

Table 2.3.4-4 SEPS Characteristics

<u>Thruster - 30 cm</u>	
Thrust	0.205 N (0.046 lbf)
Specific Impulse	49,000 N-sec/kg (5,000 sec)
Input Power	6 kW
Screen Voltage	2,900 V dc
Propellants	Mercury
Beam Diameter	30 cm (1 ft)
Overall Diameter	38 cm (14 inches)
Length	1.6 cm (6 $\frac{1}{4}$ inches)
Weight	8 kg (17.9 lb)
<u>Power Processing Unit (PPU) - (One per Thruster)</u>	
Type	Silicon Control Rectifier
Power Efficiency	87%
Size	0.04m ³ (1.54 ft ³)
Weight, Each	35 kg (77.2 lb)
<u>Propellant Tank (One per 4 Thrusters)</u>	
Material	Stainless Steel
Operating Pressure	414 kPa (60 psia)
Expulsion	Diaphragm
Pressurization	Integral Gas (GN ₂ or Freon 113)
Size, Diameter	45 cm (17.6 inch)
Weight	9 kg (20 lb)

2.3.5 Attitude and Velocity Control Subsystem

The main features and characteristics of the attitude and velocity control subsystem (AVCS) are summarized in Figure 2.3.5-1.

The AVCS is designed to perform several post-construction functions. It controls the vehicle's attitude, points the microwave antenna, controls orbit transfer maneuvers, and regulates the vehicle's velocity to maintain proper spacing with the co-orbiting rectenna.

The AVCS is designed to perform during the following phases of flight following construction and checkout: orbit transfer from the 250 nmi construction orbit to the 300-nmi operational orbit, six months of antenna testing, transfer from the operational orbit to a 400 nmi holding orbit, a prolonged period in storage, and transfer back down to the 250 nmi construction orbit. Subsequent flight phases, starting with reoutfitting the vehicle for another mission, are not considered here.

The following text discusses the important considerations leading to the AVCS definition. The discussion, together with the supporting analyses and trade studies, is intended to define the subsystem in sufficient detail to satisfy the needs of this space construction study. It is in this spirit that many of the detailed trade studies required to fully define the AVCS components are replaced by engineering judgment. Even though a more detailed study might modify the subsystem design somewhat, it is believed that the hardware described here is representative of the type needed for the SPS vehicle, and will properly exercise the construction aspects of this study.

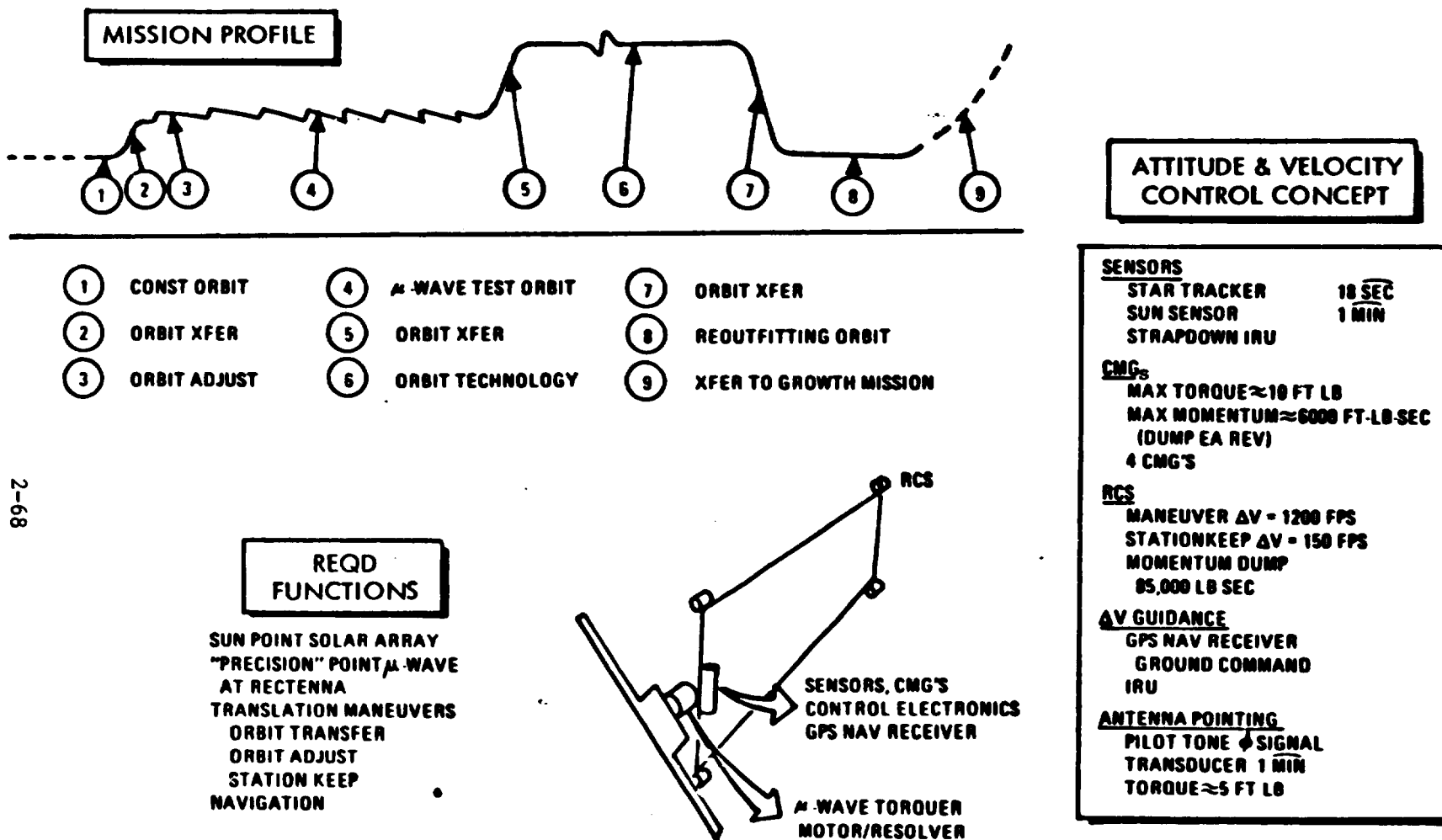
Attitude Control

A primary function of the AVCS is to control the angular orientation of the SPS test article. The attitude control requirements are different for each flight phase, and all phases (orbit transfer, experiment operation, and storage) must be considered in selecting an attitude control scheme. The discussion begins by first examining attitude control needs during the six-month microwave experiment.

Two attitude control requirements must be met. The solar array must be oriented toward the sun, and the bearing axis of the microwave antenna must be oriented so that the antenna can be accurately pointed toward the co-orbiting rectenna. These requirements are satisfied by aligning the long axis of the vehicle perpendicular to the orbit plane and orienting the solar arrays toward the sun with the accuracies listed in Figure 2.3.5-2.

An important consideration in selecting a preferred attitude control concept is the required orientation accuracy. The SPS test article has loose attitude control requirements (precise orientation of the microwave antenna about its bearing axis is not considered here); therefore, all forms of attitude control are candidates.

Another important consideration is the environmental disturbance torques. The major disturbances—gravity gradient, aerodynamic and solar pressure—are illustrated in Figure 2.3.5-3. These torque-time histories serve as a basis



2-68

Figure 2.3.5-1 AVCS Summary, SPS Test Article

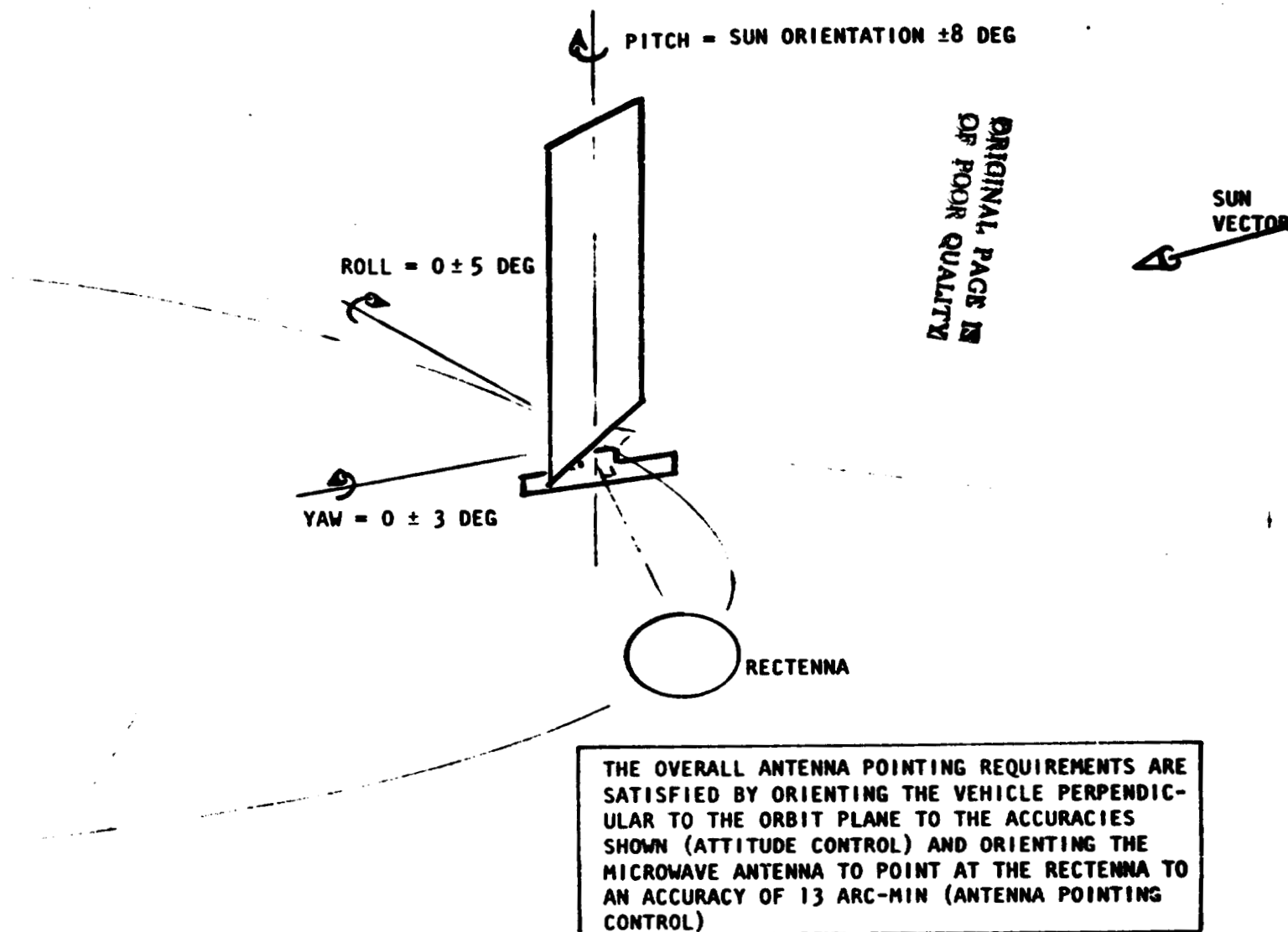


Figure 2.3.5-2. Attitude Control Requirements for the Microwave Transmission Experiment

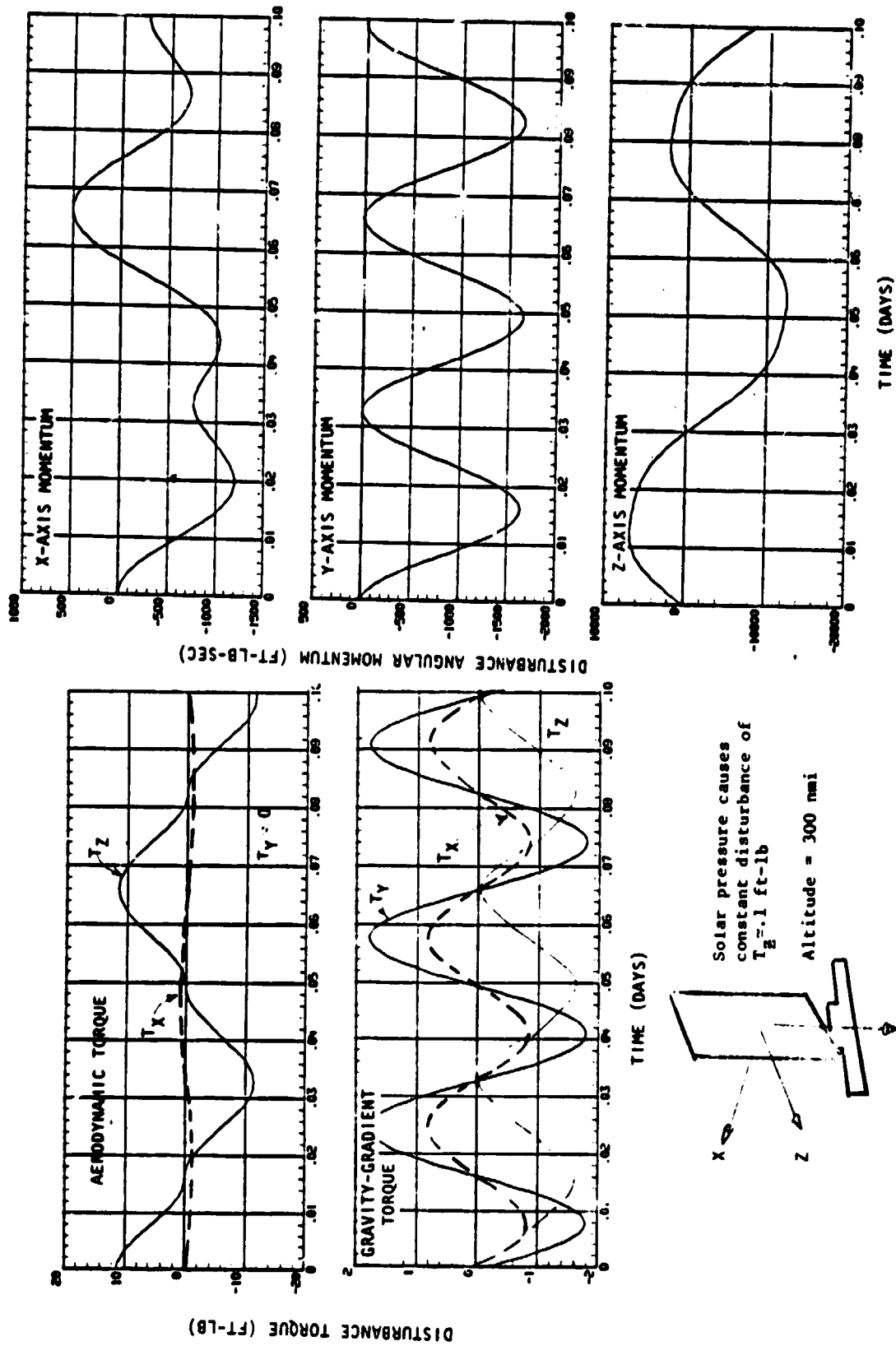


Figure 2.3.5-3. Environmental Disturbances, SPS Test Article

for considering the applicability of each of the three fundamental control concepts:

Passive. Environmental torques can be used to loosely control a vehicle's attitude. For example, gravity-gradient torques can "hold" a vehicle in a local vertical orientation. Such concepts are not applicable to the SPS test article, because the vehicle's changing attitude does not remain fixed in a torque equilibrium orientation.

Mass Expulsion. Jets can perform the entire attitude control function. If this is done, 1400 kg (3000 lb) of hydrazine is expelled during the six-month experimental phase.

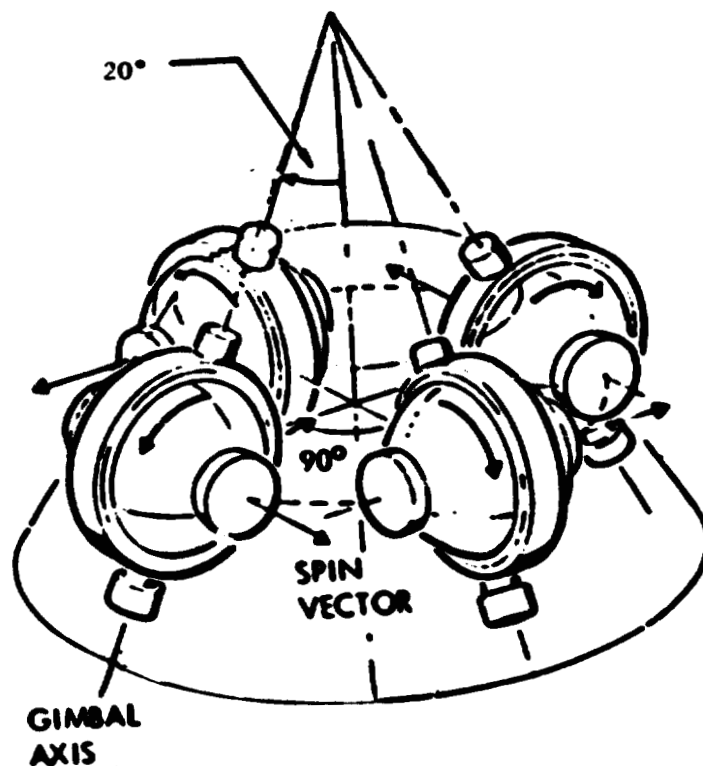
Momentum Storage and Transfer. Control wheels can be used in a variety of ways. A logical concept for the SPS test article is to store (exchange) the angular momentum caused by cyclic disturbance torques and rely on the reaction jets to counter the secular components of the environmental torques. With this concept, the propellant requirement for six months of attitude control is reduced to 70 kg (150 lb). A set of control wheels capable of exchanging the environmentally induced cyclic momentum is illustrated in Figure 2.3.5-4. Control moment gyros (CMG's) have some attractive features. They are the only devices presently available with very large momentum storage capability; and they have much larger torque capacities than momentum wheels, enabling them to settle transient disturbances faster.

Somewhat arbitrary reasons are used to select CMG's to exchange cyclic momentum and RCS jets to control the secular momentum buildup. This combination probably costs more (the cost difference is \$0.5M or less) than an all-jet system, but it provides more capability which may be required after the vehicle is reoutfitted for subsequent missions. Furthermore, this control concept stresses the construction process more.

Several types of attitude and angular rate sensors are available. Earth sensors can measure roll and pitch angle relative to an orbiting reference frame with an accuracy of approximately 1/4 degree. Sun sensors can measure two displacement angles relative to the sun (1 arc-sec to 1 arc-min accuracy); star sensors can provide three-axis angle measurements relative to inertial space (1 arc-sec to 20 arc-sec accuracy); and gyros can provide inertial rate measurements (0.1 deg/hr to 10 deg/hr accuracy). A number of different combinations of these devices can satisfy the SPS test article requirements.

The following considerations are used as the basis for selecting a reasonable complement of sensors:

- Attitude sensing requirements are not very demanding during the microwave experiment ($\sim 0.5^\circ$ accuracy); however, more accurate sensing may be required during orbit transfer in order to reduce thrusting inaccuracy.
- The cost of attitude sensors is a much smaller percentage of the total SPS test article system cost than it is for present-day spacecraft.



CHARACTERISTICS OF EACH CMG

• CMG WEIGHT (BASE GIMBAL INCLUDED)	195 LB
• ANGULAR MOMENTUM	1600 FT-LB-SEC
• POWER REQUIREMENTS	
PEAK GYRO INPUT POWER	50 W
PEAK DURING RUN-UP	200 W
STEADY-STATE RUNNING	40 W @ 5300 RPM
• WHEEL OPERATING SPEED	7000 RPM
• SPIN BEARINGS BALL BEARINGS	204H DF PAIR
• TORQUE OUTPUT	15 FT-LB
CMG SIZE	40.1×27.0×30.5 IN.
• TOTAL WEIGHT (INCL. ELECTRONICS)	206 LB

Figure 2.3.5-4. CMG's for SPS Test Article Attitude Control

- Redundancy is important, because failure of the AVCS at high altitude (say, the 400-nmi orbit) would result in very high repair costs.

These considerations, and a desire to select sensors which are plausible and which stress space construction, lead to the components illustrated in Figure 2.3.5-5. The inertial reference unit (IRU), updated by star sensors, provides attitude and rate information during orbit transfer. The sun sensor is used during attitude acquisition to initialize the star sensors' search.

Improved attitude sensors (laser gyros, CCD star sensors, etc.) will be available when the SPS test article is flown. However, today's off-the-shelf hardware is adequate and is completely defined. For these reasons, the sensor characteristics listed in Figure 2.3.5-5 are taken from vendor catalogs.

Antenna Pointing

Two control functions combine to aim the microwave antenna at the rectenna. The attitude control system orients the antenna's bearing axis perpendicular to the orbit plane to within 5° in roll and 3° in yaw (Figure 2.3.5-2). Then, the pointing control system orients the antenna about the bearing axis to point it toward the rectenna to an accuracy of at least 13 arc-min.

Fine pointing of the antenna is performed by a continuous drive torquer which nulls the pointing error measured by a directional antenna. The directional antenna is part of the microwave antenna payload. It receives a pilot signal transmitted from the rectenna at two locations displaced from one another. Angular errors much less than 13 arc-min are sensed by comparing the phase differences between the two signals.

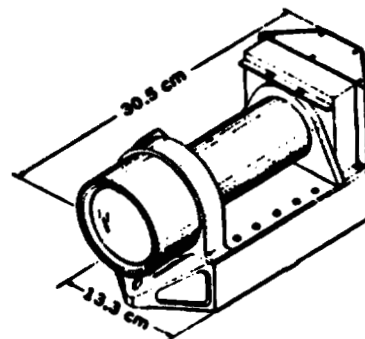
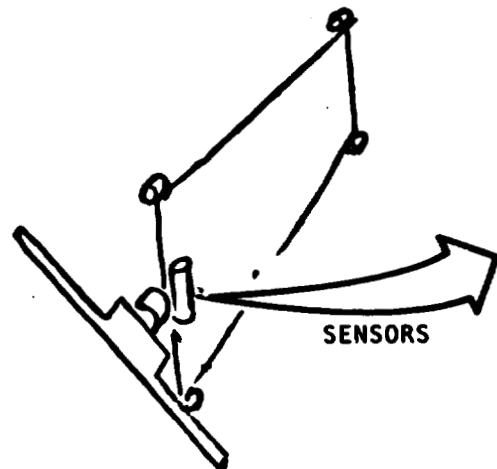
An angle measurement transducer is included in the pointing control system to provide antenna angle relative to the solar array. The transducer, together with the star sensor/IRU is used for open-loop pointing of the antenna with sufficient accuracy to get within the directional antenna's field of view. The angle transducer is also available for controlling the antenna's relative orientation during other phases of flight.

The drive motor must have sufficient torque to overcome friction and environmental disturbance torques, and to accelerate the antenna to track the rectenna. A peak drive torque capacity of 7.0 N·m is sufficient as indicated in Table 2.3.5-1.

Orbit Transfer and Maintenance

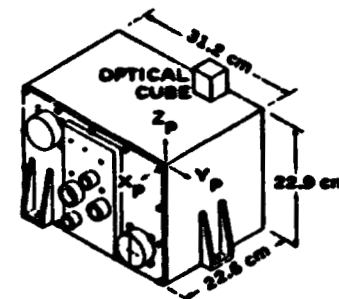
The AVCS must perform guidance and attitude control functions during orbit transfer and velocity corrections for orbit maintenance. Most of the components required for these functions are required for other functions and have been discussed previously.

The additional equipment requirements include hardware to determine the vehicle's orbital parameters and its position relative to the rectenna, as well as sensors to measure the velocity change caused by orbit transfer thrusting maneuvers. The most effective way to satisfy these requirements is to use the Global Positioning System (GPS) for navigation data.



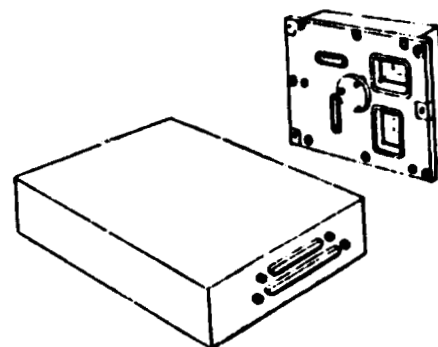
STAR SENSORS

TYPE	TRACKER
FOV	8x8 DEG
POWER	4 WATTS
ACCURACY	10 SEC (1 σ)



INERTIAL REFERENCE UNIT

POWER	7.5 W/CHANNEL
RANDOM DRIFT	0.015 DEG/HR (3 σ)



TWO-AXIS SUN SENSOR

FOV	± 32 DEG
POWER	2.5 W
RESOL.	<15 SEC
STAB.	1 MIN

Figure 2.3.5-5. Sensors for SPS Test Article Attitude Control

Table 2.3.5-1. Antenna Pointing Drive Torque Requirements,
SPS Test Article

	Torque (N·m)
Friction	1.0
Gravity gradient	0.6
Aerodynamic	0.1
Solar pressure	Negligible
Tracking acceleration	3.0
50% contingency	<u>2.3</u>
Torque requirement	7.0 (5.2 ft-lb)

GPS navigation data are provided by a small antenna, which receives information from four GPS spacecraft, and on-board electronics to process data. This system will locate the SPS test article and the rectenna to an accuracy of less than 10 m.

Orbit transfer is achieved by first computing the required ΔV maneuver parameters on the ground, using GPS navigation data and vehicle attitude data. Maneuver parameters (attitude and velocity change) are transmitted to the vehicle. Then, the AVCS controls orbit transfer by using angle and angle rate data from the IRU together with the RCS jets and CMG's to maintain the proper attitude.

Structural Requirements

Special care is required to prevent unstable interactions between the AVCS and the vehicle's soft structure. The easiest method to ensure stable operation is to design the structure to be stiff when compared to the control system. Analyses for many other space vehicles indicates that stable operation is achieved if the vehicle's fundamental vibration frequency is at least 5 to 10 times greater than the control system's characteristic frequency. When sufficient structural stiffness does not exist, the AVCS control logic can be shaped to stabilize the low frequency vibration modes. However, this approach can be risky when more than a few modes must be stabilized. The main concern grows out of the inability to accurately identify and measure motions of more than a few low-frequency modes.

The approach taken here is to develop adequate separation between the structural and control frequencies wherever possible and to actively stabilize low-frequency modes when separation is not possible. This approach is examined in the following text for the AVCS functions most likely to couple with structural vibrations: vehicle attitude control and antenna pointing during the microwave experiment.

Attitude Control. The potential for unstable interactions between the attitude control loops and the SPS test article's structure is again examined by comparing frequencies.

The vehicle's structural frequencies and associated modes are presented in Section 2.3.1 (see Figure 2.3.1-7). The lowest frequency mode liable to couple with the pitch control loop is a torsional mode at 0.010 Hz, and the mode most likely to couple with the roll and yaw control loops is the first transverse bending mode at 0.029 Hz. It is these frequencies which must be compared with the control frequencies.

The control frequencies of a simple attitude control system (i.e., control loops with rate and position feedback only) are established by two considerations—transient and steady-state response characteristics. The transient response requirements are easily met by assuring that the control frequency is at least two times greater than the fastest disturbance torque. A control frequency of 7×10^{-4} Hz ensures that the attitude control system can compensate for environmental disturbances without a significant transient response. A somewhat higher frequency is desirable to settle the transients caused by firing jets, but a frequency less than one-tenth of the structural frequency is adequate.

The control frequency must also provide enough "stiffness" so that the attitude errors caused by the environmental torques do not exceed the allowable values (5° in roll, 3° in yaw, and 8° in pitch). The required control stiffness and the vehicle's mass moment of inertia then establish the control system frequency. The control frequency requirements for adequate steady state response are listed in Table 2.3.5-2, along with the transient control frequency requirement and the structural frequencies. The maximum control frequency requirement is compared to the structural frequency in the right-hand column. Note that a frequency separation greater than ten can be achieved. Reasonable structural frequency requirements are: first torsional mode >0.007 Hz and first bending mode >0.007 Hz.

Table 2.3.5-2. Attitude Control Frequency Separation

Axis	f_c , Control Frequency Requirement (Hz)		f_s , Structural Frequency (Hz)	f_s/f_c
	Steady State	Transient		
Roll	$\geq 4.4 \times 10^{-5}$	$\geq 7 \times 10^{-4}$	0.029	≤ 41
Pitch	$\geq 3.7 \times 10^{-4}$	$\geq 7 \times 10^{-4}$	0.010	≤ 14
Yaw	$\geq 1.7 \times 10^{-4}$	$\geq 7 \times 10^{-4}$	0.029	≤ 41

Antenna Pointing Control. The microwave antenna pointing control system can excite vibrations of the antenna and the solar array. However, only modes which can be excited by the drive motor and which can be sensed by the directional antenna (which is mounted on the microwave antenna) can interact with the control system.

The lowest frequency mode computed in Section 2.3.1 is a 0.010 Hz torsional mode of the vehicle, which nominally does not displace the directional antenna. However, stiffness and mass asymmetries, as well as drive axis friction, can cause a small amount of motion of the directional antenna in that mode. Thus, good design practice dictates that the pointing control frequency be less than 0.010 Hz. Because this motion can only occur as a second-order effect, a closer frequency spacing of 5 is permissible ($f_c \leq 0.0020$ Hz).

Next, the control frequency required to point the antenna accurately is determined and compared with the foregoing requirement. Again, the control frequency is established by the antenna's inertia and the "stiffness" needed to overcome the environmental disturbances to point accurately. In this case, the control system must be stiff enough to balance the gravity-gradient torque, which increases as the long axis of the antenna is rotated off of its local vertical orientation, plus the aerodynamic and solar pressure disturbances. The gravity gradient torque calculation is complicated because the maximum offset pointing angle is related to how well the orbit of the SPS test article is matched to that of the rectenna.

The control frequency required to achieve a residual error of 13 arc-min is plotted as a function of the altitude error between the two vehicles in Figure 2.3.5-6. Notice that the frequency requirement ($f_c \leq 0.0020$ Hz) is satisfied when the altitude error is kept to less than 5 km. Matching orbits to this accuracy is readily achievable, as discussed in Section 2.1.

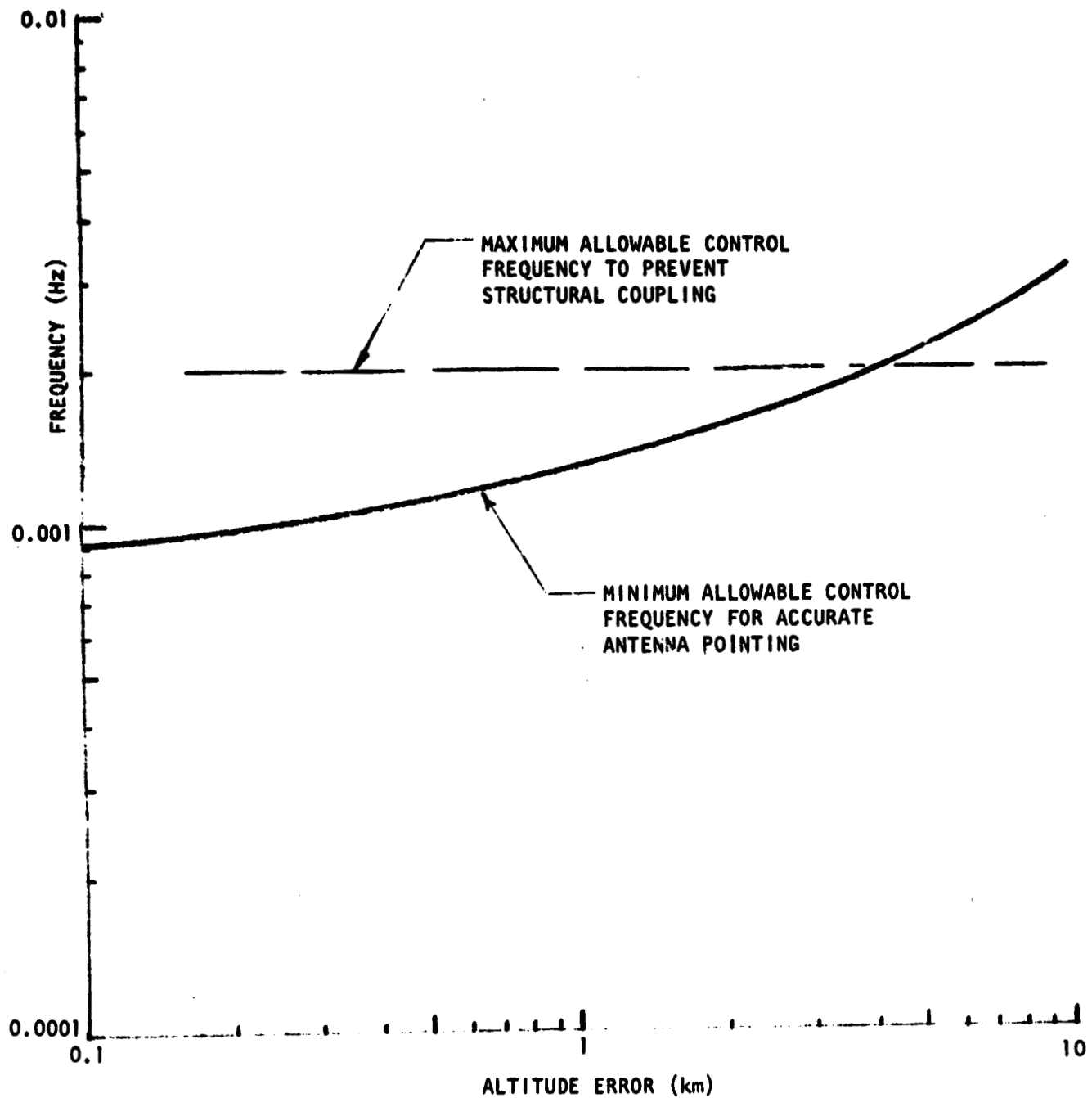


Figure 2.3.5-6. Antenna Pointing Control Frequency Requirements,
SPS Test Article

2.3.6 Tracking, Telemetry and Control Subsystem Definition

Summary

During low earth orbit or during geosynchronous orbit, the communications and tracking system of the Solar Power Satellite (SPS) Flight Test Article uses S-band and Ku-band links to provide, in addition to tracking, reception of commands at a maximum rate of 216 k bits/s. The system also provides a transmission capability for telemetry, television, and data at a maximum rate of 50 M bits/s. S-band links may be established with a ground station and both S-band and Ku-band may be routed through NASA's Tracking and Data Relay Satellite System. A simultaneous capability to communicate with the coorbiting rectenna platform, the Space Shuttle Orbiter, GPS, or other spacecraft is also provided on S-band. See Figure 2.3.6-1.

S-band Links

As shown in Table 2.3.6-1, there are three S-band links: (1) PM to orbiter, STDN or SCF, (2) FM direct to ground, and (3) PM to TDRSS and there to TDRS on the ground. The return link on (1) is split into high (2250-2300 MHz) and low (2200-2250 MHz). If the SPS Test Flight Article transmits on low, the orbiter relays this signal to TDRSS (or STDN) on high or vice versa. In general, however, the orbiter is not needed for relay and links (1) other than orbiter, (2) and (3) are adequate for most command and telemetry functions. The exception is when higher rates than indicated are needed; then, the Ku-band provides the near continuous high-data-rate capacity. Link margins are given in the special issue on Space Shuttle Communications and Tracking, IEEE Transactions on Communications, November 1978, Pages 1494, 1521 and 1604. Table 2.3.6-2 provides mass and power estimates. The grand totals for S-band and Ku-band communication subsystems including wiring and antennas are 200 kg mass and 1200 watts power.

Ku-Band Links

The Ku-band subsystem for the SPS Flight Test Article operates as a two-way communications system with the ground through the Tracking and Data Relay Satellite System (TDRSS). The advantage of the Ku-band link is the large increase in data rate capacity both on the forward link as well as the return. See Table 2.3.6-1. This increase in data rate is largely due to the 0.9 meter parabolic antenna with 1.6 degree beamwidth and 38.5 dB gain. An uncertainty in pointing up to 10 degrees (20 degree full-cone angle) is allowed for by using a slow spiral scan search pattern in acquisition. The maximum search time is 3 minutes. The subsystem described here is the communications portion of the Ku-band Integrated Radar and Communications Subsystem for the Space Shuttle.

Note that Links (1) and (2) have less than 40% real-time coverage, whereas Links (3) and (4) have more than 95% due to the SPS Flight Test Article being in low earth orbit and the good coverage given by TDRSS.

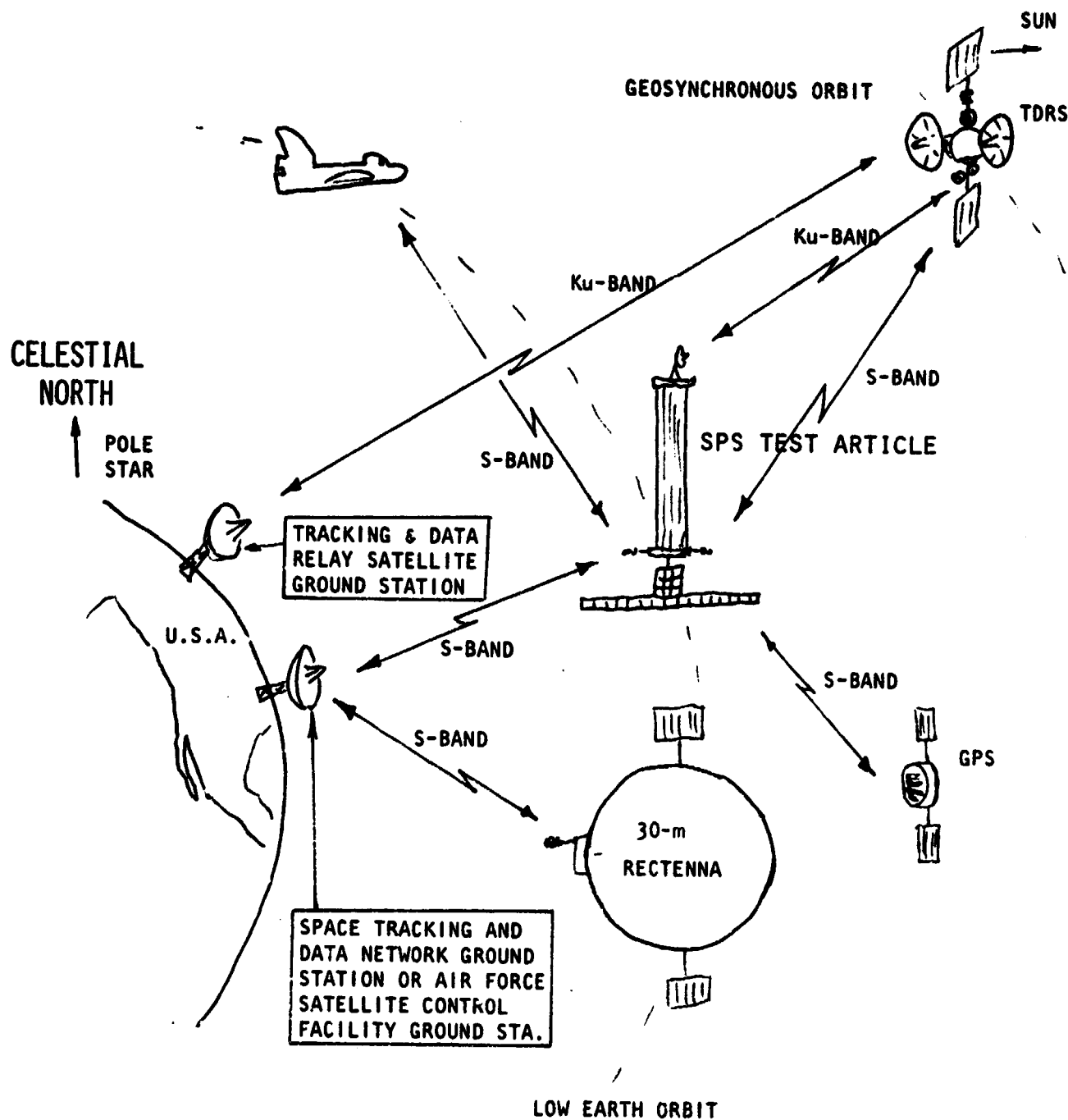


Figure 2.3.6-1. Communication Links for SPS Flight Test Article

Table 2.3.6-1: SPS Flight Test Article Link Parameters

LINK	ONE WAY OR TWO WAY?	FREQUENCY	DATA RATE	NOTES
<u>S-LINK</u> PM TO ORBITER (OR DIRECT TO STDN OR SCF)	TWO	RETURN 2200-2300 MHz FORWARD 2025-2120 MHz	192 Kb/s 72 Kb/s	THIS LINK IS RELAYED TO STDN, SCF, OR TDRS. SCF HAS 256 Kb/s (RETURN) RF POWER = 6 W ANTENNA = 4 QUAD OMNIS
FM TO GROUND (STDN OR SCF)	ONE	RETURN 2250 MHz (10 MHz BANDWIDTH)	4 Mb/s	RF POWER = 10 WATTS ANTENNA = 2 HEMIS. OMNIS
PM TO TDRS (THROUGH TDRSS)	TWO	RETURN 2200-2300 MHz FORWARD 2025-2120 MHz	192 Kb/s 72 Kb/s	RF POWER = 100 WATTS ANTENNA = 4 QUAD OMNIS TIME COVERAGE: $\geq 95\%$
<u>Ku-LINK</u> TO ORBITER OR TO TDRSS	TWO	RETURN 14.85-15.15 MHz FORWARD 13.75-13.80 GHz	50 Mb/s DIGITAL OR 4.5 MHz ANALOG TV 2 Mb/s PAYLOAD 192 Kb/s TELEMETRY 216 Kb/s COMMANDS	RF POWER = 50 WATTS ANTENNA = PARABOLIC (0.9 M DIAMETER) TIME COVERAGE: $\geq 95\%$ HAS DATA & PN RANGE

Table 2.3.6-2. SPS Flight Test Article
LRU Mass and Power Summary

LRU	Mass (kg)	Power (W)
<u>S-Band</u>		
PM transponder	15.8	63
FM processor	8.1	30
Doppler extractor	7.4	16
Power amplifier (100 W)	14.4	400
Pre-amplifier	11.6	25
FM transmitter	3.0	120
FM processor	5.2	9
Switch assembly	3.0	2
<u>Ku-Band</u>		
Electronic assembly	95.0	489
Signal processor		
Deployed assembly		
Total with wiring and antennas	200	1200

2.3.7 Thermal Analysis and Thermal Control Subsystem Definition

The primary thermal analysis effort related to the SPS flight test article involves the microwave antenna klystron panels and the solar electric propulsion system (SEPS) units. These are the only aspects reported herein.

Thermal Control of 121-Klystron Panel

An important objective of the 1985 solar power experiment (Reference 1) will be the demonstration of the feasibility of rejecting waste heat from a high-power-density klystron panel. Present plans call for the simulation of the 50-kW klystron tubes which will later be available, by a greater number of 1-kW tubes which reject the same amount of heat per panel. This approach calls for 121 klystrons mounted on one 3-meter by 3-meter panel, generating 38.5 kW of waste heat. The Red Book (Reference 2) also specifies a maximum external klystron temperature of $T_R = 195^\circ\text{C}$.

The configuration analyzed is depicted in Figure 2.3.7-1. Heat is carried from the high-temperature zones (output cavity and collector) of each klystron to the radiating surface immediately above by means of heat pipes. It is estimated that this can be accomplished with a 5°C drop resulting in a radiator root temperature of 190°C . The lower surface is made up of nearly continuous waveguide tubes which provide a second radiating surface. However, the transfer from the klystron heat source to the bottom surface will be less efficient since it is accomplished by radiation and a limited amount of conduction. It is estimated that the klystron-facing surface of the waveguide plane will reach 115°C and the opposite surface will radiate to space at $T_W = 95^\circ\text{C}$.

The radiator performance of the top surface must be modified by a fin effectiveness associated with a finite heat pipe spacing. According to Lieblien (Reference 2), effectiveness can be expressed in terms of non-dimensional fin width.

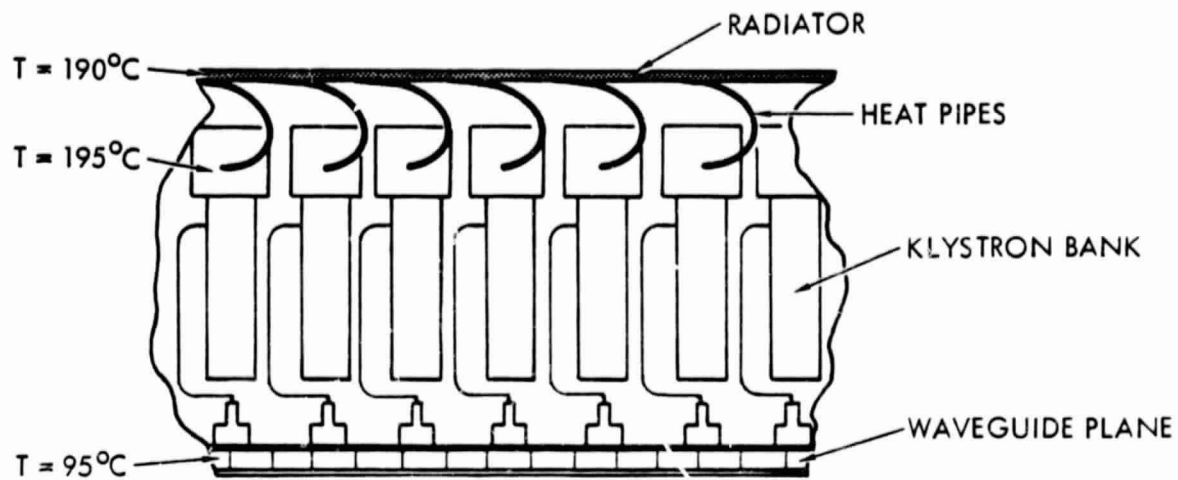
$$X = \ell \sqrt{\frac{\sigma \epsilon T_0^3}{k \delta}} \quad (1)$$

For an effective fin width $\ell = 76.2$ mm, a blackened aluminum radiator of 0.762 mm thickness δ , and a root temp T_0 of 463°K (190°C) the X parameter has the value 0.55, giving a fin effectiveness of 0.75 (Reference 2).

$$\dot{Q}_{\text{tot}} = A \left[\epsilon \eta \sigma T_R^4 + \epsilon \sigma T_W^4 \right] = 24 \text{ kW} \quad (2)$$

This is less than two-thirds of the desired 38.5 kW. In order to achieve the higher level of heat rejection, the radiator effectiveness must be increased and the conduction to the waveguide plane must be improved so as to raise the temperature of the latter. Another alternative is to allow klystron temperatures to rise (to an estimated 250°C) in order to reject the required heat from the present configuration. This is only an acceptable solution if klystron lifetime is not reduced significantly by the elevated temperature.

CLOSE-PACKED KLYSTRON PANEL
(24 KW REJECTION LEVEL)



16 KLYSTRON PANEL
(WITH CONVERTERS)

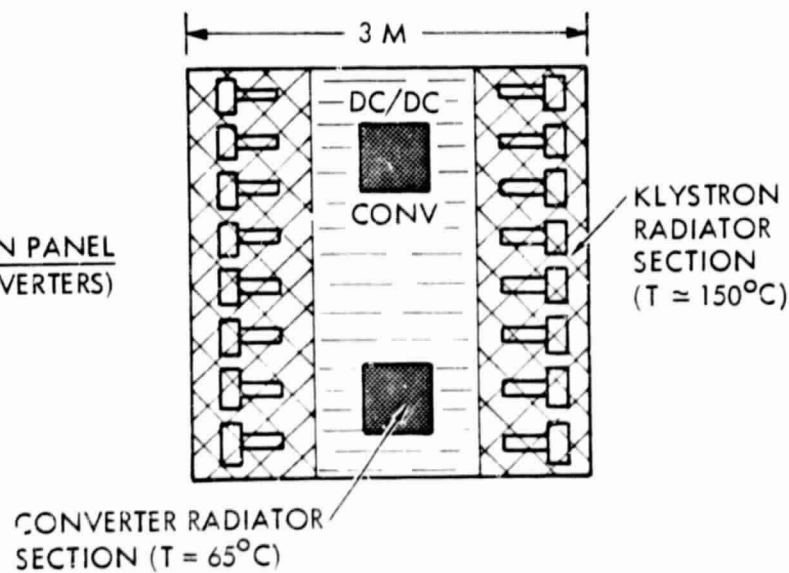


Figure 2.3.7-1. Klystron Panel Configurations

Thermal Control of 16-Klystron Panels

The remainder of the klystron tubes are mounted, 16 to a panel, along with two dc/dc converter units (see Figure 2.3.7-1). The total heat dissipation for a 3-meter by 3-meter panel is listed in Table 2.3.7-1.

Table 2.3.7-1. 16-Klystron Panel Heat Dissipation Requirements

Source	Heat Load (kW)	Radiating Temperature (°C)
Klystrons (16)	5.09	190
Converters (2)	2.50	65
Total		7.59

If the total load is radiated at the lower temperature, the required active radiating area is 16.2 m². This area is nearly equal to the two sides of the 3-m by 3-m panel and would require special methods to ensure effective radiation from the waveguide surface. An alternative approach, shown in Figure 2.3.7-1, uses only the radiator surface, but operates at two temperatures. All of the converter waste heat can be dissipated by 4.7 m² at 65°C while the remaining area can dissipate the klystron heat load at an effective temperature of 137°C or higher.

Heat Dissipation Requirements for SEPS Unit

Another concentrated source of power on the SPS flight test article is the solar electric propulsion system (SEPS). The high-temperature surfaces of the thruster electrodes will cool by self-radiation, provided no obstructions are present. The power processing units are enclosed and require specific provisions for heat rejection. Each 6-kW SEPS unit must dissipate approximately 0.9 kW in the power processor at a maximum temperature of about 60°C.

Orientation of a SEPS unit depends on its thrust program and thus cannot assume a favorable orientation with respect to the sun. For this reason, it is necessary to provide some means of preventing reverse heat flow from radiator surfaces exposed to direct solar heating. Also, there must be enough unexposed radiator surface to reject the required heat load. These requirements are usually met by providing pairs of opposed one-sided radiator panels. Backflow of heat is prevented by louvers or variable-conductance heat pipes. Each SEPS unit requires two opposing surfaces of 2.5 m² each. These may be combined to serve a module containing several units.



Rockwell International
Space Division

References

1. Solar Power Satellite Concept Evaluation/Activities Report, NASA/JSC, JSC-12913 (July 1977).
2. Lieblien, Seymour, "Analysis of Temperature Distribution and Radiant Heat Transfer Along a Rectangular Fin of Constant Thickness," NASA TN D-196 (November 1969).

NOMENCLATURE

<u>Symbol</u>	<u>Explanation</u>
A	Area
Cp	Specific heat
D	Girder depth
\bar{i}	Solar radiation fraction
I_{sc}	Solar constant
k	Thermal conductivity
L	Length
l	Fin width
p	Open fraction
Q	Energy flow rate
T	Absolute temperature
t	Time
W	Width
X	Nondimensional width
Greek Letters:	
α	Solar absorptivity
δ	Thickness, depth
ϵ	Thermal emissivity
η	Effectiveness
θ	Angle of incidence
ρ	Density
σ	Stefan-Boltzmann constant
τ	Thermal time constant
$\bar{\tau}$	Graybody shape factor

Subscripts:

c	Pertains to conduction
m	Pertains to mesh
o	Initial or base value
R	Pertains to radiation
W	Pertains to girder web or to waveguide

C-2

2.4 MASS PROPERTIES

Table 2.4-1 presents the mass summary statement for the SPS Flight Test Article configuration under study.

2.4.1 Rationale for Analysis

Basic structure masses were based on structures analysis and sizing. The docking port masses were based on modified Apollo/Soyuz units. The rotary joint mass was calculated from a layout. The secondary structure for the SPS consists of the solar blanket tie-down brackets.

The solar panel mass was based on the standard Lockheed panel of 0.752m x 4m dimension with a mass of 3.147 kg. The remainder of the electrical power and distribution mass was based on analysis and requirements.

The attitude control mass, consisting of CMG's and the RCS were based on requirements reflected by the satellite's mass properties and mission requirements.

The mass of the TT&C, Thermal and Information Management and Control are estimates based on prior studies. The mass of the Microwave and Communication Systems were based on scaling algorithms. Propellant mass was based on satellite mass properties and mission requirements.

Discussion

For the analysis of this project one may consider the microwave system as a payload of the SPS Test Article spacecraft. The microwave system payload mass represents 24% of the total satellite initial LEO (wet) mass. The major mass item is the electrical power and distribution system which is 36% of the total satellite initial LEO (wet) mass. The solar panels account for 30% of the EP&D system.

The structure and mechanisms represent 17% of the total satellite mass. The docking ports constitute 44% of the structure and mechanism mass.

The SEP orbit transfer system mass is approximately 22% of the total satellite gross weight. This gives a mass ratio of 0.115.

Table 2.4-1
Mass Summary - SPS Flight Test Article
(Mass in Kg)

<u>Structure & Mechanisms</u>	(6,472)
Basic Structure	594
Secondary Structure	32
System Control Module	2,268
Mechanisms	(3,578)
Docking Ports	2,838
Rotary Joint Module - MW Ant. End Only (1)	740
<u>Electrical Power & Distribution</u>	(13,730)
Solar Energy Collector	(4,091)
Solar Panels	4,091
Battery System	(1,134)
Batteries	943
Charger	103
Wire Harness & Control	88
Distribution	(7,261)
Conductor	(4,822)
EPD Wire Harness	1,503
Ion Propulsion Harness	1,798
Antenna Harness	1,473
Slip Ring/Brushes	48
Equipment	(2,439)
Blanket Switch Box	893
EPD Panel	962
Ion Propulsion Switch Box	584
Supports & Secondary Structure	(1,244)

Table 2.4-1 (Cont)
Mass Summary - SPS Flight Test Article

<u>Attitude Control</u>	(2,050)
Control Moment Gyro	93
Reaction Control System (Inert)	1,957
<u>TT&C</u>	(136)
<u>Thermal</u> (Battery & Equipment Cooling & Radiator)	(230)
<u>Microwave System</u>	(9,141)
Klystrons (279)	8,175
Thermal Test Array	386
Phase Control Test Array	580
<u>Information Management & Control</u>	(800)
Data Management	500
Instrumentation	300
TOTAL - SATELLITE, Dry (Initial LEO)	32,559
RCS Propellant	5,239
TOTAL - SATELLITE, Wet (Initial LEO)	37,798
Rotary Joint - Elect Prop. Only End (1)	740
TOTAL - SATELLITE, Wet; GEO Mission	38,538
ORBIT TRANSFER PROPULSION	
Inert (6 Modules)	4,967
TOTAL - GEO Burn-out	43,505
Propellant (Mercury)	5,680
TOTAL - GROSS MASS	49,185

2.5 CONSTRUCTION REQUIREMENTS - SPS TEST ARTICLE

The following presentation identifies general and specified requirements applicable to construction equipment and processes which are inherent in the specific preliminary design of the Space Power Satellite Test Article (Drawing 42665-27).

These construction requirements are inputs to the space construction analyses of Task 2.0. As discussed in this report introduction, the intent is to narrow down the total range of options by providing the important guidelines and constraints affecting construction strategy, along with characteristics of the major component parts which must be handled during the construction process of this specific project. Further, the key dimensional tolerances potentially interacting with the construction accuracies are also included.

2.5.1 Overall Strategy

The following are specific, predetermined construction approaches inherent in the design.

- o The basic structural beams of triangular cross-section are fabricated by a beam builder machine similar to that developed by General Dynamics (Reference 1). The material is a non-metallic composite of low thermal coefficient of expansion.
- o Basic structural beams are welded together at right angles to form a truss.
- o The major modular installations are accomplished using a type of androgynous mating, interleaving petal, docking/berthing port similar to that identified as baseline for the shuttle program. These ports are welded into the ends of the beams.
- o There are several diagonal bracing struts which are based on the "dixie-cup", hollow, tapered tube concept developed by Rockwell International and Langley Research Center. These utilize a ball and socket joint concept at each end, which is self-latching upon assembly.
- o The electrical power and signal wire runs are composed of segments joined at junction boxes and attached to outsides of beams between the various installed modules.
- o The overall configuration was developed to permit reach to critical installation points by use of the Shuttle Orbiter RMS, assuming the structure can be built using a construction fixture attached to the Shuttle Orbiter payload bay. In this concept the constructed spacecraft is progressively transported across the top of the orbiter along the Y axis. Other approaches are not precluded.

2.5.2 Component Inventory

As a means to help quantify the magnitude and nature of the construction process, an inventory of the significant component parts has been developed. Table 2.5.2-1 lists the quantity (number of parts), the overall dimensions and the mass which must be handled during construction. Also noted are key construction features which relate to transport/handling or joining parts together or transporting parts.

2.5.3 General Construction Sequence Guidelines

The following general guidelines apply to planning an effective construction sequence.

- o Set up construction fixture early in project (probably first activity).
- o The longitudinal beams must be fabricated prior to assembling any cross beams or transverse beams to them. It is probably desirable to manufacture the longitudinal beams first to avoid the necessity of storing cross beams or using two beam machines simultaneously.
- o Construct basic structure prior to attaching subsystem modules and flexible items such as electrical power and signal lines. Note that paralleling electrical power and signal lines can be installed as a beam is fabricated or installed.
- o Install nickel-hydrogen batteries toward end of the construction project, provide for thermal conditioning (radiators) at time of installation, and put batteries on-line as soon as possible to avoid extended periods of storage in charged condition.
- o Consider thermal constraints on flexible plastic wire coverings and other materials which might be brittle at low temperatures. Schedule for deployment during periods of solar heating when required (or provide other thermal conditioning).
- o Install large-area solar arrays as late as possible to avoid destabilizing influence of drag forces.

2.5.4 General Tolerances

Table 2.5.4-1 defines the construction tolerances for the dimensions of the component parts and their interfaces which are judged to be critical to mission success of the spacecraft. All other interfaces will have tolerances specified which are consistent with good engineering practice. A description of the rationale and analysis effort which resulted in Table 2.5.4-1 appears in Appendix B.

Table 2.5.2-1 Component Inventory - SPS Test Article

ITEM DESCRIPTION	QUAN	SIZE HANDLED			HEIGHT OR DIA (m)	MASS (Kg)	KEY CONSTRUCTION FEATURES
		LENGTH (m)	WIDTH (m)				
Microwave Antenna	1	15	3		3.5	9,141	Large, massive, deploy- able assembly; one berth- ing port
Rotary Joint	2	2.3	-		2.0 Dia	2,286	Moderately large, no mas- sive module, one berthing port
Sep Assembly 2nd Panel	2	5.6	1.5		1.2	1,774	Long, narrow module; one insertion port
Single Panel	4	12.0	1.5		1.2	1,781	
System Support Housing	1	11.6	4.0		1.7	2,361	Large module two berthing ports
Docking Port End Fittings	8	2.0	-		2.0 Dia	~ 6	Small, but relatively dense, insertion & weld to join
Longitudinal Beams	2	215.8	1.4		1.2	441	Extremely long, thin, low density
Cross Beams	6	20.6	1.4		1.2	126	Relatively long, thin, low density
Struts, Double Tapered	4	2.6	-		.3 Dia	~ 5	Long, thin shape; ball end
RCS Module	4	3.0	2.5		2.0	1,779	High density, compact module. Berthing port installation
Bridge Fitting	1	11.6	3.5		1.7	~ 150	Low density trusswork module/structure, two berthing port install'n

Table 2.5.2-1 - Component Inventory - SPS Test Article
(Continued)

ITEM DESCRIPTION	QUAN	SIZE HANDLED			MASS (Kg)	KEY CONSTRUCTION FEATURES
		LENGTH (m)	WIDTH (m)	HEIGHT OR DIA (m)		
Solar Array Blankets	25	4.0	.8	1.0	164	Flexible, folding material deployed and tensioned
Electrical Power Distribution Boxes	25	1.5	.7	.3	~ 36	Small items
Solar Array Attach Brackets	90	1.5	.2	.1	Negl	Light, small items
Junction Boxes	12	.5	.2	.2	~ 30	Small items
Retention Clips - Wire Segment	1,050	.06	.04	.08	~ 1 (total)	Large number of small items
Wire Bundles, Power	100	2	-	<.1 Dia	10.5	Short items
	42	4 to 6	-	<.1 Dia	21	Moderate length, flexible
	26	8 to 12	-	<.1 Dia	38	Shorter than orbiter bay
	18	42	-	<.1 Dia	153	Long, flexible items to be deployed
Signal and Data Lines	21	4 to 6	-	<.1 Dia	4.0	Relatively flexible, long, thin items to be deployed
	12	8 to 12	-	<.1 Dia	8.0	
	5	42	-	<.1 Dia	33.5	

2-94

Science Systems Division
Space Systems Group



Table 2.5.4-1. Critical Construction Tolerances—SPS Test Article

ITEM DESCRIPTION	CRITICAL DIMENSION	TOLERANCE ALLOCATION	SYSTEMS AFFECTED BY CRITICAL DIMENSIONS	CONSTRUCTION OPERATION
MICROWAVE ANTENNA	DOCKING PORT ALIGN.	$\pm 0.1^\circ$	ANTENNA	GROUND FAB
ROTARY JOINT	DOCKING PORT ALIGN.	$\pm 0.1^\circ$	ANTENNA & SEP	GROUND FAB
SEP ASSEMBLY	NONE	-	-	-
SYS. SUPPORT HOUSING	DOCKING PORT ALIGN.	$\pm 0.1^\circ$	ANTENNA & SEP	GROUND FAB
DOCKING PORT (STRUCT.)	FACE ALIGN WITH BEAM END (± 0.1 CM)	$\pm 0.1^\circ$	RCS, SYS. SUPPORT HOUSING	ASSEMBLY
LONGITUDINAL BEAM	LENGTH (± 0.1 CM)	$\pm 0.1^\circ$	SYS. SUP. HOUSING	FABRICATION
CROSS-BEAM	TWISTED	$\pm 0.2^\circ$	RCS	FAB/ASSEMBLY
	BOWED (± 2.5 CM)	$\pm 0.1^\circ$	RCS	FAB/ASSEMBLY
STRUT	NONE	-	-	-
RCS MODULE	DOCKING PORT ALIGN.	$\pm 0.1^\circ$	RCS	GROUND FAB
BRIDGE FITTING	NONE	-	-	-
SOLAR ARRAY BLANKETS	↓	↓	↓	↓
EPD BOXES	↓	↓	↓	↓
SOLAR ARRAY ATTACH BRACKETS	↓	↓	↓	↓
JUNCTION BOXES	↓	↓	↓	↓
WIRE SEGMENTS	NONE	-	-	-



2.5.5 References

1. General Dynamics

Space Construction Automated Fabrication Experiment Definition Study (SCAFEDS) Part II, Mid-Term Briefing. Briefing No. CASD-ASP77-011, 9 November 1977.

3.0 DEFINITION OF ADVANCED TECHNOLOGY COMMUNICATIONS PLATFORMS

Definitions of two similar antenna platform construction projects are presented in the following pages. Their major similarities lie in the areas of communication antenna design, solar array design, RCS and orbit transfer propulsion, TT&C, and in guidance and navigation. Major differences appear in the design of the basic structure to which the subsystems are attached. Therefore, to avoid needless repetition, the features common to both projects are discussed together, while separate descriptions are provided for structural concepts and those aspects closely related to attachments to those dissimilar structures.

ORIGINAL PAGE IS
OF POOR QUALITY.

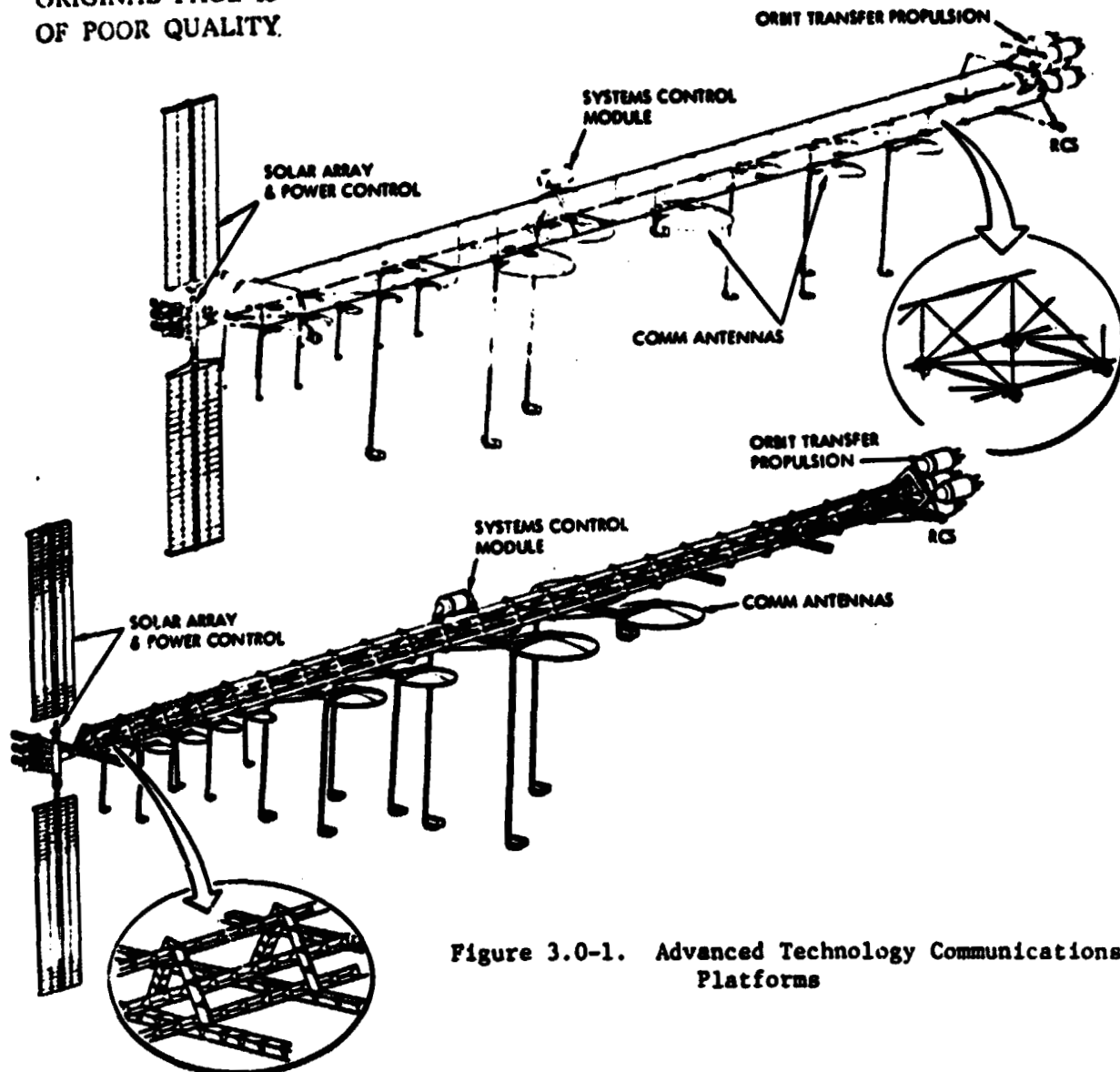


Figure 3.0-1. Advanced Technology Communications Platforms

3.1 ADVANCED COMMUNICATIONS PLATFORM PROJECT SCENARIO

The purpose of this section is to provide a "word picture" of the major factors likely to influence the design concept for this project. It includes a brief summary of the overall motivating environment surrounding the project, general operating modes suited to the project objectives and servicing/growth considerations related to the scope and objectives of the project. It serves as an abbreviated approach in establishing the top level system requirements for use in concept synthesis and design analyses.

3.1.1 General

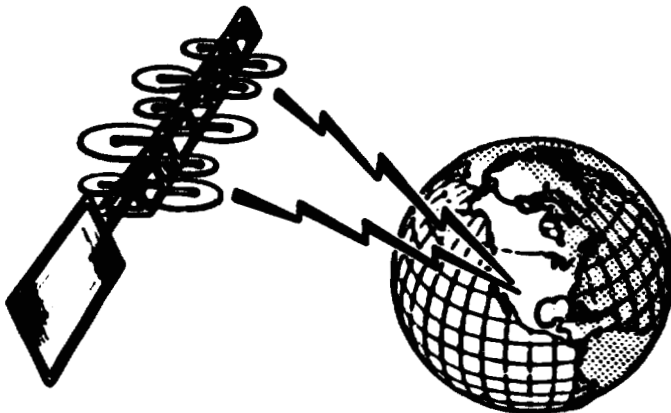
The scenario for the Advanced Communications Platform is outlined in Figure 3.1-1. This scenario presumes the current mushrooming worldwide growth in both domestic and international space communications will continue. This growth is particularly important to the rapidly developing third world countries. It further presumes the available space in the geosynchronous arc will become overcrowded with the continued application of the present individual satellite concept. Higher capacity approaches designed for more efficient use of the available frequency spectrum and with merged political/economic interests will be required to meet the projected growth needs. Much has been written about the issues and interactions between the efficient utilization of the "geo-sync" natural resource and the need for safeguarding the future interests of all nations, even those not now in a position to fully exploit or even begin to exploit the use of their "fair share" of this resource. It is beyond the scope of this study to resolve these problems, but the study assumes that solutions will be found, and that more efficient concepts will be implemented.

The emphasis here has been to "leapfrog" the political arena and focus on the technical nature of more efficient advanced communications systems. Toward this end it is noted that current technology yields satellite service lifetimes of 5 to 7 years. Present plans call for replacement of existing satellites in the 1983 time period. These replacement systems are already under contract and on the drawing boards. Thus, the earliest that a large advanced communications platform could appear is in the 1990 time period, and this is the timeframe selected for the communications project scenario.

In focusing on the technical nature of the communications concept design, further emphasis has been placed on general sizing to U.S. needs. These needs are perhaps better known than world-wide traffic projections, but more importantly, the U.S. will likely be the first to apply advanced "platform technology." This, then, along with the above discussion is the general background and motivating environment surrounding the Advanced Communications Platform project. More specific characteristics are discussed in the following subsections.

3.1.2 Platform Concept Approach

The purpose of the advanced communications platform is to provide high performance point-to-point communication links covering the entire continental United States. The platform will supplement existing services provided by the common carriers, increase traffic capacity, and it will provide for direct



OPERATING SCENARIO

GEO ORBIT—USA ACCESS
STABILIZED EARTH POINTING
EW & NS STATIONKEEPING
UP TO 20 YRS SERVICE LIFE
PROVIDE UNINTERRUPTED SERVICE

SERVICING SCENARIO

UNMANNED/REMOTE
5-7 YR SERVICE INTERVAL
RESUPPLY STATIONKEEPING PROP
REPLACE FAILED/DEGRADED MODULES

GROWTH SCENARIO

EXPAND CAPACITY, POSS NEW SERVICES
ADD 18-30 GHZ ANTENNAS, NEW MODULATION ELEC
ADD SPACE-TO-SPACE LINK(S)
ADD ELEC POWER

PROJECT SCOPE

1990 TIME PERIOD
SATISFY PROJECTED GROWTH FOR CURRENT
SERVICES & INTRO NEW SERVICES
TELEPHONE/TELECONFERENCE, VIDEO....

REDUCE GEO CONGESTION
COULD BE GLOBAL SYSTEM

CONFIGURATION/DESIGN IMPACTS

- EPS SIZED FOR CONTINUOUS GEO OPS INCLUDING OCCULTATION PERIODS
- ACCURATE BEAM POINTING/STABIL INCLUDING DURING STATIC-KEEP
- ACCESS FOR SERVICING & GROWTH
- LOCATIONS FOR ADDED ANTENNAS
- PROVISION FOR ADDED ELEC POWER

Figure 3.1-1. Advanced Communications Platform Scenario

links to areas where landline and radio relay networks are relatively "thin." It will perform the functions of the seven U.S. domestic satellites that now contribute to crowding of the geostationary arc at western longitudes. The platform will be required to provide multiple, high-gain spot beams covering the continental U.S., in contrast to the single CONUS coverage beams of each of the seven current satellites. The system will operate in the 4- and 6-GHz bands currently in use, with additional bands at 12 to 14 GHz, and will have the potential for future growth into the 20- to 30-GHz region of the spectrum if this proves feasible and desirable.

The platform concept produces an inversion of complexity in the sense that the roles now played by the ground and by the space segments will be interchanged. Currently, communications satellites have one or two simple antennas in the 1-m to 3-m size range and carry relatively little in the way of switching equipment. Ground terminals, which are few in number, use large antennas, in the 10-m to 30-m range, with complex switching networks. Complexity inversion requires the space platform to carry a multiplicity of large (10 to 20 m) highly sophisticated antennas, each generating many independent beams that will demand complexity in the switching and accessing networks in space. By contrast, the number of ground terminals will become very large, but the equipment will be simpler and much less expensive, using antennas, for example, in the 1- to 4-m range. In addition, ground networks will be much simplified.

The needed complexity inversion is made possible by the development of on-orbit construction and assembly techniques along with the transportation capability afforded by the Space Shuttle. The constraints on satellite and antenna size formerly imposed by the launch vehicle and its shroud are thus removed, not only permitting, but encouraging, the use of orbiting platforms supporting multiple large antennas, each optimized to its own communications task, and carrying large solar arrays to supply power for a complex of amplifiers, switches, and processing networks.

3.1.3 Operating Scenario

The overall operating scenario for the communications platform is depicted in the mission profile of Figure 3.1-2. The complete system will be constructed and checked out in LEO. Orbit transfer propulsion modules will then be delivered and mounted. The fully assembled platform will then be transported to GEO at a longitude serving US communications needs. Upon arrival at its mission station the appropriate flight modes will be activated and the communications system will be initialized. The platform system will then be ready for communications operations and will begin absorbing the projected traffic demands.

A communications platform requiring space construction and sized for future needs will represent a significant investment in both technology development and flight hardware. To assure an adequate return on this investment, a 20-year service life is required. This long life, together with its high capacity, creates several important implications. First, the extremely high capacity of such systems means millions of users are dependent upon its continued operation, and the need for uninterrupted service is paramount. Second, the long operational life implies the need for on-orbit servicing. Together (long life and

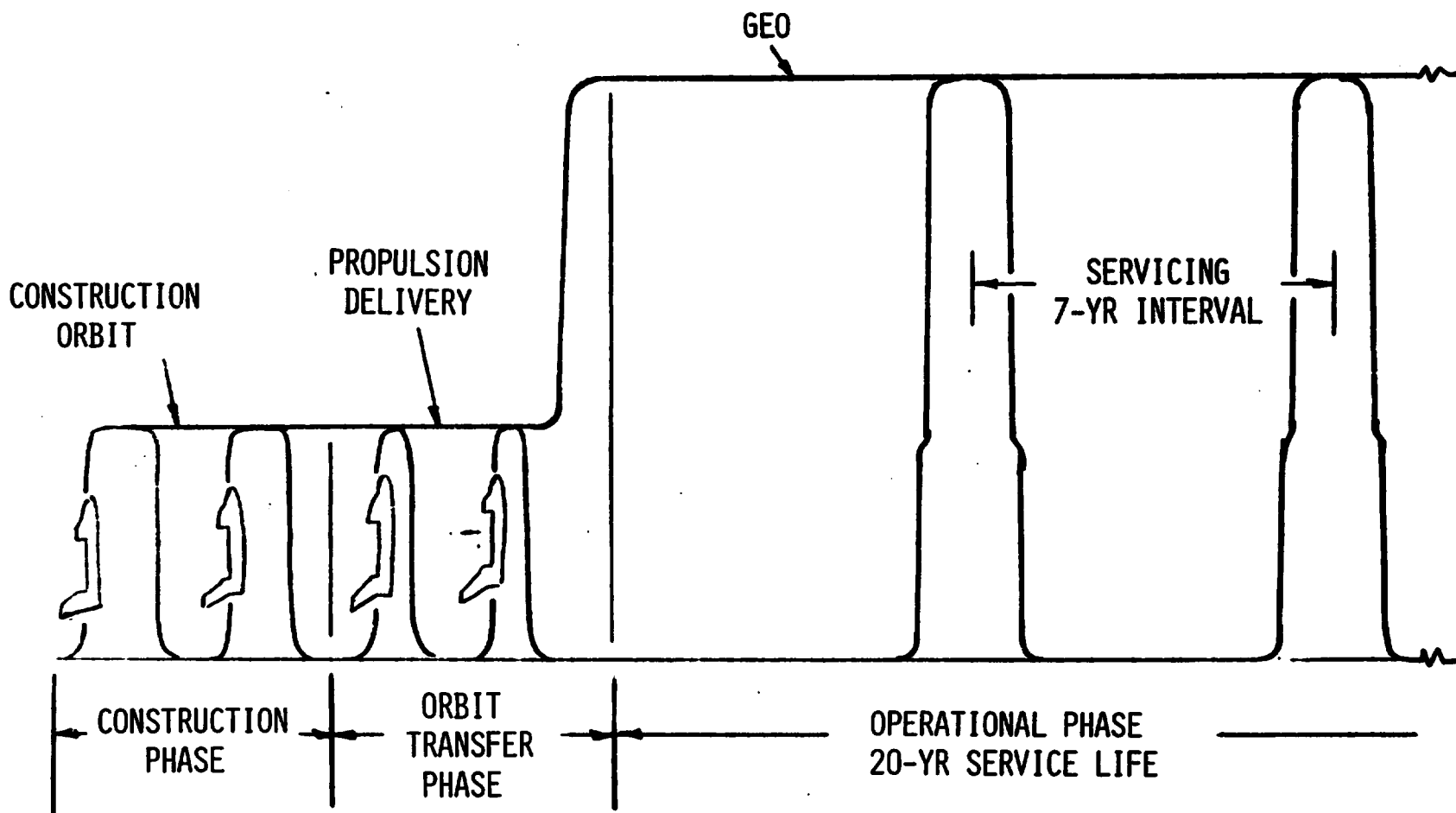


Figure 3.1-2. Mission Profile Advanced Communications Platform

ORIGINAL PAGE IS
OF POOR QUALITY

Satellite Systems Division
Space Systems Group



uninterrupted service) they imply the need for servicing approaches which minimize or completely non-interfere with the on-going communications operations. In fact, all routine platform operations as well as servicing and growth installation operations must be performed with minimal or no interruptions in services.

Another requirement introduced by the need for uninterrupted service is the sizing of energy storage capacity. This must be sized to maintain full service through maximum sun occultation periods. Sun occultations can occur due to both earth and moon shadowing. Earth shadowing occurs over a two month span, twice per year, near the equinox periods and has a maximum shadow interval of approximately 1.1 hours. Moon shadowing is much less frequent and is coupled to the lunar eclipse cycle and specific platform ephemeris characteristics. The moon shadowing intervals can be as long as 3 hours, but are governed by the specific eclipse geometry which varies from event to event. The combined set of conditions producing worst case moon shadowing is very rare and may not occur over the life of the platform. Thus, for the concept definition presented herein the earth shadowing interval was used for establishing energy storage requirements.

In addition to continuous service the platform must provide a stable earth pointing base for precision pointing the high performance communications antennas. To reduce the amount of antenna/platform steering required to maintain beam coverage patterns, north-south stationkeeping is required in addition to the usual east-west drift control. All stationkeeping maneuvers must be "soft" in nature and sufficiently isolated from the beam steering dynamics to maintain antenna pointing stability.

Thus, the critical requirements derived from the platform operating scenario are: a 20 year service life with a goal of uninterrupted service.

3.1.4 Servicing and Growth

Servicing and growth considerations are also important elements in the overall project scenario. However, in keeping with the preliminary nature of the system definition presented here, the scope of servicing considerations is necessarily limited. Trades between reliability, redundancy and level of servicing are inappropriate. Emphasis is on the assurance that the project design not preclude on-orbit servicing, thus, allowing these trades to be made in the future when the design definition reaches the appropriate level of detail.

In addition to the need for long life and uninterrupted service, there is another important driver which is perhaps unique to the Advanced Communications Platform and which significantly affects servicing and growth requirements—it is the impact of rapid technological progress on the platform growth process. The rapid technological progress being made on nearly all fronts of the micro-electronics/data processing industry will stimulate increased requirements for updating the flight and ground hardware. New developments bring on higher efficiencies with improved cost-effective economies which must periodically be incorporated into the platform to maintain competitive operations.

Servicing concepts for meeting these requirements must also consider the time period of their application. As indicated earlier in the scenario discussed, the 1990 time period was assumed for the introduction of the Advanced Communications Platform. It is not likely that manned capabilities will be extended to geosynchronous orbit in time to support this schedule. Manned geosync operations will probably appear during the 20 year lifetime of the platform, but should not be baselined into the initial platform servicing concepts. In this light, servicing options centered on remote-teleoperator concepts were selected for this study. Manned servicing, if cost effective, could perhaps be introduced later in the platform mission along with the updated growth mission electronics.

Commensurate with remote servicing approaches and with the gross levels of configuration definition available in these early stages of system conceptual design, servicing considerations here have emphasized the changeout of major elements or modules. These would also apply to the module updating changeouts associated with system growth and technology advances. Some example replacement operations to meet these needs could involve new ways to repair and/or add solar array panels without interrupting service, replacing failed CMG units or expended RCS propellant modules/quads and could also include ways to install new power/signal wire runs for new technology elements without interrupting service.

A final important servicing consideration is the issue of scheduled versus unscheduled maintenance. The relatively high costs for transportation to GEO will likely preclude early platform concepts planned solely around unscheduled servicing. However, once sufficient numbers of GEO systems designed for on-orbit servicing are in place unscheduled maintenance may have a more prominent role. If the proper levels of failure tolerance are designed into the GEO systems, the failures of several platforms could be "stored up" until they would utilize a full maintenance trip. With this concept servicing would be conducted on a demand basis somewhere between "pure" scheduled and "pure" unscheduled approaches. Since this study is aimed at early communications platform concepts a scheduled maintenance approach was selected with a 7-year servicing interval.

The length of the interval was mainly based on current satellite design life values. Present designs typically offer a 7-year life. Increases in service life might be expected with future advances in reliability, but these would tend to be offset by increases in complexity associated with the high capacity communications platforms. This coupled with the possible further need for revisits to update and/or add capacity to the system led to the selection of the 7-year servicing interval for this study.

All of the above scenario conditions result in the top level system requirements summarized in Table 3.1-1. These requirements form the basic framework from which the individual subsystems requirements and concepts were derived.

Table 3.1-1. Advanced Communications Platform Project Requirements

Mission Objective

- Provide order-of-magnitude increase in U.S. space communications network capability

Operational Time Period

- 1990 IOC

Operational Orbit

- Geosynchronous equatorial, good access to U.S.

Mission Flight Operations

- Orientation—principal axes, Y-POP and Z-nadir
- Comm. antennas precision steer with RF autotrack
- Platform performs E-W and N-S stationkeeping
- Continuous, uninterrupted communications services are desired
- Platform service life—20 years

Construction and Orbit Transfer

- Design for construction in LEO
- Design for low-thrust chemical propulsion LEO-to-GEO orbit transfer

Servicing

- Design for seven-year service interval
- Consider remote teleoperator available initially
- Consider direct man-in-the-loop for growth only
- Consider design goal to provide servicing without interrupting communications services

Growth

- Consider ways to add communications capacity
- Consider need for updating electronics to rapidly progressing technology
- Consider design of growth installations to preclude interruptions in communications services

3.2 CONFIGURATION DESCRIPTIONS—ADVANCED COMMUNICATIONS PLATFORMS

Two structural arrangement concepts were developed to implement the communications platform requirements as discussed in Section 3.1, Project Scenarios. Figures 3.2-1 and 3.2-2 illustrate these two concepts. Except for minor variations, such as the arrangement of the antennas and the attaching concept of the system control module, most of the subsystems are identical between the two concepts. The variations are a result of the different structural arrangement concepts selected for development in this study.

The figures illustrate a composite of the three configurations for each concept. The configuration in LEO just prior to orbit transfer will be as illustrated except that all of the antennas will have their feed horn folded as shown on one of the large antennas. The GEO operational configuration will have all of the antennas extended, but will only have two propulsion modules remaining. The three first-stage burn propulsion modules will have been jettisoned. The third configuration is the LEO checkout arrangement which will have all antennas deployed, but the orbit transfer modules will not have been installed at this time. Drawings 42662-25, Erectable Communications Platform, and 42662-26, Space-Fabricated Communications Platform, define these two concepts (Appendix A).

3.2.1 Configuration Description - Erectable Communications Platform

This antenna platform concept consists of an erectable type structure assembled of tapered struts with ball end fittings engaging receptacle type unions. The solar array produces 133 kW of electrical power which includes a 50% allowance for growth. The GN&C system utilizes CMG's and RCS for attitude control and stationkeeping. The platform is boosted to its operating orbit utilizing low-thrust chemical fueled engines. The 16 antennas are arranged in two groups (1) eight 4-6 GHz "C" band receivers and transmitters and (2) eight 12-14 GHz "K" band receivers and transmitters. Growth capability for additional antennas are also provided.

During orbit transfer the solar arrays are folded parallel to the longitudinal axis of the platform which is also the direction of acceleration. Each antenna horn and boom support is also retracted during the orbit transfer mode. The reflector portion of each antenna, however, is in the deployed position.

The platform structure consists of double tapered tubes with ball-type end fittings. The tubes are formed from two conical tubes jointed at their large ends. This concept permits "dixie cup" type packaging of the structural members for transport. Most of the tube assemblies are joined to each other through a receptacle type of union member, creating a pinned joint. However, the antenna mounting concept requires fixed-type joints in order to react the orbit transfer thrust loads. For this condition, the strut ends and the receptacles are designed to transmit moments. The support arrangement for the RCS pods, the systems module, and the orbit transfer propulsion modules utilize struts arranged to form A-frame reaction members. This arrangement results in only axial loads being introduced into these members. Most of the struts are a common length and size. However, the two load conditions described above use unique struts to fulfill their individual requirements.

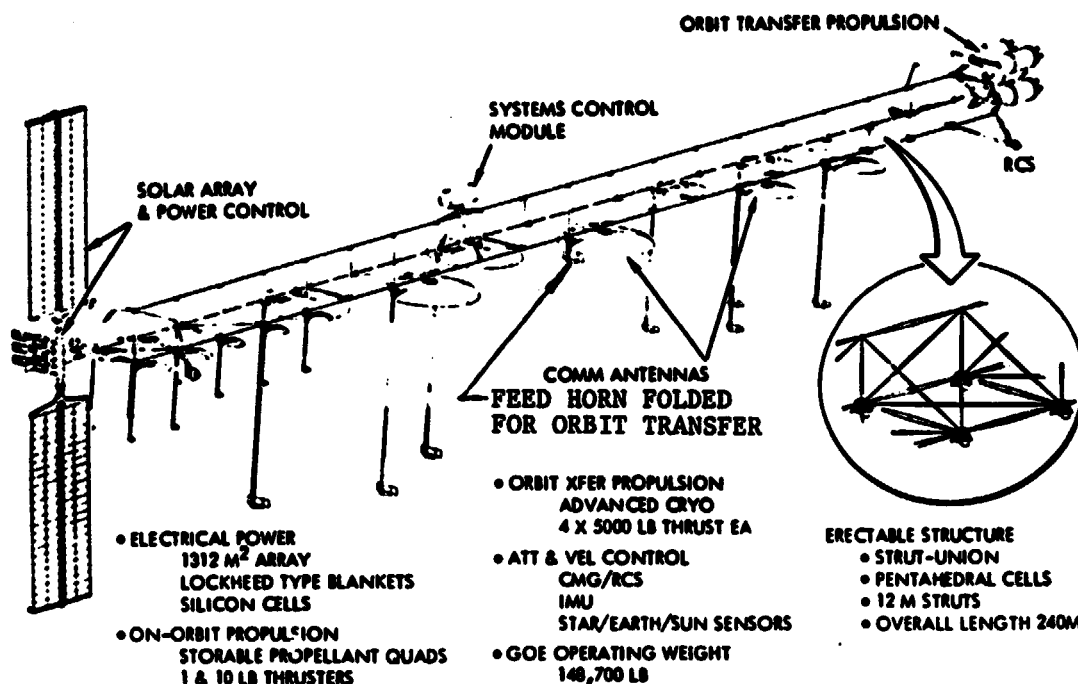


Figure 3.2-1. Erectable Communications Platform Concept

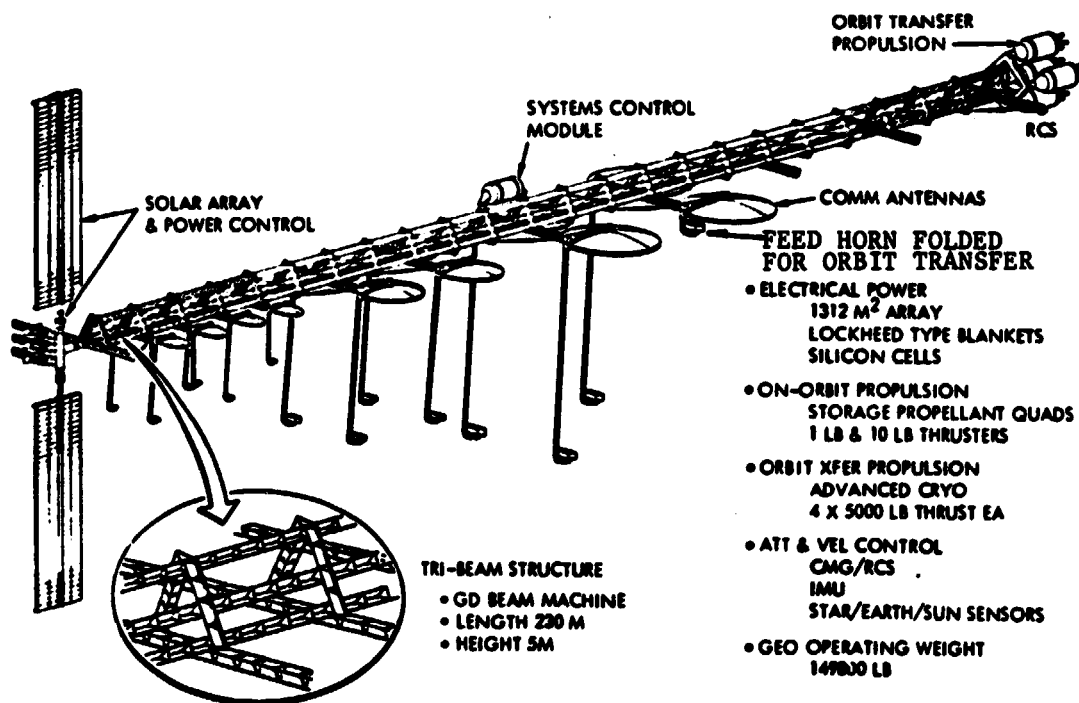


Figure 3.2-2. Space Fab. Communications Platform Concept

The struts are assembled into a linear, pentahedral, structural arrangement. The size of the pentahedrons are dictated by the reach envelope of the orbiter RMS required for assembly of the struts. The size of the individual struts is dictated by the orbit transfer induced loads and by the control stiffness required.

All of the larger modular items such as the antennas, the GN&C/ATT&C module, the orbit transfer engines, and support structure are attached to the structure via berthing ports. The berthing port concept is the three-petal, neuter concept, baselined for the Shuttle orbiter. Because all of the berthing activities are accomplished by using the orbiter RMS, no velocity attenuation is required. Consequently, the berthing ports, both on the structure and on the modules contain no attenuation systems. Structural latches are provided only on the mating module. This permits a final checkout of the active latching system on the ground immediately before transport and assembly in orbit. A utilities interface is provided at each berthing port and each interface will be unique to its particular utilities requirements.

Smaller units such as the electrical junction boxes may be secured to the struts with clamping-type devices that are compatible with the structural capability of the struts. The electrical lines may also be secured to the struts with clamping-type wire-supporting clips.

The solar arrays are mounted to a rotary joint which provides a 360° rotation capability perpendicular to the orbit plane. A 24° nodding capability is also provided to permit full sun illumination during all sun beta angles. A folding capability for orbit transfer is also provided. The orientation of the solar array wings minimizes platform disturbance torque caused by solar pressures. Each solar array wing consists of four SEPS concept panels.

The battery power storage system which is sized to provide continuous operation during the orbit eclipse periods is packaged into three independent units. Each package of batteries include the battery chargers and controls, thermal control insulation and meteoroid protection, and its own heat rejection radiator system. Each unit is a replaceable item.

The rotary joint provides for the power transfer from the power generation system to the platform through a slip ring assembly. Data and control signals between the central control processor and the power generation system is also transferred thru the rotary joint via a dedicated slip ring assembly. The rotary joint as a unit or subassembly is attached to the platform structure via a berthing port. A power and data/control signal interface is also established at this joint.

A system module containing the GN&C CMG's and sensor, the TT&C receivers, transmitters, antennas, etc., and a central data/signal processor is provided in a centrally located position on the platform. Thermal control, meteoroid protection, and heat rejection radiator systems are provided as part of the module to support these systems.

A communications message switching control unit is centrally located within the C-band antenna complex and a similar unit is also centrally located within the K-band antenna complex.

The last items to be installed will be the orbit transfer propulsion modules. The propulsion modules attach to the supporting structure utilizing berthing ports to effect the joint and to establish the lines interfaces. The five modules are arranged to permit an initial firing of three modules and staging to two modules. The three initial modules will be jettisoned during the staging operation. Both the initial and final stages will be aligned to thrust through the c.g. of the platform.

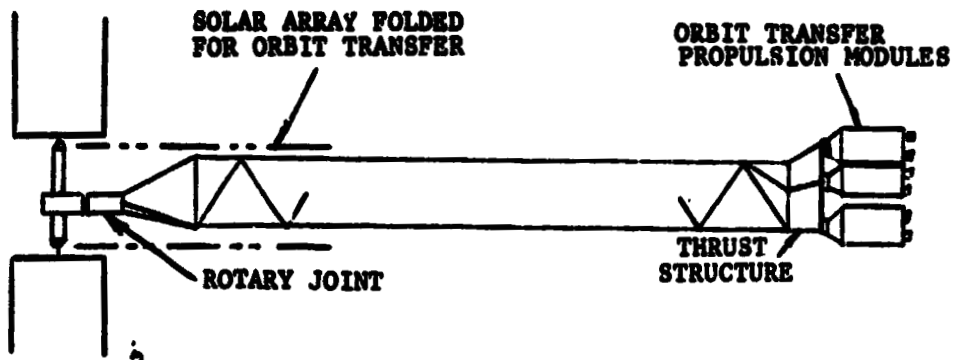
The complete platform less the propulsion modules has an estimated weight of 60,500 kg (133,400 lb).

Trades

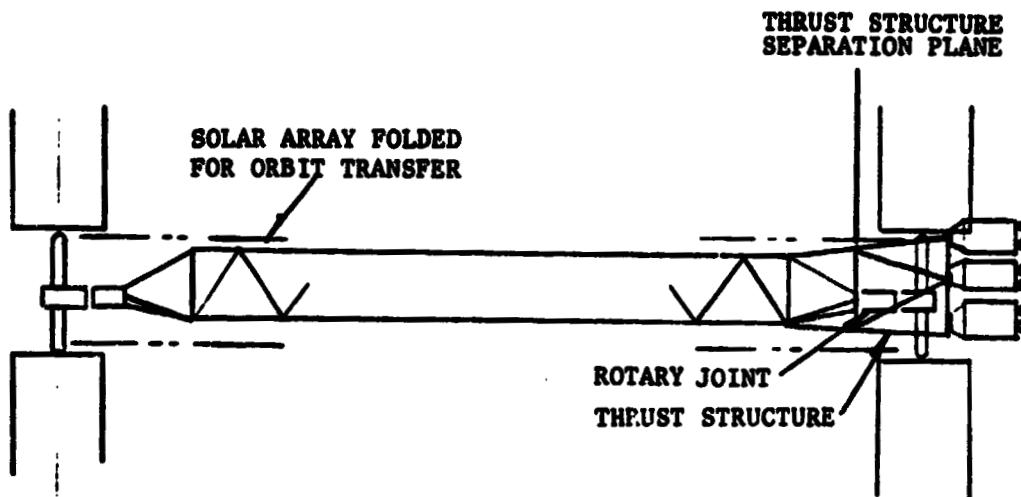
A trade-off study was made concerning the location of the solar arrays. Figure 3.2.1-1 represents the two configurations evaluated. Concept "A" has the total solar array located at one end of the platform opposite to the orbit transfer propulsion system. During orbit transfer the solar arrays are folded, as shown. This arrangement induces only tension loads on the solar array which can be accepted by the solar array deployment and support system and by the individual solar panels.

The alternate arrangement, Concept "B", places the solar arrays on each end of the platform. This arrangement has the advantage of providing a more balanced configuration which would be particularly advantageous to the sizing of the CMG's. This balanced arrangement would eliminate the solar pressure torque disturbance. Since the sizing driver for the CMG's is the solar pressure influence, the CMG's may not be required for this concept. The RCS propellant quantities would also be significantly reduced with the elimination of the CMG dumping requirement.

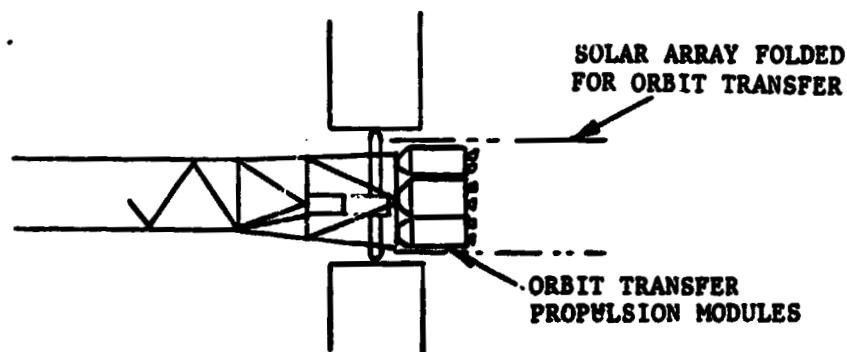
However, this arrangement would require an additional rotary joint, and additional power distribution lines. The additional rotary joint, however, could very well balance out the cost of elimination of the CMG's. Consideration of the reliability of the two power generation systems could require greater power capability in each system to account for a failure mode. Consideration of the orbit transfer mode imposes the issues of array folding and thrust loads. The arrays, folded parallel to the thrust axis as shown, induce undesirable compression loads on the array system. Folding the arrays to permit tension loads only as depicted in Figure 3.2.1-1 (Concept B') exposes the solar panels to propulsion module plume impingement which is undesirable also.



CONCEPT A



CONCEPT B



CONCEPT B'

Figure 3.2.1-1. Solar Array Location Concepts

Consequently, the array location, as shown in Concept A, was selected for this phase of the construction systems analysis study.

3.2.2 Configuration Description—Tri-Beam Space-Fabricated Platform

Many features of this configuration are similar if not identical to those of the erectable concept of the communications antenna platform. Consequently, this description will concentrate on those features that are unique to this concept.

This concept represents an antenna platform consisting of a space fabricated structure, 133 kW of power, including a 50% growth allowance, and a low-thrust chemical-fueled orbit transfer system, with a G&N CMG/RCS control system. The 16 antennas are arranged in two groups: (1) eight 4-6 GHz C-band receivers and transmitters, and (2) eight 12-14 GHz K-band receivers and transmitters. Growth capability for additional antennas is also provided.

During orbit transfer, the solar arrays are folded parallel to the longitudinal axis of the platform which is also the direction of acceleration. The antenna horn and boom support is retracted during the orbit transfer mode. The reflector portion of the antenna remains in the deployed position.

The platform structure consists of members fabricated in orbit by a single beam builder and assembled by use of appropriate fixtures. The configuration is dictated by the reach envelope of the orbiter RMS, by the loads induced during orbit transfer, and by the required control stiffness. The individual beam configuration and the beam builder device are from the General Dynamics SCAPE study concepts.

The installation of the larger modular units utilizes the berthing port concept. The description of this installation concept is identical to that discussed for the erectable antenna platform concept.

Smaller units such as the electrical junction boxes will be secured to the structure with clamp-type devices that are compatible with the structural beam configuration and load capability.

The electrical lines are secured to the structure with special clips. The clips may require pre-punched holes in the post members of the beams.

The electrical power generation system, including the solar arrays and the power storage battery arrangement, and the rotary joint through which the electrical power is transmitted to the antennas and subsystems, are identical to the concept description for the erectable platform.

The systems module contents and installation concept are identical to that of the erectable platform, as also is the communications message switching control units.

The last items to be installed will be the orbit transfer support structure and the orbit transfer propulsion modules. The support structure interfaces with the three longitudinal members of the platform structure by means of berthing ports. The propulsion modules attach to the supporting structure in the same manner.

The five modules are arranged to permit an initial firing of three modules and staging to two modules. The three initial modules will be jettisoned during the staging operation. Both the initial and final stages will be aligned to thrust thru the C.G. of the platform.

The complete platform, less the propulsion modules, has an estimated weight of 61,000 kg (134,200 lbs).

3.3 SUBSYSTEMS DEFINITION

Detailed descriptions of the subsystems for the two Advanced Communications Platforms projects are presented in the following section. In each subsystem discussion there is an introductory summary description which includes design requirements, a detail description, and a discussion of rationale or analytical effort accomplished to support the design of the subsystem. The structural subsystems for the erectable platform and the space-fabricated platform are separately described in Sections 3.3.1 and 3.3.2, respectively. However, the remaining subsystems discussions include considerations for both platforms, since only minor differences are required between them. The order of subsystems presentation is: electrical power, microwave, thermal propulsion, attitude and velocity control, and TT&C. As for the previous project, the mass properties statement and construction requirements follow the subsystems definition.

PRECEDING PAGE BLANK NOT FILMED

3.3.1 Space-Erectable Truss Structure Definition

Objectives

The objectives of the structural engineering reviews and analyses conducted in this space construction study were:

- To ensure construction system study realism by representing structural configurations that are indeed suitable for the total spectrum of mission requirements.
- To ensure identification and understanding of those particular requirements for structural integrity which significantly impact construction.
- To support the total systems weight analysis through definition of component structural sizes.

Erectable Structure Configuration Description

The structural configuration of this erectable communication platform, pictorially described on Drawing 42662-25 (Appendix A), is that of a pentahedral truss. The truss typical bay dimension of 12 meters presents a truss 12 m wide and 8.48 m high, with a total length of 240 m. This truss is the basic strongback to which the 6.0-, 7.5-, 13.8-, and 20.5-meter-diameter communication antennas, solar panel array, thrust structure and propulsion modules, control moment gyro package, and RCS thruster modules are mounted. All of the foregoing items (except the antennas) are mounted to the strongback through pin-ended axially loaded truss-type transition structures. The antennas, however, are mounted to berthing ports that are supported by the end moment carrying longitudinal and lateral members (Figure 3.3.1-1). The moment carrying joints are not only required to sustain the orbit transfer thrust-induced moments, but to provide a necessarily rigid platform for the antenna in order to maintain the required pointing accuracy. The top longitudinal and pyramidal members, however, utilize pin-ended joints.

The significant differences in structural requirements placed upon the bottom longitudinals, bottom diagonals, laterals, top longitudinal, and pyramidal members comprising the basic pentahedral truss bay resulted in three different element sizes. However, all of the elements are tapered to permit "dixie cup" packaging in the orbiter. The alternative of making all these members the same would result in a structure weight penalty of 2270 kg (5000 lb). To the maximum extent practical, the trusses supporting the solar panel array and RCS thruster modules are constructed of 12-m-long tapered tubes. This was not practical, however, for the gyro package and thrust structure (Figure 3.3.1-2), where a mix of element lengths is unavoidable.

The referenced configuration drawing illustrates (on Sheet 1) the communication antenna platform in the operational mode. Sheet 2 illustrates the configuration during thrust ($T/W = 1.96 \text{ N/kg}$) for transfer to geosynchronous orbit. As shown, the antenna feed column masts are stowed to preclude a prohibitive penalizing of the antenna feed column design, large thrust vector inclination, and prohibitive joint moments. The solar panels are stowed to avoid

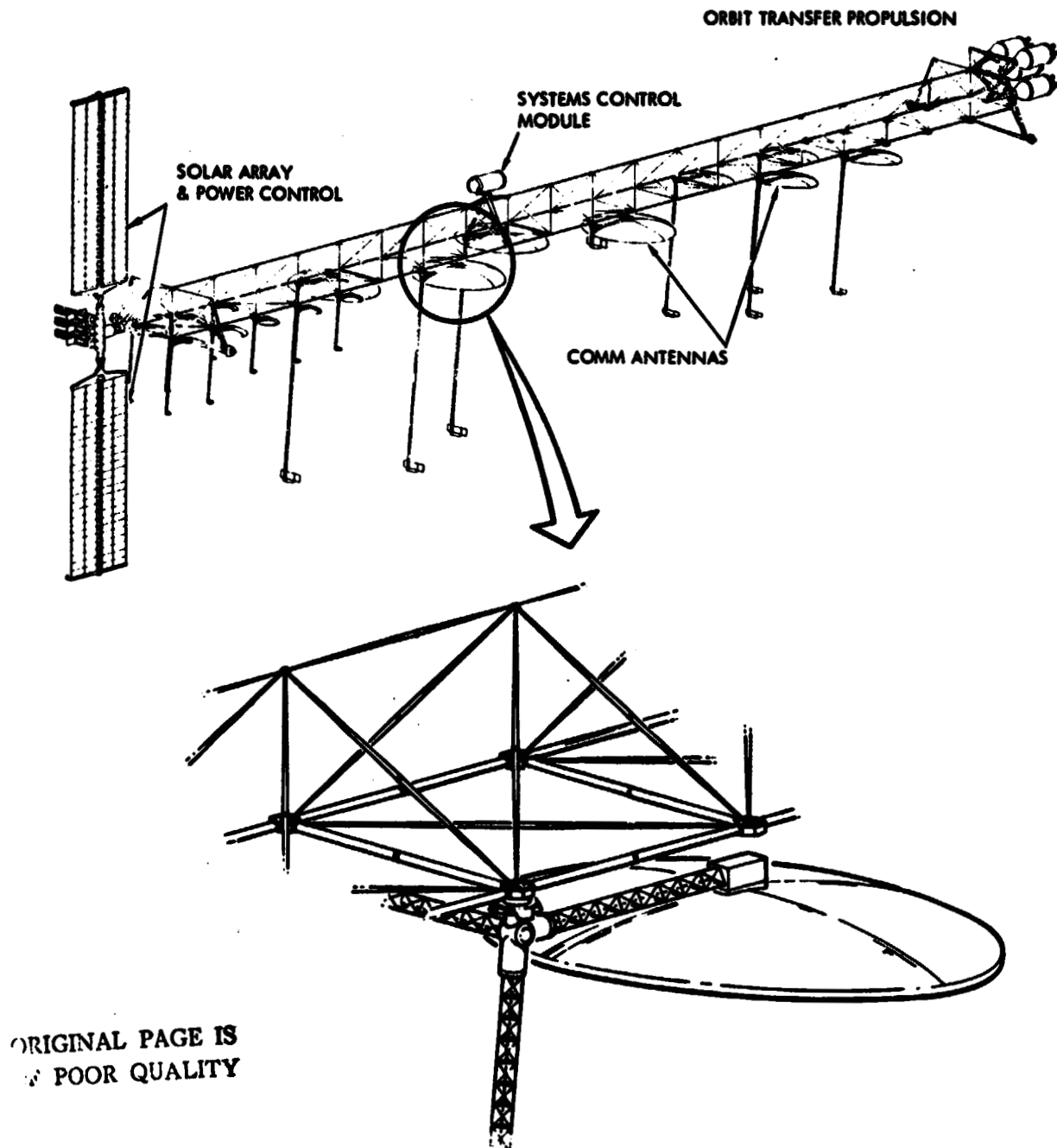


Figure 3.3.1-1. Antenna Mounting to Pentahedral Truss

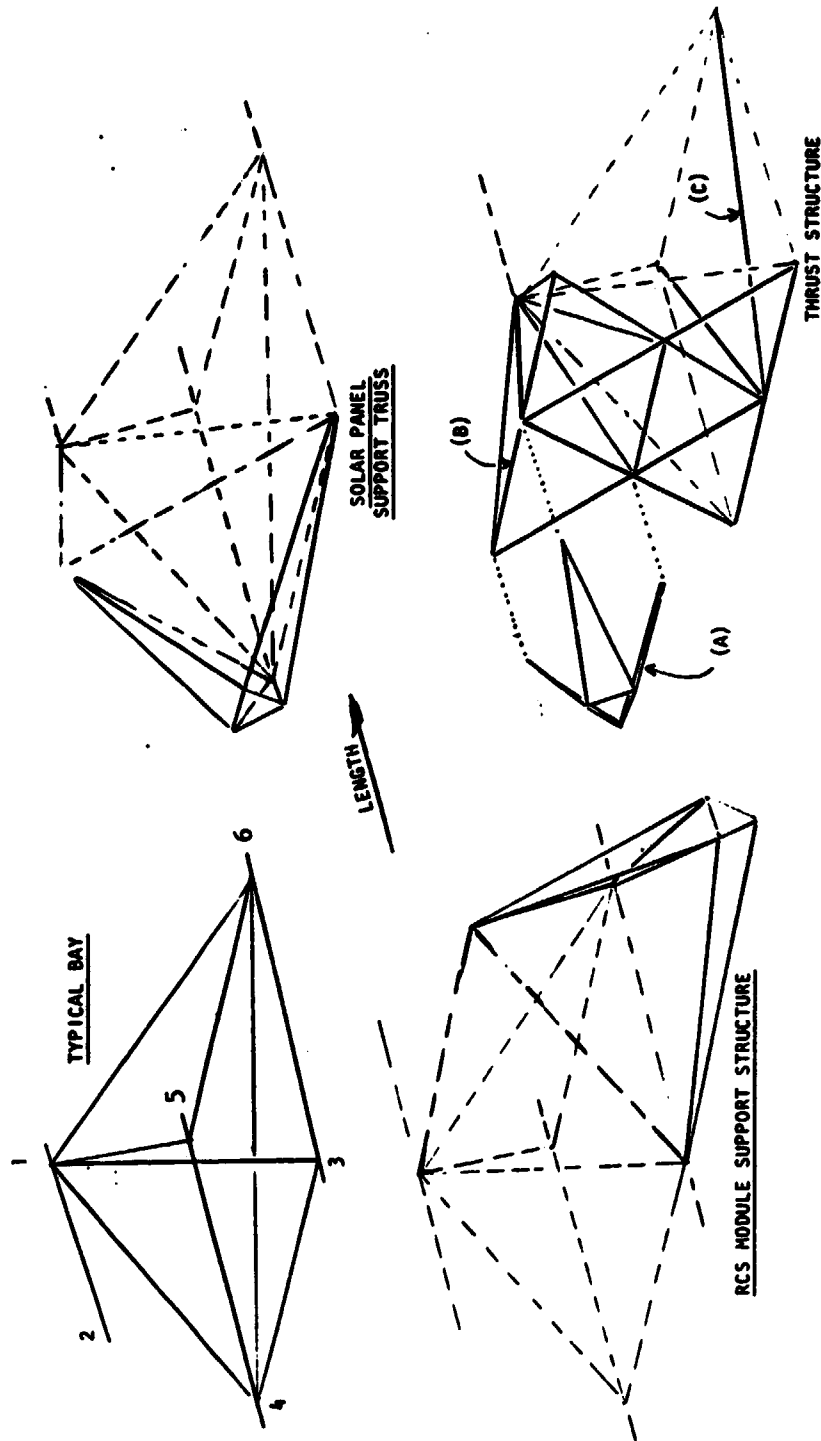


Figure 3.3.1-2. Pentahedral Truss Elements Configuration

penalizing its structural design. The antenna reflector, however, is deployed to eliminate the risk of deployment at geosynchronous orbit and because antennas of this size are designed for 1-g ground deployment with the electrical axis oriented horizontally (according to Reference 1). The reflector weights and moment arms are small compared to that of the feeds.

Attention is directed to the manner of antenna support. The attachment of the antenna reflector/feed column assembly at the base of the feed column, rather than at the base of the reflector, reduces the feed column stiffness requirements—particularly the GJ requirement.

To minimize the thrust loading impact on the reflector support column, the antennas are oriented to produce tension in this element during thrust.

The detailed structural requirements and analyses that directed the structural design of this communication antenna platform structure are described herein. However, for review convenience, a summary of the most significant requirements and design capability are shown in Table 3.3.1-1, and in further detail in Table 3.3.1-2.

Structural Requirements

The foregoing discussed configuration has been reviewed and analyzed to a level of detail compatible with the previously stated objectives. The reviews and analysis conducted were based upon the following requirements.

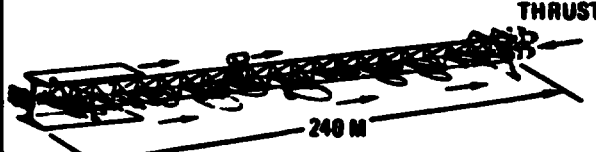

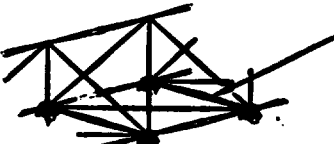
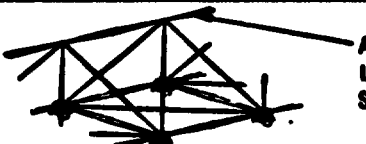
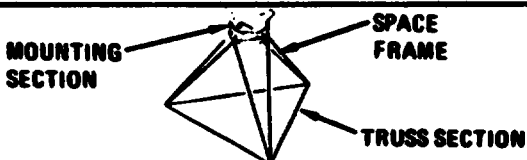
Orbit Transfer Thrust. The structure must sustain the loads induced during transfer from low earth orbit to geosynchronous orbit, in conjunction with the associated thermal gradient induced loads. The thrust loading results from the particular erectable communication antenna mass distribution defined in Section 3.4, exposed to a $T/W = 1.96 \text{ N/kg}$ (0.20). At this stage of the study maturity, to preclude any significant load amplification, each of the four thrusters provided per propulsion module will be started sequentially to provide a total thrust rise time two times greater than the minimum mode structural frequency period.

Orbit Transfer Configuration—Minimum Modal Frequency Requirement. The structural stiffness must be compatible with the guidance and control system to minimize delta-V losses to acceptable levels. This requirement has not been firmly established, but is discussed in Section 3.3.7.

Miscellaneous Loads. A review of this configuration in conjunction with prior study experience has indicated that docking, gravity gradient, solar pressure, aerodynamic drag, and RCS thruster loads for stationkeeping and attitude control are negligible compared to the thrust loading.

Operational Configuration—Minimum Modal Frequency Requirement. To permit the guidance and control system to maintain the antenna "short term" pointing accuracy within 0.03 degree, the overall structural configuration minimum modal frequency must be greater than 0.005 Hz (see Section 3.3.7).

TABLE 3.3.1-1 Erectable Communications Platform Structure - Requirements/Capability

REQUIREMENT		DESIGN CONCERN/IMPACT	DESIGN CAPABILITY
ORBIT TRANSFER - T/W = .20 TOTAL WEIGHT = 140,000 LBS TOTAL THRUST = 28,000 LBS		PENTAHEDRAL TRUSS-COLUMN BEHAVIOR	ULTIMATE AXIAL LOAD = 42,800 LBS CAPABILITY = 78,550 LBS
		BASE LONGITUDINALS - BEAM/COLUMN	DESIGN SATISFIES ULT AXIAL LOAD = 4830 LBS ULT MOMENT = 91,000 LB IN.
		TRUSS LATERALS - RIGIDITY FOR ANTENNA SUPPORT	✓
		APEX LONGITUDINAL - COLUMN BEHAVIOR	ULT AXIAL LOAD = 28,120 LBS CAPABILITY = 25,800 LBS
		RCS MODULE, GYRO PACKAGE, SOLAR PANEL, PROPULSION MODULE	SUPPORTED BY SPACE FRAMES OF PIN-ENDED MEMBERS
		MINIMUM MODAL FREQUENCY	1ST MODE (BENDING) = .14 HZ
MINIMUM MODAL FREQUENCY >.008 HZ		MINIMUM MODAL FREQUENCY	FIRST MODE (BENDING) = .026 HZ
• DIMENSIONAL STABILITY - 18 MIN. • STRUCTURE ALLOCATION - 6 MIN. (1 LB THRUSTERS)		• OVERALL TRUSS DEFLECTION • LOCAL LATERAL DEFLECTION • ANTENNA FEED DEFLECTION • ANTENNA REFLECTOR DEFLECTION	≈ 6 MIN.

3-24

Satellite Systems Division
Space Systems Group



Table 3.3.1-2. Pentahedral Truss Element
Compression Loads and Sizes

ELEMENT	ULTIMATE AXIAL LOAD (N)	ULTIMATE MOMENT (N/m)	MAXIMUM DIAMETER (cm)	MINIMUM DIAMETER (cm)	WALL THICKNESS (cm)
TYPICAL BAY					
1-2	89,530	-	44.2	22.1	0.089
4-5, 5-6	44,750 21,500	- 10,280	30.0	24.1	0.122
4-6	4,630	-	20.0	10.0	0.071
1-4, 1-3, 1-5, 1-6	6,365	-	20.0	10.0	0.071
SOLAR PANEL SUPPORT STRUCTURE					
ALL SIX SHOWN	18,600	-	30.5	15.25	0.064
THRUST STRUCTURE					
TYPE (A)	18,334	-	19.0	9.5	0.064
TYPE (B)	< (A)	-	19.0	9.5	0.064
TYPE (C)	13,530	-	30.5	15.25	0.064
RCS SUPPORT STRUCTURE					
ALL SIX SHOWN	6,230	-	20.0	10.0	0.071

Dimensional Stability. The dimensional stability of the operational configuration in the presence of thermal gradient, stationkeeping, and attitude control forces must be compatible with the total system "long term" antenna pointing accuracy requirement of 0.3 degree, or 18 minutes. The portion of this error allocated to structure is 6 minutes.

Launch Environment. All the structural elements must sustain the cargo bay launch environment. Of particular concern is the stacked arrangement of nested "dixie cup" tubes.

Structural Analysis

The structural analyses performed to support the design definition and verify the suitability of the structural configuration to satisfy the foregoing requirements are delineated herein. These analyses utilize a safety factor of 1.5 applied to limit load.

Euler Column Stability Analysis—Orbit Transfer. The Euler column stability analysis for the orbit transfer loading is similar to that shown in Section 3.3.2, except the pentahedral truss depth of 8.48 m (width—12 m) provides a significantly greater minimum moment of inertia of 0.0427 m^4 ($103,000 \text{ in.}^4$). The same loads were used.

The distributed load capability is determined, by ratio, to be $p_a = 8.05 \times 10^4 \text{ N}$ (179,000 lb). This loading could not be achieved by simple compression stress considerations; however, $40.4 \times 10^4 \text{ N}$ (90,000 lb) is compatible with a peak ultimate compression stress of $2.5 \times 10^6 \text{ N/m}^2$ (36,000 psi). With a safety factor of 1.5, the allowable load = $27.0 \times 10^4 \text{ N}$ (60,000 lb), or 3.75 times the applied limit load of $7.2 \times 10^4 \text{ N}$.

Pentahedral Truss Element Sizing. Table 3.3.1-2 describes the structural dimensions of the individual elements of the pentahedral truss illustrated in Figure 3.3.1-2. The sizing of these elements is described next.

All of the members subjected to axial compression without significant bending have a taper of 2:1. These members are sized so that the allowable axial compression load $P = 5.7 EI_m / \alpha l^2$, where I_m is the maximum moment of inertia and α is a factor to preclude magnification of thermal gradient imposed deflection and other secondary effects. The factor α was at least 1.3.

The lower longitudinal members (Elements 4-5, and 3-6 in Table 3.3.1-2) must sustain the peak axial load shown of 44,750 N (10,060 lb), adjacent to the thrust structure, and an axial compression of 21,500 N, and concurrent bending moment of 10,280 N m (91,000 lb in.) due to acceleration of the heaviest antenna mass; i.e., the 7.5-meter antenna. The taper of this column is 1.24 to 1 and was checked to satisfy the 44,750-N load by $P = 8.25 EI_m / \alpha l^2$. Here, too, the minimum value of α was 1.3. The member critical loading was the combined beam column loading for which the standard beam column analysis was used.

The peak compression stress was limited to $2.5 \times 10^8 \text{ N/m}^2$ (36,000 psi). The wall thickness provided was sized for the local buckling criteria of $0.30 E t/r$ (bending).

Orbit Transfer Configuration Modal Analysis. The minimum modal frequency of this communication antenna platform was determined by ratio from the analysis data shown in Section 3.3.2. Since the pentahedral torsional stiffness is significantly greater than that of the tri-beam, the minimum mode will be due to bending. The EI of the pentahedral truss is 4.3 times that of the tri-beam. The modal frequencies are therefore estimated to be 0.140 and 0.170 Hz at beginning and end of burn, respectively.

Operational Configuration Model Analysis. To determine the minimum natural frequency of the operational configuration of this communication antenna platform, the antenna structure stick models shown in Figure 3.3.2-5 were applied to the structure shown by the CRT plot (Figure 3.3.1-3). Since the antennas are mounted to the pentahedral trusses through berthing ports, with base rigidity dependent on the local bending characteristics of the individual elements, the structure was modeled to include this effect.

The NASTRAN analysis first modal frequency of 0.026 Hz is shown by the CRT plot on Figure 3.3.1-4 and is determined by the solar panel deflection. The EI and GJ characteristics of the solar panel boom, respectively, were 6.9×10^{12} and $52 \times 10^{10} \text{ N/m}^2$. The boom is a truss of triangular cross-section having a side dimension of one meter. The significant number of parameters affecting the stated first modal frequency is apparent. The significance of the analyses is that a frequency above 0.005 Hz is achievable.

Dimensional Stability Analysis. Several discrete analyses were performed to determine the antenna platform dimensional stability quality.

The antenna feed column thermal gradient deflections (Table 3.3.2-2) were based upon a 28°K (50°F) gradient across the column tubular members, and a coefficient of expansion of $0.36 \times 10^{-6} \text{ m/m/}^\circ\text{K}$ for the graphite composite materials.

A summary of the thermal and inertia induced rotations are shown in Table 3.3.1-3. The data pertaining to attitude control are based on one-pound thrusters.

The major rotation (Table 3.3.1-3) is 3.3 minutes and is due to a thermal gradient of 122°K (220°F) across the pentahedral truss laterals (member 5-6, Figure 3.3.1-2). The gradient shown is described in Section 3.3.5.

On the basis of the rotations shown, which are not all necessarily concurrent, or at the same point, or about the same axis, it is reasonable to expect the total rotational error will not exceed 6 minutes, as required.

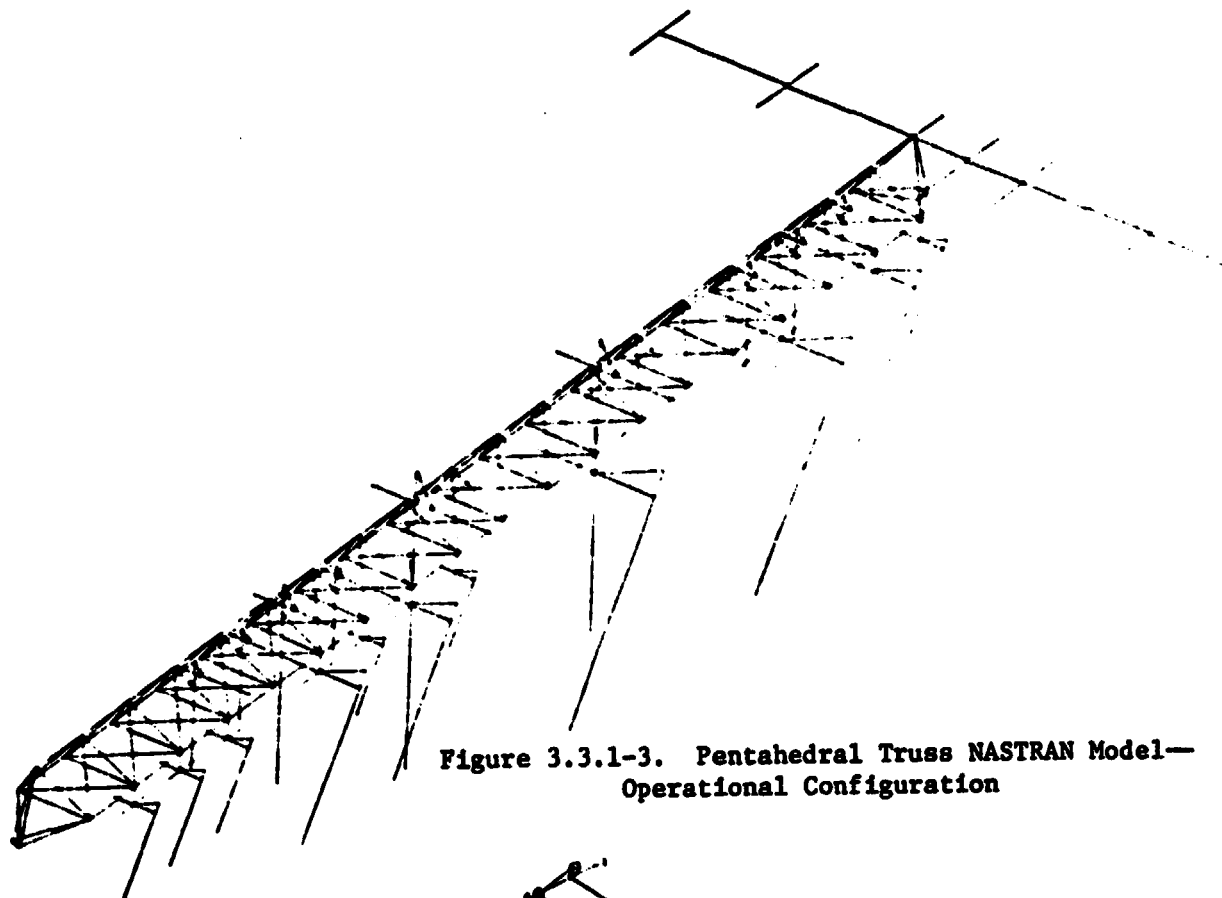


Figure 3.3.1-3. Pentahedral Truss NASTRAN Model—
Operational Configuration

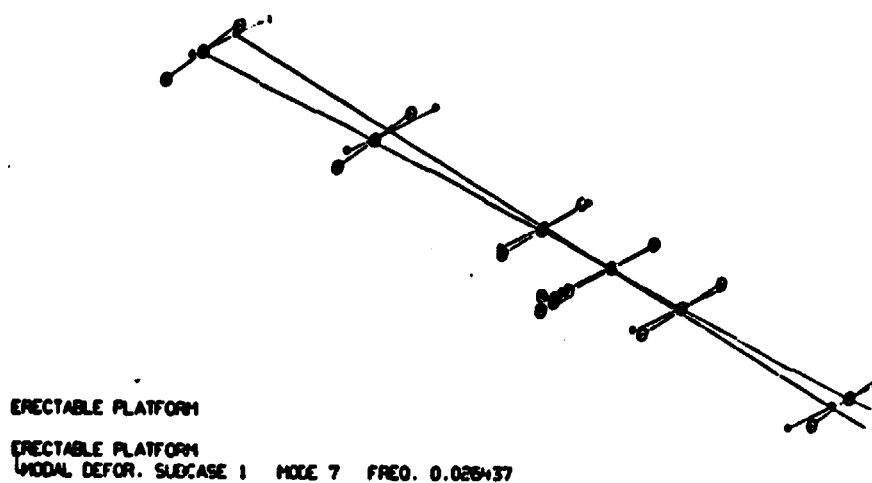


Figure 3.3.1-4. First Mode Shape—
Solar Panel Array

Table 3.3.1-3. Erectable Communication Antenna Platform Rotations
(Thermal/Attitude Control Torque)

Source	Antenna Feed Column (min.)	Antenna Reflector (min.)	Pentahedral Truss (min.)	Local Truss Elements (min.)
Thermal	2.1	<0.5	0.5 (roll axis)	3.3 (pitch axis)
Attitude Control	<0.10	<0.10	<0.10	<0.10

Dixie-Cup Cargo Bay Stacking. The natural frequency of the 20 cm(8-in.) diameter elements as stacked in the cargo bay was estimated to be 6.4 Hz (30 struts in stack). It is expected that a soft system to support the stack may be required for attenuation.

REFERENCE

1. Lockheed Wrap Rib Parabolic Antenna, Lockheed Corporation, LMSC A969503.

3.3.2 Space-Fabricated Tri-Beam Structure Definition

Objectives

See Section 3.3.1.

Space-Fabricated Tri-Beam Configuration Description

The structural configuration of this space-fabricated communication antenna platform, pictorially described on Dwg. 42662-26 (Appendix A) is that of a tri-beam with outriggers. The tri-beam utilizes the machine-made beam element (Figure 2.3.1-1), currently being developed by General Dynamics under contract NAS9-15310, as the basic structural member from which the tri-beam is fabricated. However, its basic cap thickness, diagonal chord diameter, and pretension have been increased. These increases are within the permissible envelope of changes (per conversation with the General Dynamics study manager). The tri-beam cross-section has a side dimension of 4.2 m (center-to-center of beam element) with truss behavior provided by the "X" system of diagonal tension cables (6.4-mm-diameter graphite composite). The individual bays are 10 m on center.

The tri-beam is the basic strongback to which the orbit transfer propulsion modules, solar panel array, and control moment gyro package are mounted. The 6.0-, 7.5-, 13.8-, and 20.5-meter antennas and RCS thruster modules are mounted to outriggers which are the extension of the tri-beam laterals.

The four RCS thruster module packages will be placed so that their center of mass (associated with orbit transfer) will be nominally on the neutral axis of the outriggers. The lateral braces shown are provided to preclude excessive lateral bending loads on the outriggers.

The control moment gyro package is utilized as a strongback to span 10 m as shown, and introduce acceptable levels of axial and shear loads into the tri-beam during orbit transfer thrust.

The antenna reflectors are deployed during the orbit transfer thrust maneuver (see Section 3.3.1). To minimize the induced moment about the outrigger longitudinal axis (torsion) the antenna reflector and feed column configuration are oriented as shown in the left-hand portion of the drawing. Nevertheless, the torsional moments imposed by the 20.5-m and 13.8-m reflectors would be sufficient to induce excessive angles of twist if the bracing shown were not provided.

The thrust structure concept (Figure 3.3.2-1) is a rigid frame comprised of 30-in. by 30-in. box trusses, configured to attach to the end of the beam elements. Since the individual box members are subjected to high shear, bending and torsional moments, the design provides high GJ, EI, and KAG characteristics. Also, if necessary, self-aligning ball joints can be provided in the box truss side of the interface to preclude local moments being imposed on the beam elements that would be additional to the peak axial load.

The detailed structural requirements and analyses that directed the structural design of this communication antenna platform structure are described herein. However, for review convenience, a summary of the most significant requirements and design capability are shown in Table 3.3.2-1.

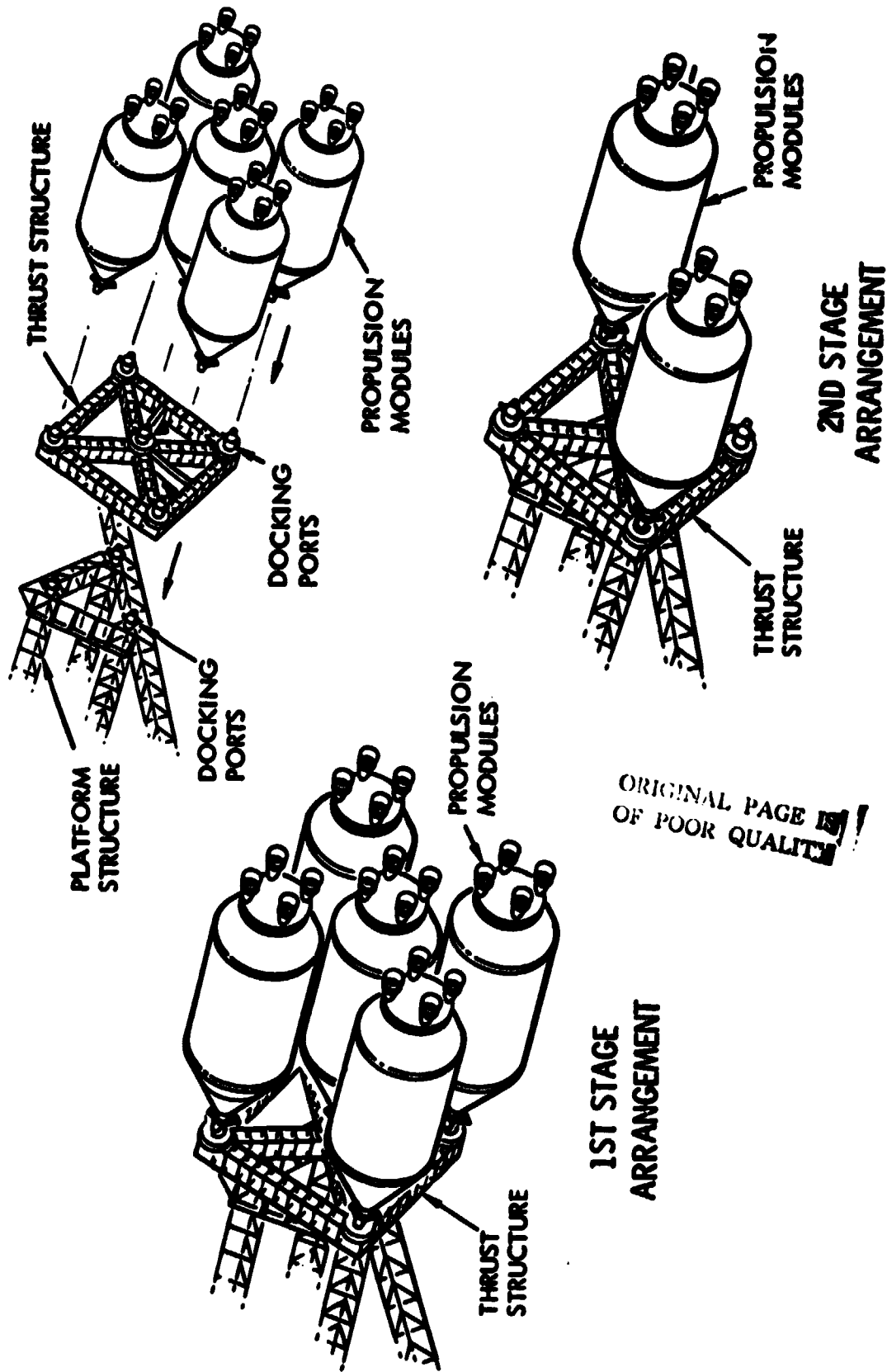


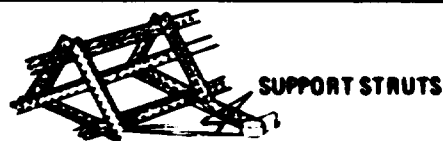
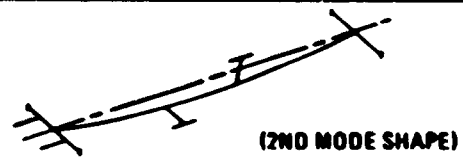


Figure 3.3.2-1. Thrust Structure Configurations

TABLE 3.3.2-1 Space Fabricated Communications Platform Structure - Requirements/Capability

REQUIREMENT		DESIGN CONCERN/IMPACT	DESIGN CAPABILITY
ORBIT TRANSFER T/W = .20 <ul style="list-style-type: none"> • TOTAL WEIGHT = 140,000 LBS • TOTAL THRUST = 28,000 LBS 		TRI-BEAM COLUMN BEHAVIOR <ul style="list-style-type: none"> • COLUMN LENGTH < 250 M • BASELINE GD BEAM CAP GAGE INCREASED TO .070 IN. 	ULTIMATE AXIAL LOAD = 42,000 LBS CAPABILITY = 48,200 LBS
		GD BEAM LOCAL CAP COLUMN BEHAVIOR - DIAGONAL CHORD DIA .000 IN.	ULT AXIAL LOAD = 5600 LBS CAPABILITY EXTRAPOLATED FROM BASELINE = 8000 LBS
		OUTRIGGER TORSIONAL & LATERAL SUPPORT - BY BRACES BACK TO TRI-BEAM	ADEQUATE
		MINIMUM MODAL FREQUENCY .25 DIA GRAPHITE DIAGONAL CABLES	<ul style="list-style-type: none"> • 1ST MODE (TORSION) = .044 HZ • 2ND MODE (BENDING) = .070 HZ
MINIMUM MODAL FREQUENCY > .008 HZ		.25" DIA GRAPHITE DIAGONAL CABLES	FIRST MODE (TORSION) = .020 HZ
<ul style="list-style-type: none"> • DIMENSIONAL STABILITY - 18 MIN • TOTAL STRUCTURE ALLOCATION - 6 MIN (1 LB THRUSTERS) 		<ul style="list-style-type: none"> • TRI-BEAM DEFORMATION • ANTENNA FEED DEFLECTION • ANTENNA REFLECTOR DEFLECTION 	~ 6 MIN.

Structural Requirements

The space-fabricated tri-beam structural requirements are identical to that delineated in Section 3.3.1 for the pentahedral truss.

Structural Analysis

The structural analyses performed to support the design definition and verify the suitability of the structural configuration to satisfy the foregoing requirements are delineated herein. These analyses utilize a safety factor of 1.5 applied to limit load. Since the baseline General Dynamics beam is used, Figure 2.3.1-1 presents the basic beam significant structural characteristics, except that the A, AE, I, and EI values have been increased by a factor of 2.33. The GJ values have been increased by a factor of 4.

Euler Column Stability Analysis

The basic Euler Column stability analysis is performed, as follows, for the limit loading shown in Figure 3.3.2-2. This loading was derived from a $\dot{r}/W = 1.96 \text{ N/kg}$ (.20) applied to the total mass distribution of this platform (mass = 63,636 kg).

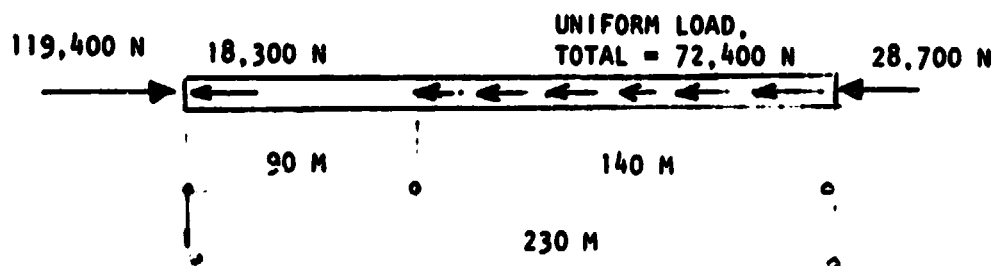


Figure 3.3.2-2. Tri-Beam Column Loading
—Orbit Transfer Configuration

Referring to Reference 1 [Table 34, Case 3b (pinned ends)] and interpolating for $a/l = 0.609$, $P/P_a = 0.4$, $K = 0.97$. The allowable distributed load is determined from $P_a = K\pi^2 EI/l^2$, where $I = 0.00994 \text{ m}^4$ (23,940 in.⁴) for the 4.2-m wide tri-beam, containing caps with an effective thickness = 1.78 mm (0.070 in.).

$$\text{Hence, } p_a (\text{allow}) = \frac{0.97\pi^2 (1.43 \times 10^{11}) (0.00994)}{(230)^2} = 25.7 \times 10^4 \text{ N}$$

This value is reduced by 7% by shear deflection effects on the 6.4-mm-diameter X-bracing. Applying a safety factor of 1.5, and the 7% reduction, the allowable distributed load = $16.0 \times 10^4 \text{ N}$ (35,980 lb). Since the applied load is $7.24 \times 10^4 \text{ N}$ (Figure 3.3.2-2), a factor of 2.2 remains to preclude any significant magnification of the offset moments, and secondary moments due to fabrication induced non-straightness (related to tolerance in cable tensioning), and thermal

gradient induced bending. The factor of 2.2 is regarded as marginally adequate; however, an increase in tri-beam depth from 4.2 to 5.6 meters can be introduced (if necessary) with no other configuration impact. The desirability of this depth increase is further discussed later in this section.

It is pertinent to note, that the compression loads due to pretension of the diagonal chord and X-bracing of the tri-beam are included in the local cap stability considerations but not in the foregoing Euler stability analyses. The Euler column stability is not influenced by the pretension loads (see Section 2.3.1).

Machine-Made Element Strength Review

Of primary concern is the peak axial loading induced in the individual open-section cap of the machine-made beam element. The peak ultimate axial load = 24,920 N (5600 lb) at the gyro package station. As stated in Section 2.3.1, the analysis presumes, pending a static test of the prototype beam, that the individual cap ultimate load capability is 6583 N (1480 lb) for the baseline 0.030-gauge cap, i.e., the value quoted in Reference 2. The baseline design is not limited by Euler buckling, but by local buckling and torsional buckling criteria. It is expected that use of the 0.070 gauge, which was provided for sufficient EI to satisfy the overall tri-beam Euler column stability requirement, increases the 6583 N value as described below.

In metals, the total axial load capability governed by local buckling criteria would be increased by the ratio of the thickness cubed. The torsional stiffness has the same ratio of increase. This ratio $(2.33)^3$ is a factor of 12.66. For composites, this value may be somewhat less. Conservatively using the ratio squared, the allowable load is 35,700 N (8000 lb). In view of the foregoing, although the baseline design exhibited a reduced axial stiffness above 2540 N because of local buckling, significant reduction is not expected in this design.

Of primary concern to this strength review, is the machine-made beam-beam joint capability. Figure 3.3.2-3 illustrates the local tension loading resulting from joint moment. The concern is the transverse bending induced in the laminate. It is strongly expected that a reinforcing member will be required across this joint, and is planned for, in the construction analyses within this study.

X-Bracing (Diagonal) Pretension Analysis. It is also important to ensure that the 6.4-mm-diameter (0.25-in.) graphite X-bracing tension cords are maintained in tension during thrust to ensure their function. The following analysis addresses this issue and is based on a cord pretension stress of $1.66 \times 10^8 \text{ N/m}^2$ (24,000 psi).

ORIGINAL PAGE IS
OF POOR QUALITY

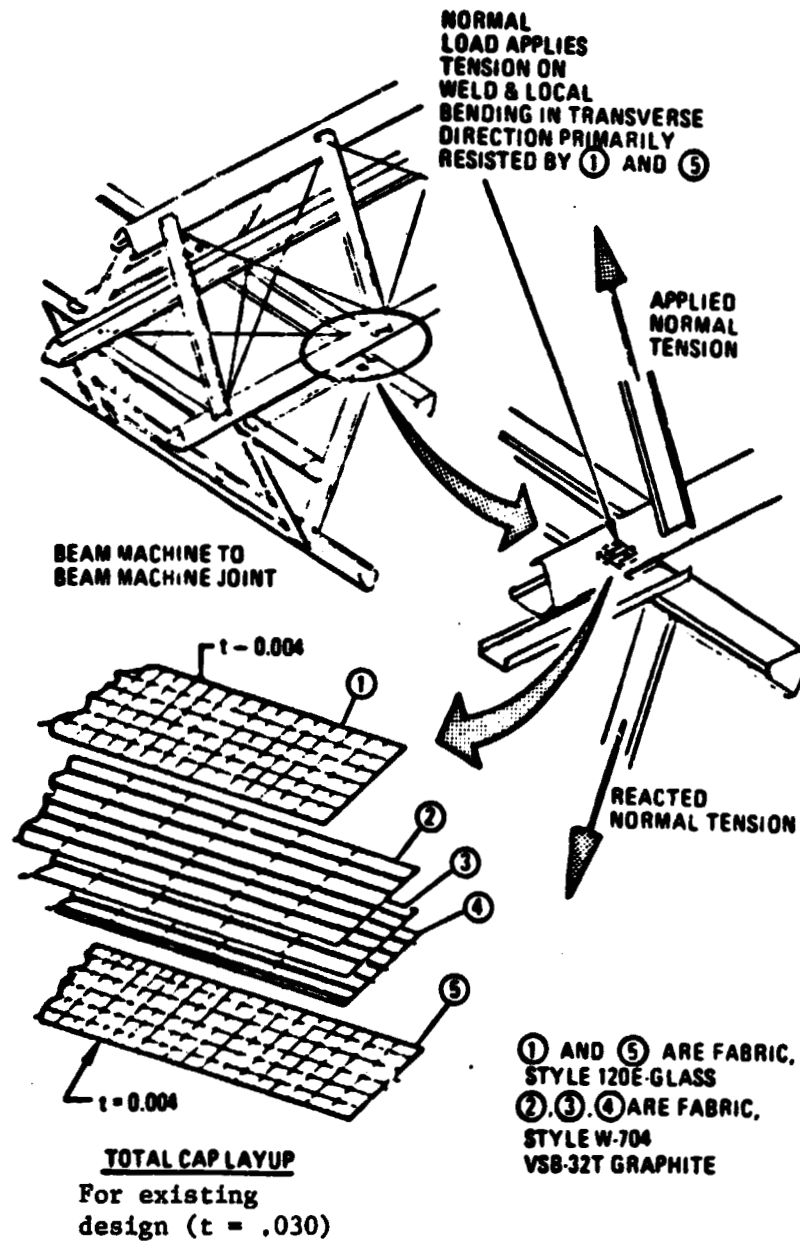


Figure 3.3.2-3. Beam-to-Beam Load Considerations

- The peak ultimate longitudinal shortening of the caps in the 10-meter bay

$$= \frac{24,920 \times 10 \times 100}{49 \times 10^6} = 0.51 \text{ cm}$$

- The cord length change with a 111°K temperature increase (along the X-axis) = 0.004 cm

- The cord length change due to peak ultimate vertical shear (along the X-axis) = 0.18 cm

$$\text{Total} = 0.694 \text{ cm}$$

The limit cord pretension induced elongation

$$= \frac{1.66 \times 10^8 \times 10.84 \times 100}{2.07 \times 10^{11}} = 0.87 \text{ cm}$$

The cord pretension induced initial elongation along the X-axis = 0.80 cm. The remaining effective elongation = 0.106 cm (0.04 in.). It is pertinent to note that the loss of pretension due to vertical shear will be avoided by relocation of the solar panel center of mass from the lower elements of the tri-beam to the upper element. This will place the total c.g. on the neutral axis of the tri-beam and essentially eliminate the vertical shear. The remaining effective elongation would then = 0.284 cm. Relocation of the solar panel also will provide a point of contraflexure in the orbit transfer load induced bending moment and, hence, increase the Euler capability and decrease the transverse deflection.

Orbit Transfer Configuration Modal Analysis. The analysis performed to estimate the minimum natural frequency of this communication antenna platform in the orbit transfer mode is discussed herein. As stated in Section 3.3.1, the antenna feed columns and solar panel are stowed. Presently, a minimum requirement has not been established. The minimum modal values are therefore presented for future guidance and control evaluations.

The analysis was performed on NASTRAN for both the start of orbit transfer (all five propulsion modules full) and end burn (two empty modules). The mass distribution used was consistent with the weights shown in Section 3.4. A stick structural model was used representing the EI, AE, KAG, and GJ characteristics of the tri-beam. The following data were obtained:

Start of Orbit Transfer

First mode (torsion) frequency = 0.044 Hz
Second mode (bending) frequency = 0.070 Hz (Figure 3.3.2-4)

End Burn

First mode (torsion) frequency = 0.062 Hz
Second mode (bending) frequency = 0.085 Hz

It is pertinent to note that an increase in tri-beam depth to a 5.6-meter design will increase the first and second mode frequencies quoted by a factor of 1.33.

ORIGINAL PAGE IS
OF POOR QUALITY

SPACE FAB COMM PLATFORM
SPACE FAB COMM PLATFORM
MODAL DEFOR. SUBCASE 1 MODE 8 FREQ. 0.070121

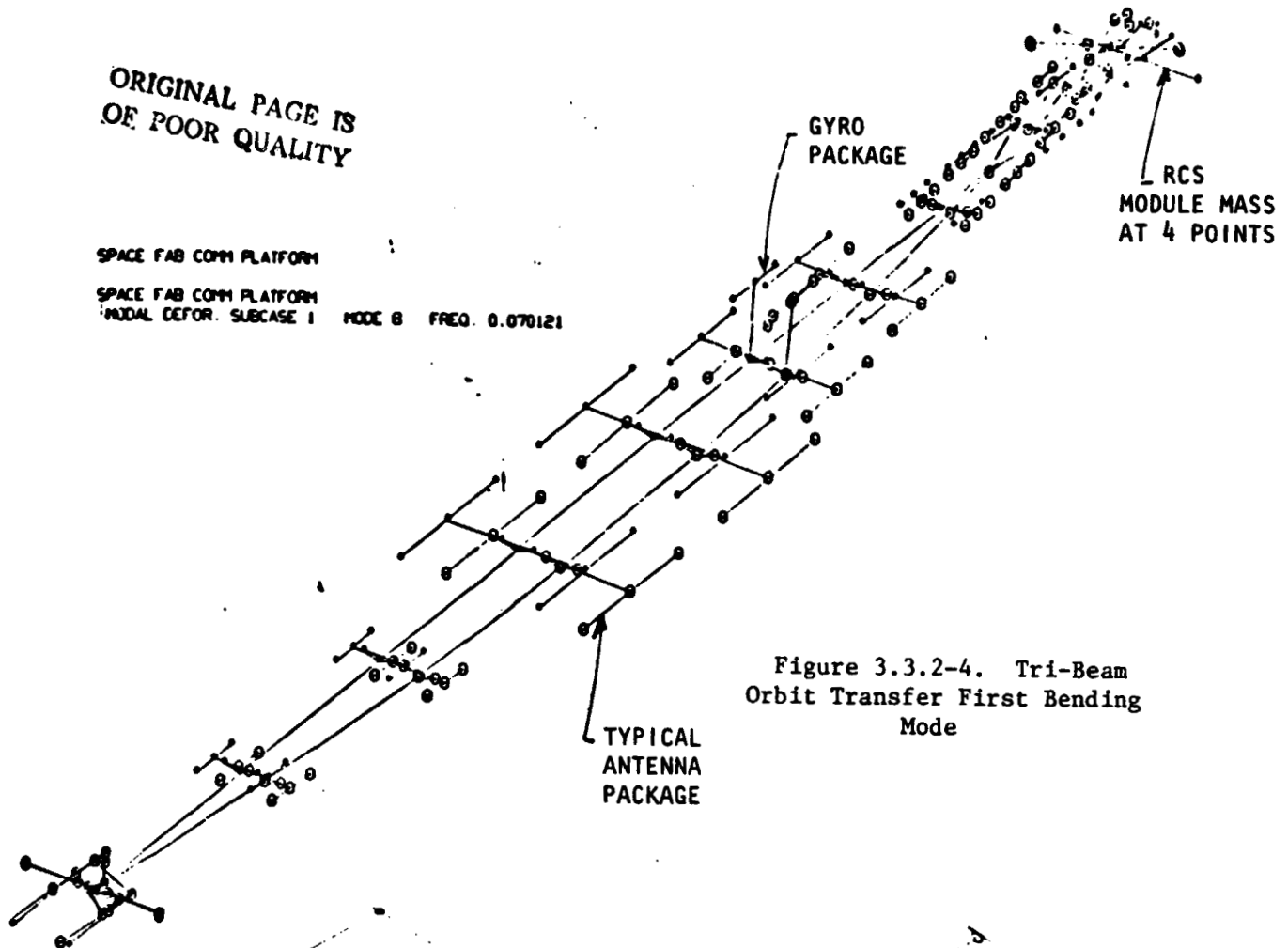


Figure 3.3.2-4. Tri-Beam
Orbit Transfer First Bending
Mode

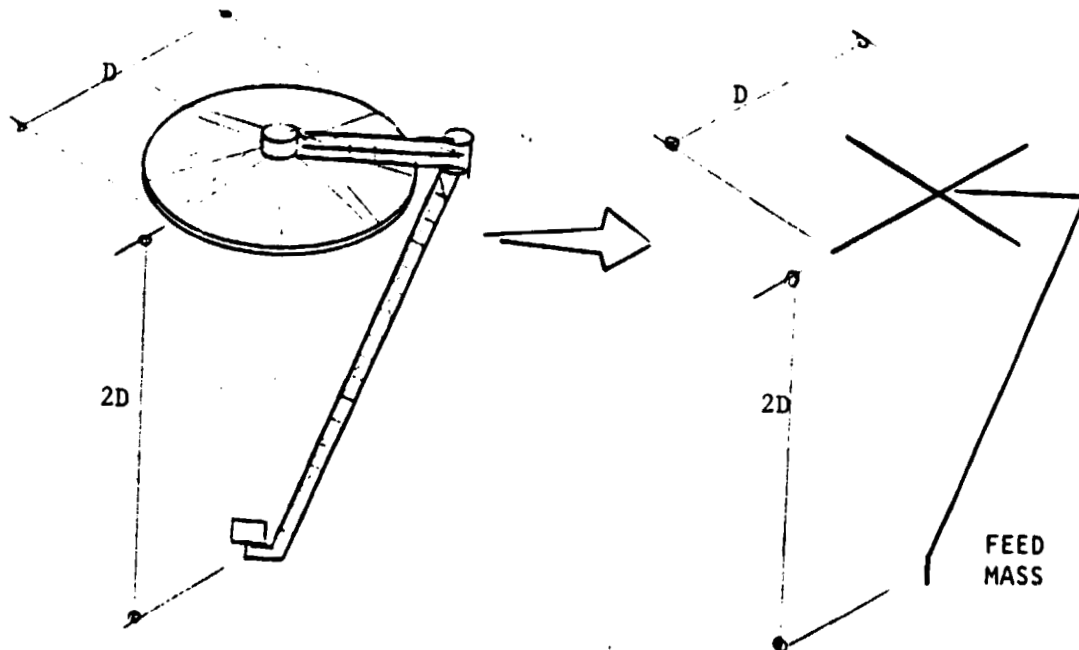


Figure 3.3.2-5. Antenna Structure Stick Model

Operational Configuration Modal Analysis. To determine the minimum natural frequency of this communication antenna platform, it was necessary to estimate the structural characteristics of the 20.5-, 13.8-, 7.5-, and 6-meter-diameter antenna feed columns, reflector structure, and reflector structure support boom. The EI and GJ data shown in Table 3.3.2-2 were derived from analysis of the derived stick model shown in Figure 3.3.2-5. The GJ and EI data shown were determined to provide a natural frequency at least = 0.10 Hz for the antenna mounted to an infinitely rigid base.

The antenna structure data shown were incorporated into a stick model containing the tri-beam EI, GJ, AE, and KAG characteristics, with the actual beam element arms to support the antennas and RCS modules. The solar panel and gyro package were supported by rigid elements. Figure 3.3.2-6 presents the first modal frequency obtained from the described NASTRAN model. The frequency is 0.020 Hz (0.005 required) and was driven by the 20-m-diameter antenna feed displacement.

The significant number of parameters that affect the stated first modal frequency is apparent. The significance of the analysis is that the frequency above 0.005 Hz is achievable.

Dimensional Stability Analysis. Several discrete analyses were performed to determine the antenna platform dimensional stability quality.

The antenna thermal gradient deflections shown in Table 3.3.2-2 were based upon a 28°K (50°F) gradient across the structure, and a coefficient of expansion of 0.36×10^{-6} m/m/°K for the graphite composite materials.

A summary of the thermal and inertia-induced rotations are tabulated below. The data pertaining to attitude control are based on use of 4.45 N (1-lb) thrusters.

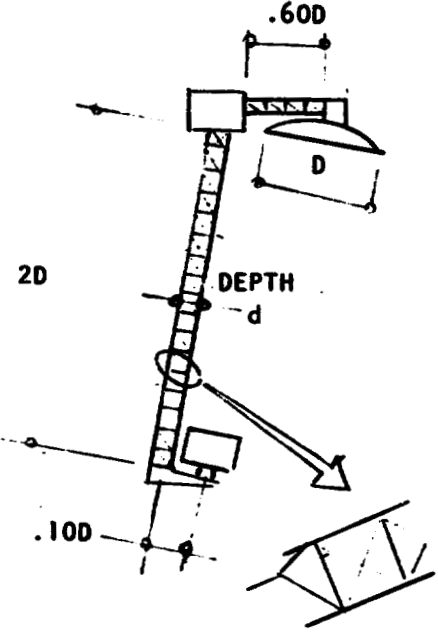
Source	Antenna Feed Column (min.)	Antenna Reflector (min.)	Tri-Beam Structure (min.)	Local Tri-Beam Element (min.)
Thermal	2.1	<.5	1.1 (roll or yaw axis)	<.30
Attitude Control	<0.10	<.10	1.8 (pitch axis)	<.10

On the basis of the rotations shown, which are not all necessarily concurrent, or at the same point, and about the same axis, it is reasonable to expect the peak error will be less than 6 minutes, as required.

REFERENCES

1. R. J. Roark and W. C. Young, Formulas for Stress and Strain, New York, McGraw-Hill.
2. Space Construction Automated Fabrication Experiment Definition Study (SCAFEDS)—Convair Division, General Dynamics, CASD-ASP77-017 (26 May 1978).

Table 3.3.2-2 Antenna Feed Column Structural Characteristics

	D (m)	FEED MASS (kg)	d (m)	EI ($\text{N/m}^2 \times 10^{-10}$)	GJ ($\text{N/m}^2 \times 10^{-10}$)	FEED COLUMN THERMAL ROTATION (AT FEED) (MIN)
	6.0	134	0.228	28	0.69	1.8
	7.5	1932	0.381	299	1.93	1.3
	13.8	140	0.456	113	2.76	2.1
	20.5	195	0.761	522	7.67	1.8
ANTENNA BOOM HAS SAME DESIGN AS FEED SUPPORT COLUMN.						

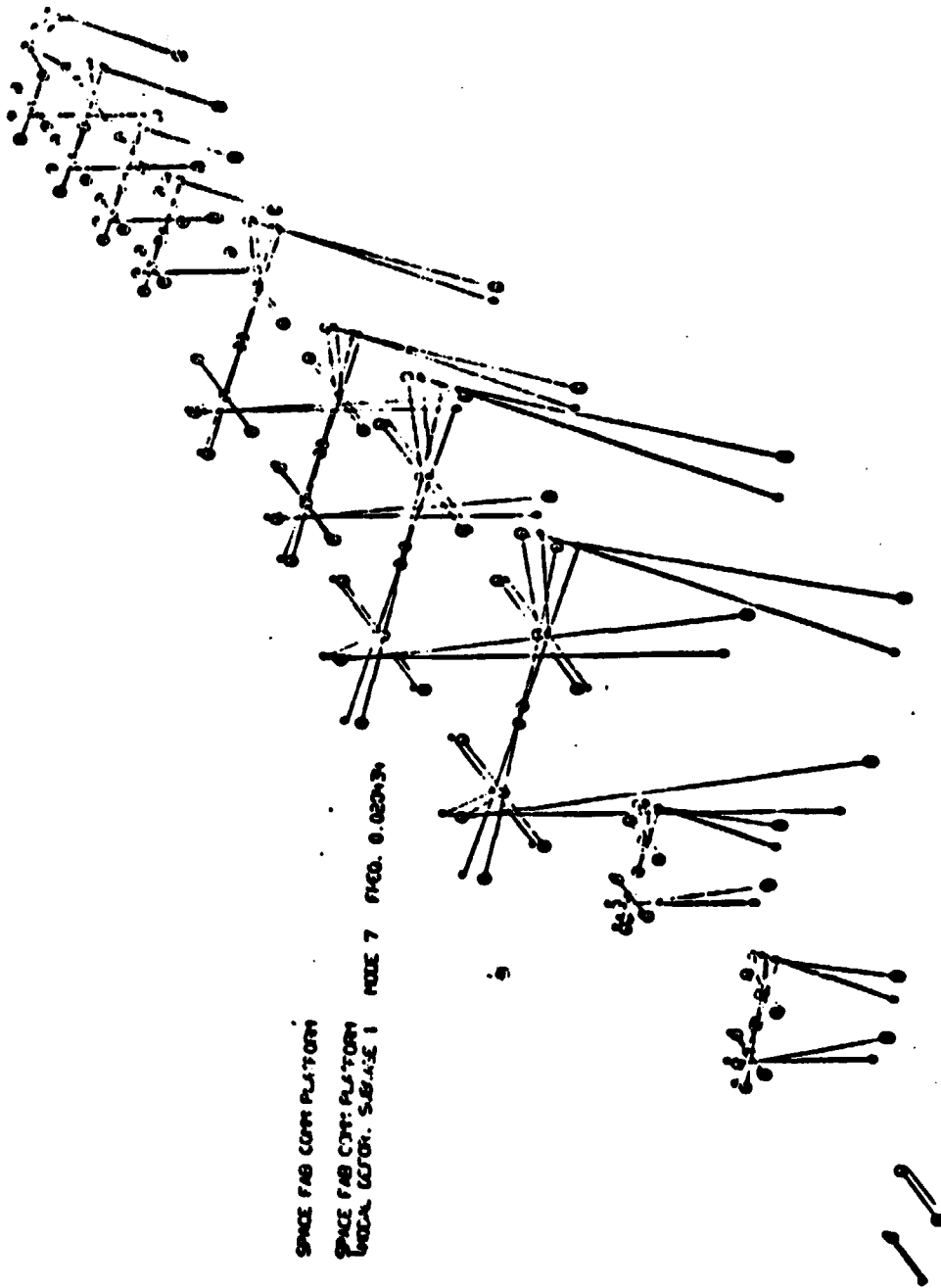


Figure 3.3.2-6. First Mode—Operational Configuration

3.3.3 Electrical Power Generation, Distribution and Control Subsystem Definition

Summary

Major components of the electrical power subsystems are summarized in Table 3.3.3-1, and the power distribution system is schematically illustrated in Figure 3.3.3-1. The electrical power system for the erectable and space-fabricated advanced communication antenna platforms are basically the same. Cable routing and length may vary slightly between the two configurations. Major components are identical and similarly located. This section pertains to either construction system.

Table 3.3.3-1. Electrical Power Generation,
Distribution and Control System

Item	Characteristic
Power generation	<ul style="list-style-type: none"> • 1312 m² solar array • High-efficiency hybrid solar cell • 336.6 W/panel EOL • 20-year life
Electrical power distribution	<ul style="list-style-type: none"> • 152 kW BOL (146 kW EOL) power at 200 V dc • Transmission efficiency, $\eta_T = 96\%$
Energy storage	<ul style="list-style-type: none"> • Nickel-hydrogen battery, 170.25-kWh
Rotary joint	<ul style="list-style-type: none"> • Slip rings, 121 2-kW @ 204.7 V
Communication Platform	<ul style="list-style-type: none"> • 118.4-kW to dc/dc converter 75 kW to antennas 37.5-kW, growth
Telemetry, tracking, and command	<ul style="list-style-type: none"> • Attitude and velocity control Low thrust chemical propulsion RCS propulsion unit • Data management • Communication • Housekeeping 5 kW @ 28 V dc and 200 V dc

The electrical power distribution system (EPDS) receives power from the power generation subsystem, a solar photovoltaic array, and provides the regulation and control required to deliver the electrical power to the various satellite loads. An energy storage system will be used to provide electrical power during the eclipse periods. Sensing devices will be situated throughout the system and will be monitored and controlled by the data management system.

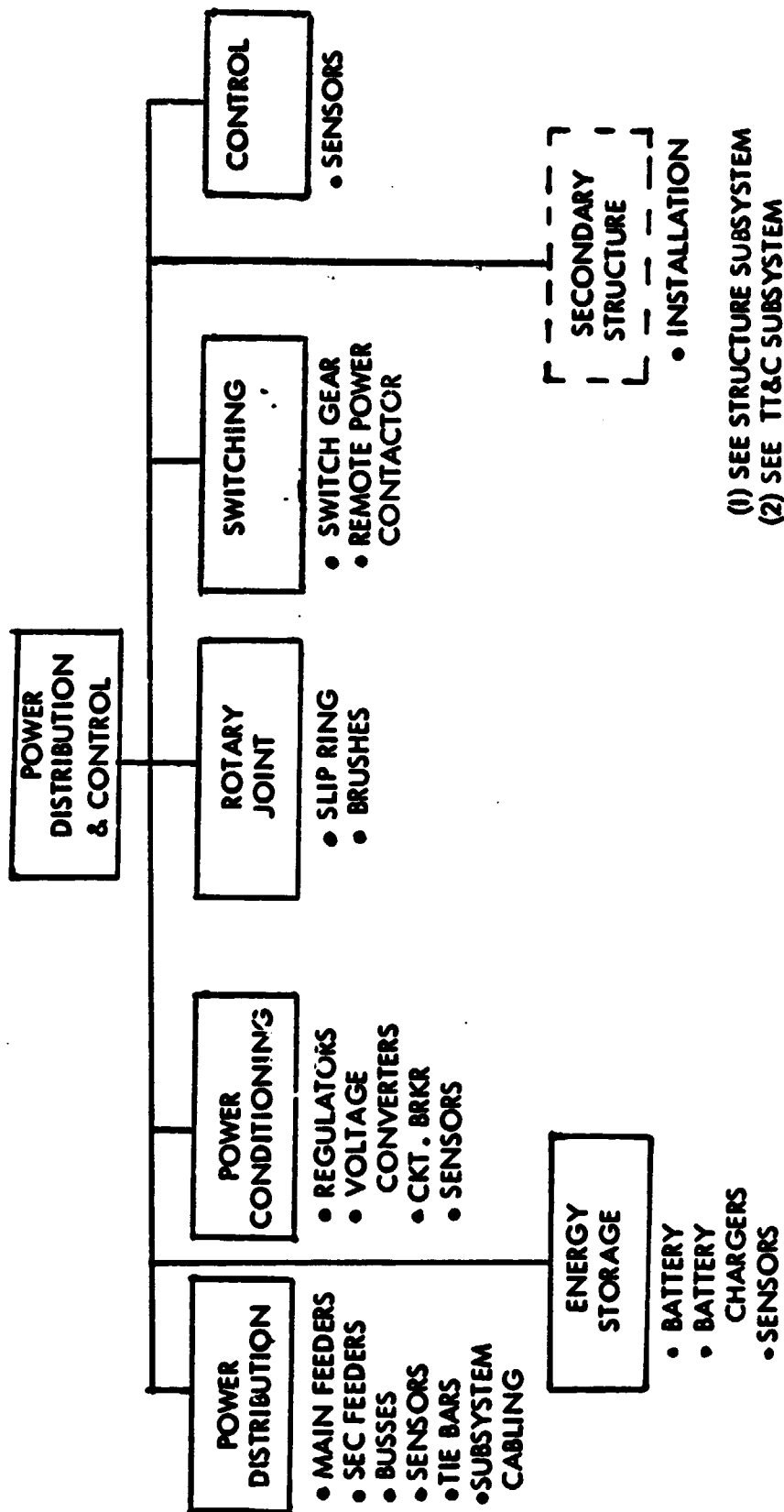


Figure 3.3.3-1. Electrical Power Distribution System Assembly

to assure circuit protection, regulation, power source switching for ecliptical periods, battery charging, and load monitoring at all times. A rotary joint will transfer the electrical power from the solar array to the communication antenna platform.

The major requirements of the electrical power subsystem are to generate and deliver electrical power at specified voltages and power levels on a continuous basis throughout the solar seasons for a duration of 20 years. The solar photovoltaic array will deliver approximately 131.16 kW of electrical energy at the end of life (EOL) of the array. The power distribution system of array to the slip rings will have a transmission efficiency of $\eta_T = 94\%$, while the transmission efficiency from the brushes to the communication antennas will be $\eta_T = 98\%$; 121.2 kW at 204.69 V will be transferred through the slip ring, and 112.5 kW at 200 V will be delivered to the dc-dc converter interface. This includes the 75 kW for the communication system plus an additional 37.5 kW for growth. Figure 3.3.3-2 illustrates the efficiency change for the electrical power distribution system for the advanced communication antenna platform.

Power Generation

Table 3.3.3-2 summarizes the physical format for the solar array. The solar photovoltaic power subsystem is based upon technology developed for the Lockheed PEP solar array design concept. An output voltage of 200 V has been selected, following telephone conversations with cognizant personnel at Johnson Space Center. Power requirements for the solar array were determined using the communication platform systems power plus an additional 50% growth factor, and applying those values to the efficiency chain which is depicted in Figure 3.3.3-2. In calculating the EOL electrical characteristics of the solar array, a magnitude of 336.6 W was used, based on the PEP solar array EOL value for wattage output per panel. Other environmentally induced losses which have been accounted for are:

- Ultraviolet radiation and micrometeoroid damage: 2%
- Electrical modules isolation diodes: 0.5%
- Voltage and power loss due to the intertie harness: 2%
- Battery charging requirements: 5%

Using values from Figure 3.3.3-2 and the above loss factors, the number of panels required for the array would be:

$$\frac{133,160 \text{ watts}}{336.6 \text{ watts} (.98)(.995)(.98)(.95)} = 435.77 \text{ panels}$$

In summary, 54 electrical panels in 8 blankets (4 meters by 41 meters each) will meet the 131.16 kW EOL power requirement (Figure 3.3.3-3).

Table 3.3.3-2. Power Generation Subsystem

Item	Characteristic
Solar array	<ul style="list-style-type: none"> • 1312 m² • Two wings, 16 meters by 41 meters • Power output, 131.16 kW (EOL) • Four solar blankets/wing
Solar blanket	<ul style="list-style-type: none"> • 164 m² (4 m × 41 m) • 54 panels/blanket • 108 electrical modules
Solar panel	<ul style="list-style-type: none"> • 3.0256 m² (4 m × 0.76 m) • 336.6 watts/panel • Two electrical modules/panel
Electrical module	<ul style="list-style-type: none"> • 1.512 m²

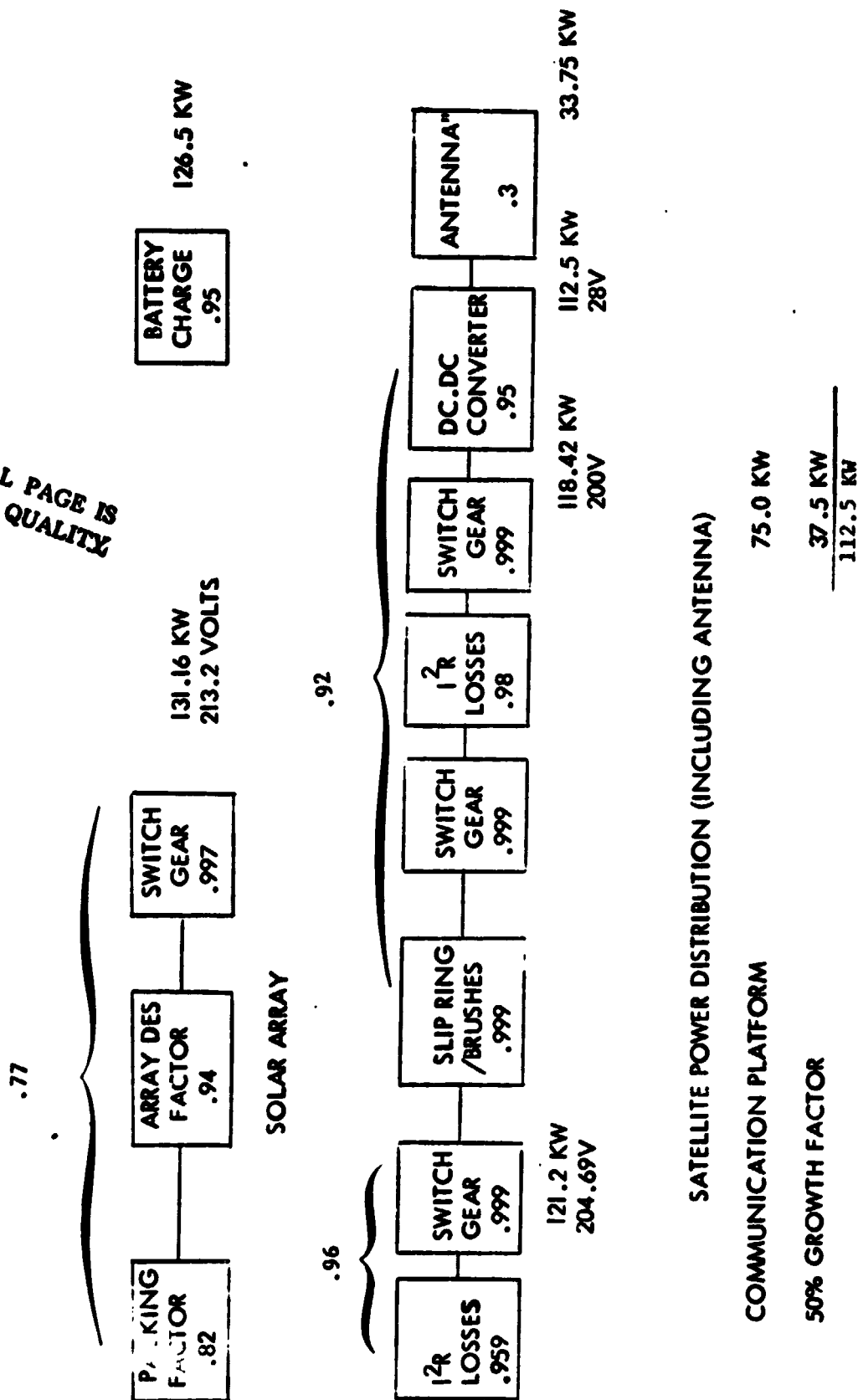


Figure 3.3.3-2. Efficiency Chain for Advanced Communication Platform System

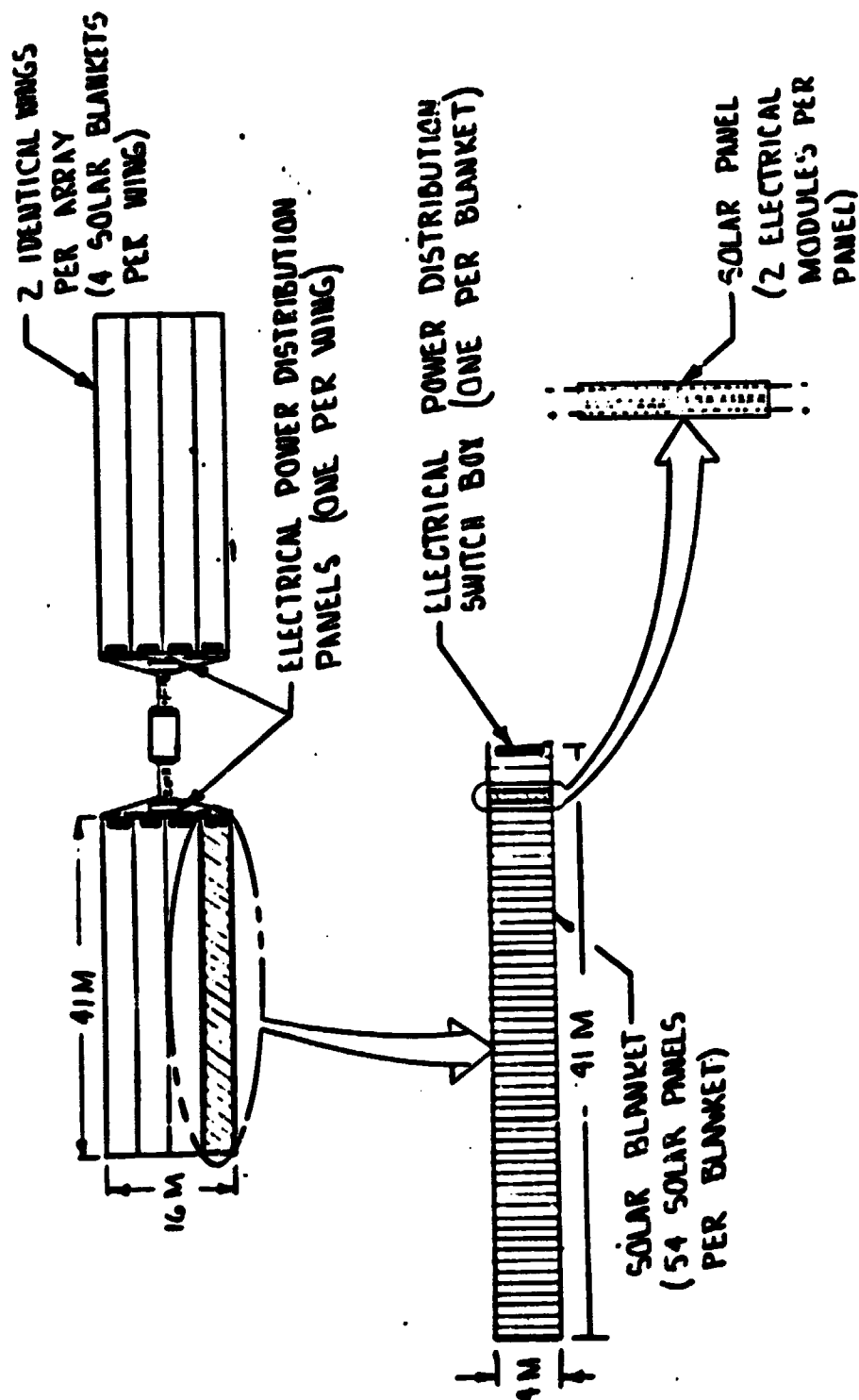


Figure 3.3.3-3. Solar Array

Power Distribution

Figure 3.3.3-1 illustrates the major assemblies comprising the EPDS. The subsystem consists of main feeders, tie bars, summing buses, regulators, voltage converters, switch gear, remote power contactors, slip rings, and brushes. Batteries and battery chargers are included for eclipse periods.

Utilizing the PEP design concept, the array harness is a flat cable conductor mounted on the back of the solar array blanket at the two long edges of the blanket. The harness folds up in the same manner as the array panels for retraction and storage. Conductor pairs from six panels will be routed to form a cable and terminate into a connector at the base of the blanket. These connectors, capable of remote manipulator handling, will be engaged into an electrical power distribution (EPD) switch box located at the base of each blanket. The number of these connectors will be minimized to augment fabrication operations in space.

The EPS switch box will consist of circuit protection devices, switch gear capable of interrupting fault loads, and series-parallel connection of panels to maintain the array voltage. Each EPD switch box will contain a regulator to maintain a 5% voltage regulation, and a data management microprocessor and signal conditioning to monitor the blanket parameters. Figure 3.3.3-4 is a simplified schematic of a typical solar array blanket.

The solar array consists of eight solar blankets fabricated in a split array of four blankets each. This split array leads to a split electrical bus. Four solar blankets, fed through their respective EPD switch boxes, are fed into an EPD panel where the individual blanket powers are summed together by the summing bus. Blanket switch gear isolates each blanket pair from the summing buses. As each blanket pair is connected, it is tied to the summing buses through the closure of each related switch gear. During this connection process, bus temperatures and current measurements must be monitored to detect any shorts throughout feeder runs of the arrays so that controlled emergency disconnects can occur under the data management system (DMS) or local breaker control to avoid catastrophic effects. The battery switch gear and bus-tie contactors will be located within the EPD panel. Sensing circuits of the DMS will monitor orbit times and will control when the battery bus will be connected and disconnected to the power buses. Bus tie bars will interconnect the power summing buses to power slip rings. The slip ring will provide for transmitting the electrical power split bus through it.

Conductors from the brushes are tied to the centrally located dc/dc converters through switch gear, to allow for isolation when performing maintenance. The dc/dc converters are tied to a summing bus for transmitting the required power through switch gear to the communication system network.

Figure 3.3.3-5 is a simplified schematic for the communication platform system.

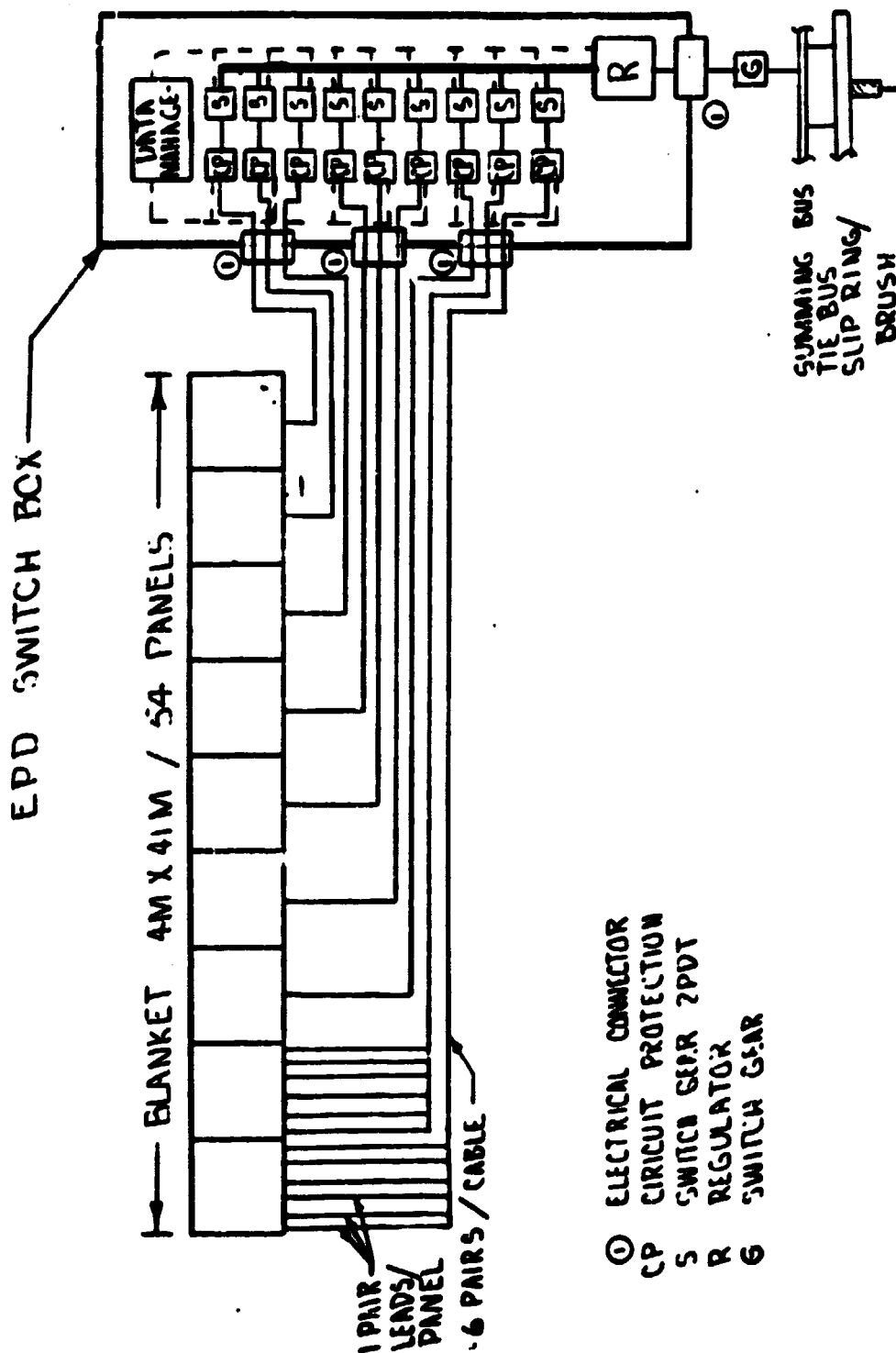


Figure 3.3.3-4. Advanced Communication Platform System
Typical Solar Array Blanket Switching Schematic (1 of 8)

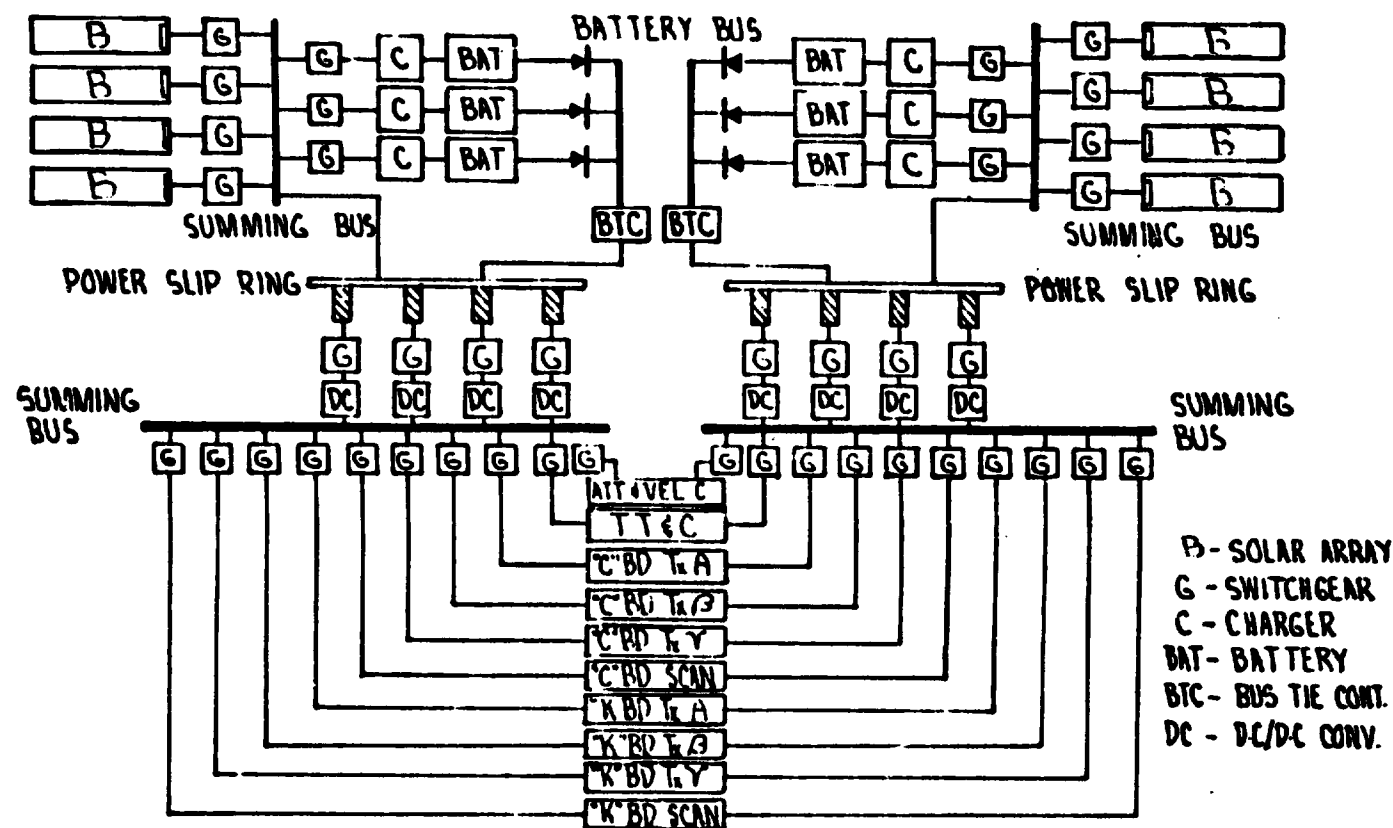


Figure 3.3.3-5. Advanced Technology Communications Platform
Simplified Schematic

Energy Storage

An energy storage system will be utilized during the eclipse periods to provide 170 kW/hr of electrical energy. Batteries and a regenerative fuel cell system have been reviewed as candidates for the energy storage subsystems. The regenerative fuel cell system was not selected at this time due to the long, costly development program required for the electrolysis unit. Among the battery types, nickel-hydrogen and nickel-cadmium batteries were evaluated as candidates. The battery evaluation was similar to that for the SPS flight test article in all major respects, and was based upon the comparative data presented in Table 2.3.2-3 and its supporting discussion in Section 2.3.2.

The parametric values for the nickel-hydrogen battery are listed in Table 3.3.3-3.

Table 3.3.3-3. Nickel-Hydrogen Battery Parameters

Item	Characteristic
Power requirement	146 kW/hr
Capacity	170 kW/hr
Charging	1.6 V
Discharging	1.25 V
Charging rate	C/10
Weight factor	18 Wh/kg
Depth of discharge	80%
Cell size	200 Ah
Number cell/battery	122
Battery weight	721 kg/battery

A new cell of a higher capacity will require development for this application. The development will be minimal as it only requires procuring a larger case which would be 17.75 cm in diameter and 30.5 cm long with a 200 ampere-hour capacity. The number of plates in the stack would be increased. Current technology would be applied and a verification test performed.

Sizing. The major consideration for using the EPD system is the power level (voltage and current) and line loss allowances. This system was sized to handle EOL power (delivered by the solar array) of approximately 131 kW at 200 volts, as shown in Figure 3.3.3-2.

Rotary Joint. The rotary joint is utilized to transfer power through slip rings and brushes from the solar array to the communication platform member of the satellite. The rotary joint will consist of two slip ring/brush sets. Each will have multiple isolated circuits of sufficient capacity to carry the assigned loads. Figure 3.3.3-6 shows a block diagram of the rotary joint.

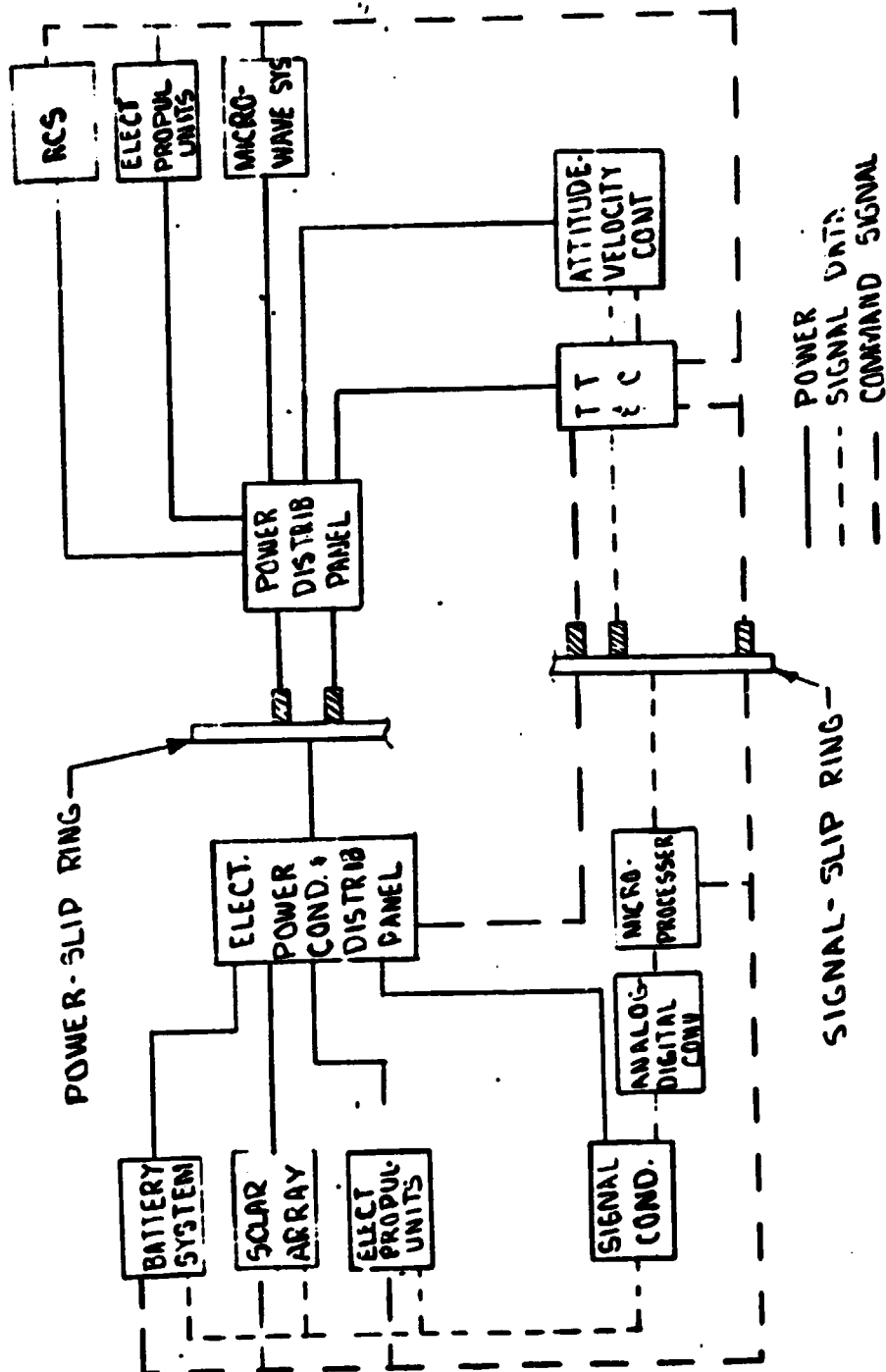


Figure 3.3.3-6. Rotary Joint Schematic

Converters. Risers from the brushes of the slip ring are tied to the dc/dc centralized converters through switch gear. The converters are tied to a summing bus to provide further conditioning and power required for the communication system.

Dc/dc converters do not exist for the capacity required for this application. TRW has a 2.4-kW dc/dc converter contracted with U.S. Army Electronic Command. Using today's technology, they can develop a dc/dc converter of 25-kW capacity by using higher power semi-conductors and drive circuits, higher power magnetics, and thermal design consistent with the new design. The control circuit design will essentially remain intact. However, the proposed changes will increase the size and weight of the converter.

Distribution. The power distribution subsystem utilizes flat copper conductors. These conductors are not considered part of the structure. They will normally be passively cooled by radiation to free space. The main feeders are sized to an average transmission efficiency of 96%. Figure 3.3.3-5 illustrates the power distribution network used on the communication platform satellite.

Conditioning. The power conditioning converts the solar photovoltaic power to the required bus voltage. A series regulator at each blanket provides the regulation of the bus voltages. The DMS monitors and series-parallelizes the panels outputs to maintain a consistent voltage. By regulating the bus supply voltage the battery circuit will not require additional regulation. Voltages to the communication system are further conditioned by the centralized dc/dc converters.

Switching. Switch gear is provided for isolation, maintenance, and conditioning. Optimum power output will be assured at all times by proper sizing and design of the submodules, their associated switch gear, and the DMS control of the switching and control to loads. Voltage and currents handled by the switch gear will be monitored by the data management system to determine their status and switched according to power demand.

Availability of switch gear for the intermediate voltage of 270-V dc rating is basically nonexistent. We have investigated this problem by inquiries to NASA-JSC and NASA-Lewis and have followed their leads describing possible study efforts without finding any space-tested hardware. NADC at Johnsville, Pa., NAC at Indianapolis, Ind., and Westinghouse have study programs for such switch gear, but no hardware development contracts have been let. Westinghouse has a 300-V dc with a current rating of 1 to 5 amperes remote power contactor and a prototype 270-V dc with a current rating of 150 amperes; neither is space qualified. Teledyne Kinetics has a 200-V dc switch with a 7-ampere rating; it, too, is not space-qualified.

Weight. A summary of weight for the electrical power system is presented in Table 3.3.3-4.

Table 3.3.3-4. Electrical Power System
Weight Summary*

	Weight (kg)
Solar array panels	1,359.36
Switch gear box	581.8
EPS wire harness	249.24
Battery system	4,910.5
Slip ring/brushes	47.86
Antenna system	
EPD harness	563.68
Switch gear box	260.4
RF harness	4,476.0
RF interconnect box	1,400.0
Secondary support structure	1,385.0
Subtotal	15,233.84
EPD Panel	265.00
Total	15,498.84

*Does not include cooling.

3.3.4 Microwave Subsystem Definition

Summary

The major features of the microwave subsystem are summarized in Figure 3.3.4-1. Each circle in the figure represents an antenna. There are three fixed-beam transmitting antennas for 3.7 to 4.2 GHz, three fixed-beam receiving antennas for 5.935 to 6.425 GHz, and two scanning antennas for filling gaps caused by overloads, failure, or rain. Also shown, is a repetition of the above for 12 and 14 GHz. It is necessary to use three antennas to provide 4.5 dB crossovers with the desired aperture weighting for good sidelobes (-35 to -40 dB). A total of 219 beams is needed to cover the continental United States when a beam size of 0.26 degree is used. The bandwidth of 500 MHz is divided into 12 channels of 40 MHz each. There are 24 channels total per band when polarization diversity is used. Since adjacent footprints cannot use the same frequency range within two footprint diameters (using -35 dB sidelobes and -24 dB crosstalk allowance), then the 24 channels must be divided by 4. Thus, the maximum capacity per six-channel beam is 6000 conversations. On the average, we will only use two 40-MHz channels per beam and the figure gives the expected capacity for the antenna platform for the continental U.S., as outlined in the mission requirements developed in Section 3.1.

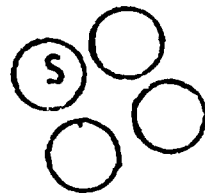
Note that the antennas are shown schematically only. Their physical placement on the platform is discussed in Sections 3.3.1 and 3.3.2. A more detailed rationale for the selection of this approach is given in subsequent sections. An isometric view of one antenna is given in Figure 3.3.4-2 to show the offset horn assembly relation to the reflector.

Subsystem Concept Definition and Rationale

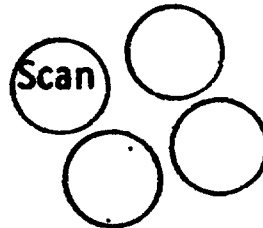
Viewed from the geostationary arc at around 98° west longitude, the continental U.S. has an angular width of about 3° in the north-south direction and somewhat more than twice this in the east-west direction. If this whole region is to be covered by high-gain spot beams then, clearly, advances in the technology of multibeam antennas will be required. Probably the largest off-axis scanning performance achieved to date is that reported by Semplak¹ of Bell laboratories. Using a dual offset reflector antenna in a Cassegrainian configuration, he carried out measurements on beams scanned off-axis by more than 20 times the full half-power beamwidth. At this extreme, he found that beam shape, although broadened, was quite acceptable, with little evidence of coma distortion. There was, however, a significant loss in peak gain amounting to about 4 dB. However, for a scan angle limited to about 10 times the beamwidth, he found the loss in gain to be no more than 0.25 dB and beam broadening completely negligible. Thus it appears that a single antenna could cover the U.S. with spot beams having a width of about 0.3° and that no beam would be off axis by more than 10 times the beamwidth. All beams would be well formed,

¹R. A. Semplak, *100 GHz Measurements on a Multiple Beam Offset Antenna*, Bell Systems Technical Journal, 56, pp. 358-398, March 1977.

UP 6 GHz



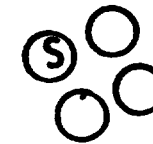
DOWN 4 GHz



UP 14 GHz



DOWN 12 GHz



DIAMETER

13.8

20.5

6.4

7.5

METERS

MASS

1.2

2.0

* 6.0

0.8

METRIC TONS

RF POWER

1.2 kW

*21.2 kW

(89 KW DC
TOTAL POWER)

FOOTPRINT 207 x 296 KM

NO. OF BEAMS/DISH - 73

$$\text{MAXIMUM CAPACITY} = \frac{1000 \text{ CONV}}{\text{CARRIER}} \times \frac{2 \text{ CARRIERS}}{\text{BEAM}} \times \frac{3 \times 73 \text{ BEAMS}}{\text{BAND}} \times 2 \text{ BANDS}$$

$$= 876 \times 10^3 \text{ CONVERSATIONS } (5.6 \times 10^{10} \text{ BITS/SEC})$$

* ADDED POWER & MASS TO OVERCOME RAIN ATTENUATION

Figure 3.3.4-1. Advanced Communications System Platform

Satellite Systems Division
Space Systems Group



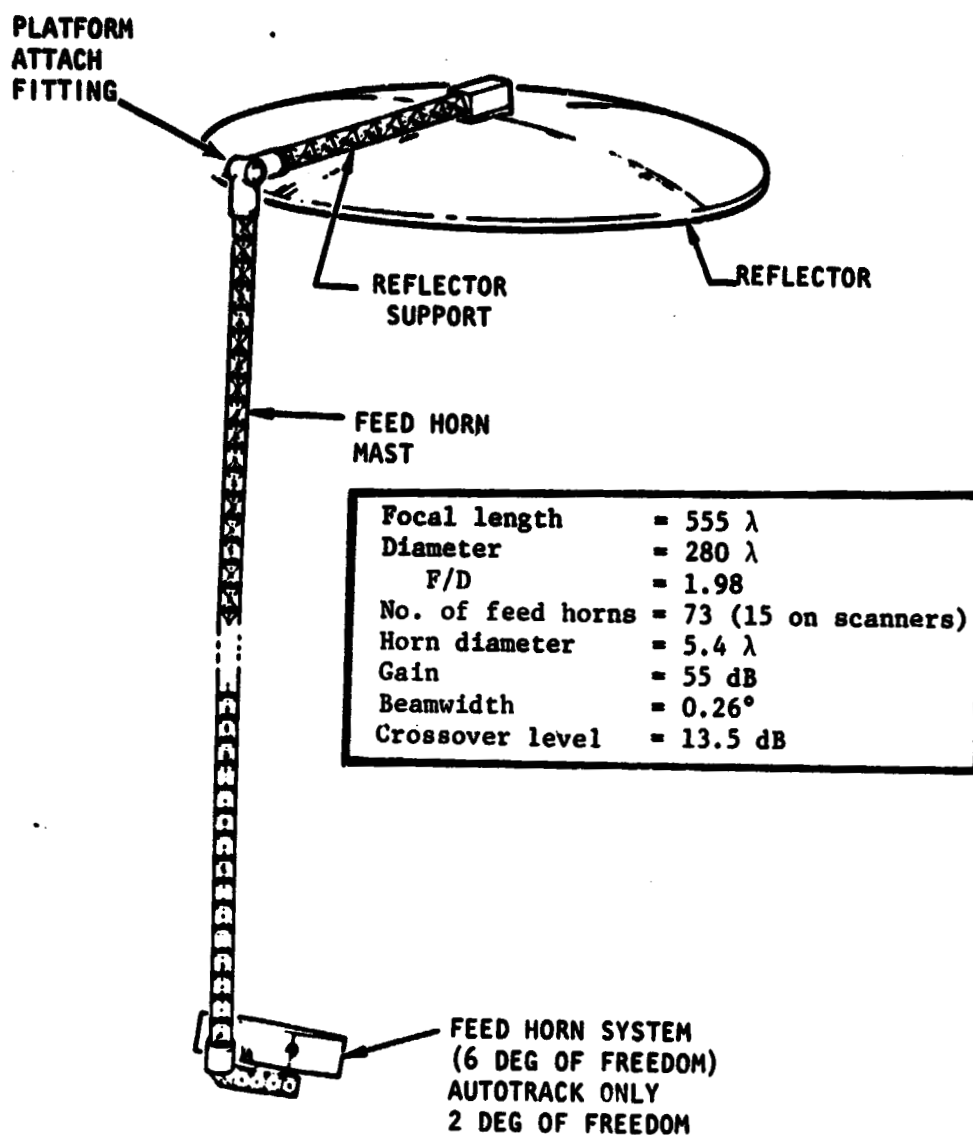


Figure 3.3.4-2. Perspective View of an
Individual Offset-Fed Parabolic
Reflector Antenna

having sidelobes nearly 30 dB down, and no beam would suffer more than 1/4 dB loss in gain. Beam intercept diameters would be 185 km (100 nmi), a size that is deemed desirable and appropriate by personnel of Bell Systems' Toll Transmission Laboratory.

In order to create the needed multiple beams, feed horns must be clustered in the offset focal plane of the reflector, preferably in a hexagonal array pattern. Even then, adjacent beam centers will be displaced by at least two beamwidths and the crossover will occur at a level of -12 dB or lower. There will, in fact, be directions in which the relative gain will be -16 dB or worse, so that the coverage provided by a single antenna is unacceptable.

The solution is to employ three identical antennas, numbered 1, 2, and 3 in Figure 3.3.4-3. Adjacent beams from antenna 1 have crossovers at the -13.5 dB level as indicated by the dashed circular contours. When beams from all three antennas are interleaved, as shown by the hexagonal pattern of small solid circles, the crossover level can be shown to be raised by a factor of 3 and becomes -4.5 dB. This assumes that the spot beams have Gaussian shapes with patterns described by

$$P(\theta) \text{ in dB} = -N \left(\frac{\theta}{\theta_N} \right)^2 \quad (1)$$

where θ_N is the angle at which the relative power level is -N dB. From the geometry it can be seen that the angular radii of the dashed and solid contours are in the ratio $\theta/\theta_N = 1/\sqrt{3}$. Equation (1) also can be used to show that nowhere in the entire coverage area will the relative gain be less than -6 dB.

This concept of beam interleaving from three antennas is applicable and realizable only over a relatively narrow frequency range in which antenna beamwidths do not appreciably change. The ratio of the highest frequency in the 6-GHz receive band to the lowest frequency in the 4-GHz transmit band is more than 1.7:1. For this reason, separate antenna systems are required for the downlink (3.7 to 4.2 GHz) and uplink (5.9 to 6.4 GHz) bands. Hence, it is convenient, in what follows, to describe antenna dimensions in terms of the wavelength at the center of the particular band in question.

Antenna Description

Due to the large size of the feed cluster in a multibeam antenna, blocking is unacceptably high in a symmetrical reflector system. Hence, the offset configuration shown in Figure 3.3.4-4 has been adopted. Both a single and a dual (Cassegrain) reflector system are shown; the former will be discussed first.

Single Offset Reflector System. The aperture diameter for the reflector has been taken to be $D = 280 \lambda$ which will yield a spot beam with a full half-power width of 0.26° . The focal length f must be large enough to ensure that the extreme off-axis beam is not appreciably degraded. This beam will be scanned through approximately 3° when pointing to either the easternmost or

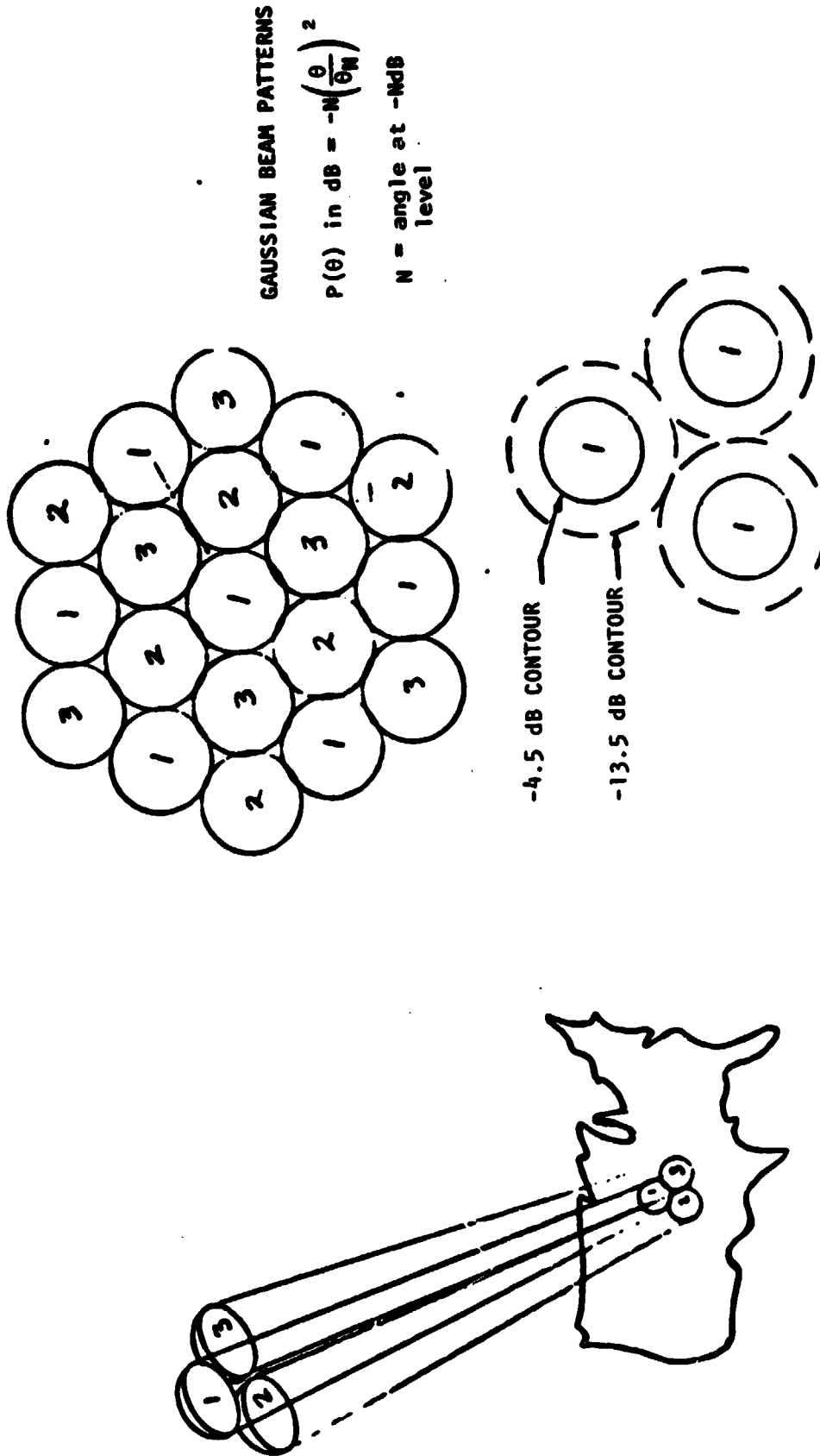


Figure 3.3.4-3. Contiguous, Interleaved Footprints with Three Antennas

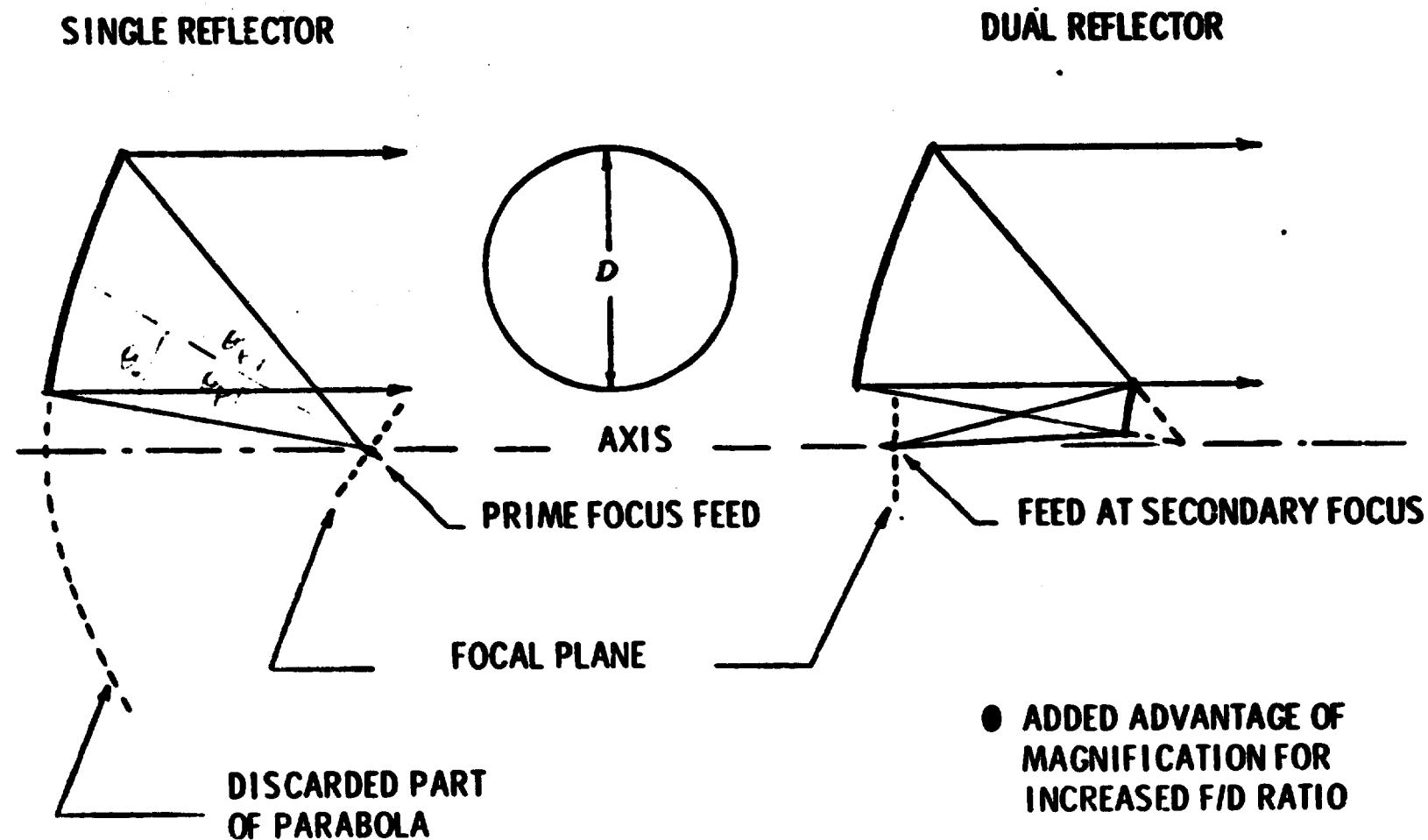


Figure 3.3.4-4. Offset Reflector without Blocking

westernmost extremity of the U.S. Off-axis beam performance can be characterized by the single parameter, due to Ruze,¹

$$X = n \left(\frac{D}{f} \right)^2 \left[1 + .02 \left(\frac{D}{f} \right)^2 \right]^{-1}$$

where n is the number of beamwidths scanned off the axis and is equal to $3/.26 = 11.5$ in this case. The parameter X has been shown² to be applicable to offset reflectors and so long as it does not exceed a value of about 3, then loss in gain and beam broadening will be negligible and the coma lobe will be below -25 dB. The value selected for focal length is 555λ which gives $f/D = 1.98$ and $X = 2.92$. From Ruze¹ the beam deviation factor is very close to unity, about 0.98.

In order to ensure that there will be no aperture blocking by the feed cluster, the offset geometry shown in Figure 3.3.4-4 has been chosen with $\theta_0 = 18.25^\circ$ and $\theta_f = 14.00^\circ$.

Feed Horn Selection. In order to permit frequency reuse it is essential that each spot beam have very low sidelobe and crosspolarization levels. Each feed must therefore act like an ideal Huygens source and, for this reason, the hybrid mode horn has been selected and is designed in accordance with the procedure of Thomas³. An edge illumination of -12 dB in the direction $\theta = \theta_f = 14^\circ$ is specified and the curves of Thomas show that $k_a \sin \theta_f = 3.7$, where $k = 2\pi/\lambda$ and a is the radius of the horn aperture. Thus, the aperture diameter of the horn is $2a = 4.9\lambda$. To find the mouth diameter of the horn it is necessary to add approximately 0.5λ to account for the depth of the corrugated grooves and for metal wall thickness. The mouth diameter is therefore 5.4λ and this is the minimum distance between horn phase centers when they are clustered. The angular separation between adjacent beams is simply equal to the minimum horn spacing divided by the focal length and reduced by the beam deviation factor. With BDF = 0.98, $f = 555\lambda$ and spacing equal to 5.5λ the angular separation between adjacent beams is 0.55° .

The crossover level for these adjacent beams may now be calculated from equation (1) in which $2\theta_N = 0.26^\circ$ for $N = 3$ dB, while $2\theta = 0.55^\circ$ at the crossover. Thus the level is -13.5 dB, as indicated in Figure 3.3.4-3.

Feed Cluster Sizing. The cluster of tightly packed feed horns arrayed in a hexagonal lattice is shown in Figure 3.3.4-5. The 73 horns, each with a mouth diameter of 5.5λ , form a cluster whose dimensions are 60.5λ wide by 34.0λ high. The circles in the pattern may also be interpreted as representing

¹J. Ruze, *Lateral Feed Displacement in a Paraboloid*, IEEE Trans. Antennas Propagat., AP-13, pp 660-665, September 1965.

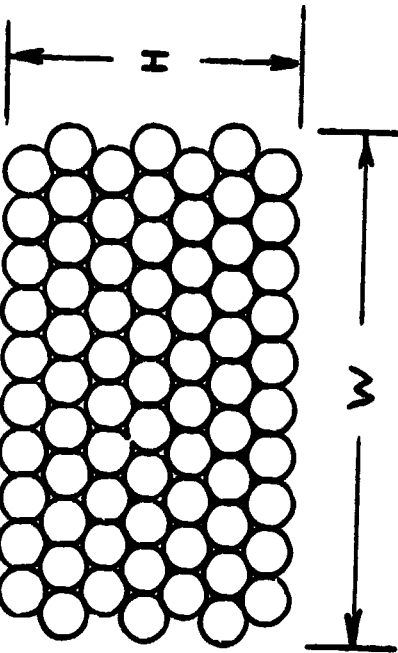
²E. A. Ohm, *A Proposed Multiple-Beam Microwave Antenna for Earth Stations and Satellites*, Bell Systems Technical Journal, 53, pp. 1657-1665, October 1974.

³B. Mac A. Thomas, *Design of Corrugated Conical Horns*, IEEE Trans. Antennas Propagat., AP-26, pp 367-327, March 1979

NO. OF BEAMS = NO. OF FEEDS = 73

FEED CLUSTER
(HEXAGONAL ARRAY OF HORNS,
5.5λ DIA.)

W = 60.5λ
H = 34.0λ



CONUS COVERAGE
(BEAMS HAVE ANGULAR
DIA. = 0.55° at
-13.5 dB LEVEL)
W = 6.05λ
H = 3.40λ

NOTE: THREE IDENTICAL ANTENNAS WITH 219 INTERLEAVED BEAMS COVERING CONUS
PLUS PARTS OF CANADA AND MEXICO WILL HAVE EFFECTIVE CROSSOVER LEVELS
OF -4.5 dB. NOWHERE IN THE COVERAGE ZONE WILL THE RELATIVE GAIN BE
LESS THAN -6 dB.

Figure 3.3.4-5. 73-Beam Offset Reflector Footprints

a single antenna's -13.5 dB circular contours, each of which has an angular diameter of 0.55° . The resulting 73 beam patterns thus cover a zone that is 6.05° wide (in the east-west direction) and 3.4° high (in the north-south direction), which is sufficient to include portions of Canada and Mexico, as well as CONUS.

Dual Offset Cassegrain Reflector System. The advantage of the Cassegrain configuration is that it provides the benefit of a long focal length in a physically compact structure; the focal distance of the main paraboloid is magnified in the ratio $m = e+1/e-1$, where e is the eccentricity of the hyperboloidal sub-reflector. One of the two foci of the hyperboloid must coincide with the focus of the main paraboloid. The location of the vertex of the sub-dish and its eccentricity then determine the location of the second focal point, where the feed must be located. It would seem that the introduction of two new parameters (vertex location and eccentricity of the hyperboloid) should not unduly complicate the design of a Cassegrain system. This is largely true for a symmetrical single-beam system in which it is only necessary to strike a balance between plane wave blocking by the sub-dish, and spherical wave blocking by the single feed horn. In the offset reflector with a single beam the same considerations apply, but it becomes more difficult to determine a geometry which eliminates both forms of blocking. When offset feeds are introduced for the formation of multiple beams in two dimensions, the design procedure becomes much more complex. Thus, for example, the addition of an offset feed requires that the sub-reflector dimensions be extended. This, in turn, causes an increase in the plane wave blocking by the sub-dish, making it larger than the spherical wave blocking by the feeds. To balance the two forms of blocking then requires a change in the Cassegrain geometry and so the process begins again.

Such an iterative design procedure has been used to arrive at the Cassegrain configuration shown in Figure 3.3.4-6 for the C-band downlink at a nominal frequency of 4 GHz ($\lambda = 7.5$ cm). The magnification factor is $m = 2.48$ which yields an effective focal length of $F = 41.66$ meters from a main reflector whose focal length is $f = 16.8$ meters. The equivalent paraboloid is defined by the angles $\theta_o = 18.25^\circ$, and $\theta_f = 14.00^\circ$ and has an aperture diameter $D = 21.00$ meters. Thus the equivalent parabola is identical to the reflector described above for the single offset reflector system. For this reason the same feed horns and feed cluster dimensions may be used; no redesign is necessary.

In the design of this system an effort was made to keep the second focus reasonably close to the vertex of the main paraboloid without requiring an unreasonably large offset in that reflector. The resulting design is a reasonable, though not an optimum one. As shown in Figure 3.3.4-7, there is a small amount of plane wave blocking caused by the extended sub-reflector. The blocked aperture area is less than 1.5%, however, and clearly occurs at the aperture edge, where illumination intensity is low (-12 dB). Thus, the loss in gain will be less than 0.1 dB.

Because of the long effective focal ratio of this system, depolarization by the reflector will be very small. According to Chu and Turrin¹ the cross-polarized losses will be suppressed to about -38 dB for this system.

¹T.S. Chu and R.H. Turrin, *Depolarization Properties of Offset Reflector Antennas*, IEEE Trans. Antennas Propagat., AP-21, pp 339-345, May 1973.

ORIGINAL PAGE IS
OF POOR QUALITY

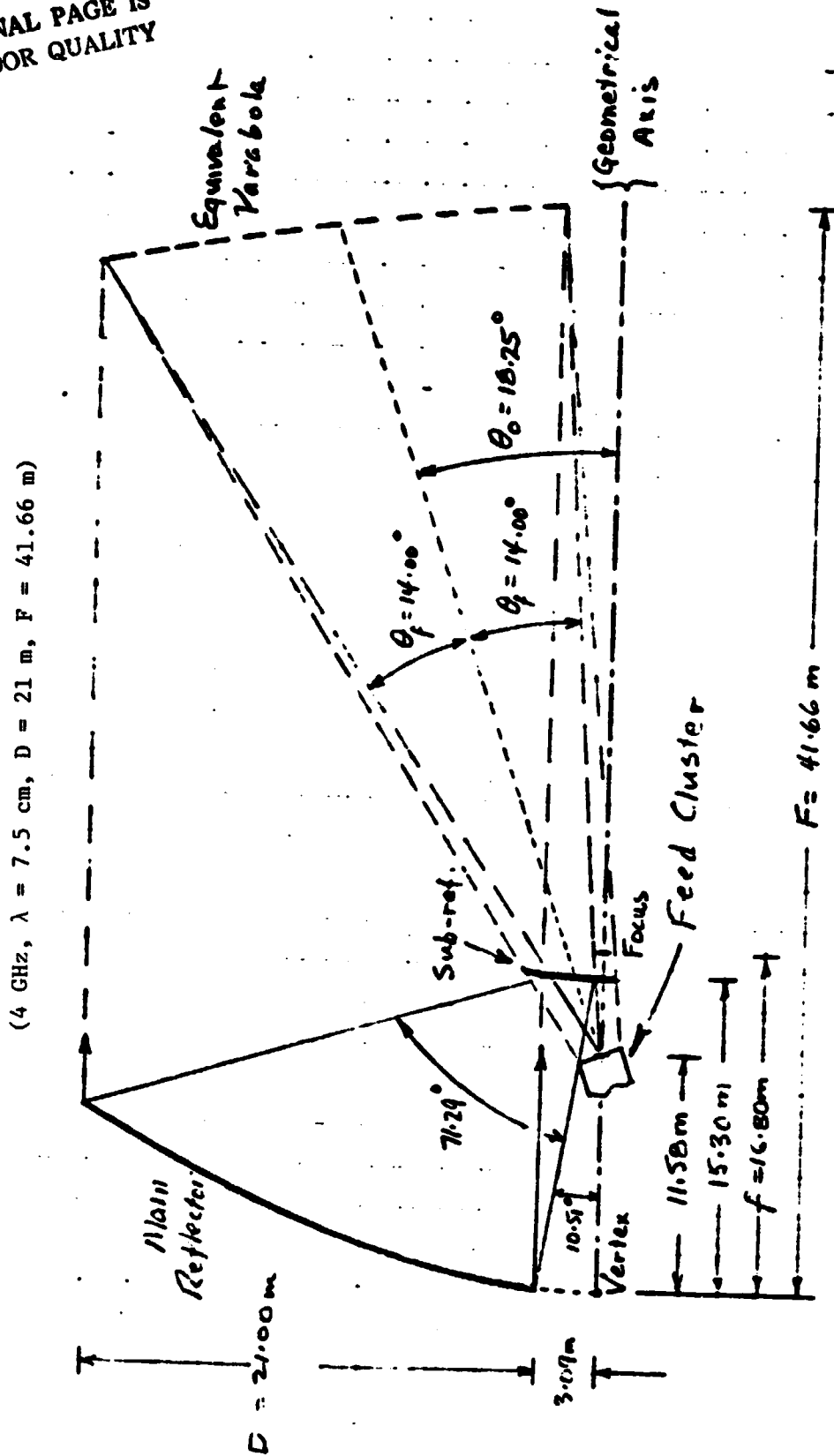


Figure 3.3.4-6. Dual Offset Cassegrain Reflector

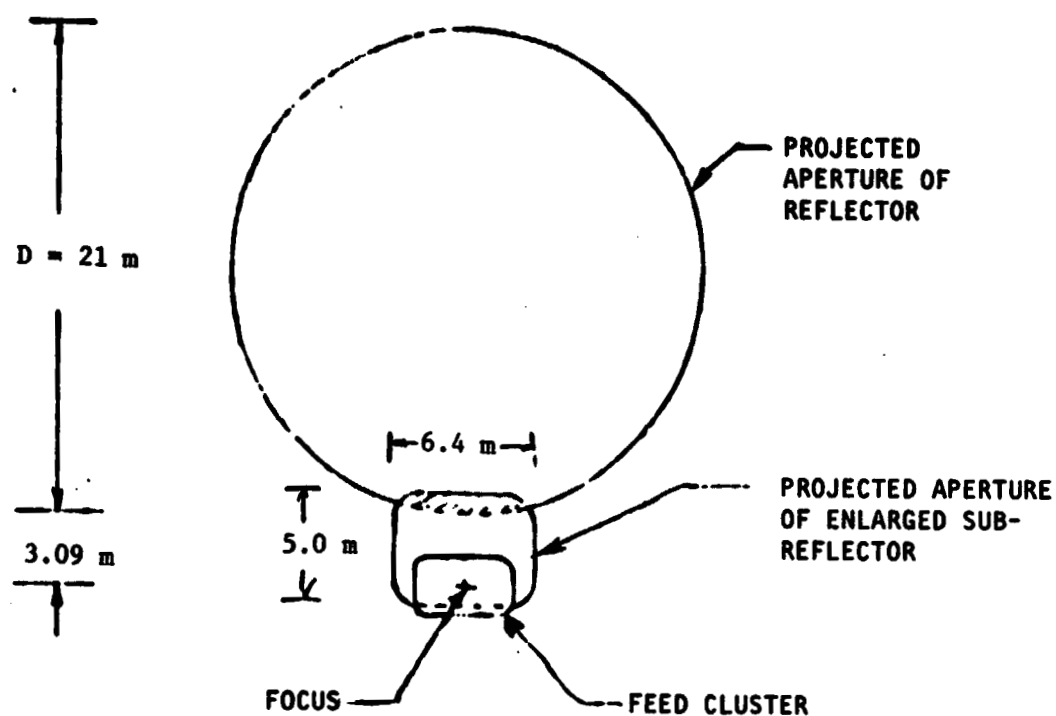


Figure 3.3.4-7. Elevation View of Dual Offset Reflector and Feed Cluster

The Cassegrain systems for the 6-GHz uplink and for the 12 to 14 GHz bands are scaled versions of the 4-GHz system.

Tolerances. Table 3.3.4-1 shows the principal tolerances that must be placed on the 21-m C-band antenna. Reflector roughness is calculated from the Ruze formula

$$\text{relative gain} = \exp \left[- \left(\frac{4\pi\sigma}{\lambda} \right)^2 \right]$$

If the loss in gain is not to exceed 0.1 dB, then the rms roughness, σ , must not exceed $\lambda/75$.

Table 3.3.4-1 Reflector Tolerances

21-M DIAMETER OFFSET REFLECTOR AT 4 GHz (HPBW = .0045 rad GAIN \approx 56.7 dB)		
PARAMETER	TOLERANCE	CRITERION
RMS SURFACE ROUGHNESS	$\lambda/75 = 1.0 \text{ mm}$	<0.12 dB GAIN LOSS
POINTING ACCURACY	$\pm .45 \text{ mr}$	1/10 (HPBW)
AXIAL DEFOCUSING	$\pm 21 \text{ cm}$	<0.1 dB GAIN LOSS
TRANSVERSE FEED DISPLACEMENT	$\pm 1.9 \text{ cm}$	1/10 (HPBW)

Pointing accuracy is required to be held to one-tenth of the half-power beamwidth, i.e., 0.45 milliradians. A transverse displacement ϵ_t of any feed in the focal plane will cause a beam squint of about ϵ_t/F radians. Since half-power beamwidth is given by $1.28 \lambda/D$ radians, it is seen that transverse feed displacement must be restricted to

$$\frac{\epsilon_t}{\lambda} = 0.128 \frac{F}{D} = 0.256.$$

The tolerance on axial feed displacement (defocusing) is much looser. The quadratic phase error due to axial displacement ϵ_a is

$$\delta = \frac{2\pi\epsilon_a}{\lambda} (1 - \cos \theta_f)$$

and the resulting loss in gain may be determined from the relation,

$$\text{loss in dB} = 20 \log_{10} \left(\frac{\sin \delta/2}{\delta/2} \right) .$$

From these relations, using $\theta_f = 14^\circ$, it is easily seen that no more than 0.1 dB loss in gain will occur if axial displacement, ϵ_a , does not exceed 2.8λ .

A detailed analysis of the tolerances required of the sub-reflector in the Cassegrain system has not been performed. Certainly, its surface roughness should be as good as (but need not exceed) that of the main reflector. Angular misorientation and transverse displacement of the sub-reflector will both produce beam squint and if this is not to exceed one-tenth of the beamwidth then the tolerances on these parameters appear to be of the same order as those demanded of the feed. It appears that axial displacement has more serious consequences for the sub-reflector, due to the inherent magnification of the Cassegrain configuration, than for the feed cluster, but since it is already rather loose for the latter (2.8λ as derived above), the tolerance required should present no problem.

Automatic Tracking Control. For purposes of telemetry, tracking, and control of the communication platform there will be a ground control station, preferably located somewhere near the center of the CONUS coverage zone, that is in contact with the platform. This is the logical location from which to transmit continuous pilot tones (in one of the guard bands within each of the communication channels) for the purpose of implementing an active autotrack system on the platform.

One way to do this is to use three adjacent feed horns (near the center of a cluster) to receive the pilot signal. Difference signals obtained from pairs of these horns then yield error signals in three directions at 120° to each other. These error signals are then amplified, processed, and used to servo-control the feed cluster in two orthogonal directions, namely E-W and N-S.

Two difficulties are apparent with this scheme. First, extraction of the pilot signal from the three horns will involve couplers and/or diplexers which will degrade the performance of the communications channels in these feed horns. Second, the crossover level between adjacent beams is too low, -13.5 dB, as explained earlier. The solution is to use entirely separate feeds which are located at A, B, C, and O, as shown in Figure 3.3.4-8. Simple geometry shows that round waveguides of diameter up to $d' = 0.89\lambda$ may be accommodated in the interstices between adjacent feed horns of the communications channels. Since the cutoff wavelength of the dominant TE_{11} mode is $\lambda_c = 1.705 d'$, it is clear that λ/λ_c must be in the range 0.66 to unity, which is quite satisfactory for a small waveguide feed.

Figure 3.3.4-9 also makes it clear that the spacing between adjacent pairs of these feeds is exactly one-half that between adjacent communications channel horns. From equation (1) it then appears that the crossover level should be raised by a factor of 4, from -13.5 dB to -3.4 dB. However, the small feeds create a nearly uniform illumination of the offset reflector aperture,

ORIGINAL PAGE IS
OF POOR QUALITY

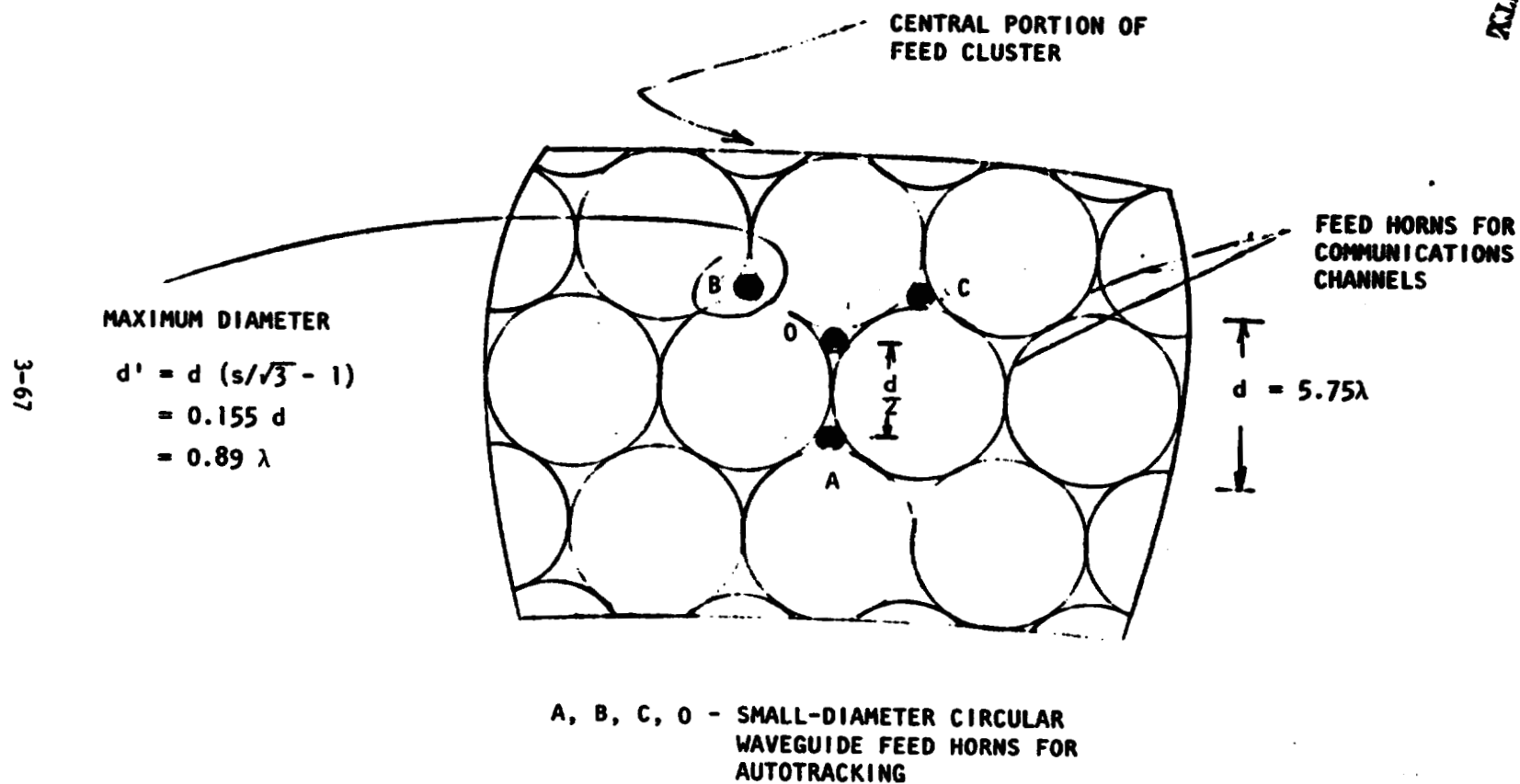


Figure 3.3.4-8. Autotrack Feed System

in contrast to the tapered illumination of the hybrid mode horns. Hence, the spot beams from the small feeds will be narrower, approximately in the ratio of 1.02/1.28. This will lower the crossover by the square of that ratio, giving a final level of -5.3 dB, which is excellent.

For tracking purposes, pilot tone difference signals are taken sequentially from pairs of horns. Thus, the difference signal from the pair OA is a measure of the angle of arrival of the pilot tone in the north-south plane. The difference signal from pairs OB and OC are measures, respectively, of the angles of arrival in planes inclined at $\pm 60^\circ$ to the north-south plane. Obviously, these two can be combined to yield a measure of angle of arrival in the east-west plane. By suitably processing the E-W and N-S information, command signals can be obtained for servo-control of the complex feed cluster as a unit, enabling it to move in two orthogonal directions as it tracks the pilot tone. Although somewhat different from the conventional monopulse tracking system, in which the complete antenna (including reflector) is servoed, this system will yield similar precision and is therefore capable of maintaining pointing accuracy to one-tenth beamwidth.

Power Calculation

As mentioned earlier, the number of beams needed to cover the Continental United States is 219 when each spot is an elliptical 207 km by 296 km. It is necessary to use the interwoven patterns from three antennas to provide -4.5 dB crossovers when highly tapered illumination is used for the reflectors. This degree of taper is needed to provide -35 dB sidelobes. Shown in Figure 3.3.4-1 are three transmitting antennas at 4 GHz, three receiving antennas at 6.2 GHz, and two scanning antennas for filling gaps caused by overloads or failures. Separate transmitting and receiving antennas are used to aid the isolation problem between transmitters and receivers. Also shown is a repetition of the above for the 12/14 GHz.

The power calculation at 4 GHz is straightforward and rather independent of satellite location. One dB is an ample allowance for rain attenuation. Using 2.1 watts per carrier and an average of two carriers per 219 spots, the RF power required is 1035 watts. At 25% dc-to-RF efficiency, the solar array power is required to be 4.14 kW.

At 12 GHz the power required is a function of satellite location. Taking a reasonably good case of 80° west, the RF power per carrier is 30 watts. Again, at two carriers per spot, 219 spots, the RF power is 14.8 kW. The solar array power is 59 kW. Note that only 3 dB rain attenuation was allowed. Data from AT&T indicate 8 dB is needed in most cities east of the Mississippi River for the desired 0.02% outage time (1.8 hours). Indeed, Miami needs 14 dB allowance for rain, and Atlanta 10 dB. However, Miami, New Orleans, Mobile, Tampa, and Jacksonville will probably have multiple sites to ease this problem. Heavy rain falls in widely spaced cells; site diversity in these locations is needed. For other areas, we have the scanning beams which can "burn through" with the extra power required. Normal heavy rain, 16 mm/hour or greater, occurs 20 hours per year (east coast average).

For a satellite located at 135°W, the power increases substantially in rain. Mask angles approach 15° and most eastern cities require 14 dB rain margin. Atlanta needs 19 dB, and Miami needs 24 dB. To provide 16 mm/hour coverage over the east coast, a margin of 7.2 dB is calculated using 4 km of rain thickness at a mask angle of 18°. An increase in power capability of 2.63 (4.2 dB) is indicated. The solar array power becomes 155 kW. Coverage for the time between 16 mm/hour (20 hours/year) and 60 mm/hour (1.8 hours/year) is provided by the scanning beams. The power needed is estimated to be 15 beams at $21.4 \text{ watts} \times 2.63 \times 4 \text{ carriers} \times 15.8 \text{ (12 dB increase in margin)} \times 1/25 \text{ (efficiency)} = 213 \text{ kW}$. Four carriers are selected since scanning beam must have capability of densest traffic. The power requirements are summarized in Table 3.3.4-1.

Table 3.3.4-2. Solar Array Power for Satellite
at Indicated Latitude

	100°W	135°W
4 GHz	4 kW	4 kW
12 GHz (heavy rain)	59 kW	155 kW
26 GHz (extra-heavy rainfall)	26 kW	213 kW*
Total	89 kW	372 kW
*Only 20 hours per year.		

Refer to Tables 3.3.4-3 and 3.3.4-4 for link margin calculations.

Table 3.3.4-3. 4-GHz Downlink Characteristics

				Link (+)	Link (-)	Link E
Frequency						
P_T	2.1W Power Generated	dBm Per Carrier		33.3		
G_T	Transmitter Gain	dB 56 - 4.5 dB		51.5		
L_M	Modulation Loss	dB			1.0	
L_{CT}	Trans. Circuit Loss	dB			2.0	
L_{RT}	Trans. Radome Loss	dB				
ERP	Eff. Radiated Power	dBm				81.8
$d = 37,000$ km						
$(4\pi \frac{d}{\lambda})^2$	Space Loss	dB			195.8	
$\lambda = 7.5$ cm						
L_p	Propagation Loss	dB			1.0	
L_t	Tracking Loss	dB			0.4	
S_I	Rec. Signal Relative	dBm				-115.4
to Isotrope						
L_{RR}	Rec. Radome Loss	dB			1.0	
L_{CR}	Rec. Circuit Loss	dB			.3	
$L_{pol.}$	Polarization Loss	dB			.2	
G_R	Receiver Gain	dB	Sm	44.0		
$\Delta\theta = 1^\circ$						
S	Rec. Signal	dBm				-72.9
kT_f	Rec. Noise Density	dBm/Hz		171.0		
3 dB NF						
Δf	Noise Bandwidth	dBHz	40 MHz		76.0	
$N = KTA F$	Link Noise	dBm				-95.0
E_b/n_o	Link	dB				22.1
E_b/n_o	Composite	dB				
E_b/n_o	Required BER=10 ⁻⁷	dB	QPSK		14.3	
Margin		dB			7.8	

299.8

299.8

Data Rate Per Carrier = 64 M Bits/sec
1000 Conversations

Table 3.3.4-4. 12-GHz Downlink Characteristics

			Link (+)	Link (-)	Link Σ
Frequency					
P_T 30W	Power Generated	dBm per carrier	44.8		
G_T	Transmitter Gain	dB 56 dB - 4.5	51.5		
L_M	Modulation Loss	dB		1.0	
L_{CT}	Trans. Circuit Loss	dB		2.0	
L_{RT}	Trans. Radome Loss	dB			
ERP	Eff. Radiated Power	dBm			93.3
$d = 37,000$ Km					
$(4\pi \frac{d}{\lambda})^2$	Space Loss $\lambda = 2.5$ cm	dB		205.3	
L_p	Propagation Loss	dB 16 mm/Hr Rain 6 km Thick		3.0	
L_t	Tracking Loss	dB		0.4	
S_I	Rec. Signal Relative	dBm to Isotrope			-115.4
L_{rR}	Rec. Radome Loss	dB		1.0	
L_{CR}	Rec. Circuit Loss	dB		.3	
$L_{pol.}$	Polarization Loss	dB		.2	
G_R	Receiver Gain	dB 1.7m $\Delta\theta = 1^\circ$	44.0		
S	Rec. Signal	dBm			-72.9
kT_F	Rec. Noise Density	dBm/Hz	171.0		
Δf	Noise Bandwidth	dHz		76.0	
N	Link Noise	dBm			-95.0
E_b/n_o	Link	dB			22.1
E_b/n_o	Composite	dB			
E_b/n_o	Required	dB		14.3	
Margin		dB		7.8	

311.3

311.3

Satellite @ 100° West
Florida @ 80° W, 30°N
Mask Angle = 48°

3.3.5 Thermal Analysis and Temperature Control Subsystem Definition

Two types of thermal analyses were employed in developing subsystems design concepts. The first involved potential distortion effects and stress loads arising from temperature differences across structural members. The second was concerned with maintaining a viable temperature range for selected mission equipment components, generally through use of radiators. From these latter analyses, design concepts were developed for location and sizing of radiators for key components. These radiators can be considered as functionally comprising a thermal control subsystem. In the following presentation the structural thermal analyses dealing with the erectable structure elements are first presented. These are followed by thermal analysis presentations common to mission equipment on both the erectable and space-fabricated platforms.

Thin-Walled, Cylindrical Struts

The supporting structure for the erectable communications platform contains thin-walled tubular struts ranging in diameter from 0.305m (12 inches) to 0.533m (21 inches). When exposed to sunlight on one side, such tubes develop substantial cross wise temperature gradients. Tube separation distances are large enough to keep self-shadowing time down to a few minutes at most. However, an eclipse lasts long enough to produce very large drops in tube average temperatures. Cross wise temperature gradients in a single tube will produce bending moments. Relative changes in the average temperature of adjacent tubes can have more serious consequences since they may result in distortion of the structure as a whole through differential expansion.

In order to evaluate these effects, a transient, three-node thermal model was written for the SR 52 programmable calculator. This model (see Figure 3.3.5-1) considers an infinite tube heated by solar radiation impinging at an angle θ normal to the tube axis. The tube surface is characterized by a solar absorptivity α and an emissivity ϵ . The tube is divided into quadrants, symmetrical with respect to the solar direction. The two "side" quadrants are thermally identical. Circumferential condition is determined by wall thickness δ and the material conductivity k .

Radiative transport between nodes depends upon the graybody shape factor \bar{F} . Each quadrant has a projected area of $\sqrt{2} D/2$ per unit length. For this purpose the \bar{F} values were estimated to be equal to ϵF where F is the blackbody shape factor. Thus $\bar{F}_{12} = \bar{F}_{21} = \epsilon \left(\frac{2 - \sqrt{2}}{2} \right)$ and $\bar{F}_{13} = \epsilon (\sqrt{2} - 1)$ For thin-walled tubes of moderate-to-large size, radiative transport dominates conduction.

The working equations are as follows:

$$(1) \frac{dT_1}{dt} = \frac{2\sqrt{2}}{\pi} \frac{\alpha I_{sc} \cos \theta}{\delta \rho C_p} - 2 \dot{Q}_{C12} - 2 \dot{Q}_{R12} - \dot{Q}_{R13} - \frac{\sigma \epsilon T_1^4}{\delta \rho C_p}$$

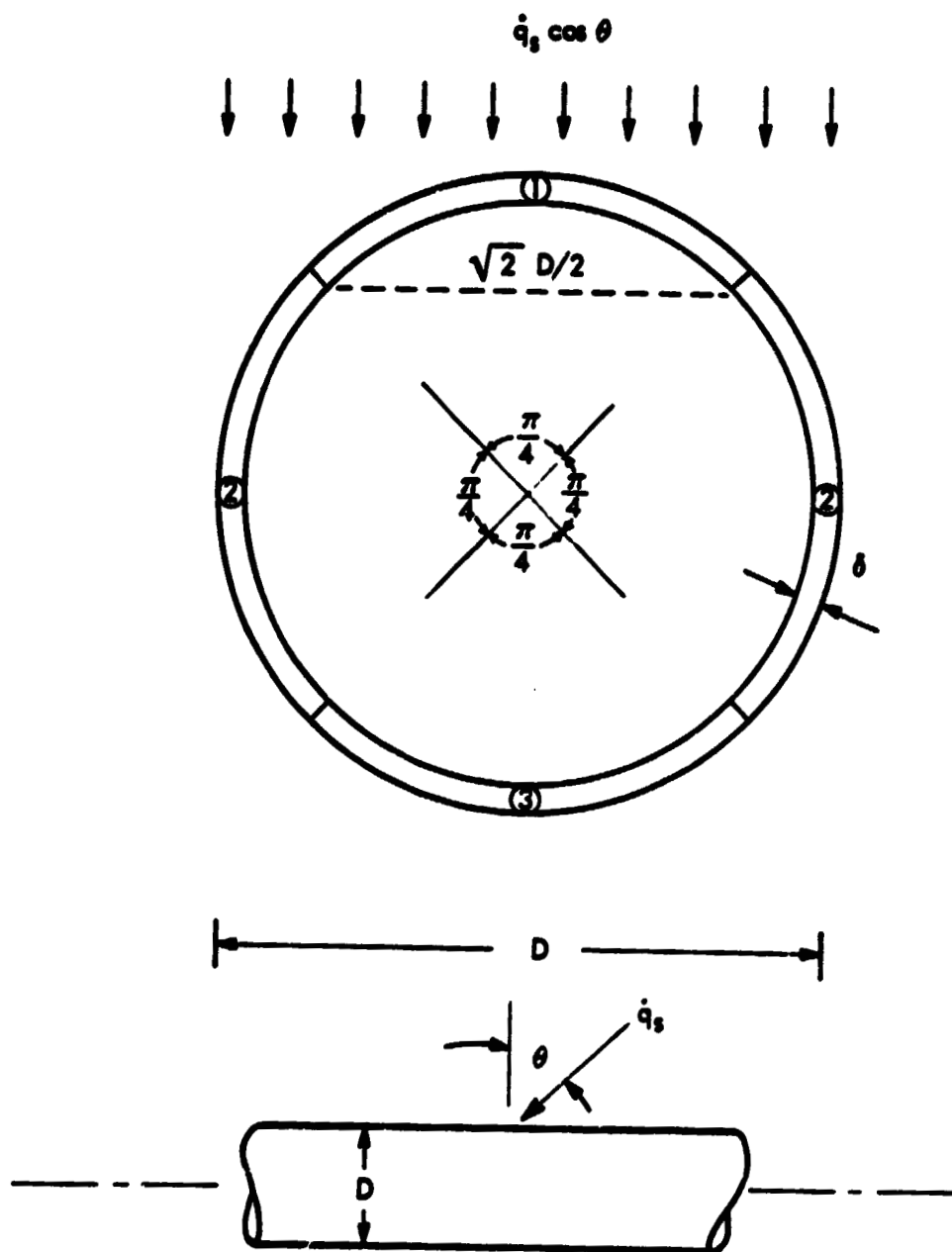


Figure 3.3.5-1. Thin-Walled Tube Thermal Model

(2)

$$\frac{dT_2}{dt} = \left(\frac{2 - \sqrt{2}}{\pi} \right) \frac{\alpha I_{sc} \cos \theta}{\delta \rho C_p} + \dot{Q}_{C12} - \dot{Q}_{C23} + \dot{Q}_{R12} - \dot{Q}_{R23} - \frac{\sigma \epsilon T_2^4}{\delta \rho C_p}$$

(3)

$$\frac{dT_3}{dt} = 2\dot{Q}_{C23} + 2\dot{Q}_{R23} + \dot{Q}_{R13} - \frac{\sigma \epsilon T_3^4}{\delta \rho C_p}$$

where

$$\dot{Q}_{C12} = \frac{16}{\pi^2} \frac{k (T_1 - T_2)}{\rho C_p D^2}$$

$$\dot{Q}_{C23} = \frac{16}{\pi^2} \frac{k (T_2 - T_3)}{\rho C_p D^2}$$

$$\dot{Q}_{R12} = \frac{2\sqrt{2}}{\pi} \frac{\sigma \bar{F}_{12} (T_1^4 - T_2^4)}{\delta \rho C_p}$$

$$\dot{Q}_{R13} = \frac{2\sqrt{2}}{\pi} \frac{\sigma \bar{F}_{13} (T_1^4 - T_3^4)}{\delta \rho C_p}$$

$$\dot{Q}_{R23} = \frac{2\sqrt{2}}{\pi} \frac{\sigma \bar{F}_{23} (T_2^4 - T_3^4)}{\delta \rho C_p}$$

The program implementing Equations 1 through 3 was checked by comparing results with those reported by Boeing (Reference 1) using a thermal analyzer program. Inputs (thermal properties, solar constant and dimensions) were held constant for the comparison. Figure 3.3.5-2 shows results for a 50.8mm (2 inch) diameter graphite-epoxy cylinder exposed to sunlight at normal incidence. There are detailed differences in the local temperatures but the overall transient behavior is quite similar. This lends confidence in the simple model for quick evaluations of other cylindrical strut transients.

Figures 3.3.5-3, 3.3.5-4, 3.3.5-5 and 3.3.5-6 show transients calculations for large and medium size graphite-epoxy struts during eclipse at GEO. For each diameter the effect of unaltered surface and selective coatings is shown. The aluminized Teflon, if practical, will reduce gradients somewhat and temperature levels considerably.

Thermal Distortion of Three-Strut Trusses

A major structural element of the erectable communications platform is a truss made up of three parallel sections. The sections are thin-walled, graphite-epoxy tubes 0.305m (12 inches) in diameter. One section has a wall thickness of 0.762mm (0.030 inch) and the other two have walls twice as thick.

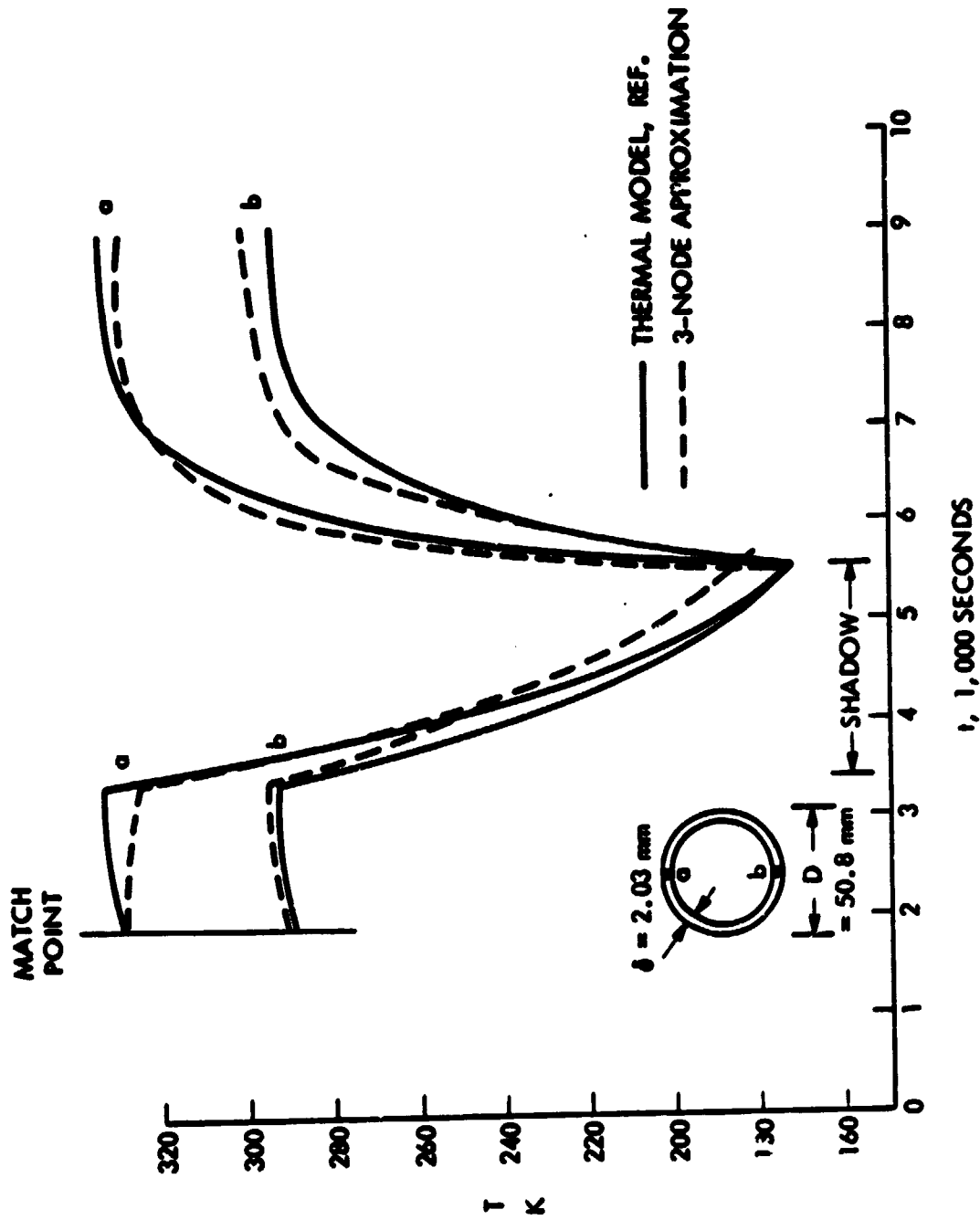


Figure 3.3.5-2. Comparison of Eclipse Temperature Predictions

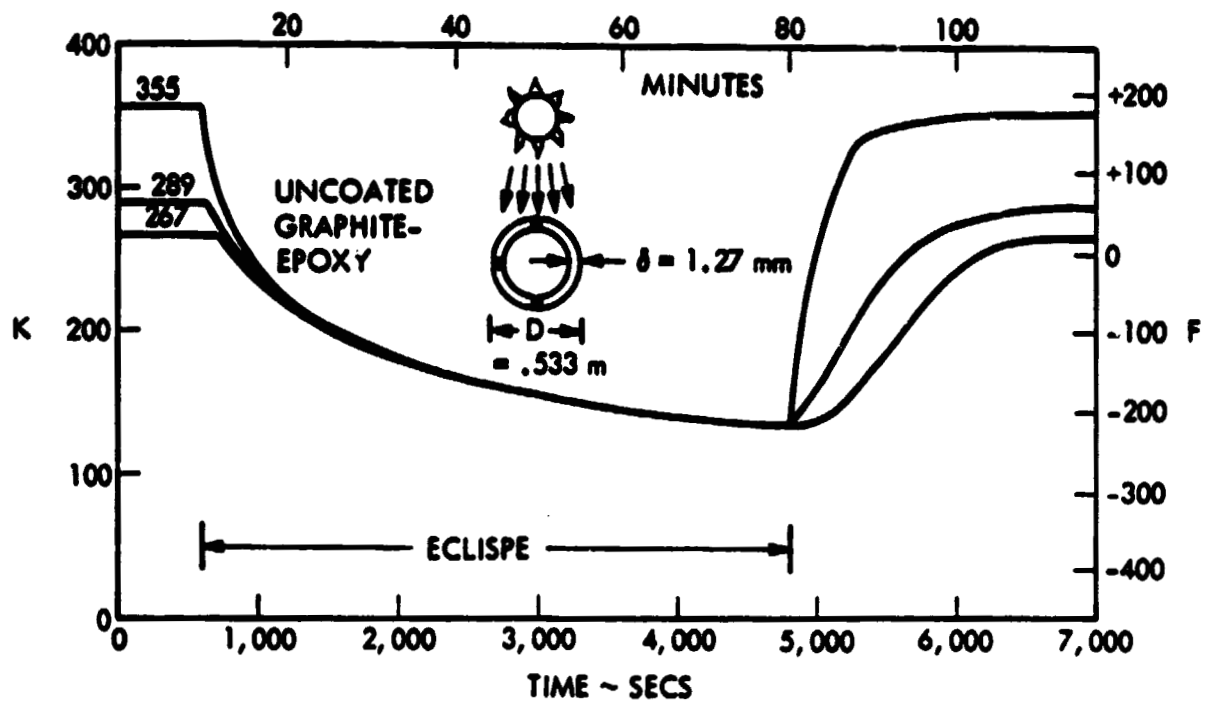


Figure 3.3.5-3. Large-Diameter Strut Temperatures—Uncoated

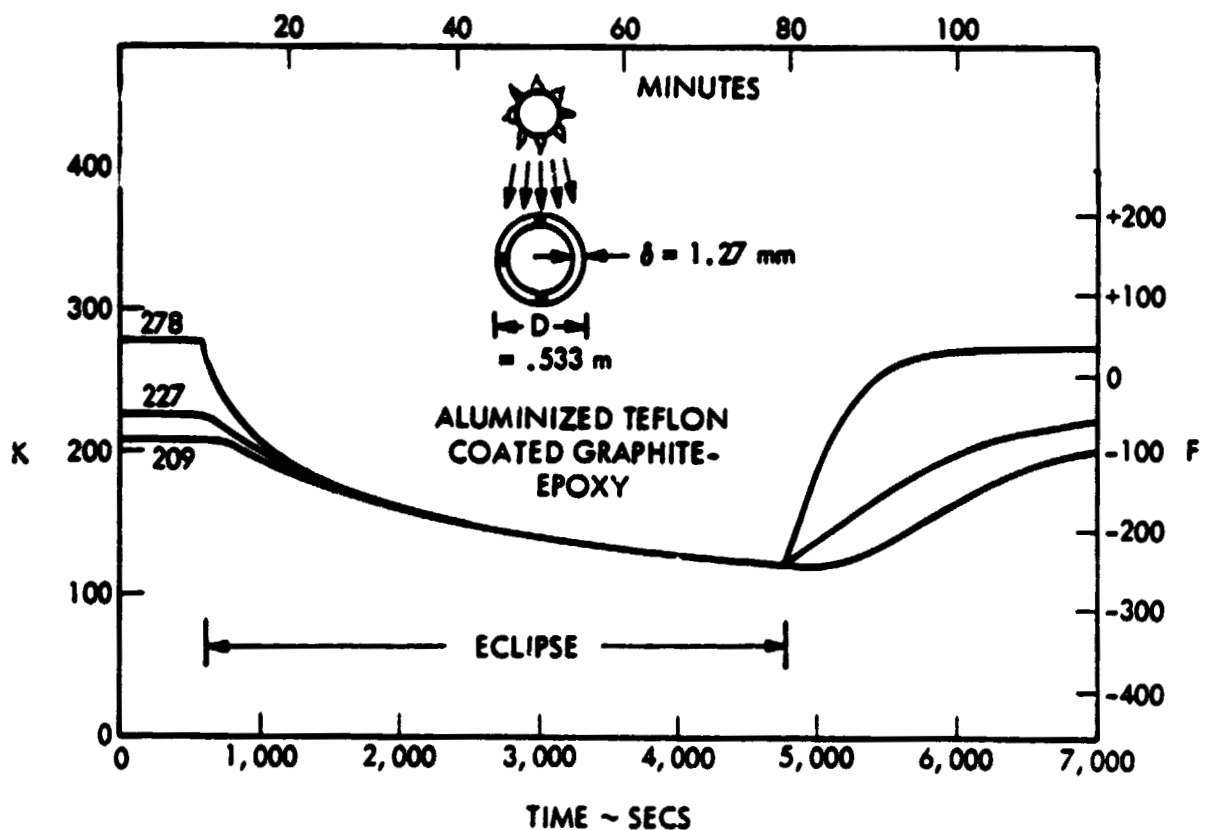


Figure 3.3.5-4. Large-Diameter Strut Temperatures—Selective Coating

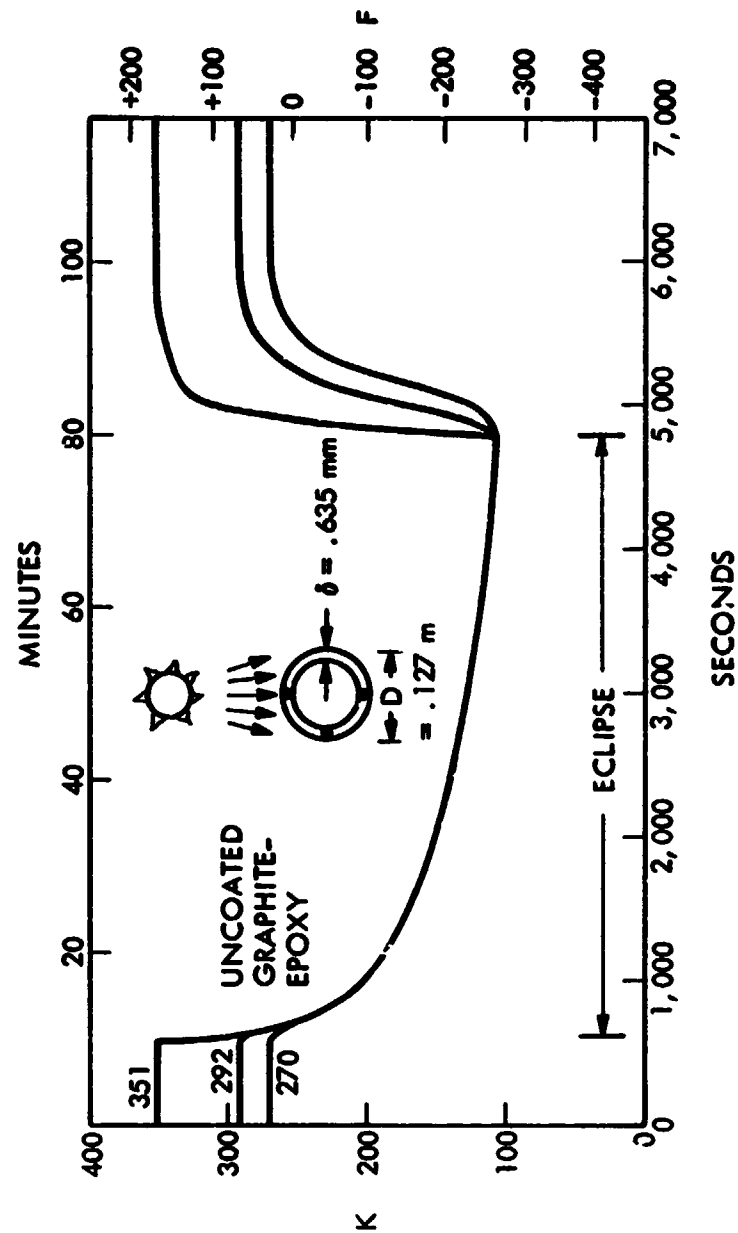


Figure 3.3.5-5. Small-Diameter Strut Temperatures—Uncoated

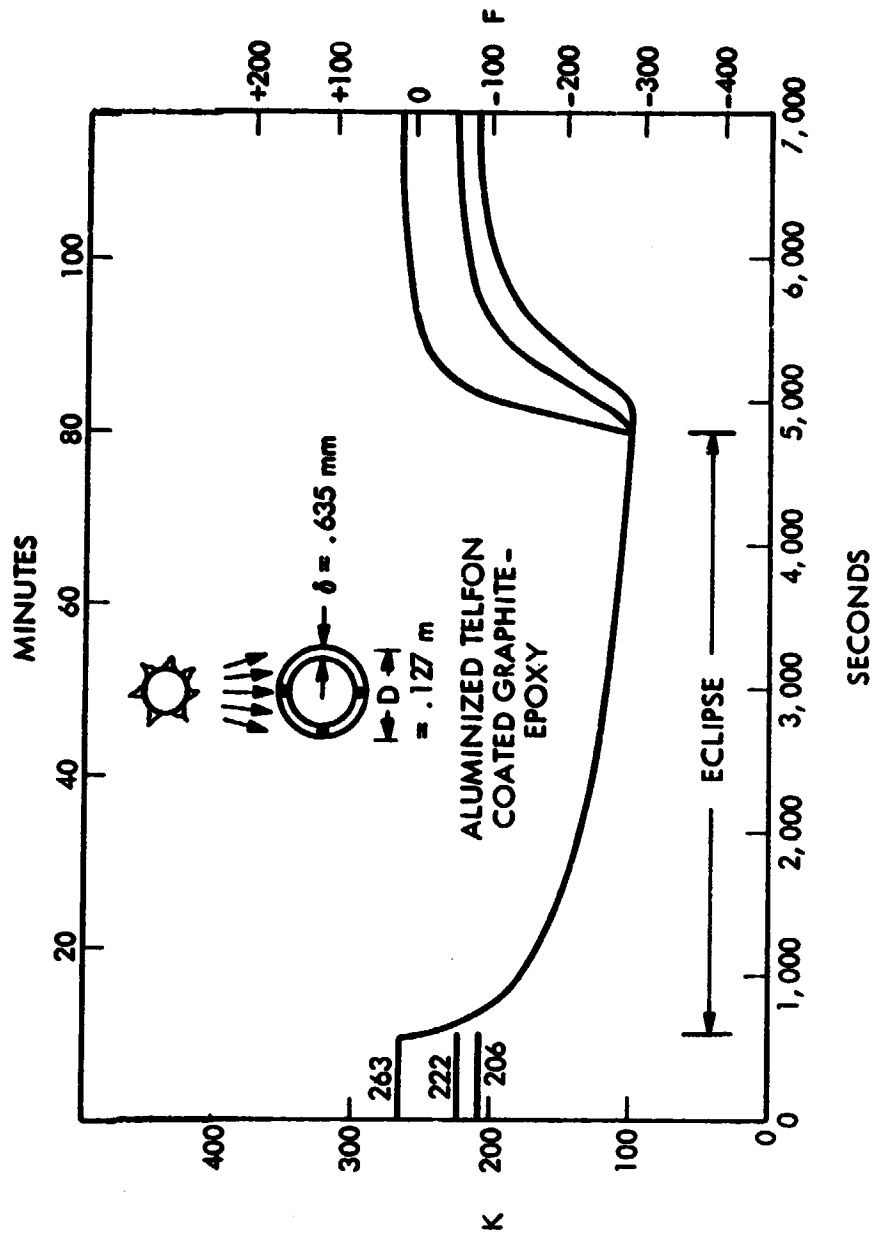


Figure 3.3.5-6. Small-Diameter Strut Temperatures--Selective Coating

During orbit, two types of thermal distortion occur. Individual tubes will develop substantial temperature differences between their sunlit and opposite sides. This will cause each tube section to bow away from the solar direction. In addition, differences in orientation, surface properties or thermal capacitance will cause changes in the average temperature of the struts, leading to distortion of the truss as a whole. No special criterion has been established for across-tube gradients as yet. Inter-tube temperature differences as great as 28 C (50 F) are acceptable.

The transient thermal model for thin-walled cylinders described in a previous section was used to evaluate the thermal gradients across the three-strut truss exposed to eclipse transients at GEO. Figure 3.3.5-7 shows gradients across individual struts and across the three-membered truss as a whole. As may be seen, the across-tube gradients are very large (150 - 200 C), particularly during emergence from the eclipse. If such gradients are found to be unacceptable, they can be reduced 30% by application of external selective surface treatment. The inter-tube gradients are more moderate (30 - 35 C) but still somewhat greater than the 28 C requirement. Selective coating or maintenance of equal tube thickness on all struts would reduce or eliminate inter-tube gradients.

Heat Rejection Radiator Subsystem

As presently conceived, the Communications Platform has several concentrated sources of heat requiring dissipation by radiating surfaces. Radiator performance is conditioned by several factors:

- (1) Orientation with respect to the sun.
- (2) Placement and orientation with respect to extended hot surfaces such as the solar array.
- (3) Temperature limitations imposed by the thermal load.

In addition, such factors as long-term reliability in a space environment must be considered. The long life requirement has led to the concept of a heat pipe radiator in which heat is taken from the load(s) by a fluid coolant and delivered to the base of a radiator equipped with heat pipes for distribution over the surface. The innate redundancy of this construction assures functional survival of the unit even after several meteoroid hits.

Heat dissipation requirements, based on a 112.5 kW communication platform, are given in Table 3.3.5-1.

Radiator performance (watts per square meter) was estimated for a variety of possible configurations. The radiator inlet temperature was assumed to be 6 C (10 F) below the load service temperature and 17 C (30 F) below the outlet temperature. A selective radiator surface ($\alpha/\epsilon = .75/.15$) was assumed. A radiator effectiveness of 0.75 was assigned. This value is probably conservative, especially for the lower range of radiator temperatures.

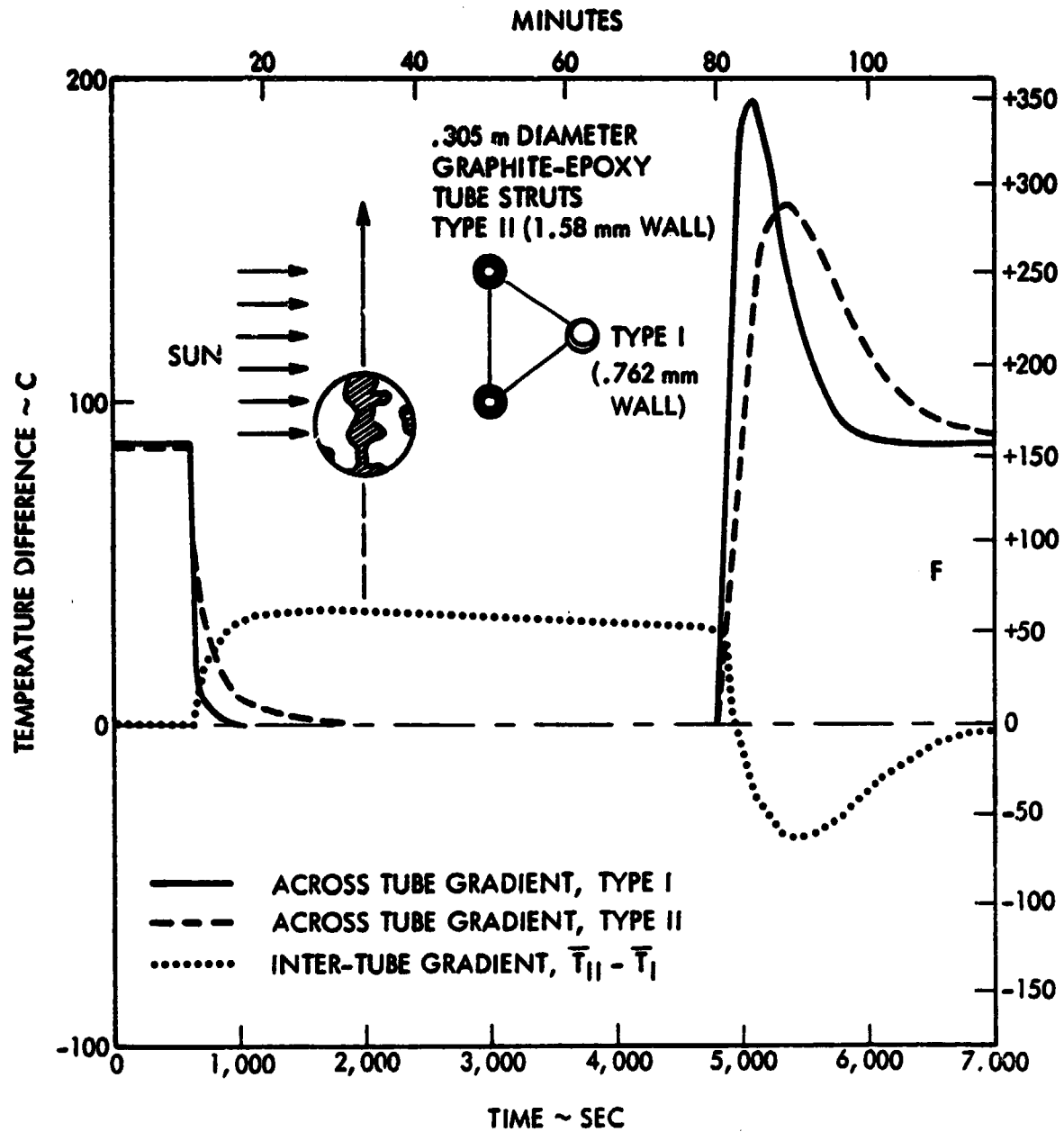


Figure 3.3.5-7. Strut Temperature Gradients during Equinoctial Eclipse

TABLE 3.3.5-1 Representative Heat Dissipation
Requirements for 112.5 kW Communications Platform

<u>Category</u>	<u>Heat Dissipation</u>	<u>Load Service Temperature</u>
dc/dc Converters	5.9 kW	74 C
Batteries (Charging)	1.0 kW	10 C
(Discharging)	18.9 kW	
Housekeeping	4.3 kW	74 C
Antennas	16.9 kW	74 C

Figure 3.3.5-8 presents estimated heat rejection rates for two-sided radiators in different thermal configurations. Poorest performance is shown by a radiator located near the solar array but mounted perpendicular to the antenna platform so that it lies in the equatorial plane. It is exposed both to solar radiation at 23 degrees and has a substantial view factor (~ 0.3) with respect to the array. Substantially better performance can be obtained by moving the radiator farther from the array and/or eliminating the solar input by maintaining the radiator in the ecliptic plane or providing a sun shield. An even greater improvement occurs when the system is in eclipse. There, solar input is absent and the cooling solar array emits less heat radiation. Luckily this enhanced performance occurs at the time of greatest battery heat load (see Table 3.3.5-1).

It is logical to group together the heat rejection associated with battery charge/discharge and that due to power conditioning into one or more modules, complete with radiator. Even though radiator performance is better during eclipse, the high dissipation due to battery discharge makes the eclipse condition the driver for radiator sizing. Since at GEO eclipse lasts for only five percent of the orbit or less, this suggests the use of phase-change material (PCM) as a way of reducing radiator size and weight. For the heat loads given in Table 3.3.5-1 the eclipse peak could be leveled out by means of 356 kg of tetradecane (melting point 5.5°C). However, the mass of the PCM containers (usually finned aluminum boxes) can be several times that of the PCM itself. Figure 3.3.5-9, adapted from Reference 2, shows a typical trade analysis which compares the mass of a radiator sized to take a peak heat load with the mass of a smaller radiator plus PCM. As Figure 3.3.5-9 shows, container mass is several times PCM mass if the temperature rise across the container is kept to a moderate value. Moreover, the weight advantage over a simple radiator is marginal even at rather low radiator temperatures. For these reasons, the PCM approach is not considered to be effective for the present application.

Thermal Dissipation from Antenna Feed

The individual antenna feed assemblies generate approximately twice as much thermal energy as radio-frequency output at the antenna. In the case of

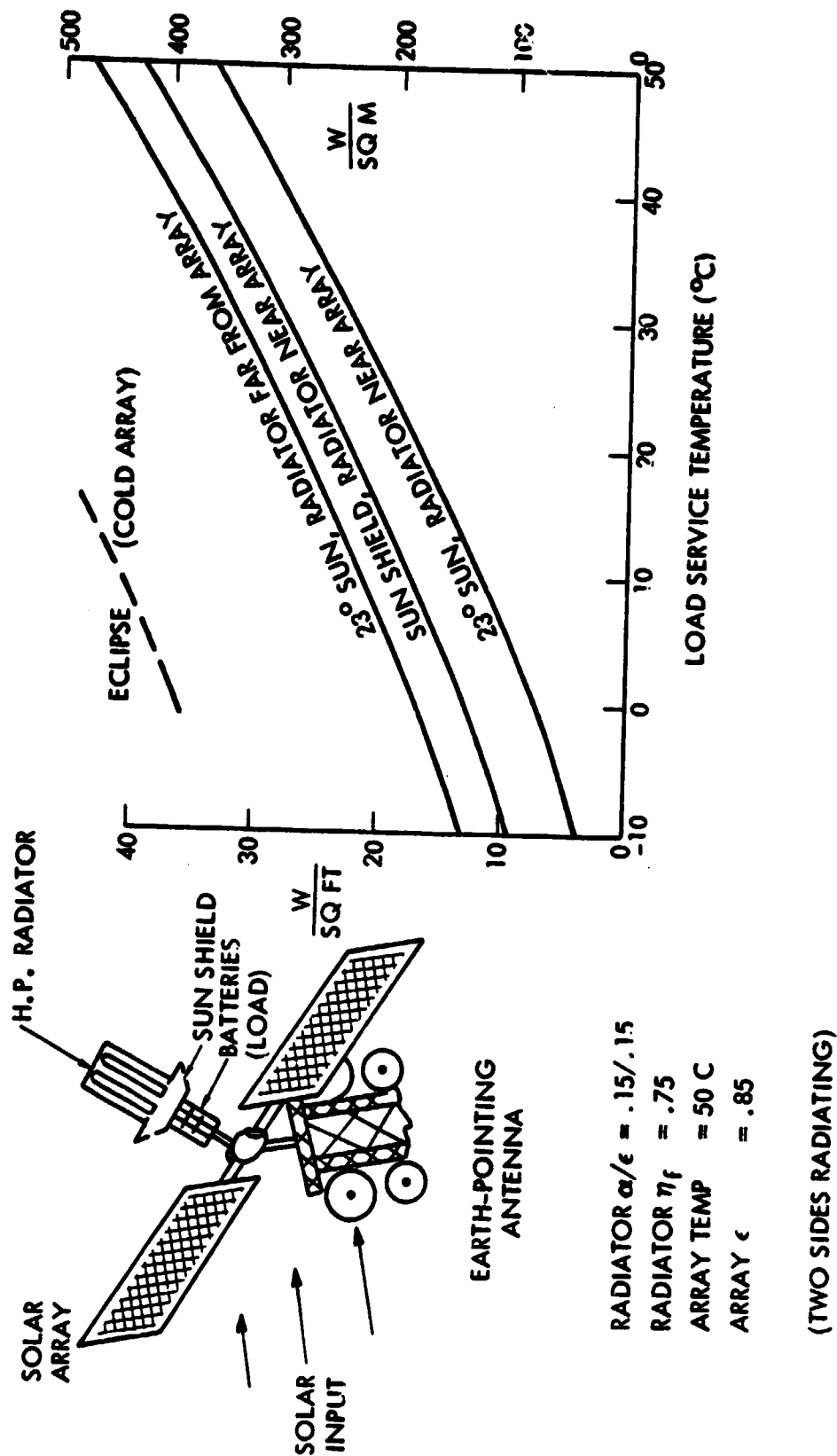


Figure 3.3.5-8. Radiator Heat Rejection Performance

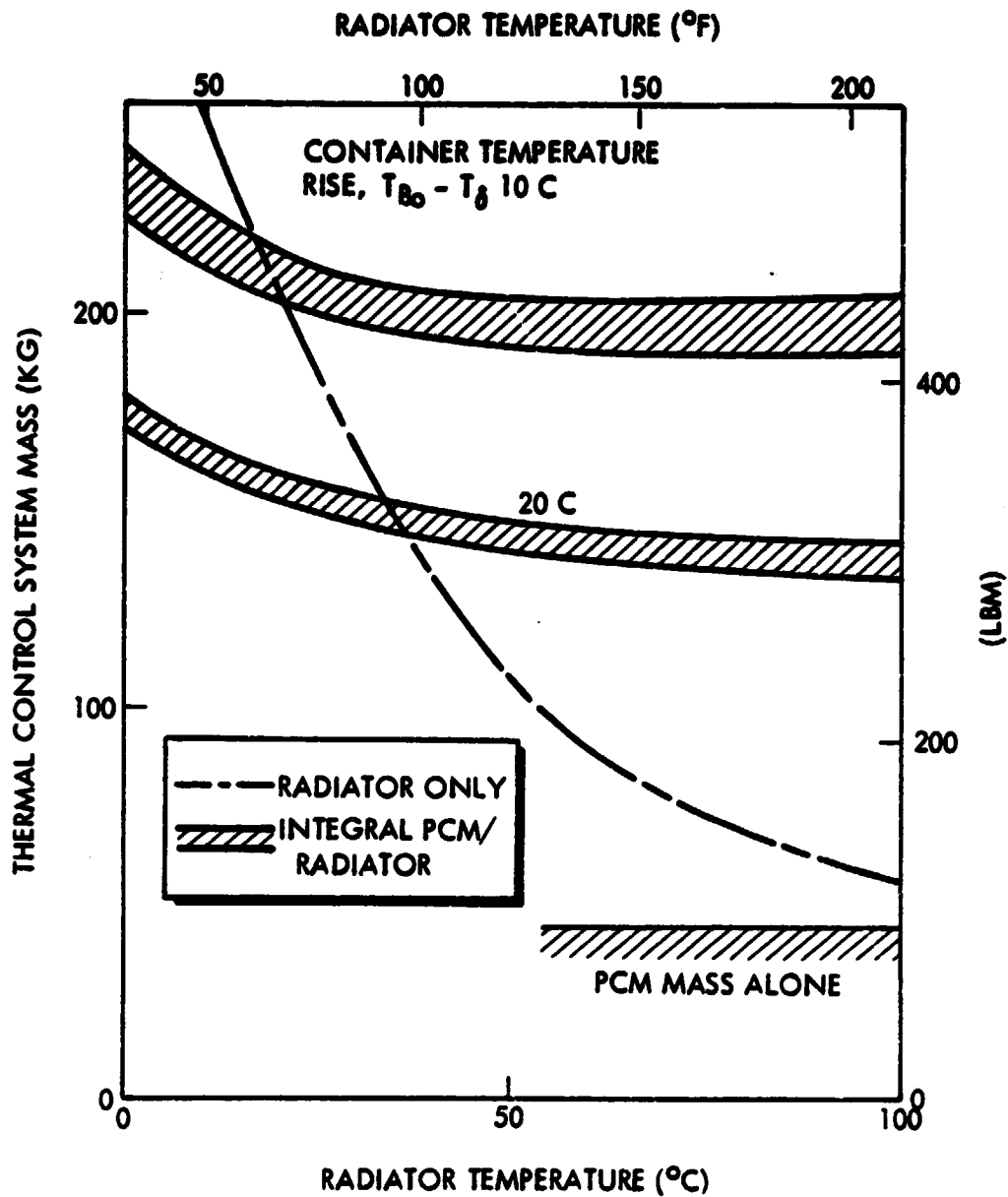


Figure 3.3.5-9. Typical PCM-Radiator Trade Analysis

such high-power assemblies as the 7.5 meter antenna, thermal dissipation from the feed is much greater than can be accommodated by surface radiation from the assembly itself. Table 3.3.5-2 summarizes the assumptions and results.

TABLE 3.3.5-2 Thermal Dissipation for
High-Power Antenna (7.5 meter)

<u>Item</u>	<u>Value</u>
Surface Temperature	45°C
α/ϵ	0.3/0.85
Net Dissipation* (Antenna Assembly only)	2.07 kW
Net Dissipation* (Radiator)	7.93 kW
Radiator Area (Two sides active)	20.7 sq m

*Assumes solar heating on one side.

Figure 3.3.5-10 illustrates a suitable geometrical arrangement. The additional radiating surface could be produced from a long strip radiator oriented along an east-west axis so as to avoid interference with the microwave beam. A similar approach is applicable to all antenna feed assemblies whose thermal dissipation requirements exceed the capabilities of their surface areas.

Heat Dissipation from Control Moment Gyros (CMG)

Continuous attitude control of both communications platforms and the SPS Test Article will be accomplished by CMG cluster (5 - 7 units) housed in a cylindrical shell 4.3m in diameter and 3 - 4m high. Heat will be generated within the shell due to mechanical friction and electrical resistance. The amount of energy dissipation is dependent on the load profile. For the communication platform an average power dissipation of 1.1 kW has been established.

Temperatures required for heat dissipation from the 83 sq m cylindrical surface have been calculated, under the assumption of full solar heating ($\theta = 0^\circ$) on one side of the cylinder (projected area 17 sq m). Under these circumstances, solar input is the dominant heat load. The working equations are as follows:

$$\dot{Q}_{\text{tot}} = \dot{Q}_{\text{solar}} + \dot{Q}_{\text{Diss}} = \alpha I_{\text{sc}} A_p + \dot{Q}_{\text{Diss}}$$

$$T_{\text{req'd}} = \sqrt[4]{\frac{\dot{Q}_{\text{tot}}}{\sigma A_{\text{tot}} \epsilon}}$$

ORI. PAGE 15
DE FOUR QUALITY

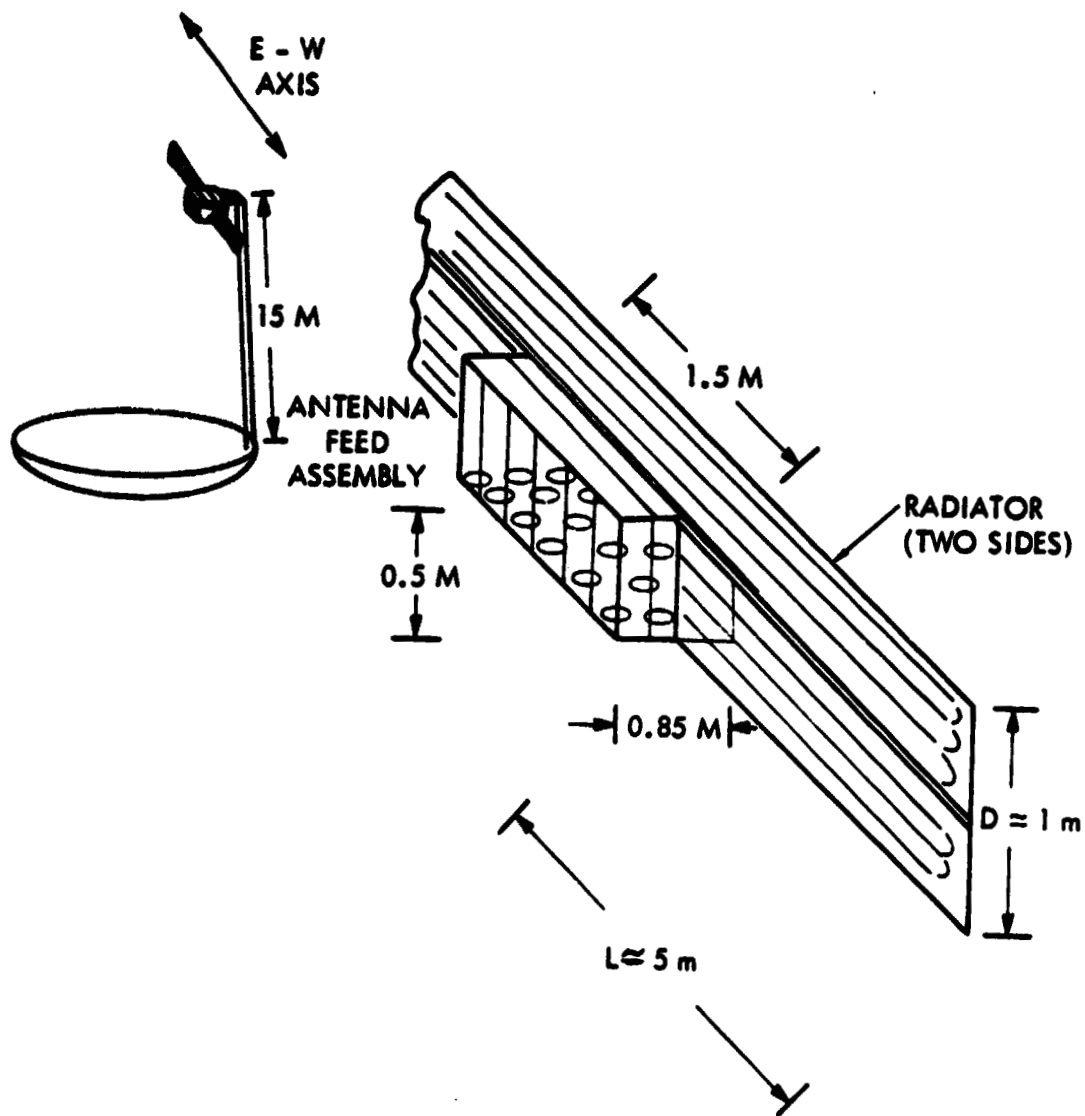


Figure 3.3.5-10. Radiator for 7.5-m Antenna Feed

TABLE 3.3.5-3 Thermal Dissipation from CMG Housing

<u>Surface</u> <u>α</u>	<u>Properties</u> <u>ϵ</u>	<u>Solar</u> <u>Input</u>	<u>CMG</u> <u>Dissipation</u>	<u>Total</u> <u>Rejection</u>	<u>Required</u> <u>Temperature</u>
0.3	0.9	7.1	1.1	8.2	-64 C
0.9	0.9	21.2	1.1	22.3	- 5 C
0.3	0.3	7.1	1.1	8.2	+ 2 C

References

1. Brogren, E. W., Barclay, D. L. & Strasayer, J. W.

"Simplified Thermal Estimation Techniques for Large Space Structures." NASA CR 145252, October 1977

2. French, E. P., et al,

"Passive Thermal Control of High Power Space Systems"
Rockwell Space Division Report SD 76-SA-0202

TABLE OF NOMENCLATURE

<u>Symbol</u>	<u>Explanation</u>
A	Area
Cp	Specific heat
D	Girder depth
f	Solar radiation fraction
I_{sc}	Solar constant
k	Thermal conductivity
L	Length
l	Fin width
P	open fraction
Q	Energy flow rate
T	Absolute temperature
t	time
W	Width
X	Nondimensional width
Greek Letters:	
α	Solar absorptivity
δ	Thickness, depth
ϵ	Thermal emissivity
η	Effectiveness
θ	Angle of incidence
ρ	Density
σ	Stefan - Boltzmann constant
τ	Thermal time constant
$\bar{\epsilon}$	Graybody shape factor
Subscripts:	
c	Pertains to conduction
m	Pertains to mesh
o	Initial or base value
R	Pertains to radiation
W	Pertains to girder web or to waveguide

3.3.6 Propulsion Subsystem Definition

The propulsion subsystems for the advanced communications antenna platform consist of an orbit transfer propulsion system for transporting the antenna platform from low earth orbit (LEO) to geosynchronous equatorial orbit (GEO), and a reaction control system (RCS) for performing stationkeeping at GEO.

Reaction Control System (RCS)

An RCS is provided for control of the antenna platform at the operational altitude in geosynchronous equatorial orbit (GEO). The RCS provides control for both translation maneuvers (stationkeeping) to maintain position in orbit over the earth reception target area, and for attitude orientation control in conjunction with the attitude and velocity control subsystem (AVCS).

Summary. The key features of the RCS are summarized in Table 3.3.6-1, and the RCS module is illustrated in Figure 3.3.6-1.

Table 3.3.6-1. RCS Summary

Propellants	N ₂ O ₄ /MMH
Pressurization gas	Helium
Total Impulse	26.2×10 ⁶ N-sec (5.9×10 ⁶ lb-sec)
Number of modules	4
Number of thrusters	16
Thrust, Each	
12 thrusters	4.4 N (1 lb _f)
4 thrusters	44 N (10 lb _f)
Total weight	12,800 kg (28,200 lb)

Requirements. Control of the antenna platform in GEO is required for the anticipated life of the vehicle which is assumed to be 20 years' duration. For purposes of sizing the RCS propellant quantities, a resupply interval of seven years is assumed. The life of storable propellant tankage, feed and propellant management devices, and other components is estimated to be 7 to 10 years.

Functional requirements for the RCS consist of (1) translation maneuvers (stationkeeping), and (2) attitude orientation maneuvers. The translation maneuvers consist of north-south stationkeeping, east-west stationkeeping, and overcoming solar pressure, with the required velocity increments shown in Table 3.3.6-2. The total velocity increment required for translation maneuvers is 427 m/sec (1400 ft/sec) for a seven-year period in GEO. The RCS thrusters are fired once per day for translation maneuvers. The RCS attitude orientation function is required for the periodic momentum dump of the AVCS control moment gyros (CMG). The total impulse per axis for pitch and yaw/roll is shown in Table 3.3.6-2. A total impulse of 2.8×10⁶ N-sec (632,031 lb-sec) for a seven-year period is dedicated for CMG momentum dumping exclusively. In addition, an equal amount of total impulse for momentum dumping is assumed to accrue from some translation maneuvers that may be synchronized to occur for momentum dumping. The RCS thrusters are fired every 12 hours (twice a day) for CMG dumping.

ORIGINAL PAGE IS
OF POOR QUALITY

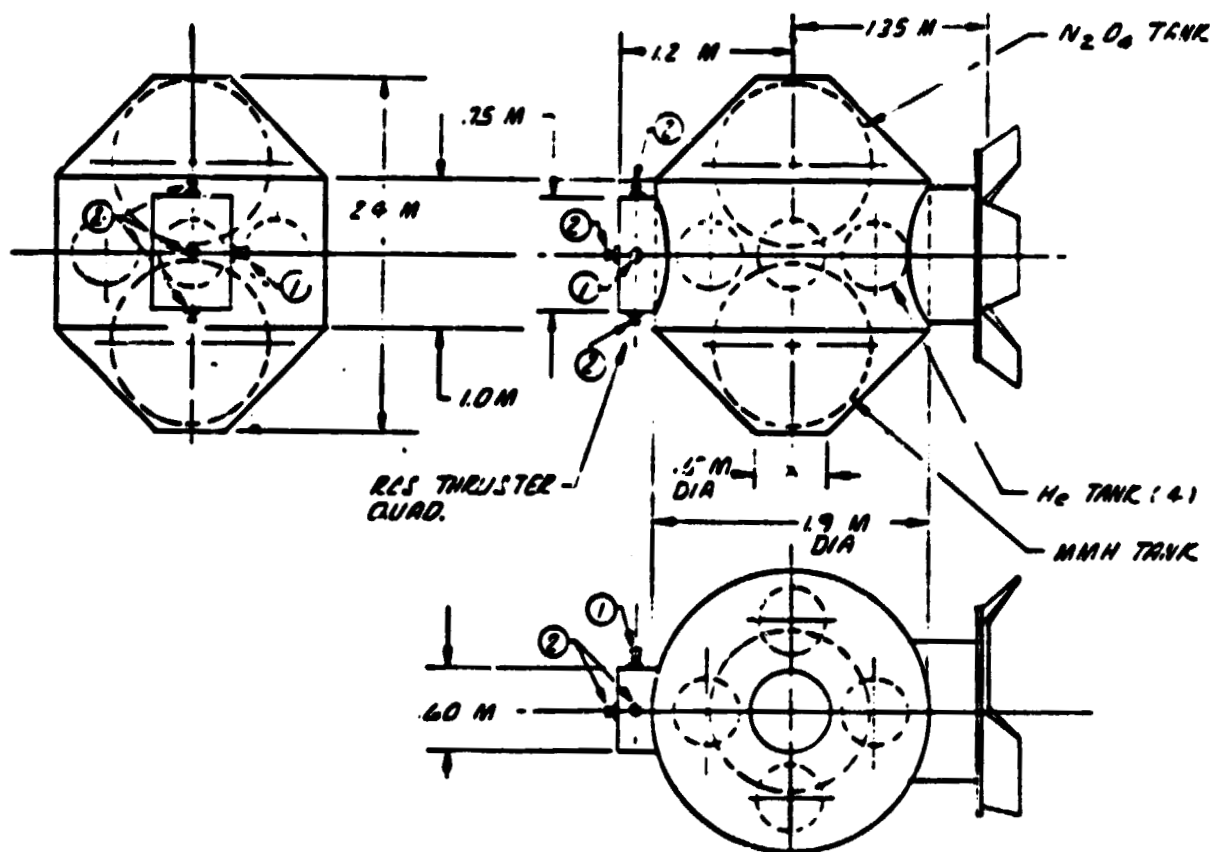


Figure 3.3.6-1. Reaction Control System (RCS) Module

Table 3.3.6-2. RCS Requirements

	$\Delta V/\text{year}$	
	m/sec	(ft/sec)
1. Translation maneuvers		
a. North-south stationkeeping	45.7	(150)
b. East-west stationkeeping (and solar pressure)	15.2	(50)
	<hr/>	<hr/>
Total translation	60.9	(200)
(One firing/day)	426.7	or (1400)/7 yr
	Total Impulse/7 years	
	N-sec	(lb-sec)
2. Attitude control CMG momentum dump		
a. Roll/yaw	2.2×10^6	(496,309)
b. Pitch	0.6×10^6	(135,722)
	<hr/>	<hr/>
Total momentum dump	2.8×10^6	(632,031)
(Two firings per day)		

Description. A 16-thruster configuration, grouped in four modules with propellants and located at the four corners of the rectangular-shaped platform, provides an RCS that meets the mission and functional requirements. This configuration is shown on Sheet No. 1 of Drawings 42662-25 (Erectable Structure) and 42662-26 (Space-Fabricated Structure), presented in Appendix A. The corner locations were selected to provide maximum-length moment arms and to avoid thruster exhaust impingement on the vehicle structure and components.

Each RCS module contains an oxidizer tank, a fuel tank, and helium pressurization tanks located within a structural shell that acts as a micro-meteoroid shield and for thermal control (Figure 3.3.6-1). On one side of the module, an assembly of four thrusters is located, with a docking port on the opposite side for mating and attachment to the platform structure.

Each assembly of four thrusters (per module) consists of one 44-N (10-lbf) thruster (N-S stationkeeping) and three 4.4-N (1-lbf) thrusters oriented for CMG momentum dumping about the pitch, roll, and yaw axes, and for E-W stationkeeping. Operation of the four-module RCS includes firing two 44-N (10-lbf) thrusters at a time for N-S stationkeeping, and alternately two or four 4.4-N (1.0-lbf) thrusters at a time for three-axis CMG momentum dump and E-W stationkeeping.

Storable propellants ($\text{N}_2\text{O}_4/\text{MMH}$) were selected for the RCS to be compatible with long-duration propellant storage for the seven year resupply interval and still provide reasonable performance. Bi-propellant RCS thrusters, such as those being developed by Aerojet [2-N (0.5-lbf), 22-N (5-lbf), and 445-N (100-lb) thrusters] provide a steady-state specific impulse of 2750 N-sec/kg (280 sec)

to 2890 N-sec/kg (295 sec). These performance values were used in sizing propellant quantities since relatively long pulse durations are required. [For N-S stationkeeping, the 44-N (10-lbf) thrusters fire for 33 seconds duration, and the shortest pulse for the 4.4-N (1.0-lbf) thruster is 13 seconds duration for pitch attitude CMG dumping.] RCS propellant requirements were based on a platform weight of 47,700 kg (105,000 lb) without RCS, and with RCS a platform weight of 60,500 kg (133,000 lb). Each RCS module contains 2294 kg (5058 lb) propellant and has an initial gross weight of 3200 kg (7050 lb) which does not include the docking port. The total gross weight of the four RCS modules is 12,800 kg (28,200 lb).

Orbit Transfer Propulsion System

A cluster of five low-thrust propulsion modules is provided for transporting the antenna platform from the construction altitude in LEO up to the operational altitude at GEO.

Summary. The key features of the orbit transfer propulsion system are summarized in Table 3.3.6-3. The low-thrust propulsion (LTP) module is illustrated in Figure 3.3.6-2.

Table 3.3.6-3. Orbit Transfer Propulsion Summary

Propellants	LO ₂ /LH ₂
Total impulse	515×10 ⁶ N-sec (116×10 ⁶ lb-sec)
Number of modules	5, parallel
Firing/staging sequence	3/2 modules
Number of engines	20
Thrust, each	22,240 N (5000 lbf)
T/W, max.	1.96 N/kg (0.2 lbf/lb _m)
Ignition weight: each	25,992 kg (57,303 lb)
5 modules*	129,961 kg (286,515 lb)
Boiloff	6%
Loaded weight: each	27,343 kg (60,280 lb)
5 modules	136,713 kg (301,400 lb)
*For antenna platform weight of 60,485 kg (133,346 lb).	

Requirements. The significant requirements for the orbit transfer propulsion module that are discussed include the following: thrust-to-weight (T/W) ratio, velocity increment, maximum size and number of modules, propellant storability, and thrust vector control (TVC).

A maximum T/W of 1.96 N/kg (0.2 lbf/lb_m) is imposed on the propulsion module design by the structural limitations of the space-fabricated structure and its tri-beam design geometry (refer to Structures section for additional details and comparison with the erectable pentahedral truss design). A common propulsion module design is used for both the erectable and space-fabricated platforms since the platform weights are comparable. This imposes a similar T/W of 1.96 N/kg (0.2 lbf/lb_m) on the erectable structure, although the structural analysis indicates that T/W values considerable in excess of this are feasible for this particular structure if the additional weight penalty

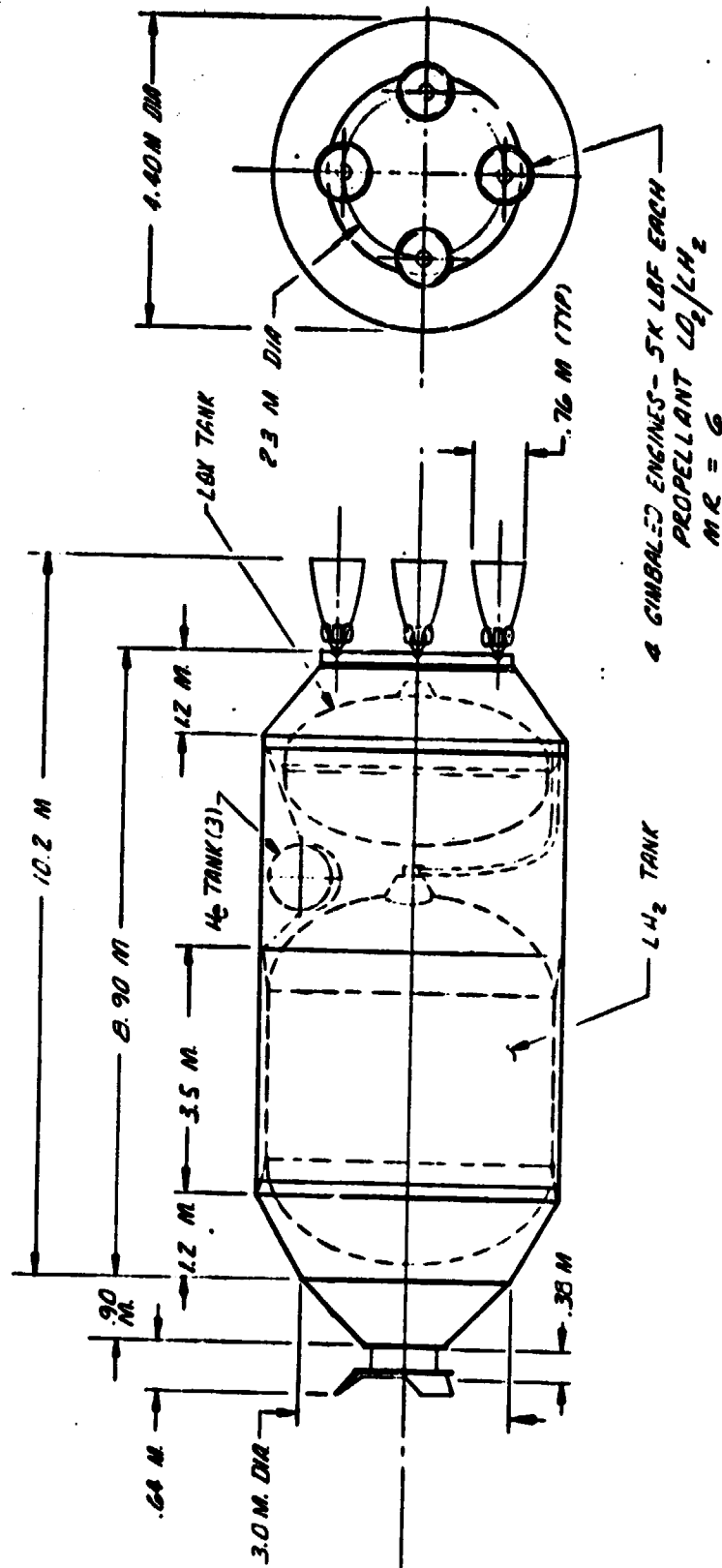


Figure 3.3.6-2. Low-Thrust Propulsion (LTP) Module

is acceptable. The maximum T/W value will determine the thrust requirements at burnout, and impact engine requirements for either the use of multiple engines with sequential shutdown to control T/W as propellants are consumed, or the use of fewer engines but with throttling requirements for T/W control.

The maximum size of the propulsion module is required to be such as to take full advantage of the current Space Shuttle orbiter payload capability and to minimize the number of orbiter flights and operational costs, since multiple modules are indicated from the magnitude of the platform weight involved. A maximum gross weight for the orbit transfer propulsion module of 28,803 kg (63,500 lb) was established. The required number of modules is determined by the platform weight requirements, the velocity increments for orbit transfer, and propulsion specific impulse values. Propellant off-loading is used in matching these requirements with the basic module.

The required velocity increments as a function of T/W is shown in Figure 3.3.6-3. This curve shows the velocity requirements for orbit transfer from a 28.5-degree inclined LEO of approximately 280 km (150 nmi) altitude to geosynchronous equatorial orbit (GEO). For a T/W range of 0.96 to 1.96 N/kg (0.1 to 0.2 lbf/lb_m), a ΔV of 4389 m/sec (14,400 ft/sec) is required, based on a two-impulse burn and Hohmann transfer. It should be noted from the curve that ΔV requirements at T/W values less than 0.96 N/kg (0.1 lbf/lb_m) increase greatly, which is due to larger gravity losses occurring with the longer trip times associated with less acceleration.

Propellant storability is a requirement for the entire elapsed time from propellant tanking to burnout. The use of cryogenic propellants requires adequate insulation for tanks to minimize boiloff propellant losses. Transit times to LEO and, subsequently, to GEO are relatively short (measured in minutes and hours), so that the elapsed time that impacts boiloff the greatest is the time required in LEO to accumulate the necessary number of propulsion modules. This elapsed time may be on the order of eight weeks, based on the following simplified scenarios:

- A single Space Shuttle orbiter is dedicated to the construction of the platform spacecraft.
- The orbiter requires a two-week turnaround period between flights.
- A total of five propulsion modules are required, and determines the orbiter flights required to transport them to LEO.

From this example, it can be seen that the fifth module arrives in LEO eight weeks after the first module.

Thrust vector control (TVC) is required for steering the spacecraft during engine burn periods. TVC about the pitch, yaw, and roll axes is required.

Description. A cluster of five cryogenic propulsion modules is provided for orbit transfer of the antenna platform. Each module is a single-stage design with four gimbaled engines of 22,240 N (5000 lbf) thrust each, using

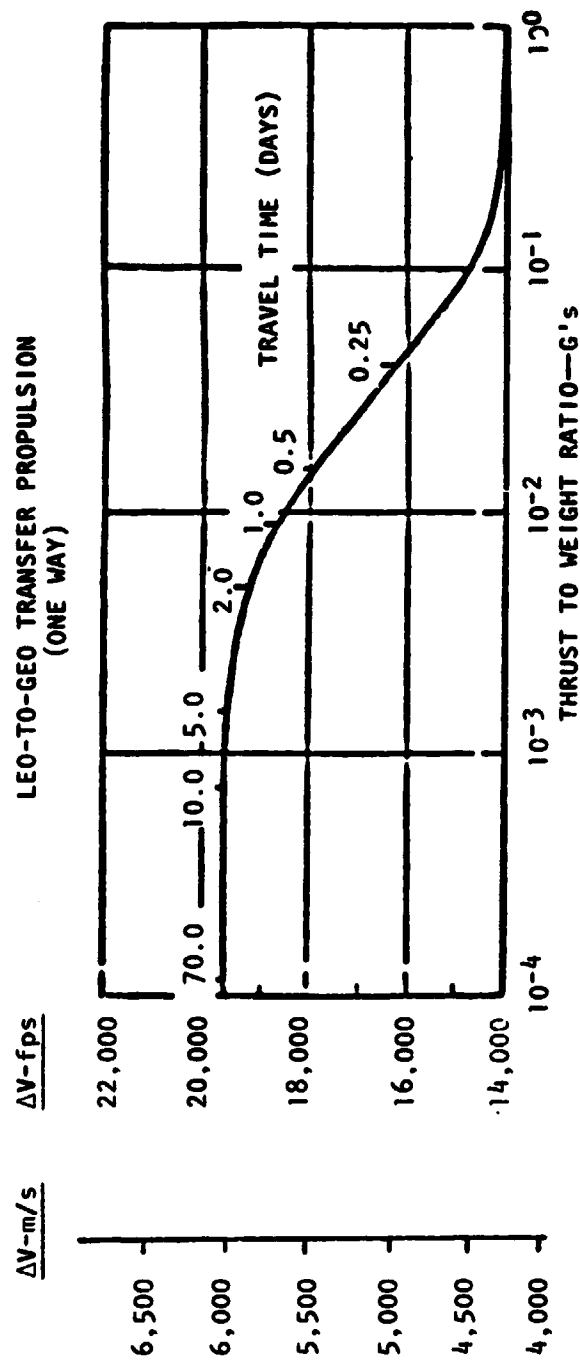


Figure 3.3.6-3. Delta-V Requirements Vs. T/W

liquid hydrogen and liquid oxygen propellants. This configuration is shown on Sheet 1 of Drawings 42662-25 (Erectable Structure) and 42662-26 (Space-Fabricated Tri-Beam Structure) presented in Appendix A. A thrust structure is provided for transmitting thrust loads from the five modules into the platform structure. Module mating to thrust structure is via docking ports.

The five propulsion modules are operated in a 3-2 firing/staging sequence. Operating in this mode, the five-module cluster is capable of transporting a maximum 63,500 kg (140,000 lb) of payload from LEO to GEO (after allowing 6% propellant boiloff from each module). The total firing time of each module is approximately 20 minutes at full four-engine thrust per module. In actual practice, durations slightly longer will result when paired engines are shut down to control T/W, and when sequential startup and shutdown by engine pairs are done in ten-second intervals in order to reduce the dynamic amplification of the platform structure during these thrust load transients.

The initial three modules require a single firing for the perigee burn, then are staged off at burnout, and the remaining two modules are fired to achieve the remaining perigee burn ΔV . A second start for the two modules is then required for the apogee burn to circularize the orbit at GEO.

With multiple engines per module, the T/W is controlled to remain below the 1.96 N/kg (0.2 lb_f/lb_m) structural limit (space-fabricated tri-beam) by sequential shutdown of engines in pairs. For example, during the three-module burn, the initial T/W is 1.4 N/kg (0.143 lb_f/lb_m) with all engines firing (266,890 N or 60,000 lb_f thrust total) and it remains below 1.96 N/kg (0.2 lb_f/lb_m) until just prior to burnout; then, if two engines are shut down on each module the T/W would be reduced to 1.1 N/kg (0.111 lb_f/lb_m) at burnout. For the remaining two-module burns made subsequently, the initial T/W is 1.6 N/kg (0.16 lb_f/lb_m) with all engines firing (177,930 N or 40,000 lb_f thrust) and it remains below 1.96 N/kg (0.2 lb_f/lb_m) for initial half of the burn ΔV , then two engines per module are shut down to bring the burnout T/W to 1.3 N/kg (0.135 lb_f/lb_m). During the orbit transfer phase, the antennae feed horn assemblies are in a retracted position, and the solar arrays which have been deployed are in a tied-down hinged (folded) position for acceleration of this phase.

Thrust vector control is provided by the gimballed engines. During orbit transfer steering, pitch is provided about the X-axis, yaw about the Z-axis, and roll about the Y-axis. The gimballed engines are ganged in pitch and yaw and differentially gimballed with the outer modules for roll control. This mode of TVC with the multiple engine configuration provides control under all conditions of 3-2 module staging and paired engine operation for T/W control or structural dynamic deamplification. Multiple engines provide the necessary flexibility for meeting these varied conditions.

The propulsion module is shown in Figure 3.3.6-2 with some details and overall dimensions. A single oxidizer tank, fuel tank, and helium pressurization gas tanks are located within a structural shell that acts as a micro-meteoroid shield. The design features the use of non-integral propellant tanks with multi-layer insulation for control of boiloff. Based on prior studies, an allowance for one-inch-thick MLI would control boiloff of LO_2/LH_2

propellants to 0.7% per week of on-orbit holding time. An allowance of 6% boiloff was assumed for an eight-week period to transport all five modules to LEO.

The overall dimensions of the module are compatible with orbiter payload bay size and the overall length is within the 10.7 m (35 ft) length target for OTV design. This is accomplished in part by the use of multiple 22,240-N (5000-lb) thrust engines which are short, and eliminates the need for nozzle retraction mechanisms.

The propulsion module design weight summary with maximum propellant loading is shown in Table 3.3.6-4. The inert weight includes allowances for subsystems such as structure, thermal control, avionics, propulsion, residual fluids and contingencies, based on prior studies of NASA Tug and USAF Orbit-to-Orbit Shuttle (OOS). With maximum propellant loading, the five LTP modules are capable of transporting a maximum of 63,500 kg (140,000 lb).

Table 3.3.6-4. LTP Maximum Propellant Load Conditions

	<u>kg</u>	<u>(lb)</u>
Maximum gross weight	28,803	(63,500)
Maximum propellant load	25,317	(55,815)
Inert weight	3,486	(7,685)
Stage mass fraction	0.879	
6% propellant boiloff	1,519	(3,349)
Usable propellant (after boiloff)	23,798	(52,466)

Each of the four engines include provisions for two-axis gimbaling for TVC. The engine is a staged combustion design based on the technology development of the Advanced Space Engine (ASE). The performance and size of the 22,240 N (5000 lbf) thrust engine is summarized in Table 3.3.6-5.

Table 3.3.6-5. Engine Performance Summary

Thrust	22,240 N (5000 lb)
Chamber pressure	10,342 kPa (1500 psia)
Nozzle expansion area	400:1
Propellants	LO ₂ /LH ₂
Mixture ratio, O/F	6:1
Specific impulse	4,580 N-sec/kg (467 sec)
Overall length	1.32 m (52 in.)
Nozzle exit diameter	0.76 m (30 in.)
Weight	49.9 kg (110 lb)

3.3.7 Attitude and Velocity Control Subsystem

The main features and characteristics of the attitude and velocity control subsystem (AVCS) are summarized in Figure 3.3.7-1.

The AVCS is designed to perform several post-construction functions. It controls the vehicle's attitude, points the solar arrays, controls the orbit transfer maneuver, and regulates the vehicle's on-station velocity.

The following text discusses the most important considerations which define the AVCS. The discussion and supporting studies are intended to define the AVCS in enough detail to satisfy the needs of this space construction study. It is in this spirit that many of the detailed trade studies required to fully define AVCS components are replaced by engineering judgment. Even though a more detailed study might modify the subsystem design somewhat, it is believed that the hardware described here is representative of the type needed for the Advanced Communications Platform, and it will properly exercise the construction aspect of this study.

Attitude Control

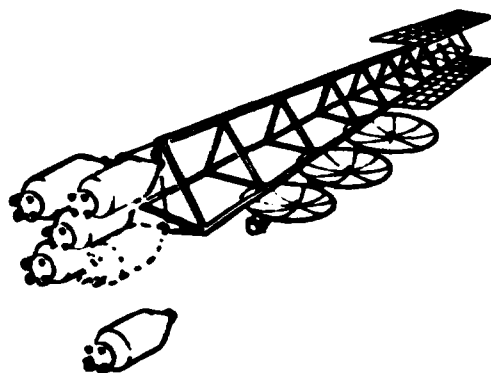
A primary function of the AVCS is to control the angular orientation of the vehicle. The attitude control requirements are different for each phase of flight, but the attitude control components are largely sized by the requirement to point the antennas accurately during nominal on-station operations.

The operational attitude control accuracy requirement is derived from the antenna pointing requirement. The antennas must be pointed with an overall accuracy of one beam width (0.258°), and then the movable feeds are positioned to steer the antenna to an accuracy of one-tenth of a beam width. (The beam steering concept is discussed in Section 3.3.8). The total antenna pointing accuracy is budgeted among the major error sources in Table 3.3.7-1. The attitude control portion appears as the first two entries. They, and other system requirements, are satisfied by orienting the vehicle with its long axis perpendicular to the orbit plane to the following accuracies: roll, 0.08° ; pitch, 0.08° ; and yaw, 0.10° .

In addition to meeting the above accuracy requirements, the AVCS must also prevent the vehicle from drifting faster than the beam steering adjustment rate of approximately 6×10^{-4} deg/sec.

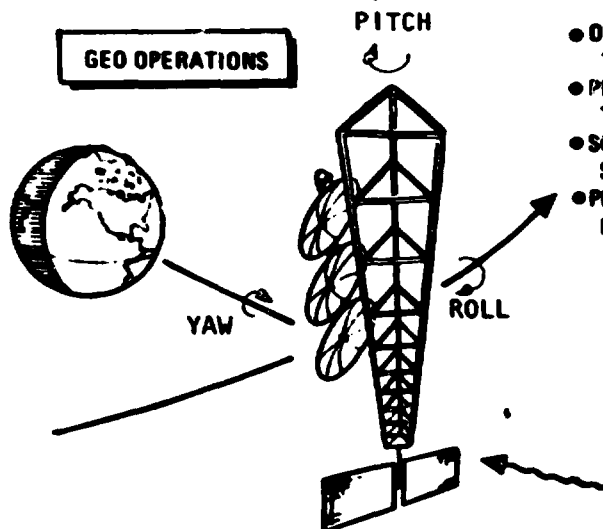
Selection and sizing of the attitude control actuators is largely dictated by the environmental disturbance torques. The angular momentum buildup values caused by the two largest disturbances are listed in Table 3.3.7-2. The most significant component of momentum buildup is the secular roll/yaw momentum caused by solar pressure acting on the offset solar array to produce a continuous 1.6 N-m torque. That torque causes a momentum vector to build up rapidly (5800 N-m-sec/hr) in the roll-yaw plane. It remains approximately inertially fixed (rotating one revolution per year), and therefore it appears alternately in the roll and yaw axes as the vehicle rotates once per day.

ORBIT TRANSFER



- STABILIZE DURING PROPULSION DELIV
- ORIENT FOR XFER MANEUVER
- GUIDE POWERED FLT
- STABILIZE DURING COASTING FLT

GEO OPERATIONS



- ORIENT & STABILIZE 100% MISSION OPS
- PRECISION POINT ANTENNAS TO USA
- SOLAR ARRAYS TRACK SUN
- PERFORM STATIONKEEPING MANEUVERS, E-W & N-S

ATTITUDE & VELOCITY CONTROL CONCEPT

SENSORS

STAR TRACKER	18 SEC
EARTH SENSOR	0.05 DEG
SUN SENSOR	1 MIN
IMU	

CMGs

PRINCIPAL AXIS ORIENTATION
DISTURB TORQUE, 1.2 FT LB (SOLAR PRESS)
MAX MOMENTUM 68,000 FT-LB-SEC
(12 HR DUMP)
7 CMG (SCALED EXISTING DESIGN)

RCS

TRANSLATION ΔV = 200 FPS/YR
MOMENTUM DUMP = 600,000 LB-SEC
(50% COMBINED W/ ΔV MANEUVER)

ΔV GUIDANCE

TDRS/GROUND TRACK & COMMAND
IMU (THRUSTING PERIODS)
TVC GIMBALLED NOZZLES

ANTENNA POINTING

FEED SYSTEM AUTO TRACK

Figure 3.3.7-1. AVCS Summary, Advanced Communications Platform

Table 3.3.7-1. Antenna Pointing Accuracy Error Budget

	Budget (deg)
Attitude determination	0.050
Control dynamics	0.100
Thermal deformation of structure and feed horn boom	0.100
Thermal deformation of antenna reflector	0.006
Manufacturing and assembly tolerance	<u>0.210</u>
RSS total (one beam width)	0.258

Table 3.3.7-2. Momentum Buildup due to Disturbance Torques

Disturbance	Roll		Pitch		Yaw	
	Secular N-m-sec/hr	Periodic* N-m-sec	Secular N-m-sec/hr	Periodic* N-m-sec	Secular N-m-sec/hr	Periodic* N-m-sec
Gravity gradient	130	20	12	1900	***	***
Solar pressure	5800**	***	55	120	5800**	***
Total	5930	20	67	2020	5800	***
*Maximum value **Alternates between roll and yaw axes ***Negligible						

Standard design practice is to use momentum exchange devices (control wheels) to compensate for the environmental disturbances and RCS jets to unload the wheels to prevent excessive wheel spin rates. This technique has the advantage of using propellant to counter the secular momentum buildup, while the cyclic momentum causes the wheel speed to oscillate about zero with a bounded maximum value. This concept works very well when the cyclic momentum buildup is much greater than the secular momentum buildup. In that case, the wheels are mainly sized by the peak cyclic momentum level and the RCS jets do not have to fire very often to unload the secular component of momentum.

The advanced communications platform is different. The secular momentum builds up much more rapidly than the periodic momentum. The simplest attitude control design is achieved by changing the vehicle's configuration to balance the solar pressure forces to produce a near-zero torque. Vehicle configuration considerations make such changes difficult to justify without extensive trade studies. Therefore, an arbitrary decision is made to size the momentum exchange devices to store 12 hours of momentum buildup. The RCS jets are fired twice a day to unload the wheels at the same time that stationkeeping maneuvers are performed. In this way, some propellant savings can be realized and the number of thruster firing cycles is reduced to a reasonable value (<100,000 firings per thruster over seven years).

The only momentum exchange devices presently available with the capacity required for 12 hours of momentum storage are control moment gyros (CMGs). A cluster of seven single-axis CMGs sized for the Advanced Communications Platform is illustrated in Figure 3.3.7-2. They possess important advantages: the seven CMGs provide for a large measure of redundancy (as few as three CMGs provide three-axis control), and the CMGs can produce large torques (~10,000 N-m) with a relatively high bandwidth (up to 15 Hz) to quickly settle the transient responses caused by jet firings.

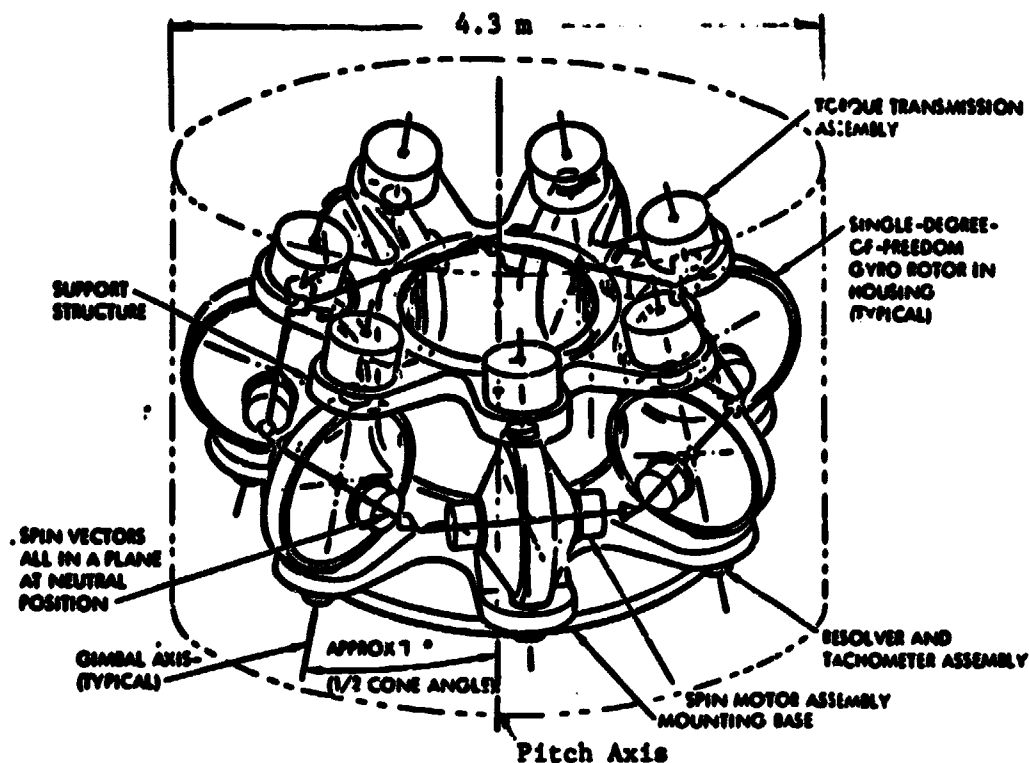
The CMGs are included as a representative momentum exchange device which satisfies the advanced communications platform's requirements. Other devices presently under development may be better suited for this application. Two examples are very large momentum wheels and the annular momentum control device (a magnetically suspended spinning hoop being tested by NASA/Langley Research Center).

A propulsion subsystem with reasonable design parameters can handle the twice-per-day momentum dumping maneuvers (see Section 3.3.6). A low thrust level of 4.4 N (1.0 lb) is selected to limit structural response and to produce acceptable thrusting durations. The attitude control RCS jets are fired to induce a vehicle rate of no greater than 6×10^{-4} deg/sec; and then the CMGs arrest the vehicle's motion over the next several minutes, thereby reducing the net momentum stored in the wheels. This maneuver is repeated 20 to 40 times to unload the total 12-hour momentum buildup.

Several types of attitude sensors are available:

Earth Sensors. These devices determine 2-axis attitude information to an accuracy of approximately 0.25° in low earth orbit, and approximately 0.05° in geosynchronous earth orbit.

ORIGINAL PAGE IS
OF POOR QUALITY



Total weight	3,000 kg
Total angular momentum	90,000 N-m-s, roll/yaw 4,000 N-m-s, pitch
Power	1-2,000 W

Figure 3.3.7-2. Single-Axis CMGs for Attitude Control,
Advanced Communications Platform

Sun Sensors. Sun sensors determine one-axis or two-axis attitude information to an accuracy of approximately one arc-min.

Star Sensors. One star sensor can determine two-axis attitude information to an accuracy 1 to 10 arc-sec. Three-axis information is established by using two sensors, or combining one or more star sensors within an inertial measurement unit (IMU). The latter concept has the advantage of providing continuous information to an accuracy of less than 1 arc-min.. However, star sensors may experience "blackout" periods when suitable stars are not in the field of view.

When the requirement to determine on-orbit three-axis attitude to an accuracy of 0.05° (180 arc-sec) in an earth staring mode is considered, together with the transfer orbit requirement to determine three-axis attitude to the same level of accuracy in more general orientations, the choice of sensors is limited to the star sensor class. A typical state-of-the-art stellar-aided IMU is selected for this project. Its characteristics were given previously in Figure 2.3.5-5.

Better sensors will probably be available for the advanced communications platforms. For example, star sensors using charged coupled device detectors, improved digital electronics and laser gyros are under development, and they will result in a lighter, more reliable sensing package.

The foregoing attitude control components sized for on-station operations are capable of controlling attitude during transfer from the construction orbit to GEO. However, thrust vector steering is also required to control the ΔV maneuvers. This topic is discussed below in the Orbit Transfer and Maintenance subsection.

Solar Array Pointing Control

Two-axis gimbal drives point the solar array at the sun. Two reasonable methods for pointing control are to close the gimbal drive loops using a two-axis sun sensor or to drive the solar array in an open-loop fashion using computed sun angle data developed on board from orbital ephemeris data and vehicle attitude reference data. Both capabilities are included to improve reliability.

Orbit Transfer and Maintenance

The AVCS controls velocity as well as the attitude. On station, the north-south and east-west velocity increments are added to maintain the vehicle's geostationary orbit. The customary practice of using ground commands to initiate these operations is used here. The velocity correction requirements are discussed in Section 3.2.

The AVCS must also control orbit transfer thrusting maneuvers. Requirements for this element of the AVCS are accurate control of the vehicle's attitude and propulsion system and, secondly, avoidance of interaction between the control system and the structural bending of the vehicle. Accurate attitude control and thrust vector control are required to minimize velocity losses and correction maneuvers to reach the desired state in the geostationary orbit.

This accuracy must be traded off against the second requirement. Control system operation can excite the structure and result in an unstable interaction. Rather than add additional, distributed sensors to the vehicle to measure structural bending, the simpler and less costly approach is to operate the control system at a frequency sufficiently less than the lowest structural frequency.

For a simplified attitude and thrust vector control system, a relationship between control frequency and total velocity error is shown in Figure 3.3.7-3. This is simplified in the sense that the vehicle is assumed to be rigid, the sensors are perfect, and there is not the ultimately required guidance loop which would reduce velocity errors by an order of magnitude. The figure shows that the total velocity error at burnout increases dramatically for control frequencies less than 0.01 Hz. However, for frequencies greater than this, velocity error is somewhat insensitive to frequency. Therefore, a minimum allowable orbit transfer control frequency of 0.01 Hz is adopted.

Structural Stiffness Requirements

Special care is required to prevent unstable interactions between the AVCS and the vehicle's structure. The approach taken here is to provide sufficient separation between the lowest structural frequency and the control system frequencies. This approach is discussed in the Structural Stiffness Requirements subsection of Section 2.3.5.

Stiffness requirements are presented and compared with vehicle vibrational frequencies in Table 3.3.7-3. They are based on the same analytical procedure described in Section 2.3.5. Adequate frequency separation exists with the present design.

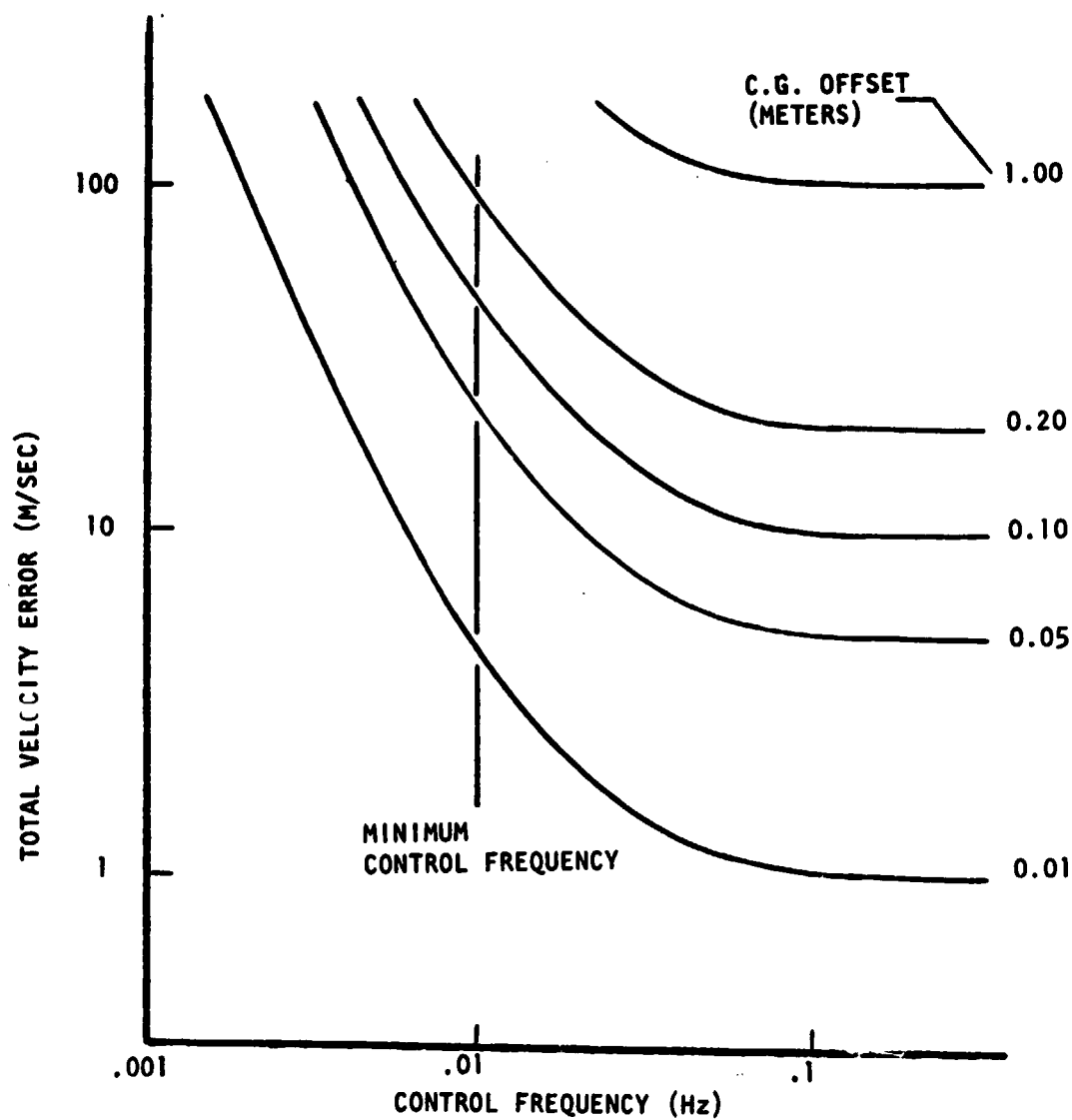


Figure 3.3.7-3. Orbit Transfer Accuracy,
Advanced Communications Platform

Table 3.3.7-3. Structural Stiffness Requirements

Flight Phase	Control Freq. (Hz)	Minimum Allow. Structural Freq. (Hz)	Fundamental* Structural Freq. (Hz)
Orbit transfer	0.010	0.050	0.070
On station	0.001	0.005	0.020
*Values from Section 3.3.2 for the tri-beam structure. The alternate structural configuration is stiffer.			

3.3.8 Tracking, Telemetry and Control Subsystem Definition

Summary

During the normal operation in geosynchronous orbit or during partial construction in low-earth orbit, the communications and tracking subsystem of the Advanced Communication Platform uses S-band and Ku-band links to provide, in addition to tracking, reception of commands at a maximum rate of 216 k bits/s. The subsystem also provides a transmission capability (return link) for telemetry, television, and data at a maximum rate of 50 M bits/s. S-band links may be established with a ground station and both S-band and Ku-band may be routed through NASA's Tracking and Data Relay Satellite System. A simultaneous capability to communicate with the Space Shuttle Orbiter (directly in LEO, indirectly while in geosynchronous orbit), GSP, or other spacecraft is also provided on S-band. See Figure 3.3.8-1.

S-Band and Ku-Band Links

While in low-earth orbit (LEO) the link capability is identical to that as given previously in Figure 2.3.6-1, and Tables 2.3.6-1 and 2.3.6-2. When the platform is in transition from LEO to GEO there should be enough rate capability available on S-band alone for the command and telemetry needs. All viewing aspects of the ascent have not been checked out as yet, however.

Once in geosynchronous orbit, there is a multitude of links available for the Advanced Communications Platform. The task here is to provide the essential needs with allowance for failures. It is reasonable to use the shuttle system less the Ku-band radar assembly as outlined previously. In addition an S-band parabolic reflector (3.4m) with 34 dB gain is needed to overcome the added space loss due to the increased range at GEO. With this addition, the Advanced Communications Platform has the following capacities as outlined in Table 3.3.8-1. Note that Link 2 has been derated in data rate to compensate for the increased range. Link 1 in this table is Link 3 in Table 2.3.6-1. The RF power required is 100 watts.

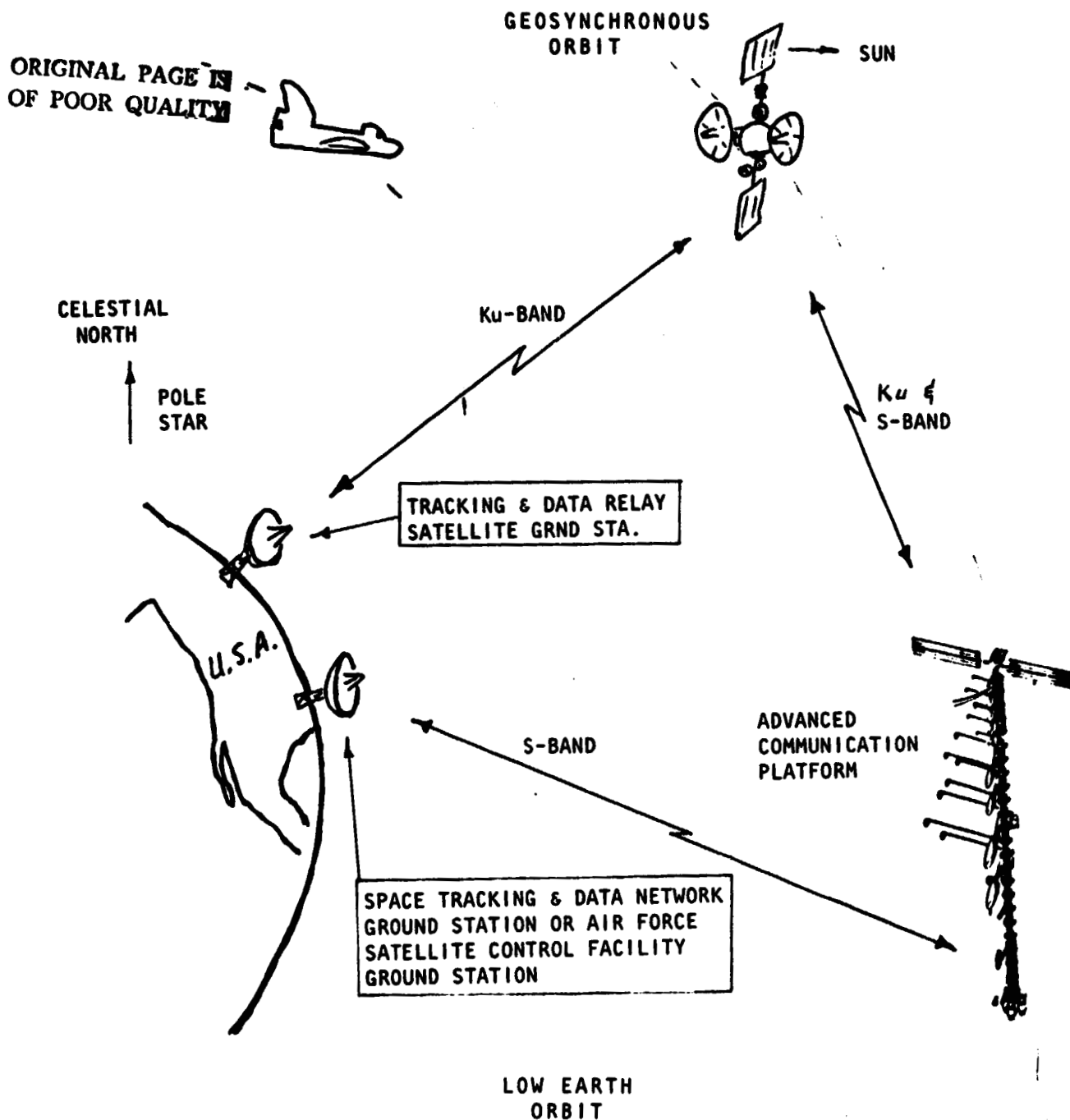


Figure 3.3.8-1. Communication Links for
Advanced Communication Platform

Table 3.3.8-1. S-Band and Ku-Band Link Capacity for Advanced Communication Platform at GEO

LINK	ONE-WAY OR TWO WAY?	FREQUENCY	DATA RATE	NOTES
<u>S-BAND</u> PM TO STDN, SCF OR TDRSS	TWO	RETURN 2200-2300 MHz FORWARD 2025-2120 MHz	192 Kb/s 72 Kb/s	RF POWER = 100 W ANTENNA = PARABOLIC (3.4 M DIAMETER) OR 4 QUAD OMNIS
FM TO GROUND (STDN OR SCF)	ONE	RETURN 2250 MHz (10 MHz BANDWIDTH)	1.6 Kb/s	RF POWER = 10 W ANTENNA = 2 HEMI OMNIS
<u>Ku-BAND</u> TO TDRSS	TWO	RETURN 14.85-15.15 GHz FORWARD 13.75-13.80 GHz	50 Mb/s DIGITAL OR 4.5 MHz ANALOG TV 2 Mb/s PAYLOAD 192 kb/s TELEMETRY 216 Kb/s COMMANDS	RF POWER = 50 WATTS ANTENNA = PARABOLIC (0.9 M DIAMETER) TIME COVERAGE $\geq 95\%$ HAS DATA & PN RANGE

3.4 MASS PROPERTIES

Table 3.4-1 presents the mass summary statement for the two platform configurations under study.

3.4.1 Rationale for Analysis

Basic structure masses were based on structures analysis and sizing. The docking port masses were based on modified Apollo/Soyuz units while the rotary joint mass was calculated from a layout. The systems control module mass are based on nominal specific unit weights.

The solar panel mass was based on the standard Lockheed panel of 0.752m x 4m dimension with a mass of 3.147 kg. For the antenna platform configurations, additional deployment and canisters were required. The remainder of the electrical power and distribution mass was based on analysis and requirements.

The attitude control mass, consisting of CMG's and the RCS were based on requirements reflected by the satellites mass properties and mission requirements.

The mass of the TT&C, Thermal and Information Management and Control are estimates based on prior studies. The mass of the Microwave and Communication Systems were based on scaling algorithms. Propellant mass was based on satellite mass properties and mission requirements.

3.4.2 Discussion

The 16 antenna modules represent 25% of the total dry weight of the project. The total electrical power system required to operate the antennas has an estimated weight of 15,817 kg, which accounts for approximately 30% of the total dry weight. Within the power generation system, which includes the solar array and the power storage batteries, the power storage battery system represents more than 31% of the weight. The power distribution system alone accounts for approximately one-half of the total electrical power system weight.

The primary structure, including the docking ports, represents approximately 20% of the total weight. The docking ports, however, contribute the major portion of this weight, 7,148 kg, compared to 3,297 kg for the basic primary structure.

The orbit transfer propulsion system weight is approximately 2.5 times the total weight of the operating communications platform being transported from LEO to GEO.

Table 3.4-1
Mass Summary - Advanced Communications Platforms
(Mass in Kg)

	Configuration	
	Erectable	Space Fab
<u>Structure & Mechanisms</u>	(12,832)	(13,330)
Basic Structure	3,297	3,795
Systems Control Module	1,537	1,537
Mechanisms	(7,998)	(7,998)
Docking Ports	7,148	7,148
Rotary Joint Module	850	850
<u>Electrical Power & Distribution</u>	(15,817)	(15,817)
Solar Energy Collector	(1,938)	(1,938)
Solar Panels	1,360	1,360
Structure & Deploy Mech.	578	578
Battery System	(4,910)	(4,910)
Batteries	4,325	4,325
Chargers	154	154
Wire Harness & Control	99	99
Switch Gear (6)	192	192
Bus Tie Connectors (2)	140	140
Distribution	(7,584)	(7,584)
Conductor	(5,337)	(5,337)
EPD Wire Harness	249	249
Antenna Harness	5,040	5,040
Slip Ring/Brushes	48	48
Equipment	(2,247)	(2,247)
EPD Panel	265	265
Switch Gear Box	582	582
RF Interconnect Box	1,400	1,400
Supports & Secondary Structure	(1,385)	(1,385)

Table 3.4-1 (Cont)
Mass Summary - Advanced Communications Platforms

	Configuration	
	Erectable	Space Fab
<u>Attitude Control</u>	(8,102)	(8,102)
Control Moment Gyro	4,491	4,491
Reaction Control System (Inert)	3,611	3,611
<u>TT&C</u>	(136)	(136)
<u>Thermal</u> (Battery & Equip. Cooling & Radiator)	(395)	(395)
<u>Communication</u>	(13,166)	(13,166)
Antennas	2,928	2,928
Feeds	184	184
Electronics	9,194	9,194
Feed & Ant. Boom Structure	519	519
Actuating Mechanism	81	81
Switch Gear Box (2)	260	260
<u>Information Management & Control</u>	(860)	(860)
Data Management	516	516
Instrumentation	344	344
TOTAL - SATELLITE (Dry)	51,308	51,805
RCS Propellant (GEO)	9,177	9,177
TOTAL - SATELLITE (Wet)	60,485	60,983
ORBIT TRANSFER PROPULSION		
Inert (5 Modules)	17,430	17,430
TOTAL - GEO Burn-Out	77,915	78,413
Propellant (max, incl. 6% Boil-Off) (LO ₂ /LH ₂)	119,283	119,283
VEHICLE GROSS MASS	197,198	197,696



3.5 CONSTRUCTION REQUIREMENTS - ADVANCED COMMUNICATIONS PLATFORMS

3.5.1 Erectable Advanced Communications Platform

The following discussion presents general and specific requirements applicable to construction equipment and processes which are inherent in the design of the Erectable Advanced Communications Platform (Drawing 42662-25).

These construction requirements are inputs to the space construction analyses of Task 2.0. As discussed in this report introduction, the intent is to narrow down the total range of options by providing the important guidelines and constraints affecting construction strategy, along with characteristics of the major component parts which must be handled during the construction process of this specific project. Further, the key dimensional tolerances potentially interacting with the construction accuracies are also included. Following the presentations of detail and unique requirements for the individual platform designs, a general discussion of common features is presented.

Overall Strategy

The following are specific, predetermined construction approaches which are inherent to the design.

- o The basic structural trusswork is composed of unions and struts. Selected joints are of a moment-carrying type, assembled as a probe and drogue. The remainder are ball-and-socket joints assembled from the side as described in Reference 1 (Section 3.5.4). Both are self-latching.
- o The major modular installations are accomplished using a type of androgynous mating, interleaving petal, docking/berthing port identified as baseline for the shuttle program.
- o The electrical power and signal wire runs are composed of segments joined at junction boxes and attached to the struts.
- o The overall configuration was developed to permit reach to the majority of critical installations points by use of the Shuttle Orbiter RMS, assuming an assembly fixture mounted to the orbiter. In this concept, the construction spacecraft is progressively transported across the top of the orbiter along the Y axis. Other orientations are not specifically precluded.

Component Inventory

As a means to help quantify the magnitude nature of the construction process, an inventory of the significant component parts has been developed. Table 3.5.1-1 lists the quantity (number of parts), the overall dimensions and the mass which must be handled during construction. Also noted are key construction features which relate to joining parts together or transporting parts.

General Construction Sequence Guidelines

The following general guidelines apply to setting up the desired construction sequence.

- o Set up construction fixture early in project (probably first activity).
- o Construct basic structure prior to attaching subsystem modules and flexible items such as electrical power and signal lines. Note that paralleling electrical power and signal lines can be installed as a beam is fabricated and/or installed.
- o Consider thermal constraints on flexible plastic wire coverings, and other materials which might be brittle at low temperatures. Schedule for deployment during periods of solar heating when required (or provide thermal conditioning).
- o Install nickel-hydrogen batteries toward end of construction project, provide for thermal conditioning (radiator) at time of installation and put them on-line as soon as possible to avoid extended periods of storage in charged condition.
- o Deploy large area solar arrays as late as possible to avoid destabilizing influence of drag forces.
- o Install orbit transfer modules as the last installation to minimize boiloff of cryogenic propellants.

General Tolerances

Table 3.5.1-2 defines the construction tolerances for the dimensions of the component parts and their interfaces which are judged to be critical to mission success of the spacecraft. All other interfaces will have tolerances specified which are consistent with good engineering practice. A description of the rationale and analysis effort which resulted in Table 3.5.1-2 is contained in Appendix 4.2.

3.5.2 Space Fabricated Advanced Communications Platform

The following discussion presents general and specific requirements applicable to construction equipment and processes which are inherent in the design of the Space Fabricated Advanced Communications Platform (Drawing 42662-26).

The presentation parallels that for the space-erectable advanced communications platform construction requirements.

Overall Strategy

The following are specific, predetermined construction approaches inherent in the design.

Table 3.5.1-1 Component Inventory
Erectable Advanced Communications Platform

ITEM DESCRIPTION	QUAN	SIZE HANDLED			MASS (Kg)	KEY CONSTRUCTION FEATURES
		LENGTH (m)	WIDTH (m)	HEIGHT OR DIA (m)		
Solar Array Wing	2	7	16	2	2,210	Accordian Deployment Rotary & Folding Joints
Solar Array Hub Module	1	11.5	5	3.5	2,396	Docking/berthing port Rotary Joint
Battery/Radiator Module	3	4	2	2	1,637	Docking/berthing port (Radiator deployment)
RCS Module	4	2.4	2.4	2.5	3,345	Docking/berthing port
20.5 m Dia Antenna	4	10.5	4.2	4.5	942	Docking/berthing port
13.8 m Dia Antenna	4	7.1	2.8	3.0	573	Deployment req'd
7.5 m Dia Antenna	4	3.8	1.6	1.7	2,389	Massive, high vol
6 m Dia Antenna	4	3.0	1.2	1.3	565	
Systems Control Ctr Module	1	7	-	4.3 Dia	5,735	One docking/berthing port Massive, large
Orbit transfer thrust module	5	11.7	-	4.4 Dia	28,949	Docking Port Attach. Massive, large

3-114

Satellite Systems Division
Space Systems Group



Table 3.5.1-1 Component Inventory (Continued)
Erectable Advanced Communications Platform

ITEM DESCRIPTION	QUAN	SIZE HANDLED			MASS (Kg)	KEY CONSTRUCTION FEATURES
		LENGTH (m)	WIDTH (m)	HEIGHT OR DIA (m)		
Struts, Double Tapered, Ball-end	150	12	-	.44 Dia	6.5	Side approach to ball/ socket joint; long, thin shape.
Struts, Bayonet End	60	12	-	.30 Dia	22.7	Axial approach to probe/ drogue jt; long, thin.
Struts, Double Tapered,	51	6	-	.25 Dia	3.3	Side approach to ball/ socket jt.; long, thin shape.
	1	10	-	.20 Dia	8.4	↓
	3	13.4	-	.20 Dia	11.2	
	20	17	-	.19 Dia	9.0	
Unions, Socket Jt. Std	16	.12	-	.21 Dia	4.5	Small items
Special	7	.12	-	.21 Dia	-	
Unions, Moment - Carrying - No Port	24	.32	-	1.2 Dia	5.7	Small items
Unions, Moment Carrying, Dock Port	18	.32	-	1.2 Dia	~5	Probe/drogue type joints. Crit. assembly sequence
Docking Ports, Fittings	11	.64	-	1.9 Dia	~10	Dense structural element

3-115

Satellite Systems Division
Space Systems Group



Table 3.5.1-1 Component Inventory (Continued)
Erectable Advanced Communications Platform

ITEM DESCRIPTION	QUAN	SIZE HANDLED			MASS (Kg)	KEY CONSTRUCTION FEATURES
		LENGTH (m)	WIDTH (m)	HEIGHT OR DIA (m)		
Interface Box 12.0 & 14.0 GHz _z	1	1.0	1.0	1.0	~700	Massive, dense berthing port installation
Interface Box 4.0 & 6.0 GHz _z	1	1.0	1.0	1.0	~700	(see above)

Table 3.5.1-2. Critical Construction Tolerances—
Erectable Communications Platform

ITEM DESCRIPTION	CRITICAL DIMENSION	TOLERANCE ALLOCATION	SYSTEMS AFFECTED BY CRITICAL DIMENSIONS	CONSTRUCTION OPERATION
SOLAR ARRAY WING	NONE	-	-	-
SOLAR ARRAY HUB	NONE	-	-	-
BATTERY/RADIATOR MOD	NONE	-	-	-
RCS MODULE	DOCKING PORT ALIGN	$\pm 0.1^\circ$	RCS	GROUND FAB
ANTENNA	DOCKING PORT ALIGN	$\pm 0.1^\circ$	ANTENNA MOD	GROUND FAB
SYST. CONTROL MOD	DOCKING PORT ALIGN	$\pm 0.1^\circ$	SYS. CONTR. MOD	GROUND FAB
ORBIT TRANSFER PROPULSION MOD	DOCKING PORT ALIGN	$\pm 0.1^\circ$	ORBIT TRANSFER PROPULSION MOD	GROUND FAB
STRUTS	LENGTH	± 0.1 CM	ANTENNA, RCS, SYS. CONTR. MOD, ORBIT TRANS. PROP.	GROUND FAB
UNIONS	NONE	-	-	-
DOCKING PORT (STRUCT.)	FACE ALIGN (± 0.1 CM)	$\pm 0.1^\circ$	ALL	ASSEMBLY
INTERFACE BOXES	NONE	-	-	-

- o The basic structural beams of triangular cross-section are fabricated by a beam builder machine similar to that developed by General Dynamics (Reference 2). The material is a non-metallic composite of low thermal coefficient of expansion.
- o Basic structural beams are welded together at right angles to form trusses.
- o The major modular installations are accomplished using a type of androgynous mating, interleaving petal, docking/berthing port similar to that identified as baseline for the shuttle program.
- o There are several diagonal bracing struts which are based on the "dixie-cup," hollow, tapered tube concept developed by Rockwell International and Langley Research Center. These utilize a ball and socket joint concept at each end, which is self-latching upon assembly.
- o The electrical power and signal wire runs are composed of segments joined at junction boxes and attached to outsides of beams between the various installed modules.
- o The overall configuration was developed to permit reach to critical installation points by use of the Shuttle Orbiter RMS, using a construction fixture attached to the Shuttle Orbiter. In this concept the constructed spacecraft is progressively transported across the top of the orbiter along the Y axis. Other approaches are not precluded.

Component Inventory

Table 3.5.2-1 lists the quantity (number of parts), the overall dimensions and the mass which must be handled during construction. Also noted are key construction features which relate to transport/handling or joining parts together or transporting parts.

General Construction Sequence Guidelines

General guidelines for the space fabricated platform are essentially the same as for the erectable platform except for the considerations specified to the beams, as follows:

- o It is probably desirable to manufacture all three longitudinal beams first to avoid the necessity of storing transverse beams and cross beams and/or using two beam machines simultaneously.

General Tolerances

Table 3.5.2-2 defines the construction tolerances for the critical dimensions of the component parts and their interfaces which are judged to be criti-

Table 3.5.2-1 - Component Inventory-
Space Fabricated Advanced Communications Platform

ITEM DESCRIPTION	QUAN	SIZE HANDLED			MASS (Each) (Kg)	KEY CONSTRUCTION FEATURES
		LENGTH (m)	WIDTH (m)	HEIGHT OR DIA (m)		
Solar Array Wing	2	7	16		2,210	Accordian deployment rotary & folding joints
Solar Array Hub Module	1	11.5	5	3.5	2,396	Berthing port, rotary joint
Battery/Radiator Module	3	4	2	2	1,637	Berthing Port (Radiator Deployment)
Bridge Fitting	1	5.3	1.5	2	16	Two attach points to ends of fab. beam
RCS Module	4	2.4	2.4	2.5	3,345	Berthing port; dense, compact module
20.5 m Dia Antenna	4	10.5	4.2	4.5	942	Berthing port
13.8 m Dia Antenna	4	7.1	2.8	3.0	573	Deployment req'd massive, high vol.
7.5 m Dia Antenna	4	3.8	1.6	1.7	2,389	↓ Two docking/berthing ports, massive, large
6 m Dia Antenna	4	3.0	1.2	1.3	565	
Systems Control Ctr Module	1	7	-	4.3 Dia	5,735	
Orbit Transfer Thrust Module	5	11.7	-	4.4 Dia	28,949	Docking port attach; massive, large

3-119

Satellite Systems Division
Space Systems Group



Table 3.5.2-1 - Component Inventory (Continued)
Space Fabricated Advanced Communications Platform

ITEM DESCRIPTION	QUAN	SIZE HANDLED			MASS (Each) (Kg)	KEY CONSTRUCTION FEATURES
		LENGTH (m)	WIDTH (m)	HEIGHT OR DIA (m)		
Fabr. Longitudinal Beam	3	~236	1.362	1.180	372	By beam builder low nat. freq. long & thin (weld to assemble)
Fabr. Transverse Beam	48	6	1.362	1.180	11	By beam builder (weld to assemble)
Fabr. Cross Beam	24	20 m to 6 m	1.362	1.180	11-42	By beam builder (weld to assemble)
Docking port end fitting - Fab Beam	22	1.5	-	2	~ 5	Weld to end of fab beam
Thrust Structure	1	8	8	3	136	Triple docking port attach
Struts, Double Tapered	12	11	-	.2	20	Ball & socket joint long, thin, light
Struts, Double Tapered	4	10	-	.15	~ 20	Ball & socket joint long, thin, light
Junction Box(es)	24	.5	.25	.25	130	Clamp to fab. beam
Wire Segments, longit , cross	Approx. 40	~10 to 20 ~ 5 to 14	- -	<0.1 <0.1	2,965 (Total Mass)	Flexible or semi-flex electrical connector at ends. Clip to beam.

3-120

Satellite Systems Division
Space Systems Group



Table 3.5.2-2. Critical Construction Tolerances—
Space-Fabricated Communications Platform

ITEM DESCRIPTION	CRITICAL DIMENSION	TOLERANCE ALLOCATION	SYSTEMS AFFECTED BY CRITICAL DIMENSIONS	CONSTRUCTION OPERATION
LONGITUDINAL BEAM	LENGTH TWISTED	+1 CM $\pm 0.6^\circ$	THRUST STRUCTURE ANTENNA, SCM, RCS	CUTOFF DURING FAB FABRICATION
TRANSVERSE BEAM CROSS BEAM	LENGTH TWISTED BOWED	+1 CM $\pm 0.2^\circ$ ± 2.5 CM	SYS. CONT. MOD (SCM) ANTENNA, RCS ANTENNA, RCS	CUTOFF FABRICATION FABRICATION
DOCKING PORT (STRUCT.)	FACE ALIGN. WITH BEAM END (± 0.1 CM)	$\pm 0.1^\circ$	ANTENNA, RCS, THRUST STRUCTURE (TS)	
THRUST STRUCTURE	OUT OF PLANE (± 4 CM) DOCKING PORT ALIGN.	$\pm 0.2^\circ$ $\pm 0.1^\circ$	ORB. TRANSF. PROP. ORB. TRANSF. PROP.	GROUND FAB GROUND FAB
STRUTS	NONE	—	—	—
JUNCTION BOXES	↓	↓	↓	↓
WIRE SEGMENTS				
SOLAR ARRAY WING				
SOLAR ARRAY HUB MOD				
BATTERY/RADIATOR MOD				
BRIDGE FITTING	NONE	—	—	—
RCS MODULE	DOCKING PORT ALIGN.	$\pm 0.1^\circ$	RCS MOD	GROUND FAB
ANTENNA MODULE	↓	↓	ANTENNA MOD	↓
SYST. CONTROL MOD			SYS. CONT. MOD.	
ORBIT TRANSF. PROP. MOD.	DOCKING PORT ALIGN.	$\pm 0.1^\circ$	ORB. TRANSF. PROP. MOD.	GROUND FAB

cal to mission success of the spacecraft. All other interfaces will have tolerances specified which are consistent with good engineering practice. A description of the rationale and the analysis effort which resulted in Table 3.5.2-2 appears in Appendix 4.2.

3.5.3 Construction Process Requirements Related to Common Features of Antenna Platform Configurations

This section discusses significant construction process requirements and considerations which are implied by the selection of features common to the design of the two antenna platform projects.

Identification of the appropriate common features and related construction issues are presented in Table 3.5.3-1. In general, the modules attached by docking port-type devices could be installed any time after the docking port is installed on the structure. This permits a large number of alternate possibilities. One major option is to install subsystem modules as the trusswork is assembled, so that there is less lost motion in translating the construction fixture back and forth. Another significant option is to first assemble all of the structure, then install the modules. Propulsion modules are considered best installed last, especially as they involve cryogenic propellants.

Because of limited reach by the remote manipulator system, special methods may be required for the larger modules to be installed. Propulsion modules might be self-installed (fly-in/dock module). If so, this would also provide reason to perform these installations after the main truss work is completed and mission equipment installed. Another practical consideration is that very large modules may require most of an orbiter payload bay to carry each one (due to volumetric, c.g., or weight limits). It is probably most efficient to do trusswork construction in as large a section as possible, thus avoiding re-positioning, setting up time and possibly use of several different support equipment devices (e.g., cherry picker, EVA, and effectors) on one mission.

3.5.4 References

1. E. Katz

Advanced Technology Laboratory Program for Large Space Structures, Parts 1 and 2, Final Report, SD 76-SA-210, November 1976 (Revised May 1977)

2. General Dynamics

Space Construction Automated Fabrication Experiment Definition Study (SCAFEDS) Part II, Mid-Term Briefing. Briefing No. CASD-ASP77-011, 9 November 1977

TABLE 3.5.3-1 Construction Implications of Design
Features, Antenna Platforms

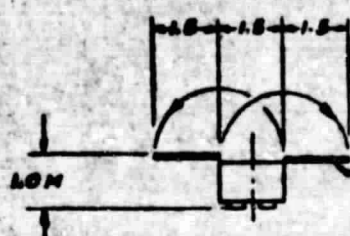
Feature	Construction Implications
<p>Androgenous docking port devices for installation of major systems modules and components.</p>	<ul style="list-style-type: none"> o Requires load-spreading interface structure between docking port ring and basic structure. Additional stowage and assembly functions required for each port. o Provides possibility of soft berthing; fly-in installation by remotely controlled vehicle or direct attach by RMS, cherry picker or other mechanism. o Provides measure of self-alignment. Installation device must give way/yield to accept this feature. o Modules may be installed during structure assembly or later as desired or appropriate.
<p>Antennas designed for single point attach to basic structure (docking port), power, signal, etc., connections integrated with attachment. separate functions which occur shortly after mechanical attachment).</p>	<ul style="list-style-type: none"> o Antennas handled as single modules from loading into Orbiter through installation to spacecraft structure. o Considerations of installing large modules apply. o Deployment follows installation to basic structure. o Concept is essential for success in geosynchronous, remotely controlled installation
<p>RCS units designed for single point attach to basic structure.</p>	<ul style="list-style-type: none"> o RCS units handled as single modules. o Considerations of installing large module apply.

APPENDIX A
PROJECT DEFINITION DRAWINGS

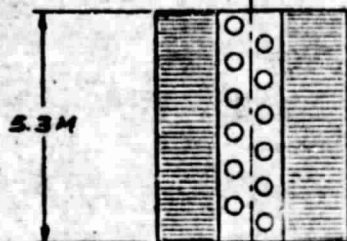
This appendix contains the definition drawings describing the major configuration features of the three construction projects. They are arranged in order of discussion in the main text, rather than by numerical order, as follows:

	<u>Page</u>
• Drawing Number 42662-27, SPS Test Article Concept Definition (3 Sheets)	A-3, 4
• Drawing Number 42662-20, SPS Microwave Antenna Configuration Concept (2 Sheets)	A-9, 10
• Drawing Number 42662-25, Advanced Communications Antenna Platform—Erectable, Low-Thrust Chem. Propulsion, 1-17-79 (3 Sheets)	A-13, 14
• Drawing Number 42662-26, Advanced Communications Antenna Platform, Space-Fab., Low-Thrust Chem. Propulsion (2 Sheets)	A-19, 20

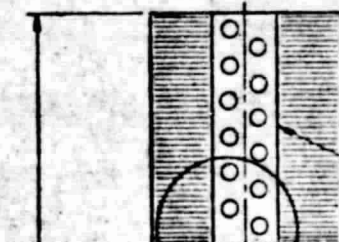
For each project, there is a general configuration sheet and a wiring arrangement schematic. Supplementary drawings describe details. Drawing Number 42662-25, Sheet 2, describes details common to the two advanced communications platforms.



2 FOLD-OUT RADIATORS
1.5 x 5.3M (DOUBLE SIDED)
EFFECTIVE AREA = 31.8M²



PLUG-IN S.E.P.
ADD-ON PANEL
- 2 REQ'D.
(SEE MAIN VIEW)



S.E.P. PANEL
- 4 REQ'D
(SEE MAIN VIEW)

FOLDOUT FRAME

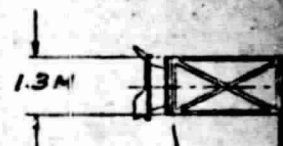
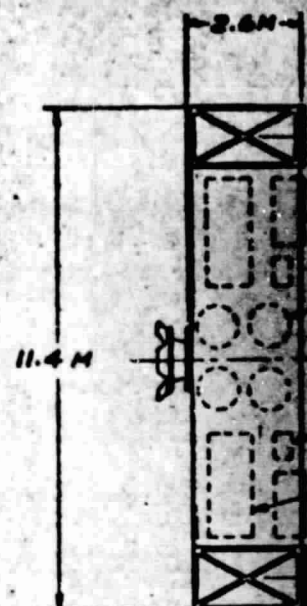
1

ORIGINAL PAGE IS
OF POOR QUALITY

MAST PLUGS-IN
ROTARY JOINT
SEE SHEET 2

S.E.P. PANEL

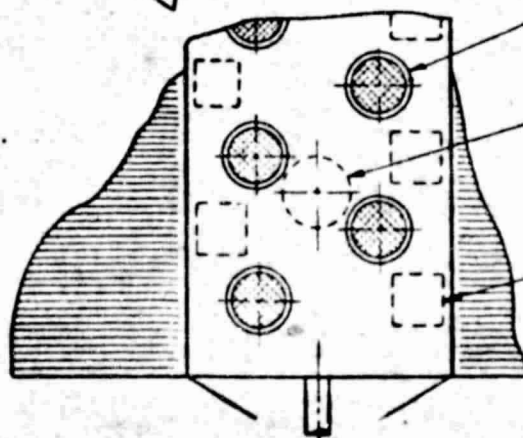
SCALE: 1/80



11.4 x 2.6M RAIL
(DOUBLE SIDED)
DEPLOYED POSITION
EFFECTIVE AREA

SYSTEM SUPPORT

SCALE: 1/80

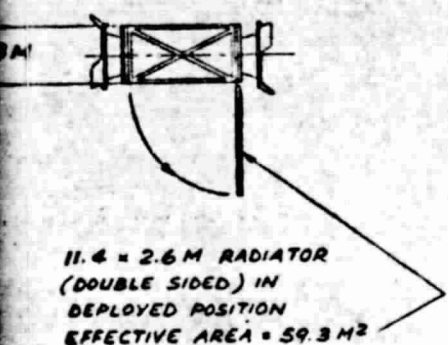
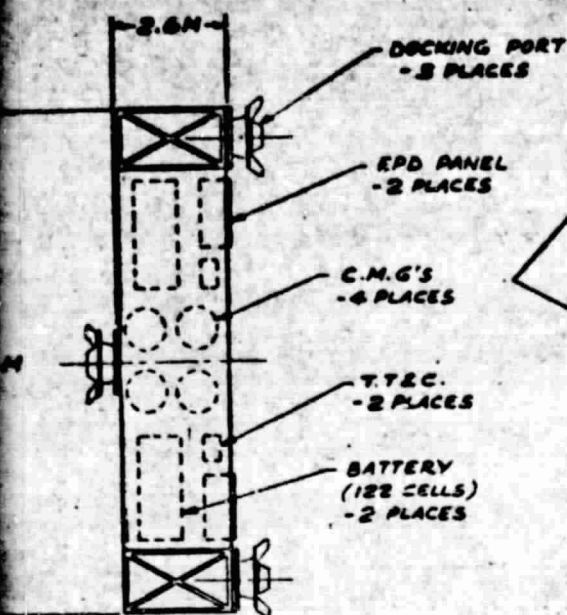


30 CM. MERCURY
ION THRUSTER
(12 PER PANEL)

PROPELLANT TANK
ONE FOR EVERY 4 THRUSTERS
(3 PER PANEL)

POWER PROCESSOR
ONE PER THRUSTER
(12 PER PANEL)

TYPICAL DETAIL



STEM SUPPORT HOUSING
SCALE: 1/20

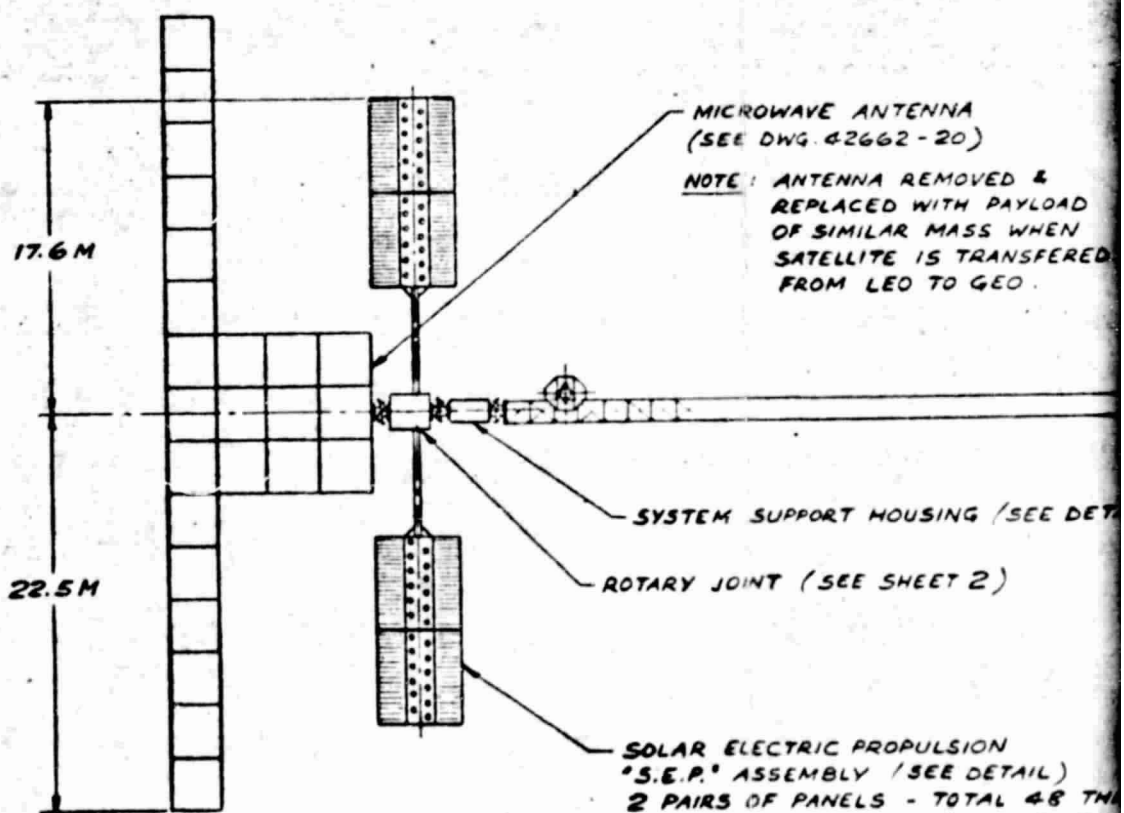
30 CM. MERCURY
ION THRUSTER
(12 PER PANEL)

PROPELLANT TANK -
ONE FOR EVERY 4 THRUSTERS
(3 PER PANEL)

POWER PROCESSING UNIT -
ONE PER THRUSTER
(12 PER PANEL)

FOLDOUT FRAME
2

FOR BREAKDOWN OF
COMPONENTS FOR
THIS END SEE SHEET 2



ORIGINAL PAGE IS
OF POOR QUALITY

NOTE: S.E.P. ASSEMBLIES 'PLUGGED'
FOR LEO TO GEO TRANSFER
AFTER MICROWAVE TEST
HAS BEEN COMPLETED.

215.2 M

5 SOLAR BLANKET BAYS AT 41.6 M = 208.0 M

MEMBER) AT 1.434 M

CROSS BEAM (6 PLACES)

LONGITUDINAL BEAM (2 PLACES)

C.G.

62.7 M

+X

+Y

+Z

ORIGINAL PAGE IS
OF POOR QUALITY

STRUCTURAL CONFIGU

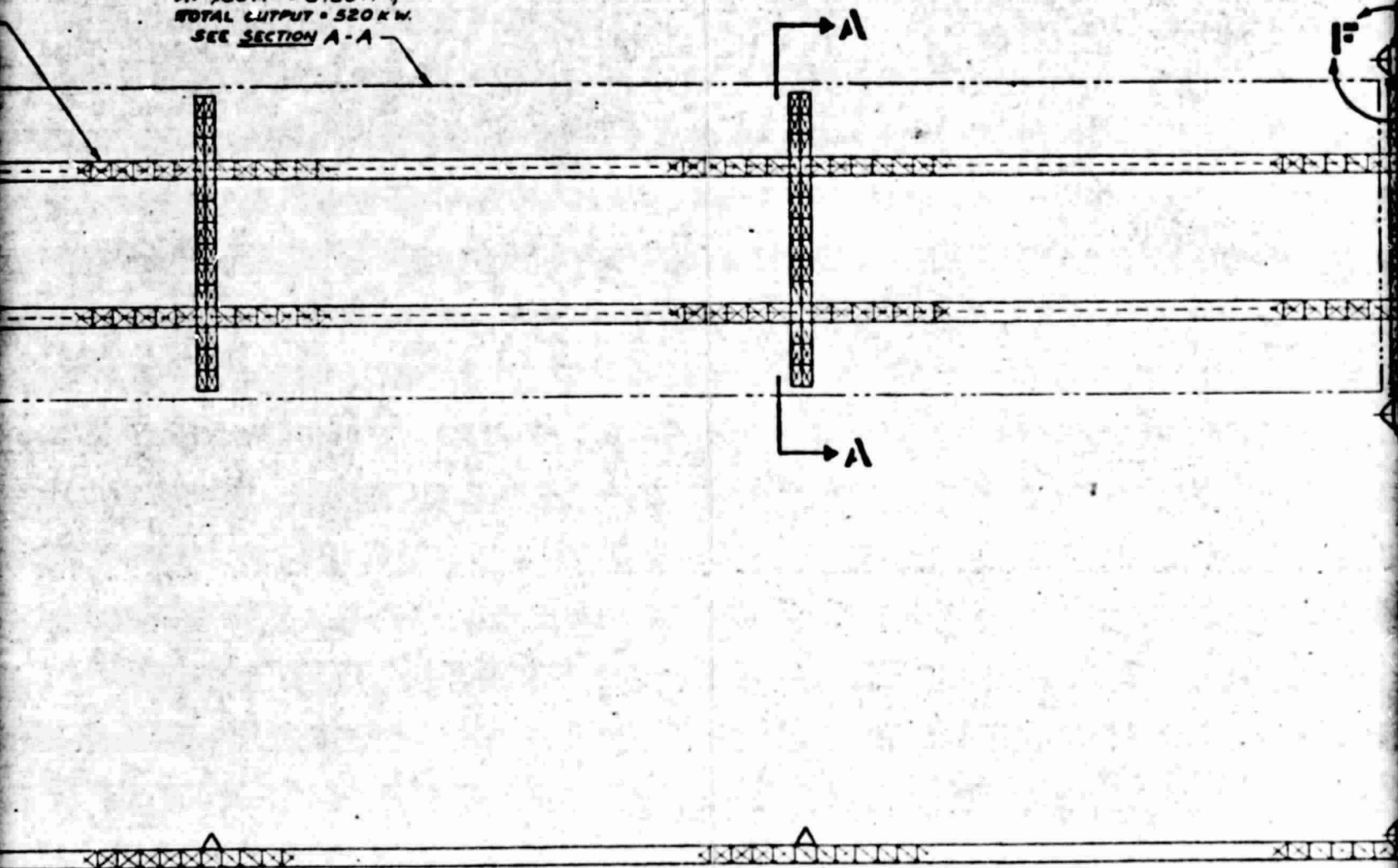
SCALE: 1/200

FOLDOUT FRAME

3

1 - 208.0 16

28 SOLAR BLANKETS
AT 158 M² = 3950 M²,
TOTAL OUTPUT = 520 KW.
SEE SECTION A-A

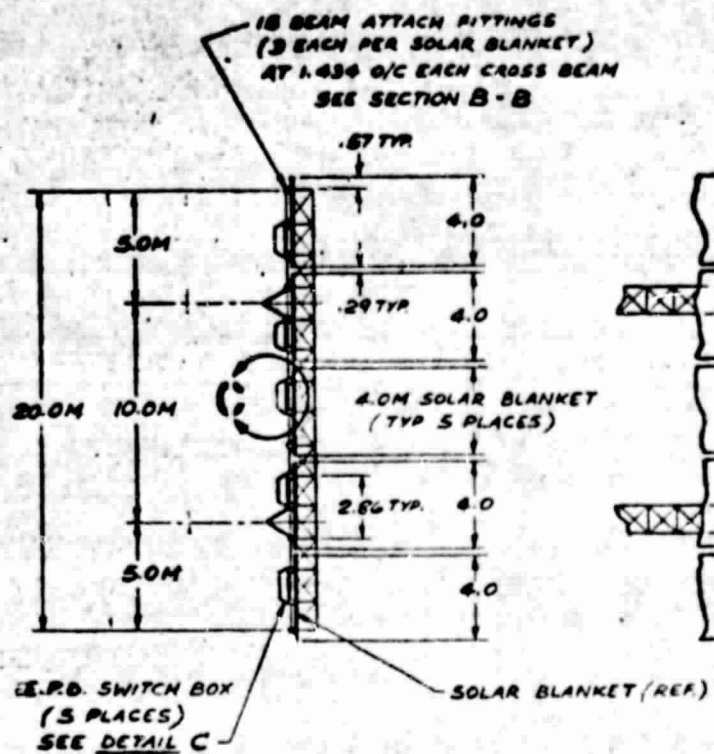
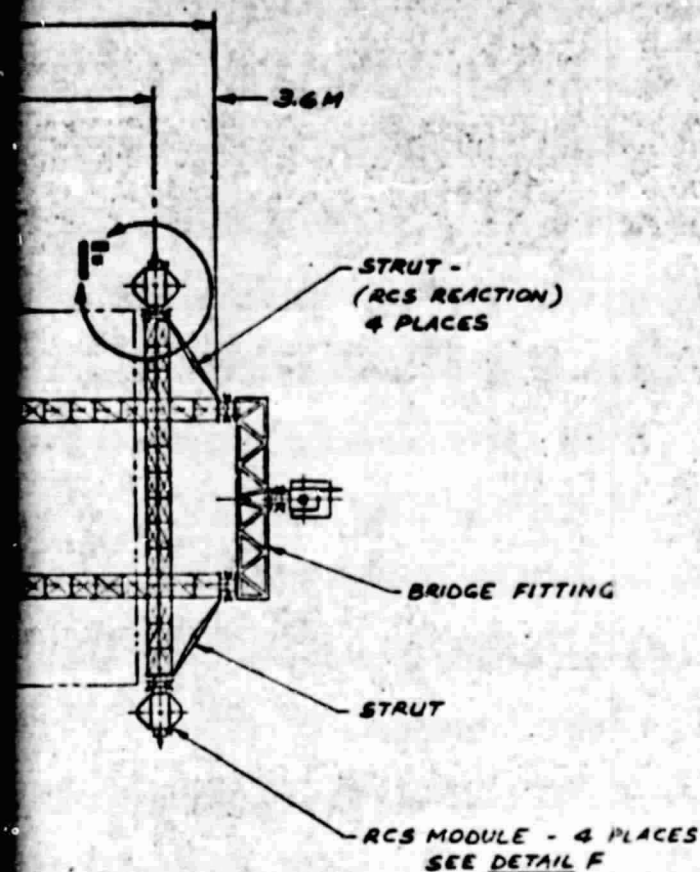


ORIGINAL PAGE IS
OF POOR QUALITY

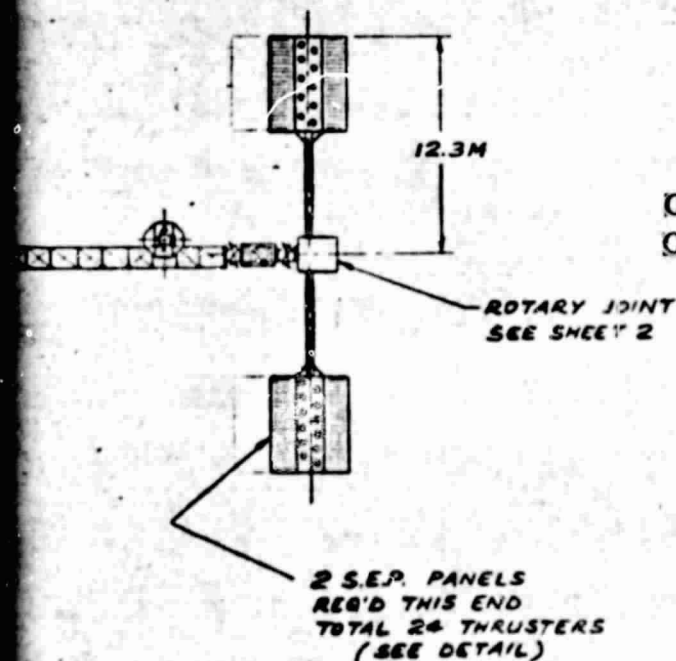
CONFIGURATION

1/200

FOLDOUT FRAME

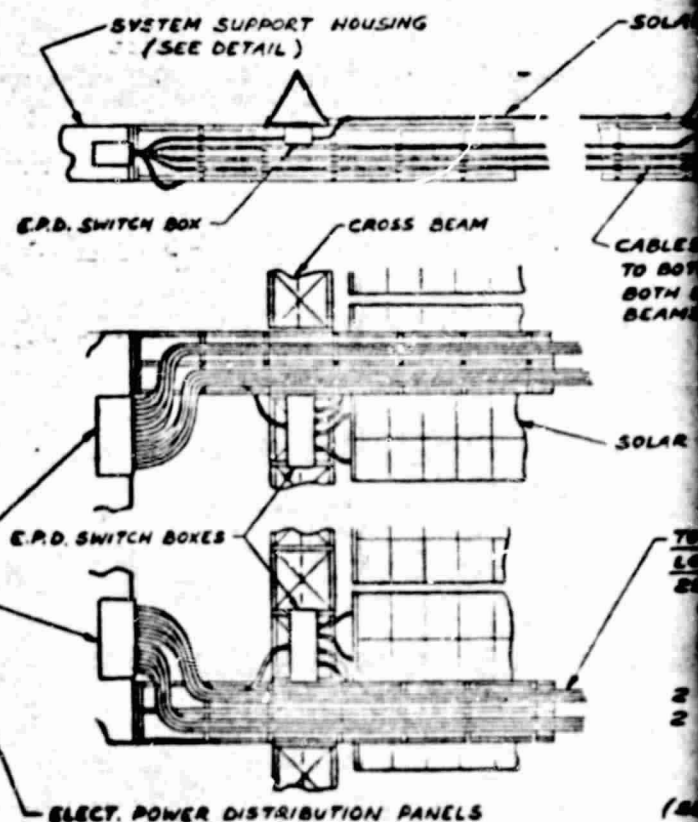


SECTION A-A



ORIGINAL PAGE IS
OF POOR QUALITY

FOLDOUT FRAME



CABLE ROUTING DE

NOTE: S.E.P. PANELS "PLUGGED-IN"
FOR LEO TO GEO TRANSFER
AFTER MICROWAVE TEST
HAS BEEN COMPLETED.

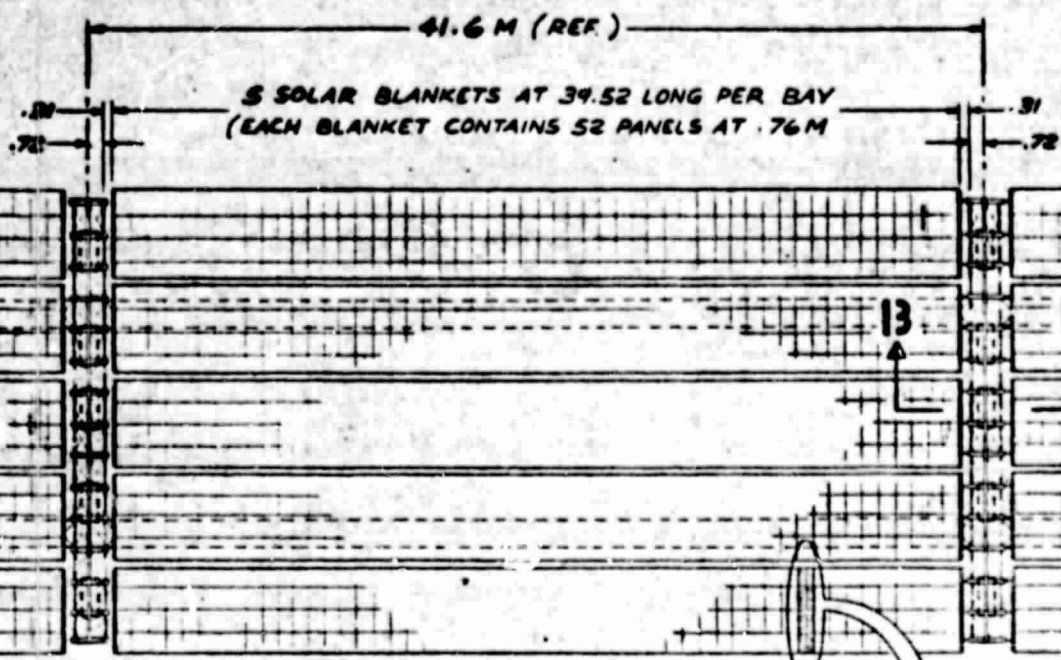
ET)
BEAM

NET

BLANKET (REF.)

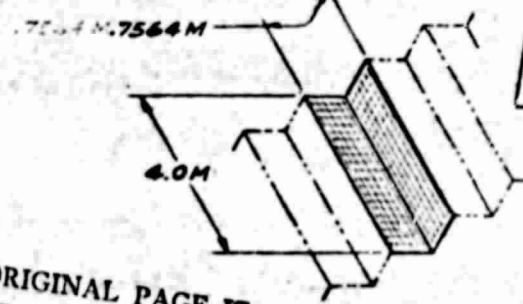
SOLAR BLANKET

ROUTING DETAILS



SOLAR BLANKETS ASSEMBLED TO STRUCTURE

SCALE: 1/160



ORIGINAL PAGE IS
OF POOR QUALITY SOLAR PANEL DETAIL
(ONE FOLD)

FOLDOUT FRAME

2.03 MM (.080") DIA.
DIAGONAL

CAP MEMBER

1.414 M

BEAM

PLUG-IN
RETENTION

PREPUNCHED SLOT
BEAM CROSS MEMBER

DETAIL 1E

SOLAR BLANKETS

CABLES INSTALLED
TO BOTH SIDES OF
BOTH LONGITUDINAL
BEAMS.

SOLAR BLANKET

TOTAL CABLES ON BOTH
LONGITUDINAL BEAMS:

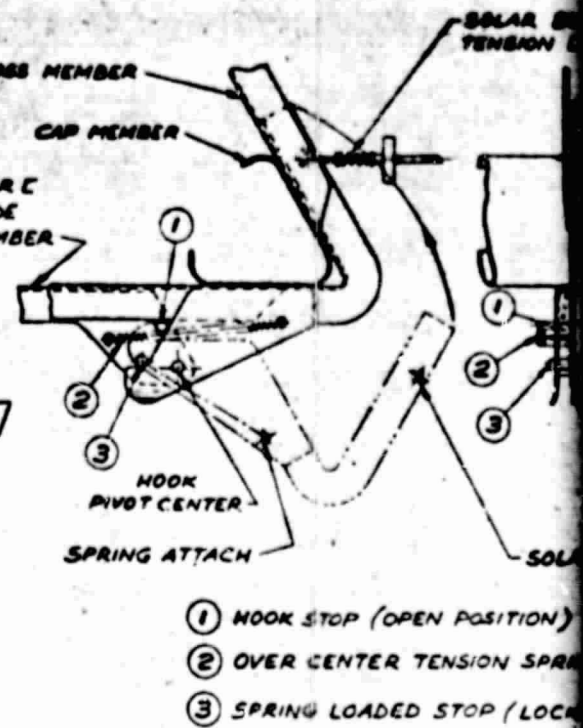
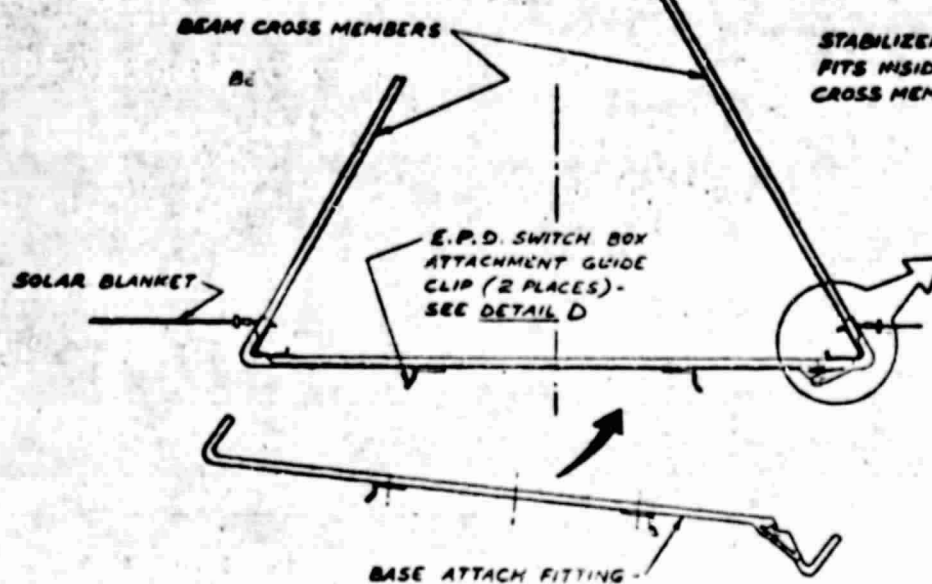
- 25 POWER CABLES
(ONE FROM EACH SOLAR
BLANKET VIA E.P.D.
SWITCH BOX) TO
E.P.D. PANEL.
- 2 DATA CABLES &
2 POWER CABLES
FROM E.P.D. PANEL
TO OPPOSITE END
OF STRUCTURE.

(SEE WIRING DIAGRAM - SHEET 3)

CABLE SECURED
IN HOLDERS

CABLE BEING
INSTALLED TO
LONGITUDINAL
BEAM (TYP.)

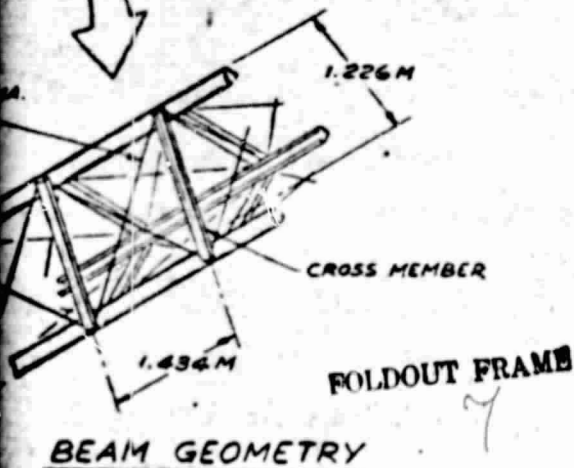
MANIPULATOR



SECTION 13-13

BEAM BASE SOLAR BLANKET ATTACHMENT

SCALE: 1/8 & 1/2



PLUG-IN SHAFT WITH RETENTION LATCH

SPRING CABLE RETENSION CLIP

ORIGINAL PAGE IS OF POOR QUALITY

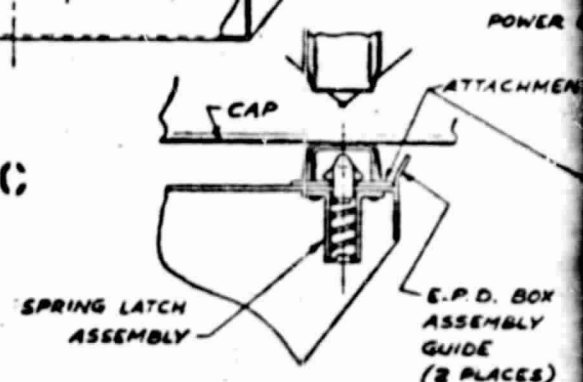
RED SLOT IN CROSS MEMBER

E.P.D. SWITCHING BOX MOUNTED TO UNDERSIDE OF CROSS BEAM - (VIA 2 ATTACHMENT DEVICES) AS SHOWN; ONE REQ'D FOR EACH SOLAR BLANKET

MANIPULATOR HANDLING APERTURE IN UNDERSIDE OF ELECT. BOX

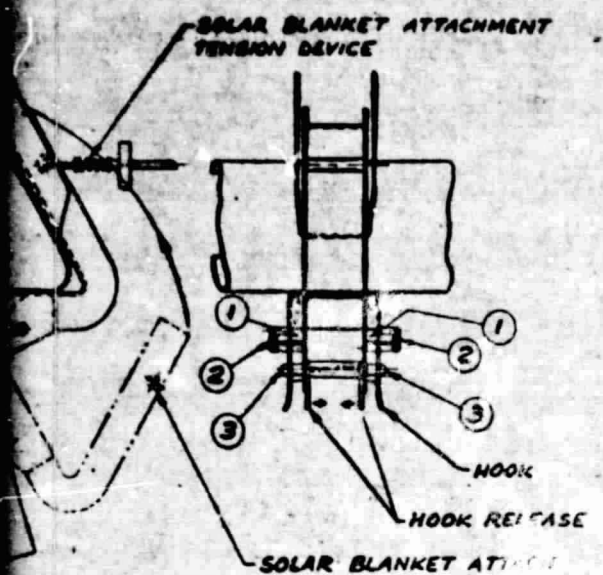
MANIPULATOR

DETAIL C SCALE: 1/8



DETAIL D SCALE: 1/8

CABLE HOLDER



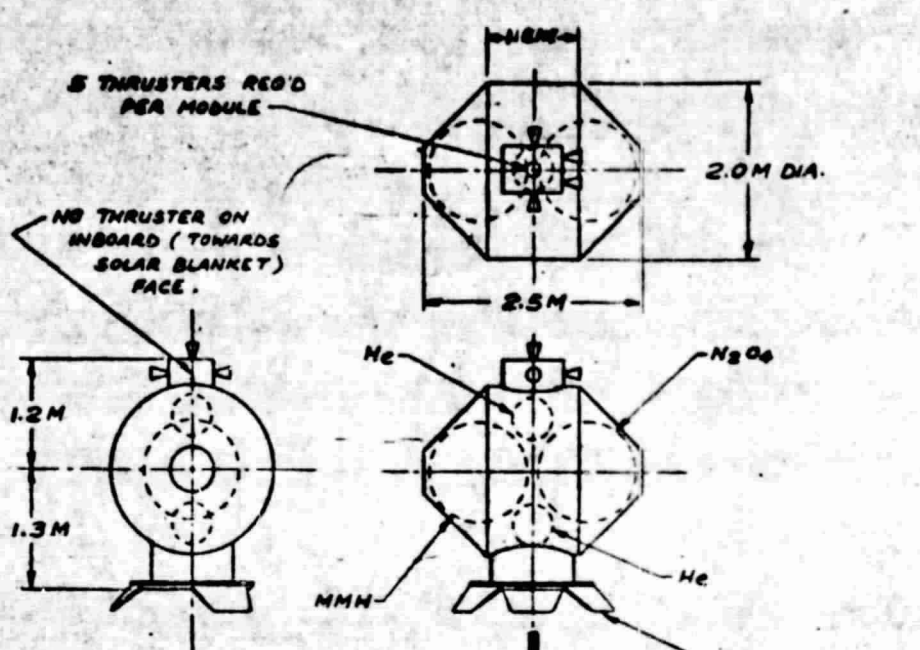
STOP (OPEN POSITION)

CENTER TENSION SPRING

SPRING LOADED STOP (LOCKED CLOSED POSITION)

BLANKET ATTACHMENT DEVICE

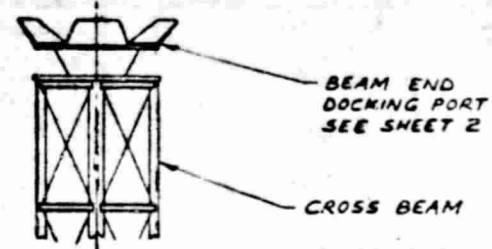
FILES: 1/8 & 1/2



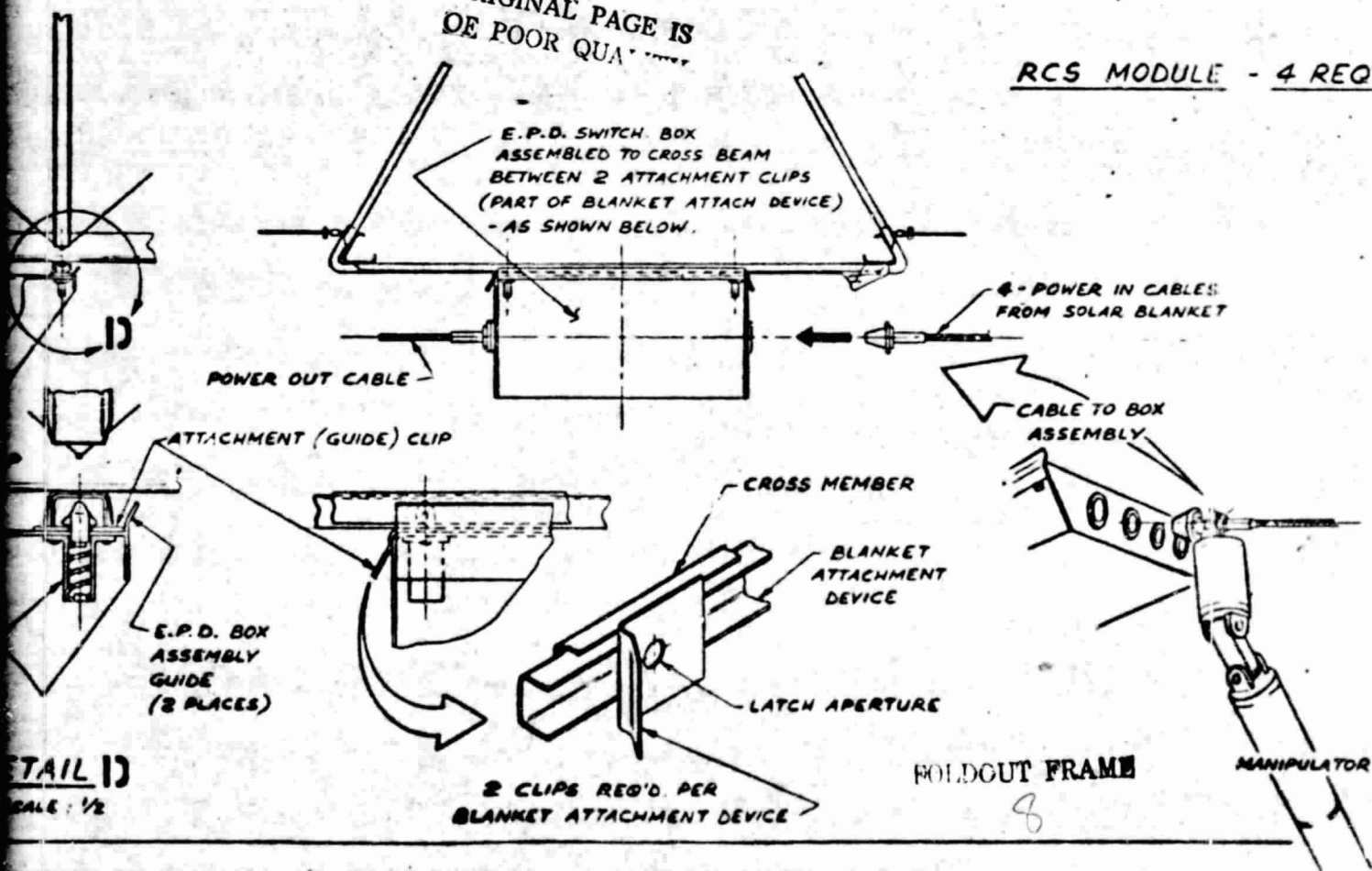
DETAIL 1

SCALE: 1/40

NOTE: 2 REQ'D AS SHOWN
& 2 OPPOSITE HAND,
(DETERMINED BY
ORIENTATION OF
DOCKING PORT)



RCS MODULE - 4 REQ'D



DETAIL 12

SCALE: 1/2

2.0M DIA.

N₂O₄

He

DOCKING PORT

BEAM END
DOCKING PORT
SEE SHEET 2

CROSS BEAM

- 4 REQ'D.

ORIGINAL PAGE IS
OF POOR QUALITY

FOLDOUT FRAME

ABBREVIATIONS USED -

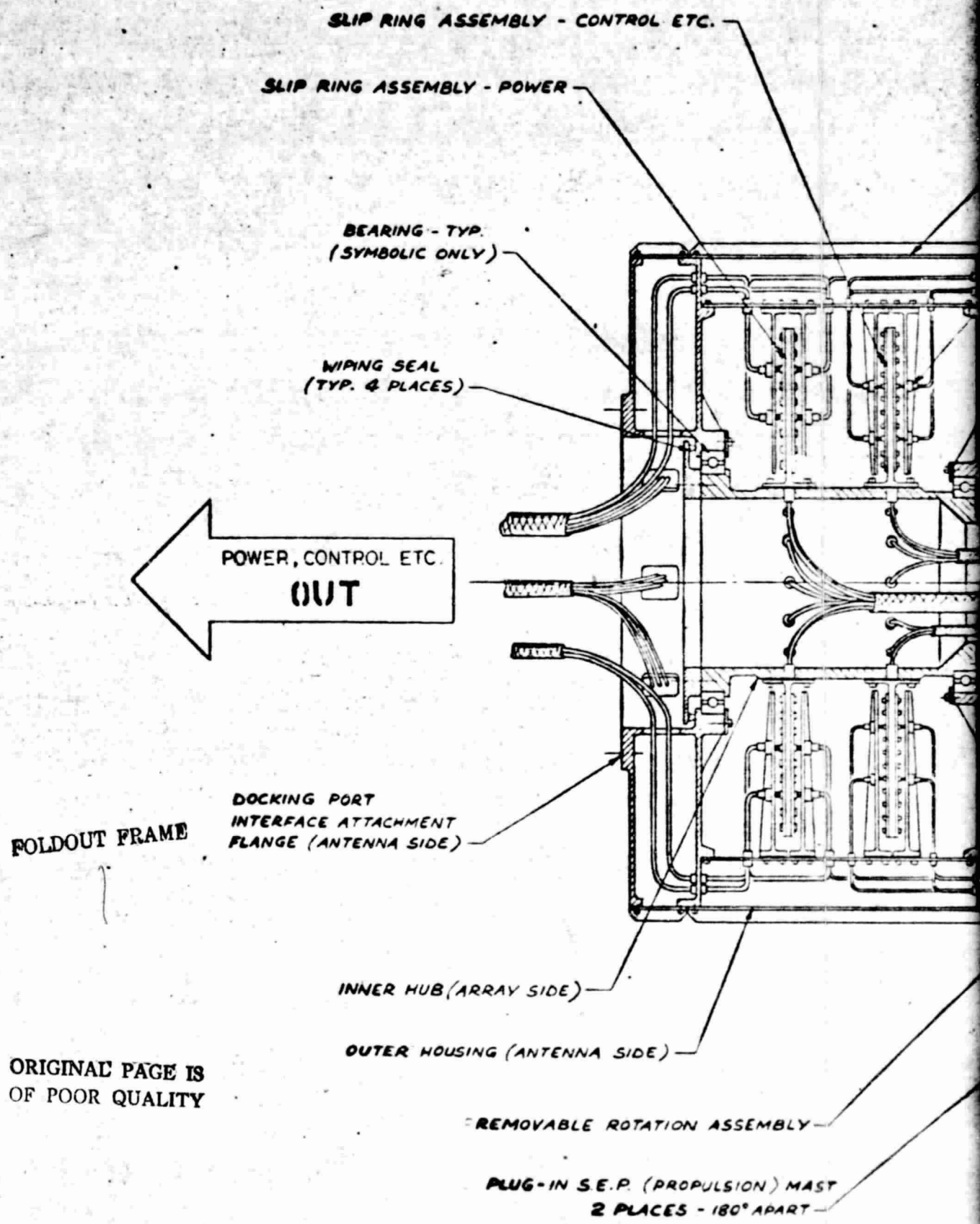
S.E.P. SOLAR ELECTRIC PROPULSION
E.P.D. ELECTRIC POWER DISTRIBUTION
R.C.S. REACTION CONTROL SYSTEM

PRECEDING PAGE BLANK NOT FILMED

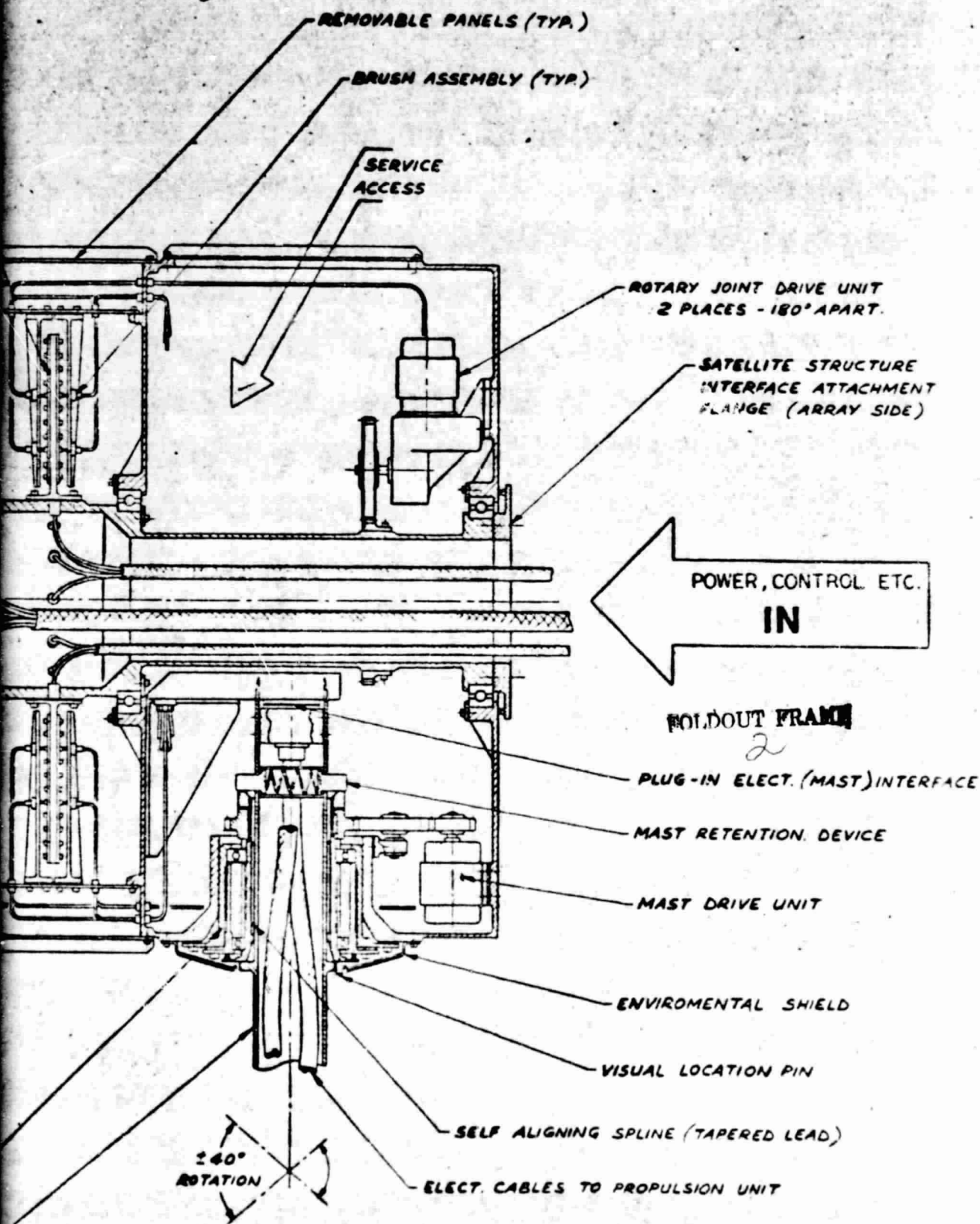
MANIPULATOR

3

DATE	NO. 8166	ROCKWELL INTERNATIONAL CORPORATION	PAGE
NOTED	DATE 1/3/79	SPACE DIVISION	A-3,4
1201 LARKSPUR BOULEVARD, BERKELEY, CALIFORNIA			
SPS TEST ARTICLE CONCEPT DEFINITION			42662-27 SHEET 1 OF 3



ORIGINAL PAGE IS
OF POOR QUALITY

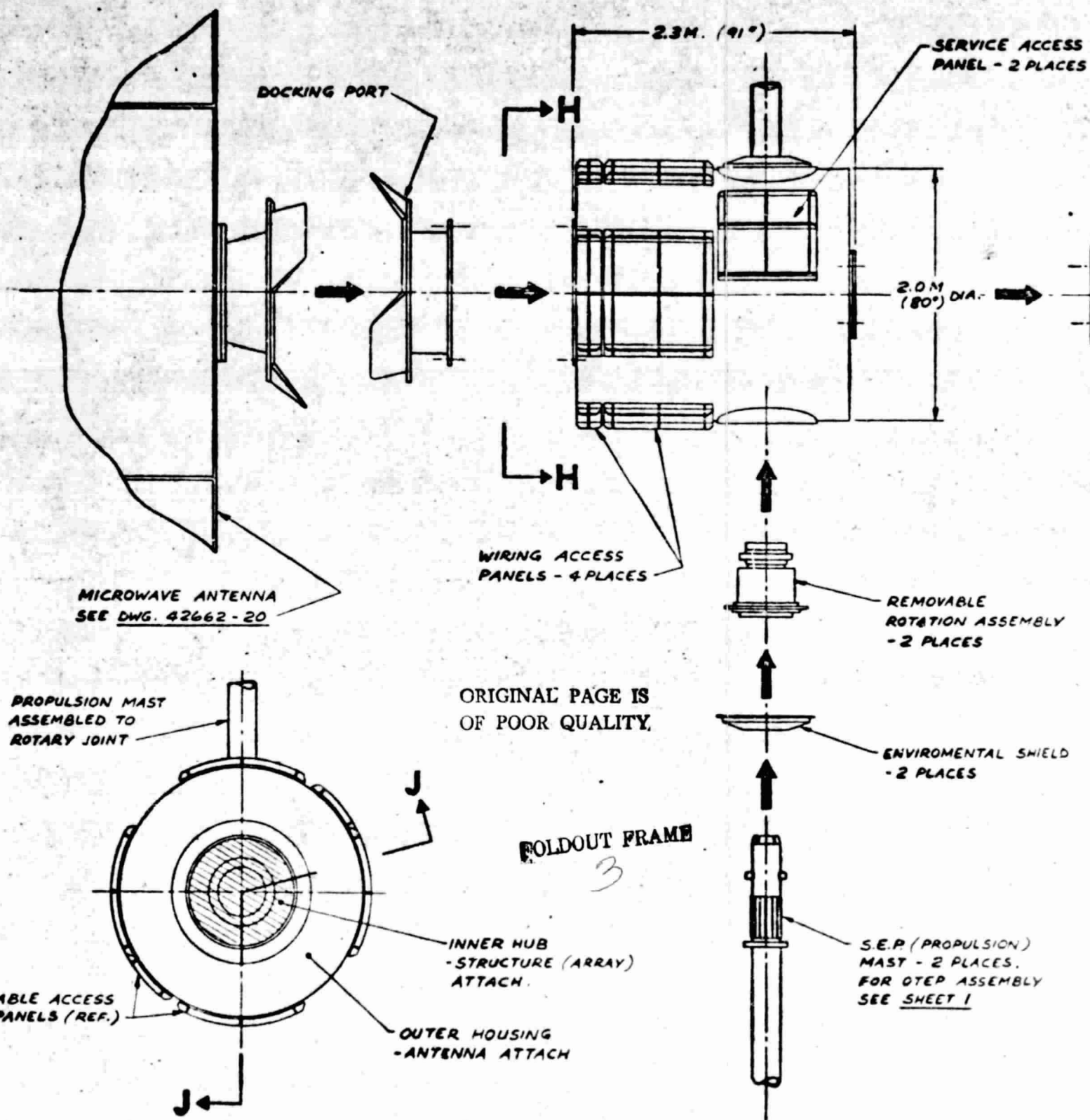


MICRO
SEE B

PROPULSION
ASSEMBLED TO
ROTARY JOINT

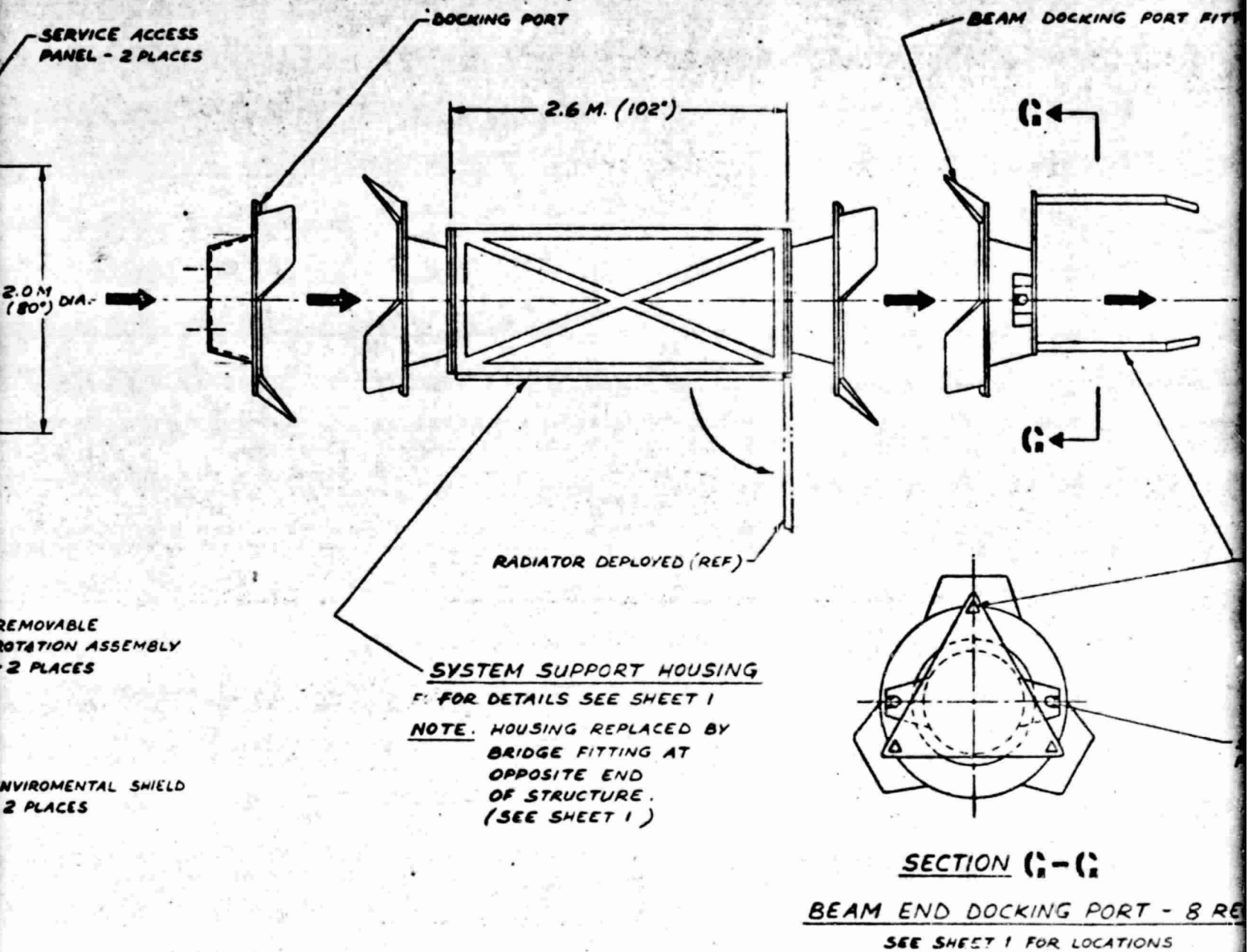
REMOVABLE ACCESS
PANELS (REF.)

ORIGINAL PAGE 18
OF POOR QUALITY



ROTARY JOINT & COMPONENT ASSEMBLY

SCALE: 1/20



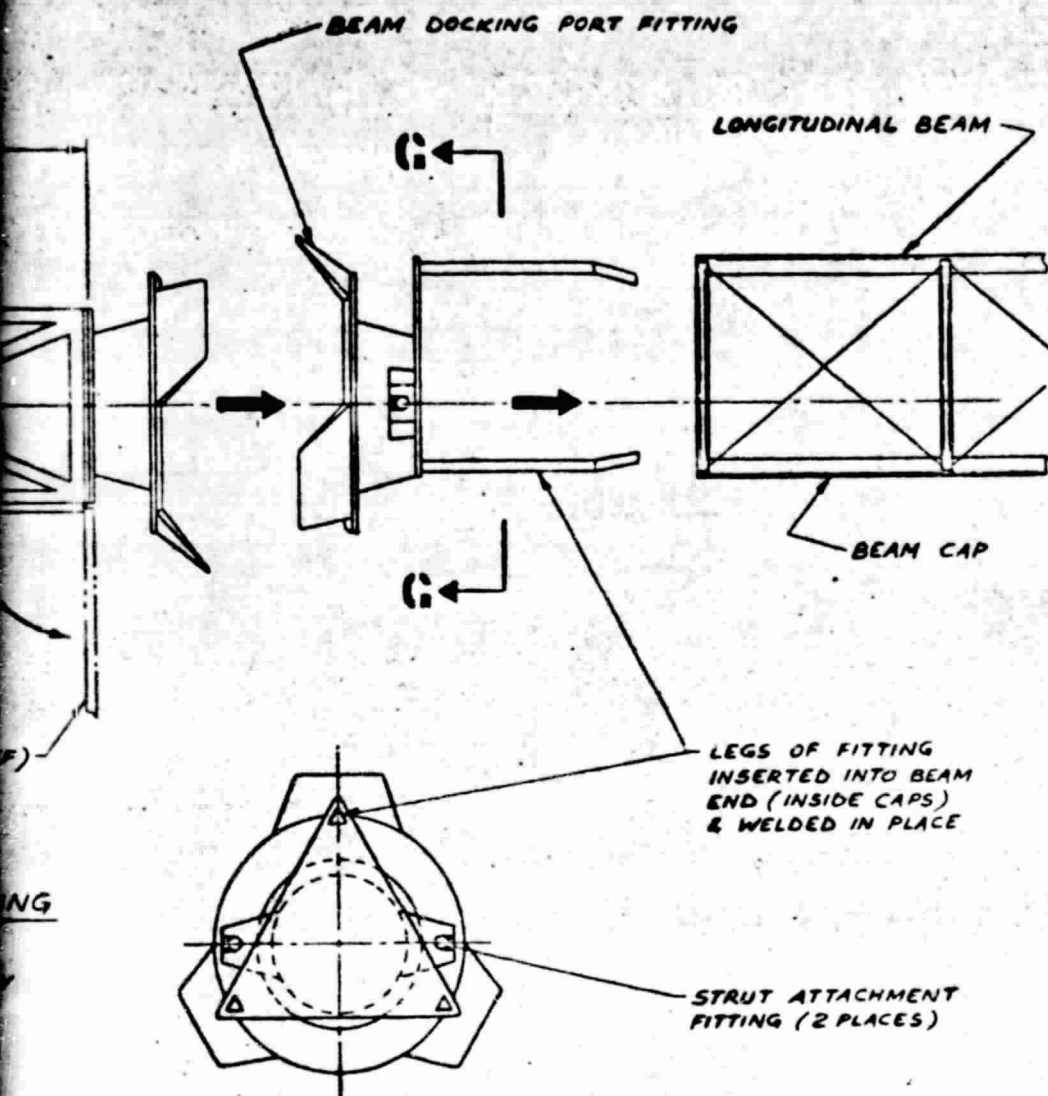
P (PROPULSION)
ST - 2 PLACES.
OTEP ASSEMBLY
SHEET 1

ORIGINAL PAGE IS
OF POOR QUALITY

FOLDOUT FRAME

ASSEMBLY

DATE	BY
NOTED	DATE
SPS	
CON	



SECTION G-G

BEAM END DOCKING PORT - 8 REQ'D

SEE SHEET 1 FOR LOCATIONS

FOLDOUT FRAME
5

ORIGINAL PAGE IS
OF POOR QUALITY

DESIGN	BY BUCK	ROCKWELL INTERNATIONAL CORPORATION	PAGE A-5,6
NOTED	DATE 1/2/70	SPACE DIVISION	
		1001 LAFAYETTE BOULEVARD, BIRMINGHAM, AL 35202	
SPS TEST ARTICLE CONCEPT DEFINITION			42662-27 SHEET 2 OF 3

ORIGINAL PAGE IS
OF POOR QUALITY

FOLDOUT FRAME

S.E.P. (PROPULSION) ASSEMBLY
2 PLACES (THIS END)
SEE SHEET 1 FOR DETAILS

TT&C UNIT

J-BOX

DOCKING INTERFACE

RCS MODULE

DOCKING INTERFACE

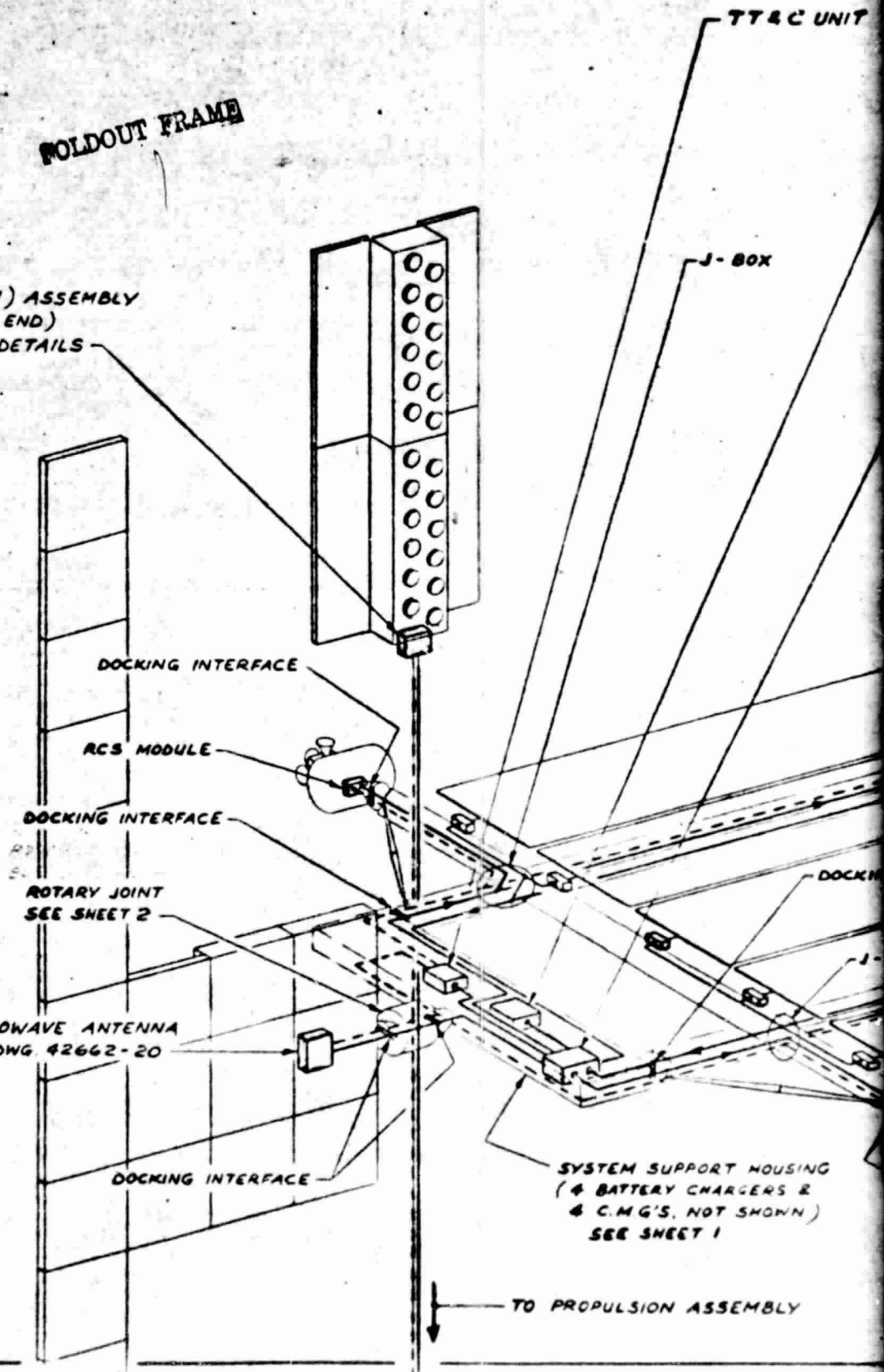
ROTARY JOINT
SEE SHEET 2

MICROWAVE ANTENNA
SEE DWG 42662-20

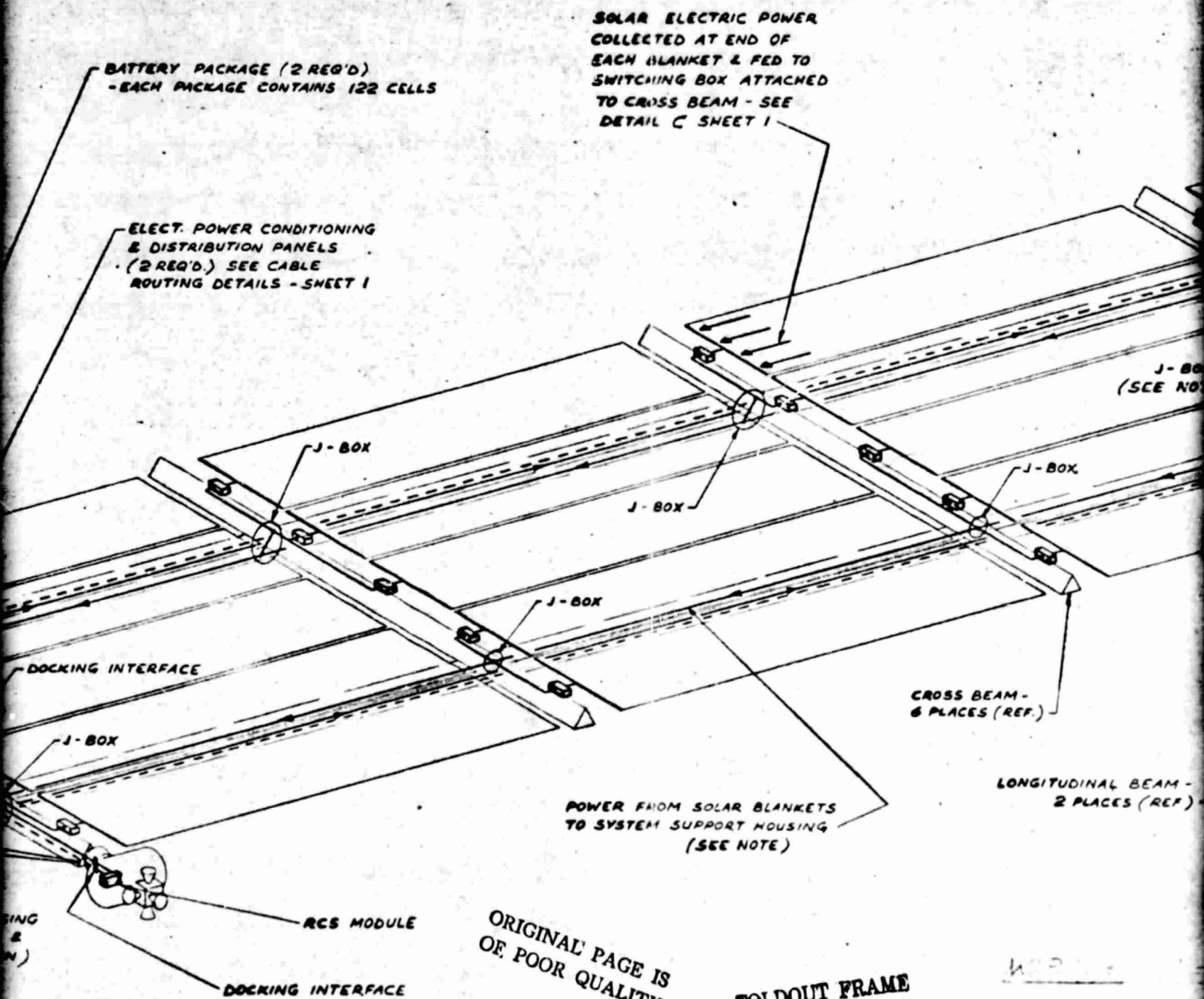
DOCKING INTERFACE

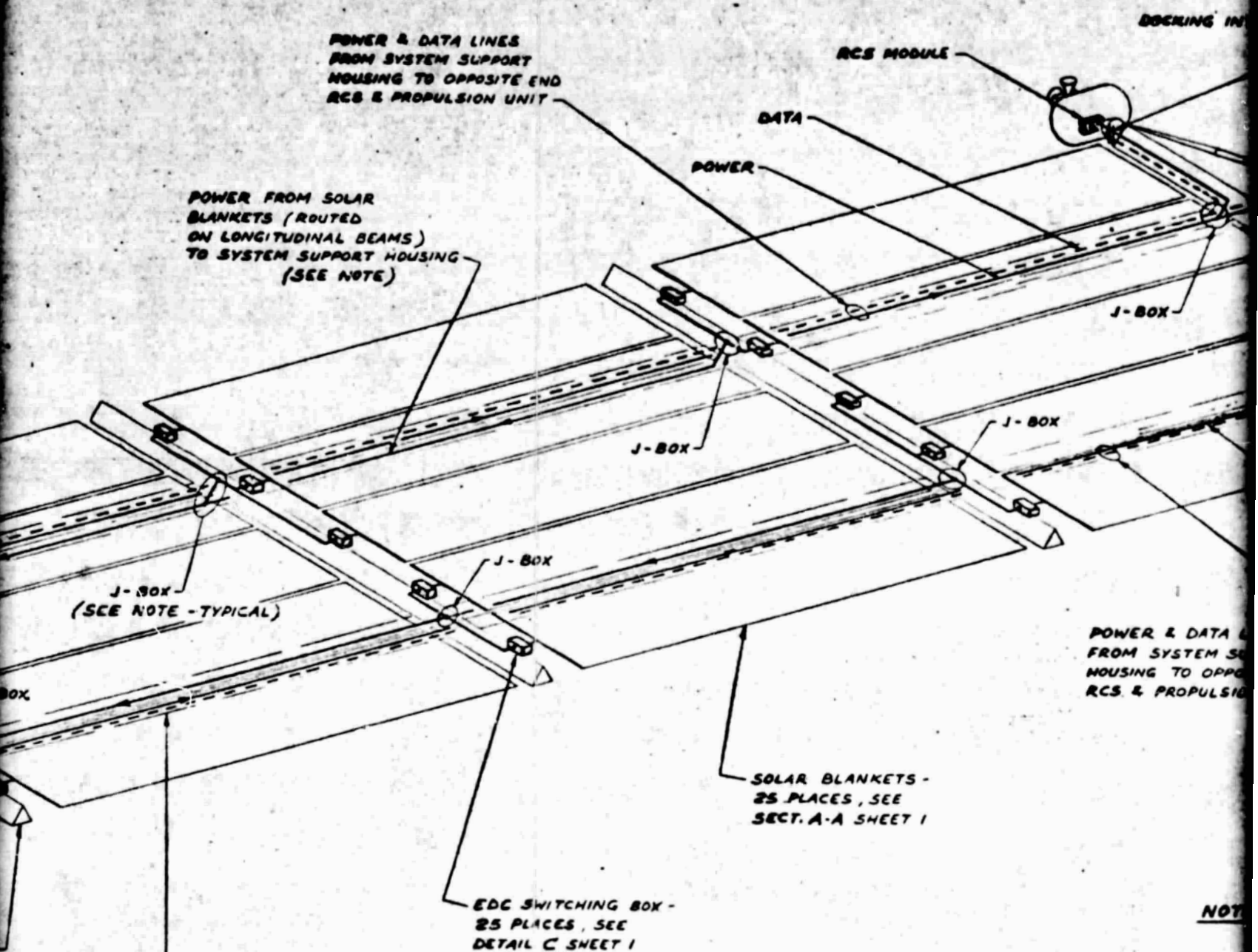
SYSTEM SUPPORT HOUSING
(4 BATTERY CHARGERS &
4 C.M.G.'S, NOT SHOWN)
SEE SHEET 1

TO PROPULSION ASSEMBLY



E UNIT



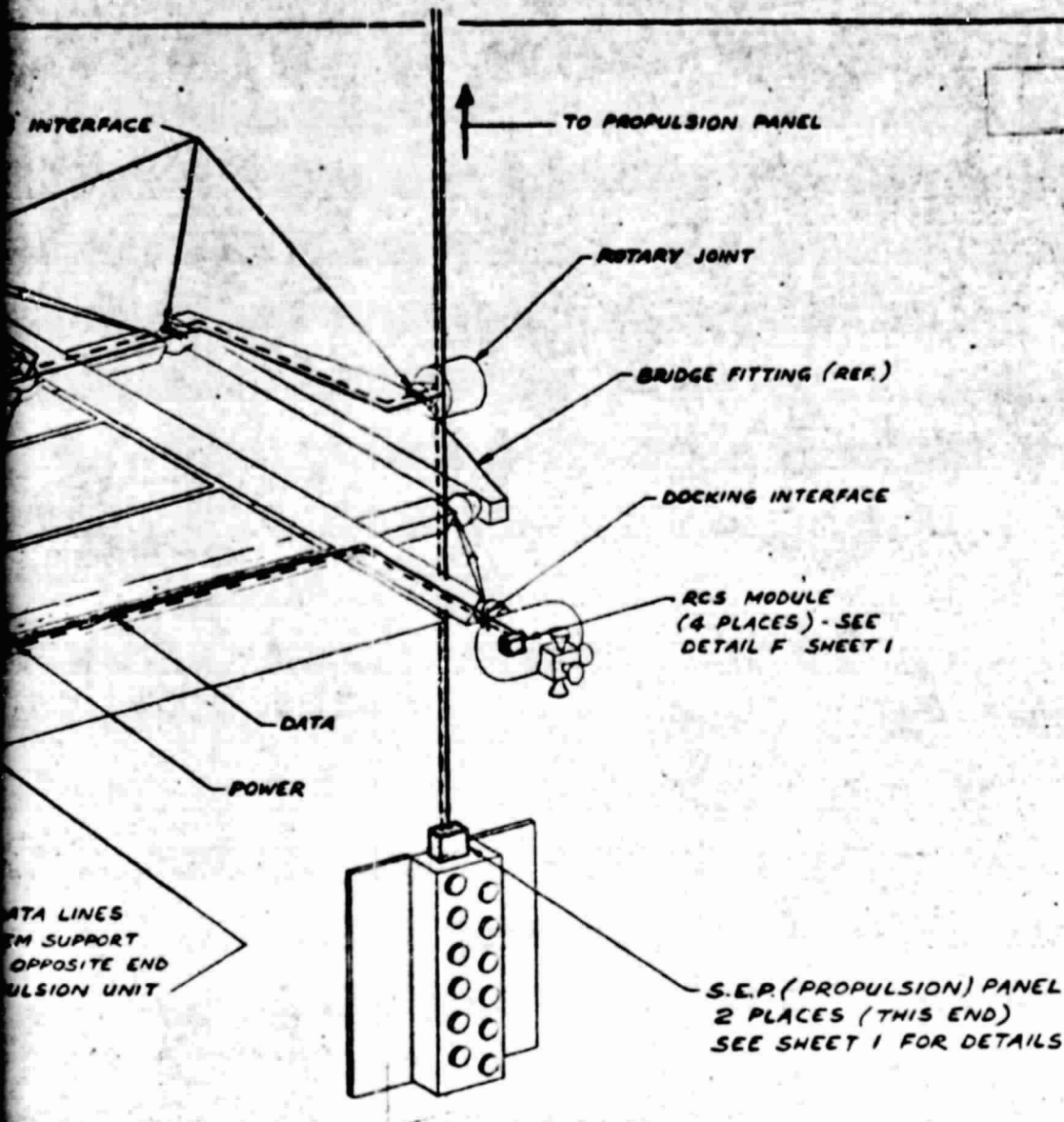


ORIGINAL PAGE IS
OF POOR QUALITY

FOLDOUT FRAME
3

WIRE ROUTING SCHEMATIC

SPS TEST ARTICLE (LADDER CONFIGURATION)



NOTE -

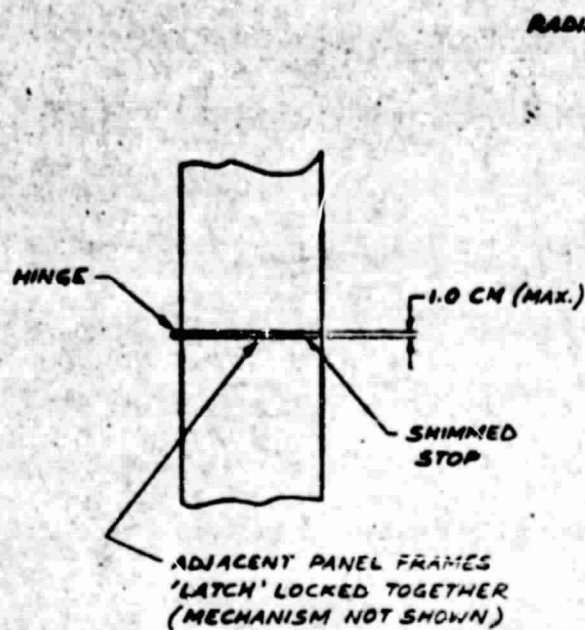
THE POWER OUTPUT FROM EACH SOLAR BLANKET SWITCH BOX IS AN INDIVIDUAL CABLE FEEDING DIRECTLY INTO THE DISTRIBUTION PANELS LOCATED IN THE SYSTEM SUPPORT HOUSING.
THE J-BOX CALL-OUTS FLAG THE NEED FOR PHYSICAL ATTACHMENT & THE BUNDLING OF INDIVIDUAL CABLES ONLY.
- NOT FOR POWER DISTRIBUTION :

ORIGINAL PAGE IS
OF POOR QUALITY

FOLDOUT FRAME
4

5

DATE	BY	ROCKWELL INTERNATIONAL CORPORATION	PAGE A-78
APPROVED	DATE	SPACE DIVISION	
		401 LAMAR AVENUE, BOSTON, MASSACHUSETTS	
SPS TEST ARTICLE CONCEPT DEFINITION			42662-27 SHEET 3 OF 3



DETAIL I

RADIATOR (HEAT PIPE) SURFACE

(A) 18 PANELS

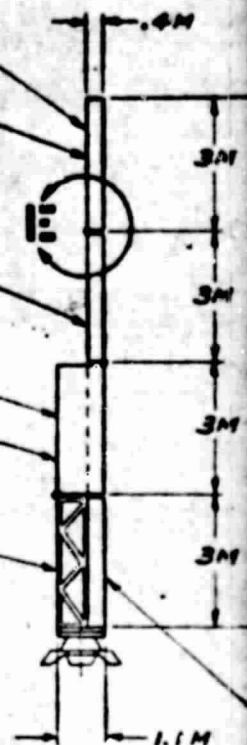
(B) 3 PANELS

(C) CENTER PANEL

(B₁) OUTBOARD PANELS

(B₂) 3 PANELS

NOTE. SAME AS B
(.4M THICK)
+.7M FOR
STRUCTURAL FRAME.

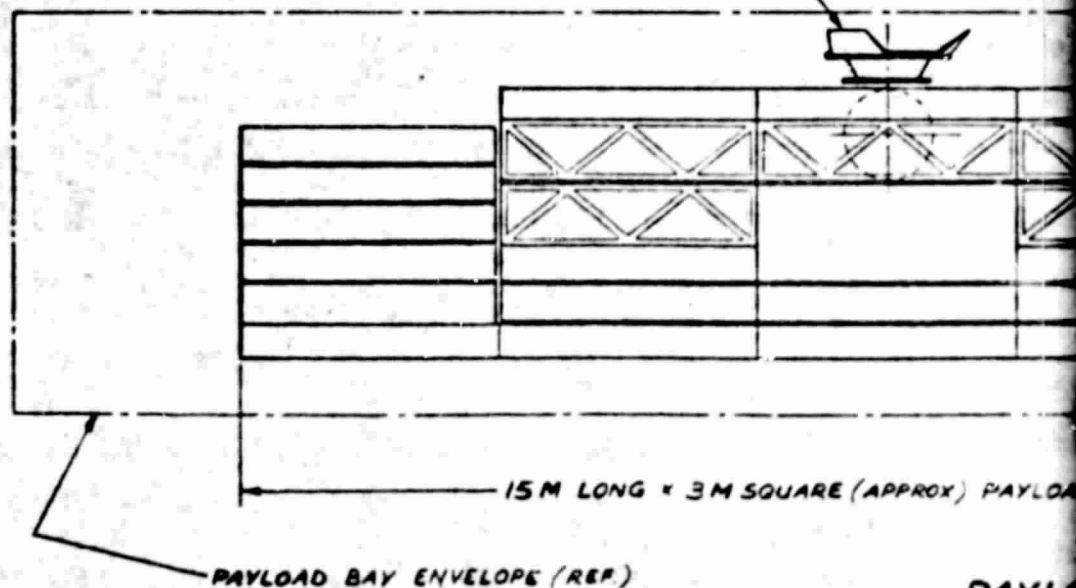


SECTION D-D

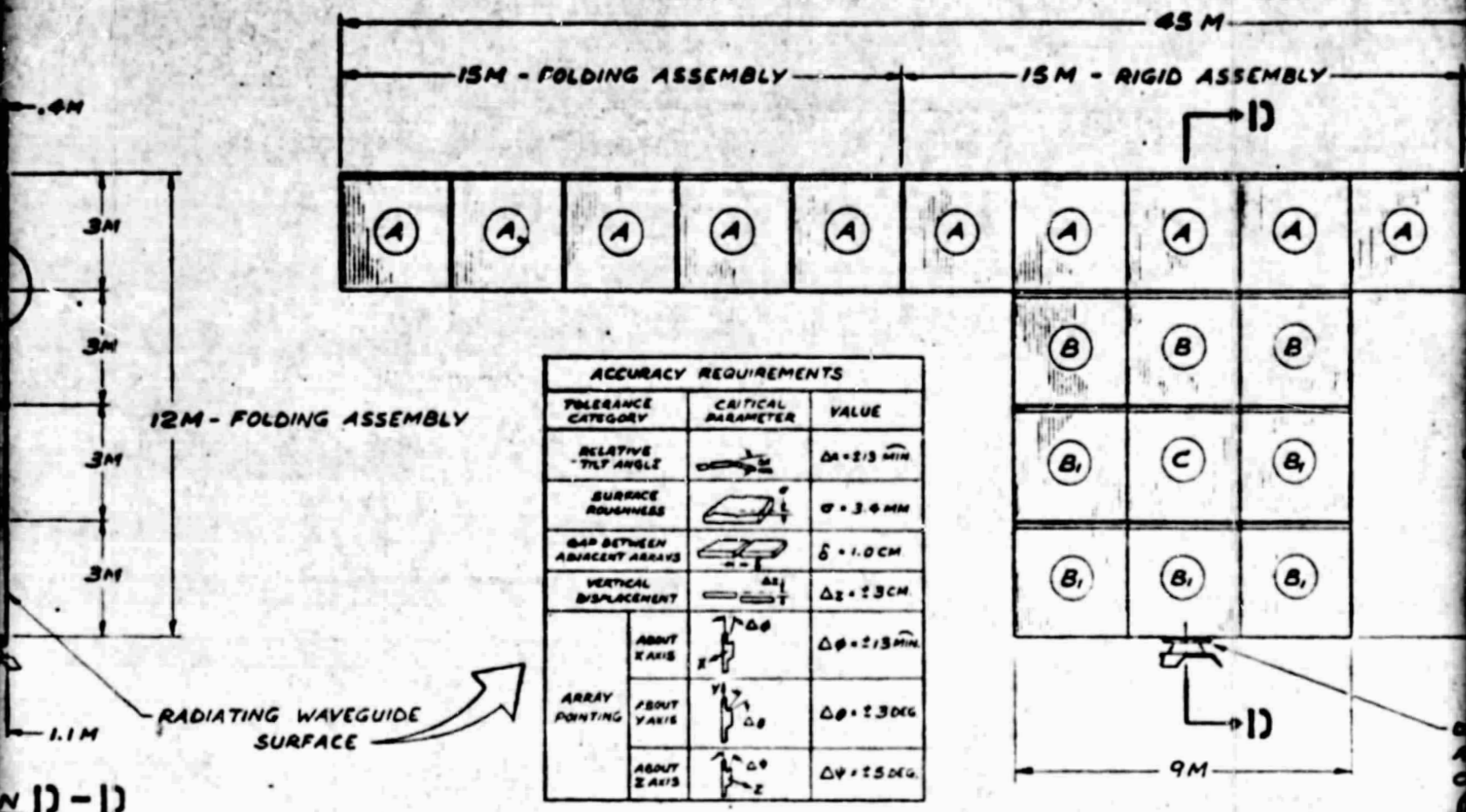
ORIGINAL PAGE IS
POOR QUALITY

FOLDOUT FRAME

DOCKING PORT SHOWN STOWED
WITHIN ENVELOPE (POSITION OPTIONAL)



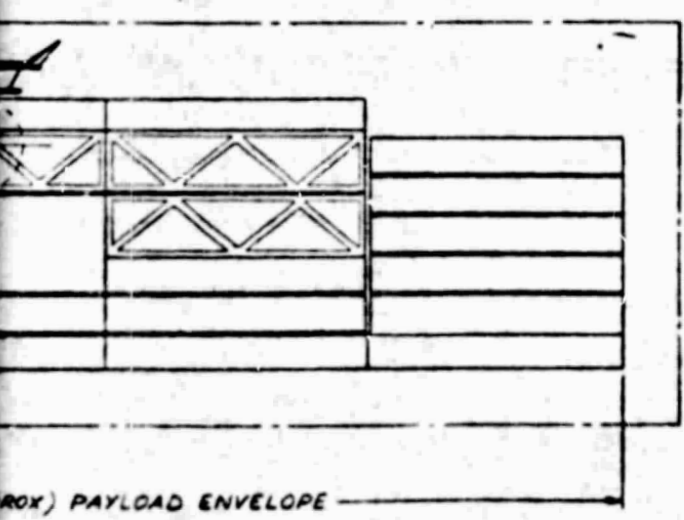
PAYLO



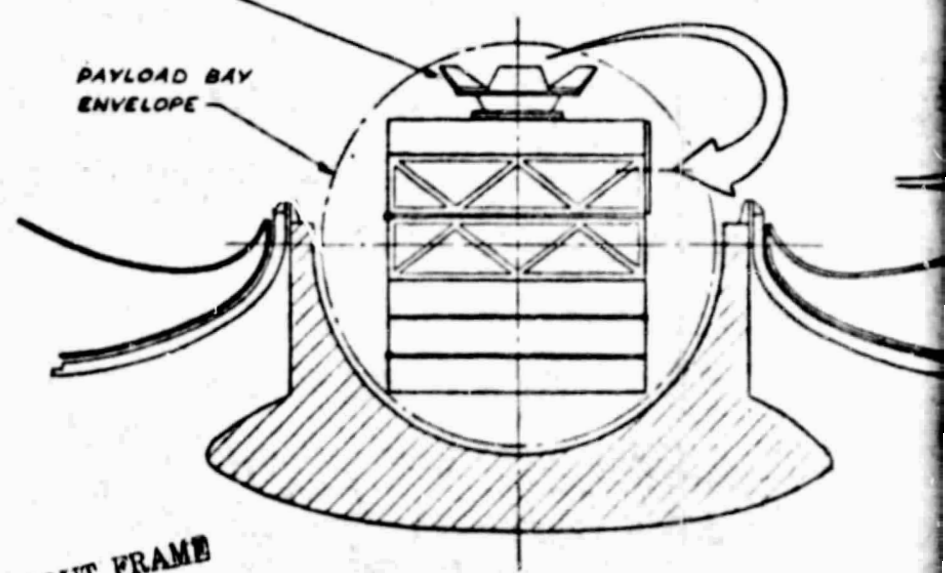
ORIGINAL PAGE 13
OF POOR QUALITY

AFTER OPENING PAYLOAD BAY DOORS
REMOVE DOCKING PORT & SECURE TO
TOP CENTER PANEL OF ANTENNA

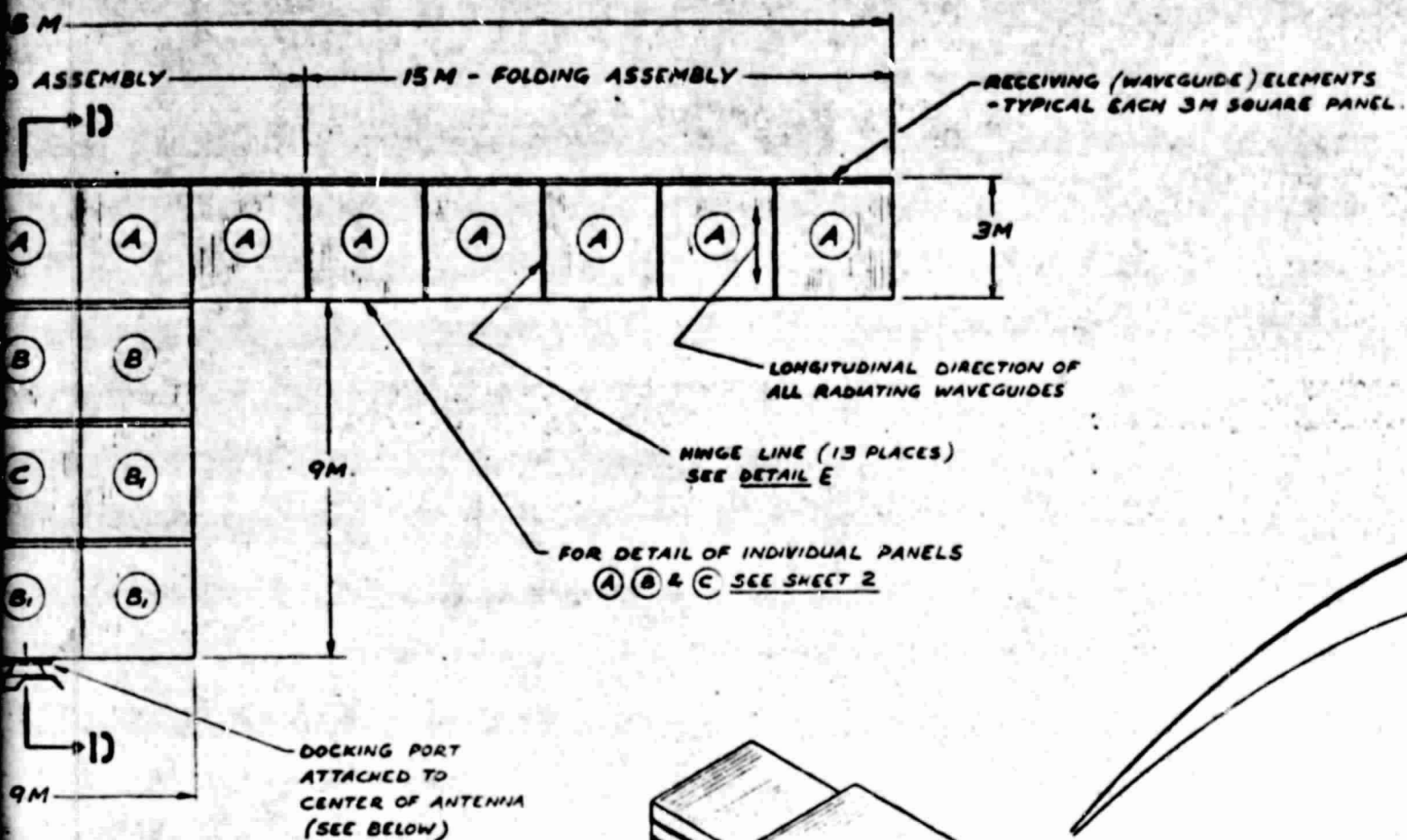
MICROWAVE ANTENNA (DEPLOYED)
SCALE: 1/80



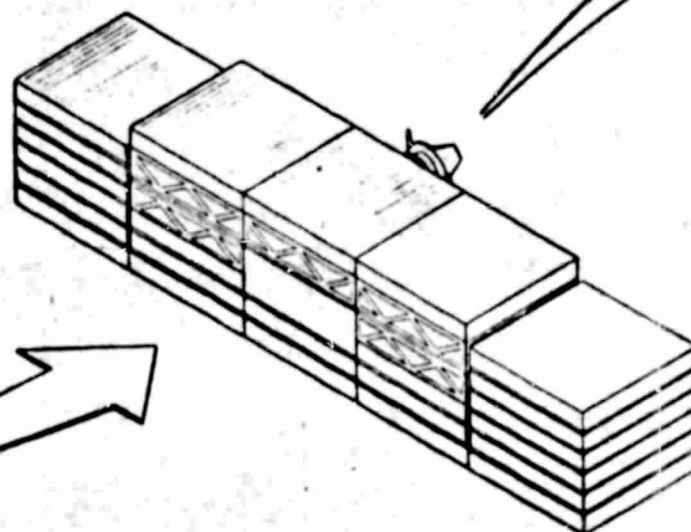
PAYLOAD PACKAGING ENVELOPE FOLDOUT FRAME
SCALE: 1/40



SECTION THRU PAYLOAD BAY



INA (DEPLOYED)
1/80



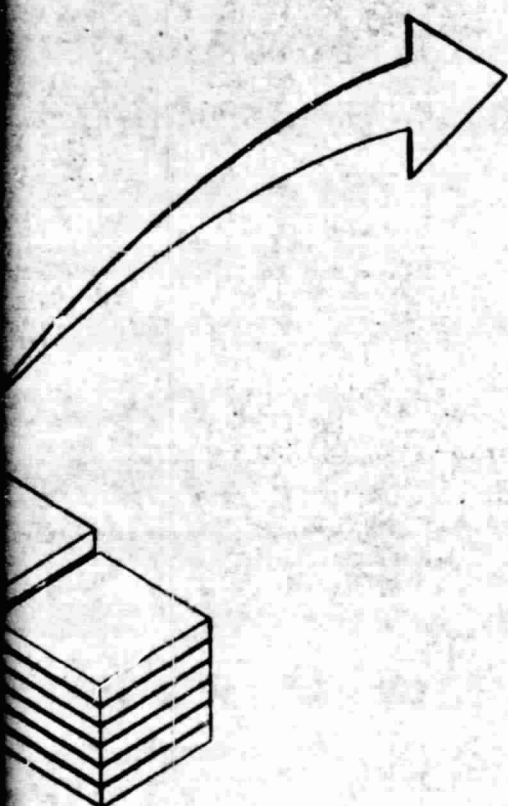
FOLDOUT FRAME
3

REMOVE ANTENNA FROM
PAYLOAD BAY AS AN
'UN - OPENED' PACKAGE.

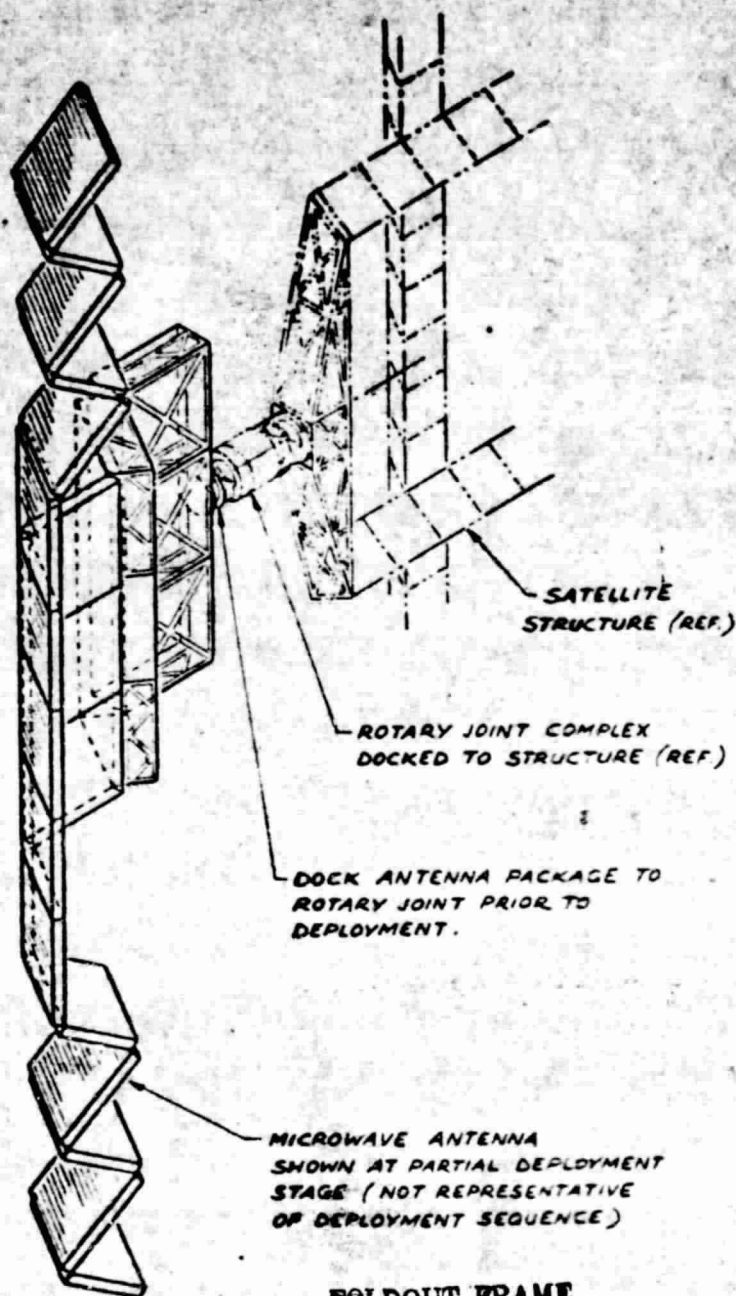
ORIGINAL PAGE IS
OF POOR QUALITY

PAYLOAD BAY

(WAVEGUIDE) ELEMENTS
EACH 3M SQUARE PANEL.



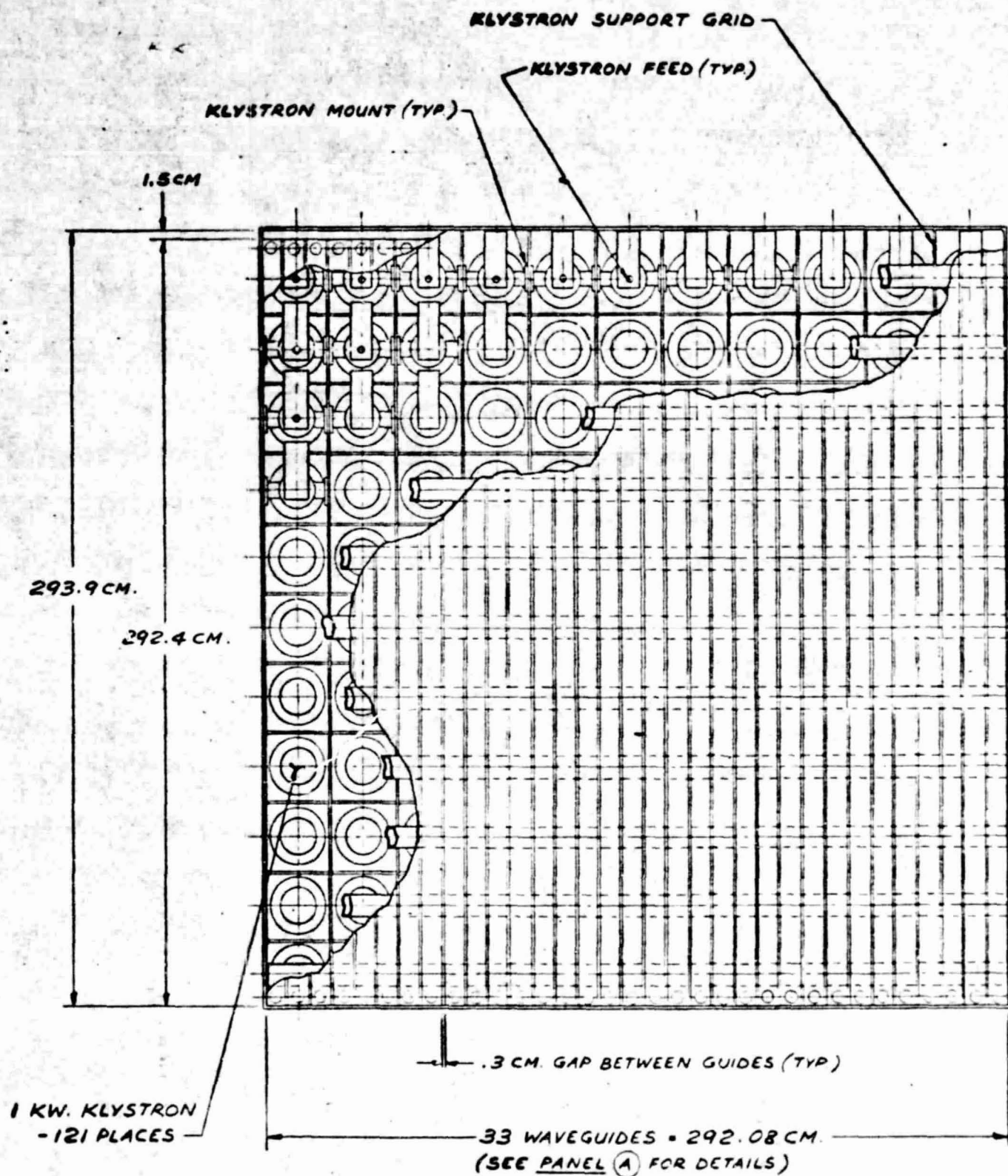
ANTENNA FROM
AS AN
PACKAGE.



FOLDOUT FRAME

ORIGINAL PAGE IS
OF POOR QUALITY

DATE	12/12/72	NOCKWELL INTERNATIONAL CORPORATION SPACE DIVISION 1411 LAKESHORE BOULEVARD, SUITE 100, ANN ARBOR, MI 48106	PAGE A-9,10
BY	BUCK		
SPS MICROWAVE ANTENNA CONFIGURATION CONCEPT			42662-20 SHEET 1 OF 2



ORIGINAL PAGE IS
OF POOR QUALITY

FOLDOUT FRAME

SUB-ARRAY C - ON

2 RECEIVING ELEMENTS
148.06 CM & 152.02 CM LONG
WITH .3 CM GAP BETWEEN

FLOATING (SOFT)
WAVEGUIDE END
SUPPORT (66 PLACES)

WAVEGUIDE OR COAX - TYP.
(KLYSTRON TO CROSS FEEDER)

BOX FRAME
SEE PANEL (A)

KLYSTRON FEED (TYP)

KLYSTRON MOUNT (TYP)

KLYSTRONS MOUNTED
VERTICAL IN PANEL

THERMAL RADIATING
SURFACE - SEE PANEL (A)

CROSS FEEDER WAVEGUIDES
8.46 CM WIDE $\frac{2}{3}$
4.23 CM WIDE $\frac{2}{3}$
WITH .050 CM THICK WALL
- 295.38 CM LONG

BOX FRAME
SEE PANEL (A)

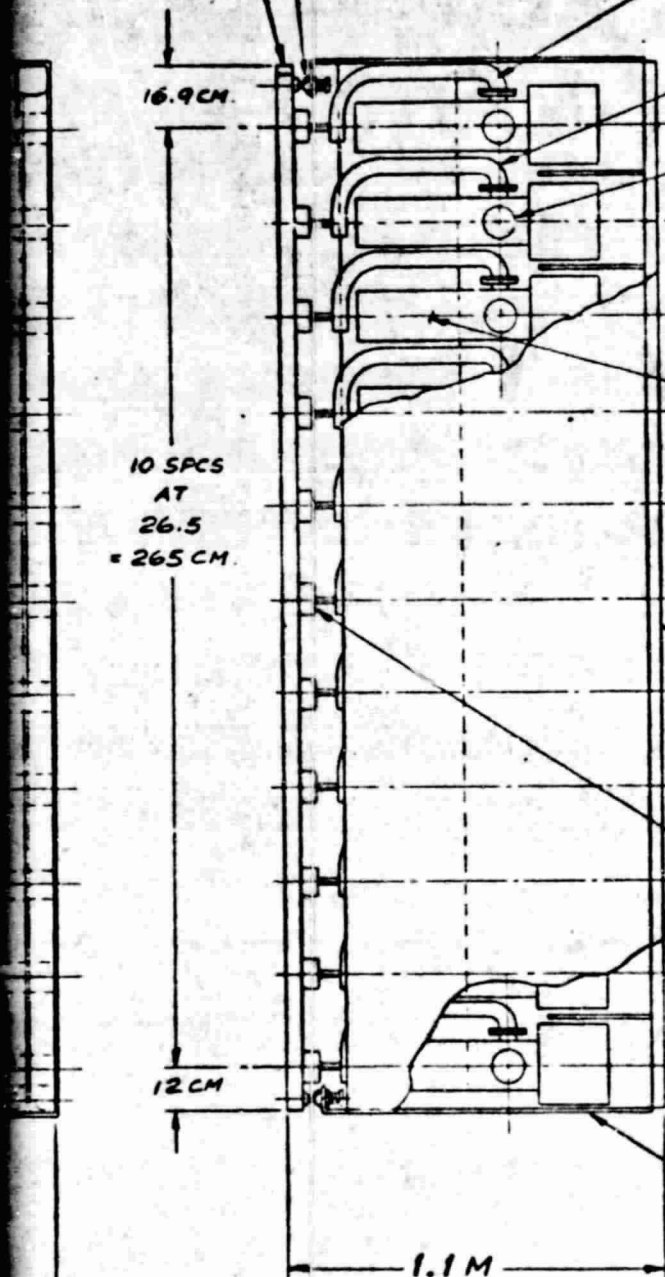
293.9 CM

RAD
(33)

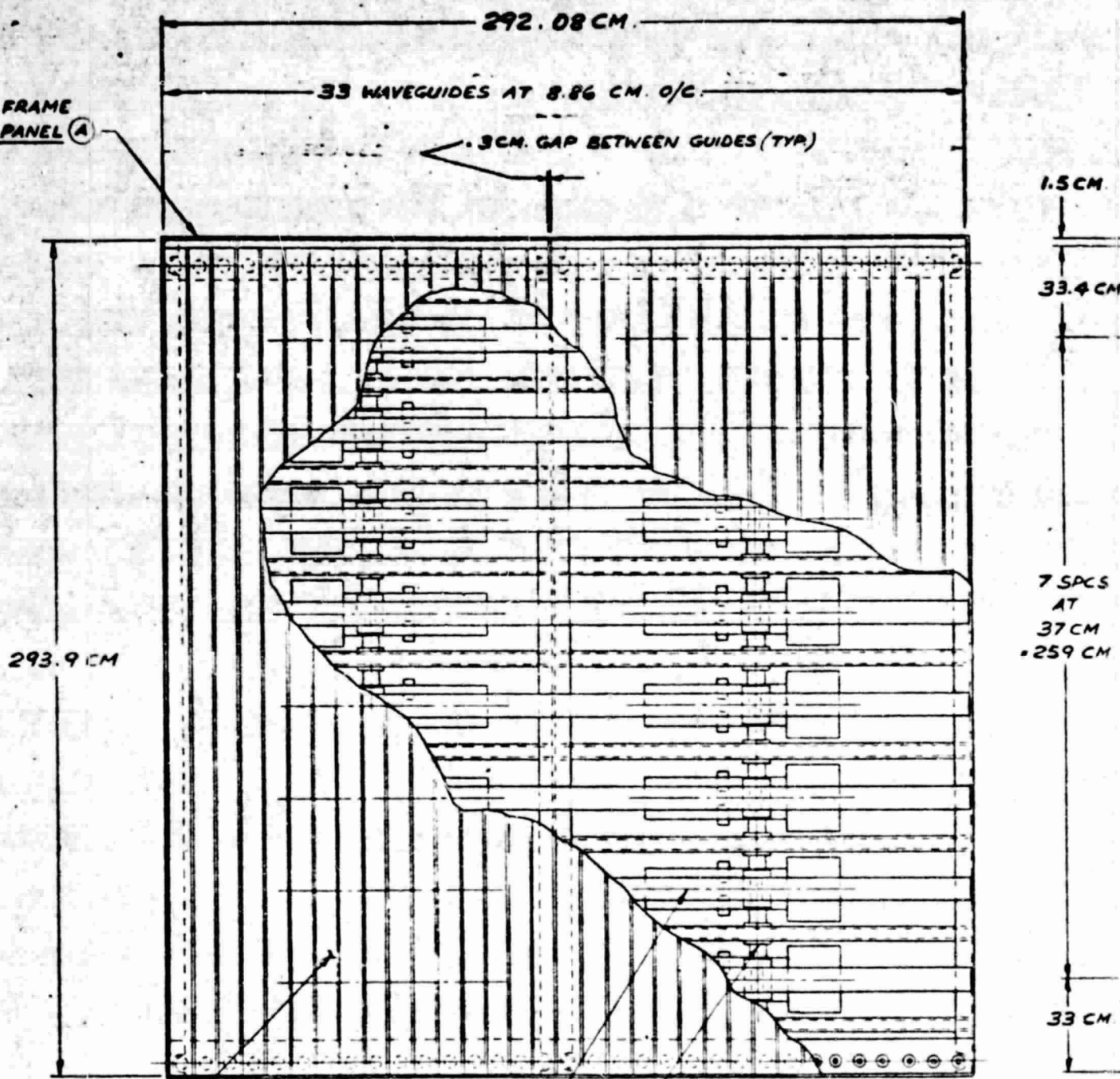
WOLDOUT FRAME
2

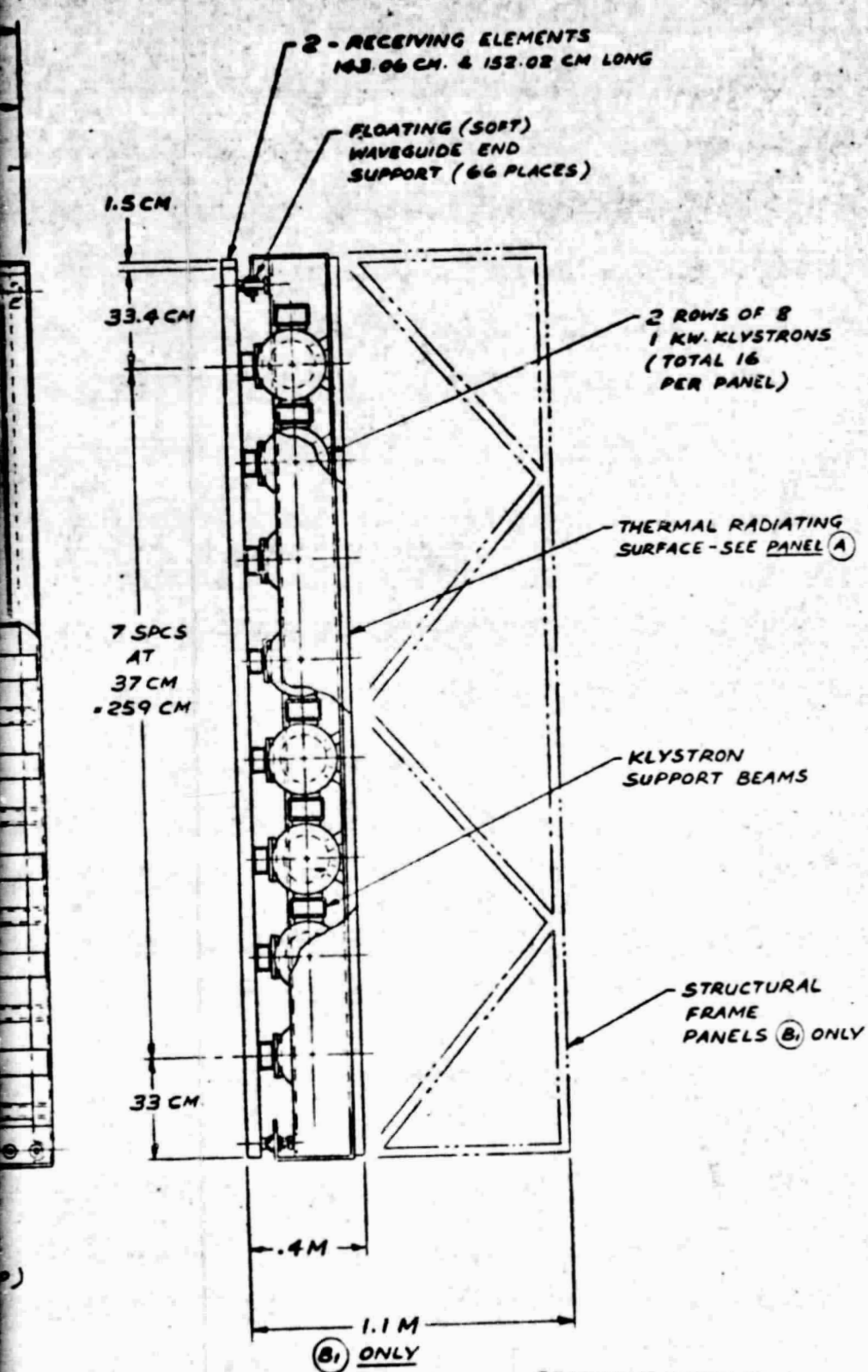
ORIGINAL PAGE 19
OF POOR QUALITY

- ONE REQ'D



BOX FRAME
SEE PANEL (A)

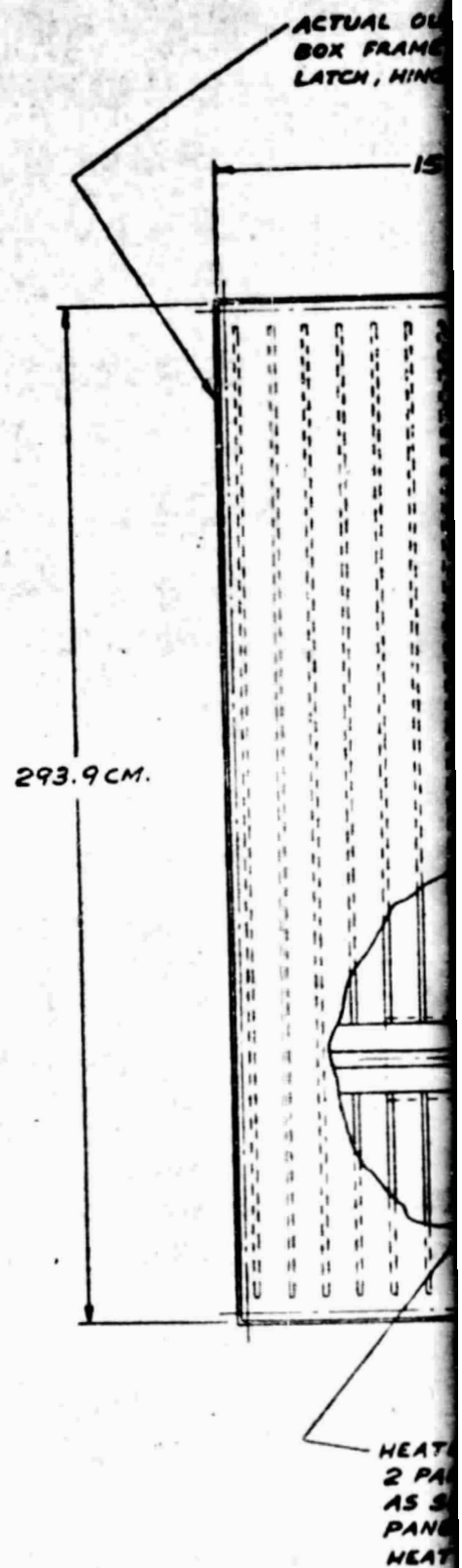




ORIGINAL PAGE IS
OF POOR QUALITY

FOLDOUT FRAME

B REQ'D



ACTUAL OUTSIDE DIMENSIONS OF
BOX FRAME DETERMINED FROM
LATCH, HINGE & STOP DESIGN

KLYSTRON SUPPORT
STRUCTURE

FLOATING (SOFT)
WAVEGUIDE END
SUPPORT
(66 PLACES)

150 CM.

141 CM.

9 CM.

293.9 CM.

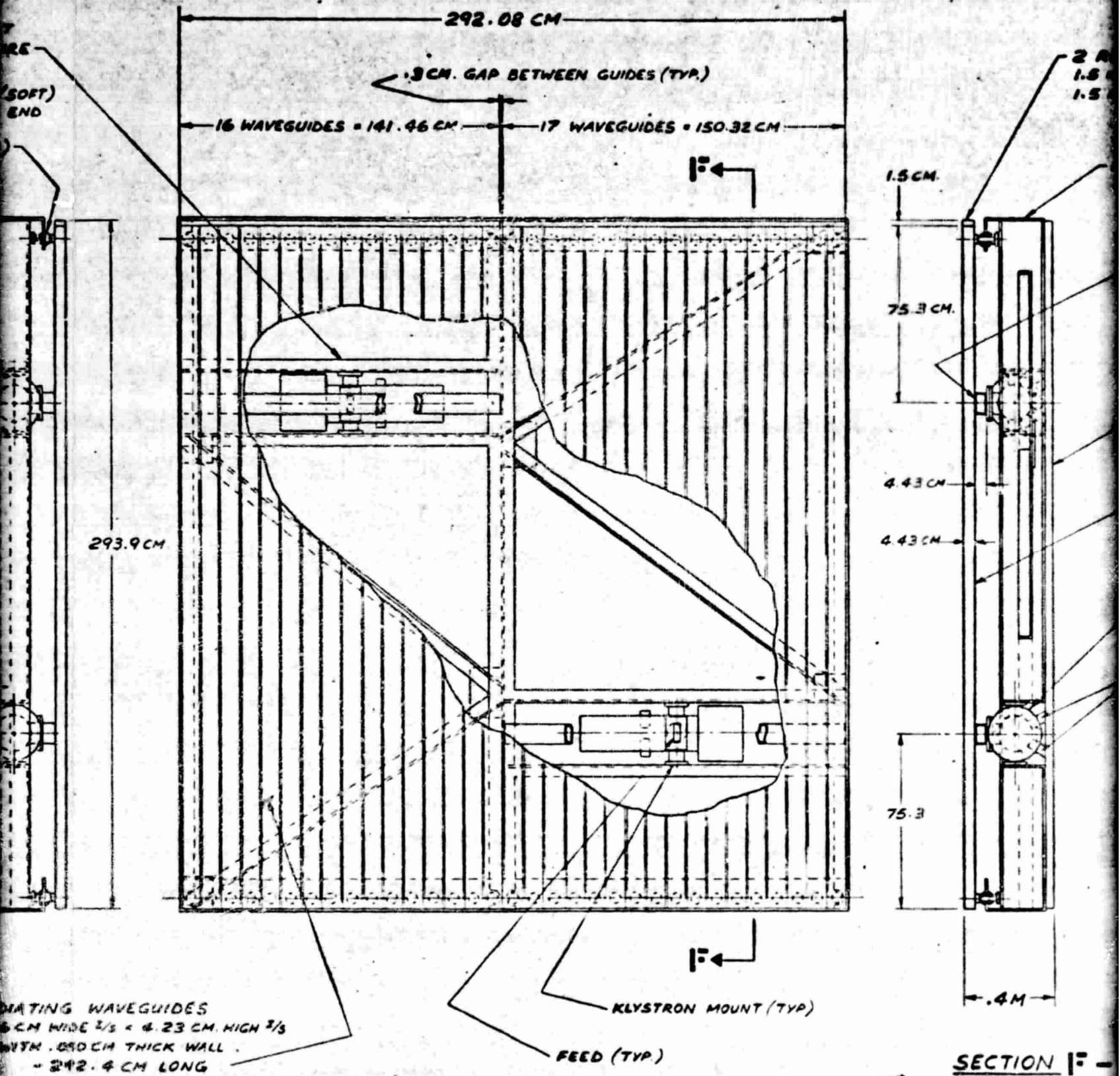
HEATPIPE RADIATOR PANELS -
2 PANELS PER SUB-ARRAY
AS SHOWN (TYPICAL FOR ALL
PANEL (A) THRU (C) EXCEPT FOR
HEAT PIPE ARRANGEMENT)

ORIGINAL PAGE IS
OF POOR QUALITY

RADIATING WAVEGUIDES
8.46 CM WIDE $\frac{2}{3} \times 4.23$ CM
WITH .050 CM THICK WALL
- 292.4 CM LONG

FOLDOUT FRAME

SUB-ARRAY PANEL (A) - 15



DIATING WAVEGUIDES
6 CM WIDE 2/3 x 4.23 CM. HIGH 2/3
WITH .050 CM THICK WALL
- 292.4 CM LONG

PANEL (A) - IS REQ'D.

ORIGINAL PAGE IS
OF POOR QUALITY

FOLDOUT FRAME

SECTION I

2 RECEIVING ELEMENTS
 $1.5 \times 4.43 = 143.06 \text{ CM}$ &
 $1.5 \times 4.43 = 152.02 \text{ CM}$

BOX FRAME STRUCTURE

CROSS FEEDER WAVEGUIDES
 (2 PLACES) $8.46 \times 4.23 \text{ CM}$, $3/5$
 $\times .010 \text{ CM WALL}$
 1 AT 143.06 CM &
 1 AT 152.02 CM LONG

THERMAL RADIATOR
 SURFACE

RADIATING WAVEGUIDE
 (33 PLACES)

1 KW. KLYSTRON
 (2 PLACES)

THERMAL RADIATOR
 FEEDS (TYP.)

FOLDOUT FRAME

ORIGINAL PAGE IS
 OF POOR QUALITY

SLOT - SLOT SPACING
 $1\frac{1}{2}$ BOTH DIRECTIONS
 ALL SLOTS $\frac{1}{2}$ RESONANT

WAVEGUIDE ARRAY
 WITH STAGGERED
 LONGITUDINAL
 RADIATING
 SLOTS

WALL COMMON TO
 BOTH WAVEGUIDES

FEEDER
 WAVEGUIDE
 WITH INCLINED
 COUPLING SLOTS

TRANSVERSE FEEDER GUIDE & RADIATING
 WAVEGUIDE SLOT DETAIL (TYP ALL PANELS)

SECTION I-I

SCALE 1/10	DR BUCK DATE 12-77 WEEK	ROCKWELL INTERNATIONAL CORPORATION SPACE DIVISION 1515 LAURELWOOD BOULEVARD, BERNET, CALIFORNIA	PAGE A-11, 12
SPS MICROWAVE ANTENNA CONFIGURATION CONCEPT			42662-20 SHEET 2 OF 2

20 BAYS @ 12.0 M = 240

SOLAR PANELS DEPLOYED
FOLDED FOR ORBIT TRANSFER

—TIEDOWN STRUTS FOR ORBIT
TRANSFER (PYRO SEPARATION SYS)

✓ 12.0 GHz & 12.0 GHz
RF SIGNAL INTERFACE BOX

SYSTEM CONTROL CENTER MODULE
CONTAINS MODULES OF TT&C UNITS, CONTROL
MOMENT CYROS (CMG), & GUIDANCE, CONTROL

7.0 M

43 M

LEIVER GROUP.
ANGULAR BODIES
1.73 M WIDE x .43

5 M DEPTH

FOLDOUT FRAME

-20.5 M. DIA C-BAND TRANSMITTER ANTENNA GROUP
[.76 M PER SIDE TRIANGULAR BEAMS
FEED HORN SIZE: 4.51 M LONG * 2.54 M WIDE * 1.5 M DEPTH]

ORIGINAL PAGE IS
OF POOR QUALITY

SEE SHEET 2 ZONE 25-30 FOR TYPICAL DETAIL

18

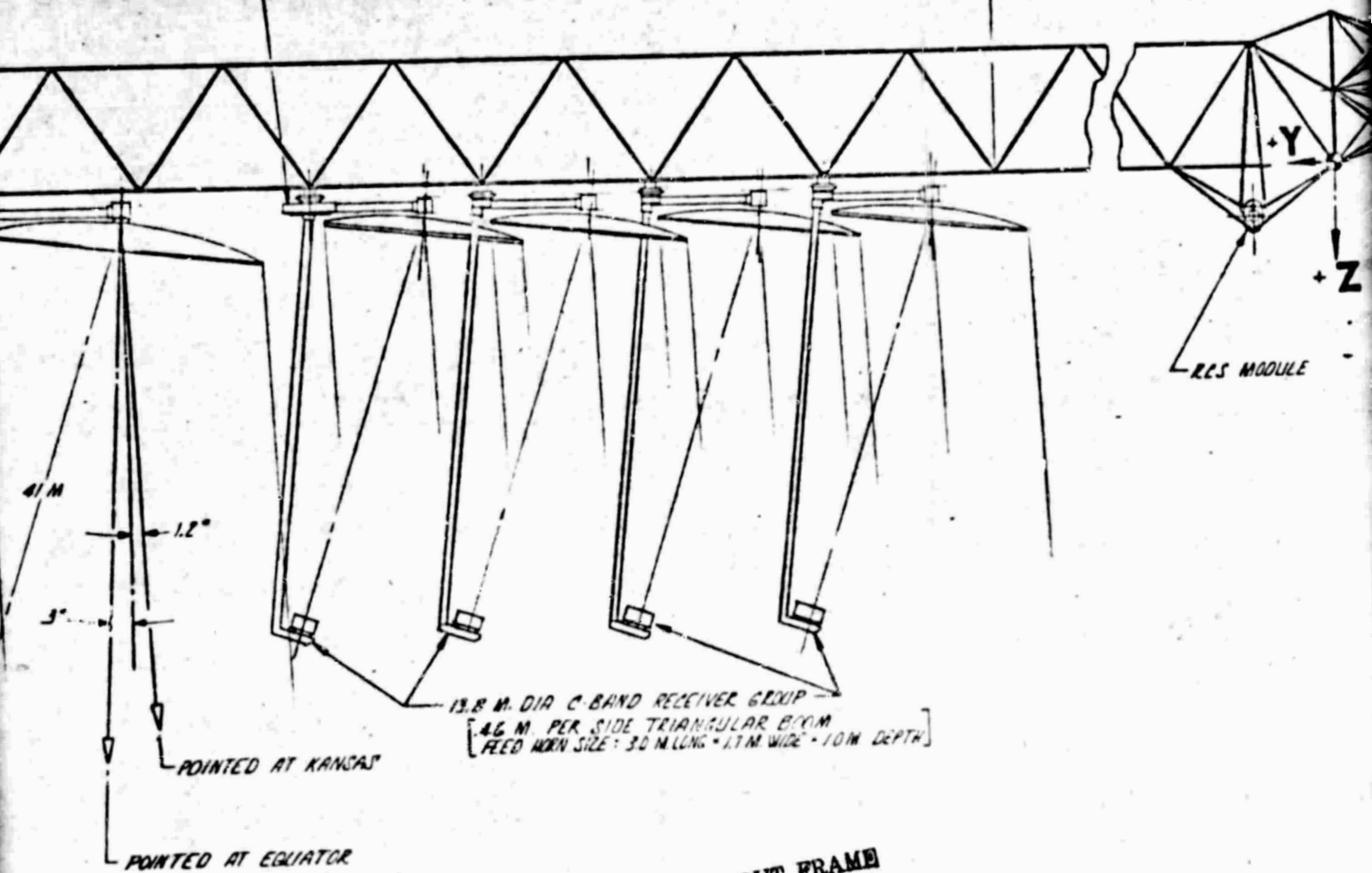
17

16

12.0 M = 240 M

STRUCTURE ALLOCATED FOR
FUTURE GROWTH
(4 BAYS @ 12 M = 48 M)

4.0 GHz & 6.0 GHz RF SIGNAL INTERFACE BOX



ORIGINAL PAGE IS MOLDOUT FRAME
OF POOR QUALITY

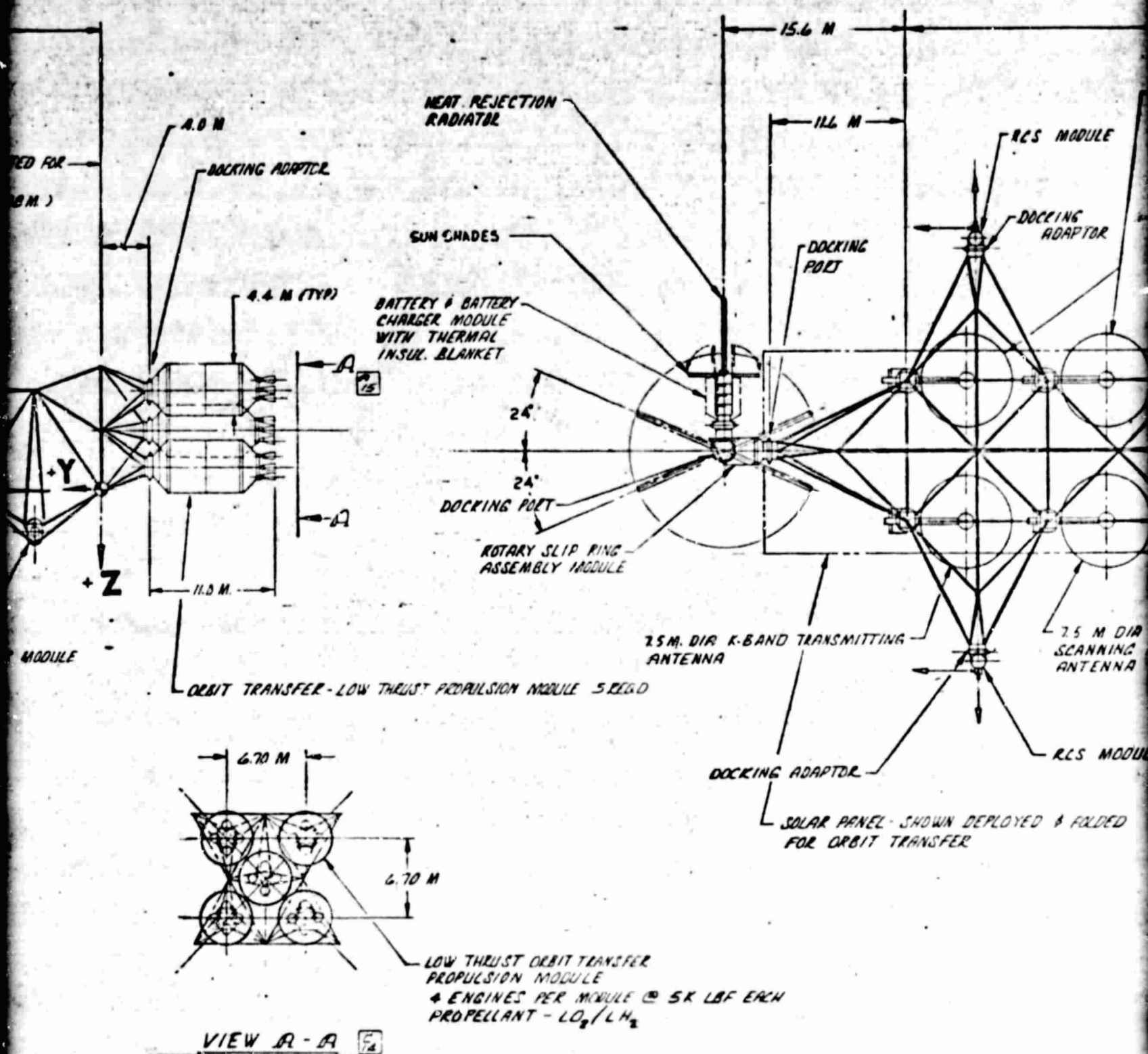
42662-25

1

18

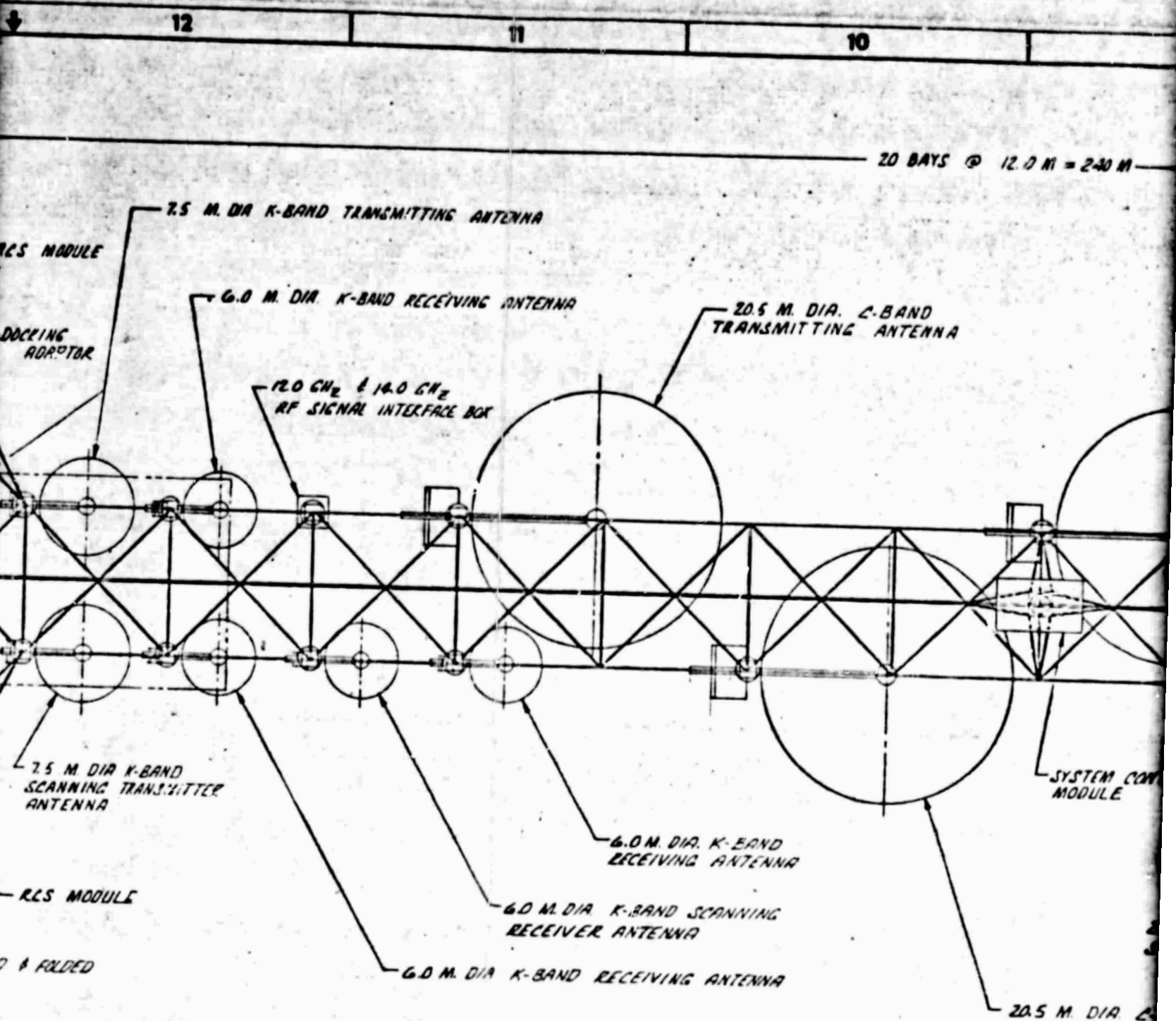
17

16



ORIGINAL PAGE IS
OF POOR QUALITY

FOLDOUT FRAME

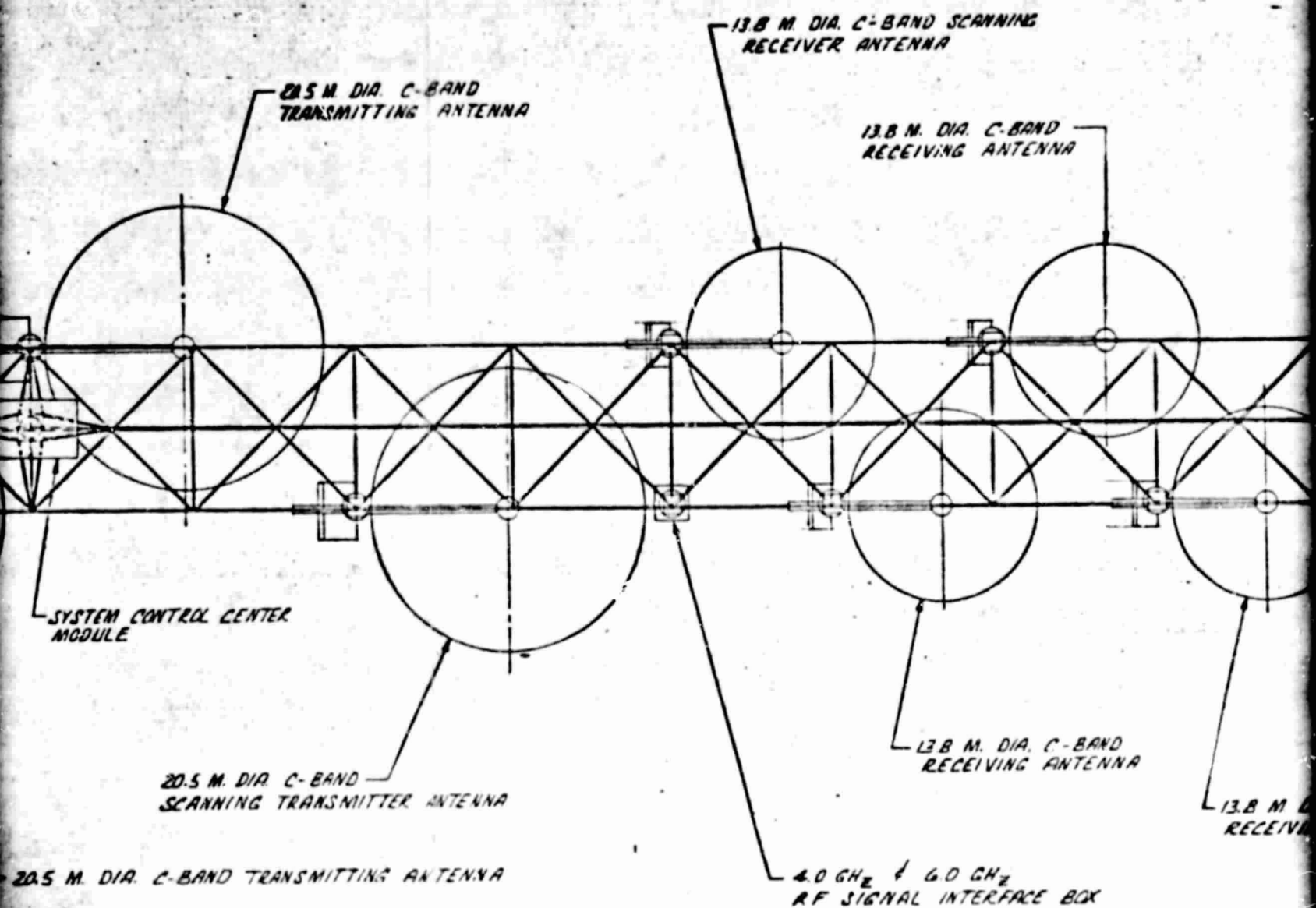


ORIGINAL PAGE IS
OF POOR QUALITY

WITHOUT FRAME
5

42662

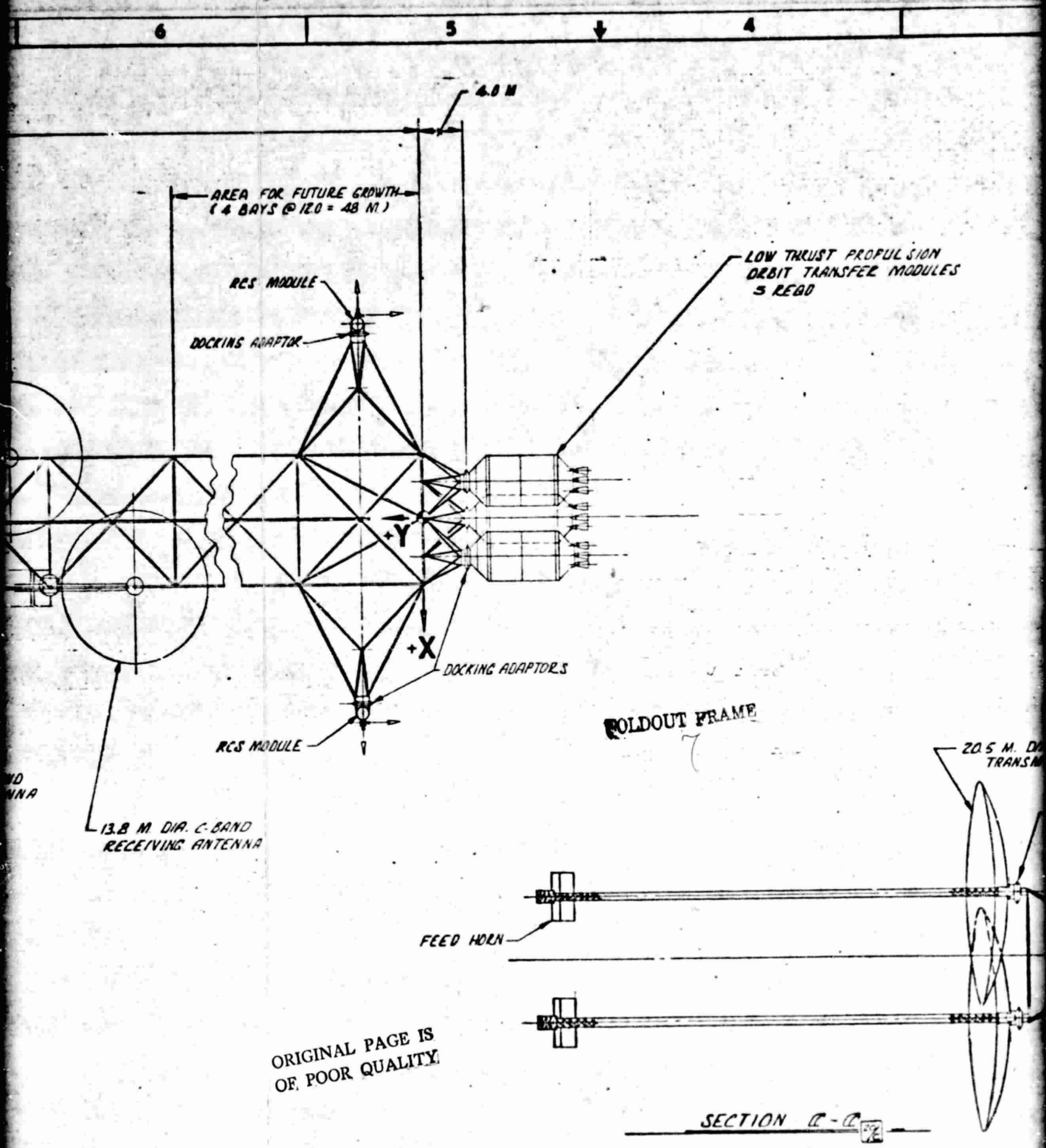
9 8 7 6
M = 240 M

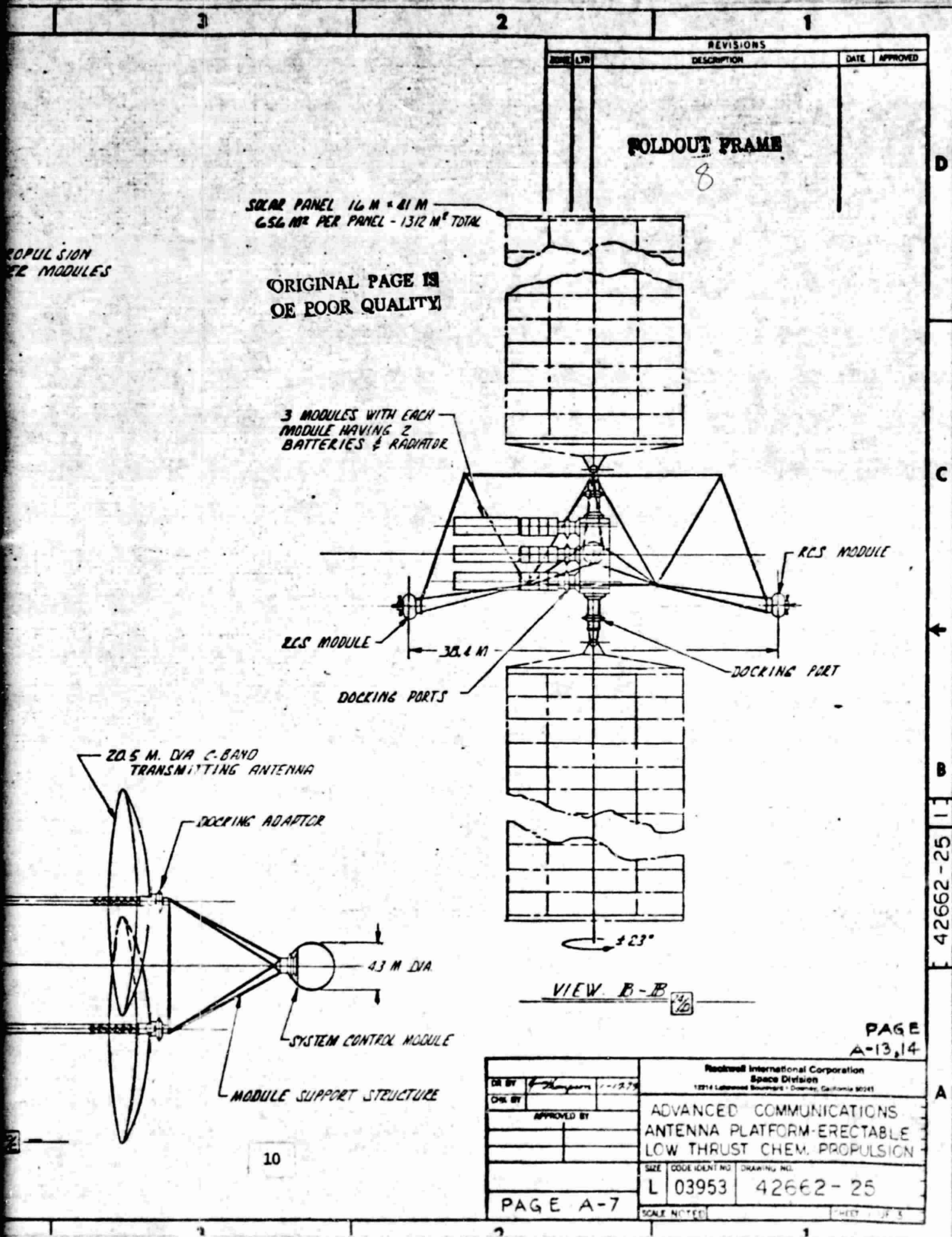


ORIGINAL PAGE IS
OF POOR QUALITY

FOLDOUT FRAME
6

42662-75

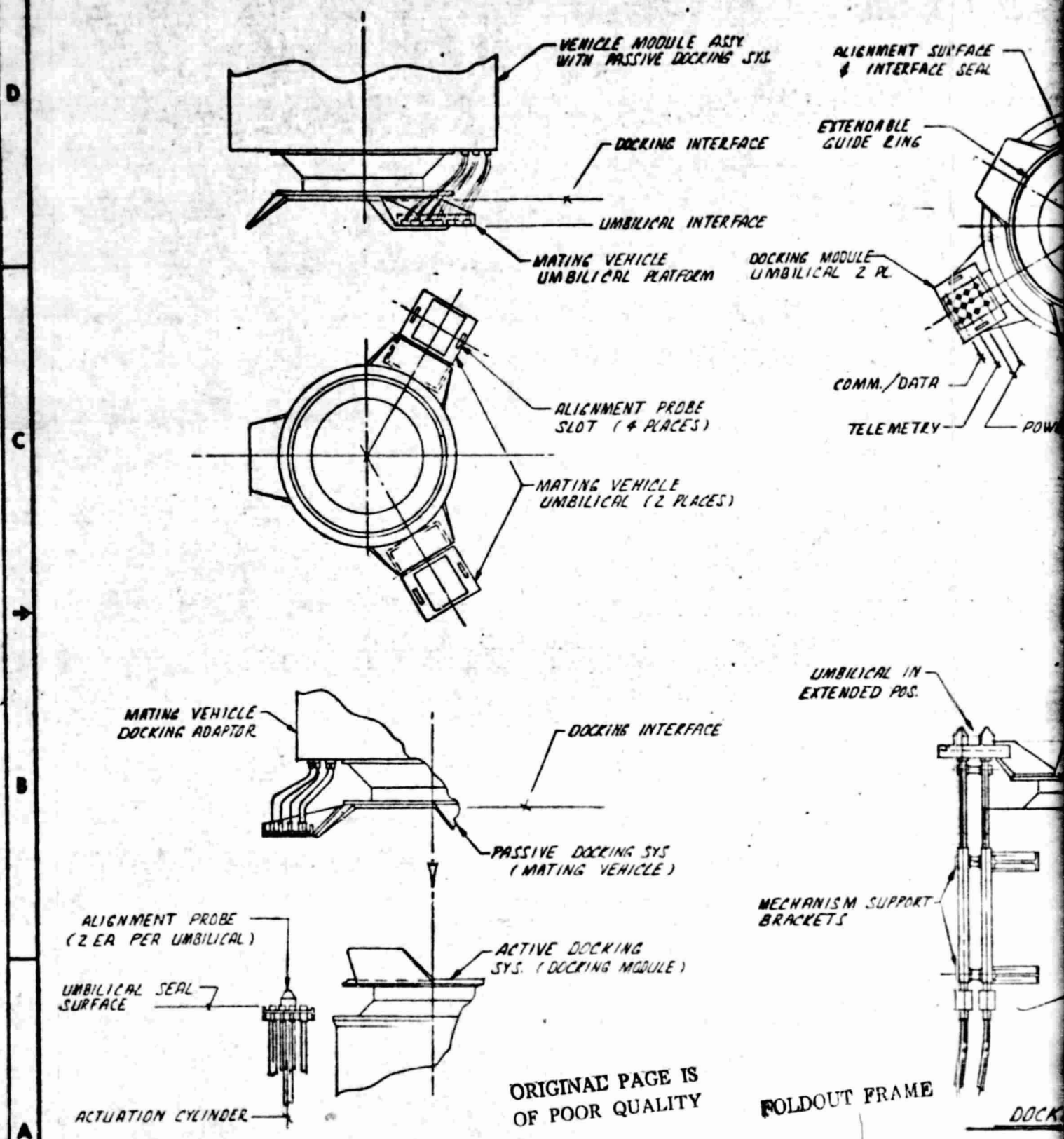




PAGE
A-13,14

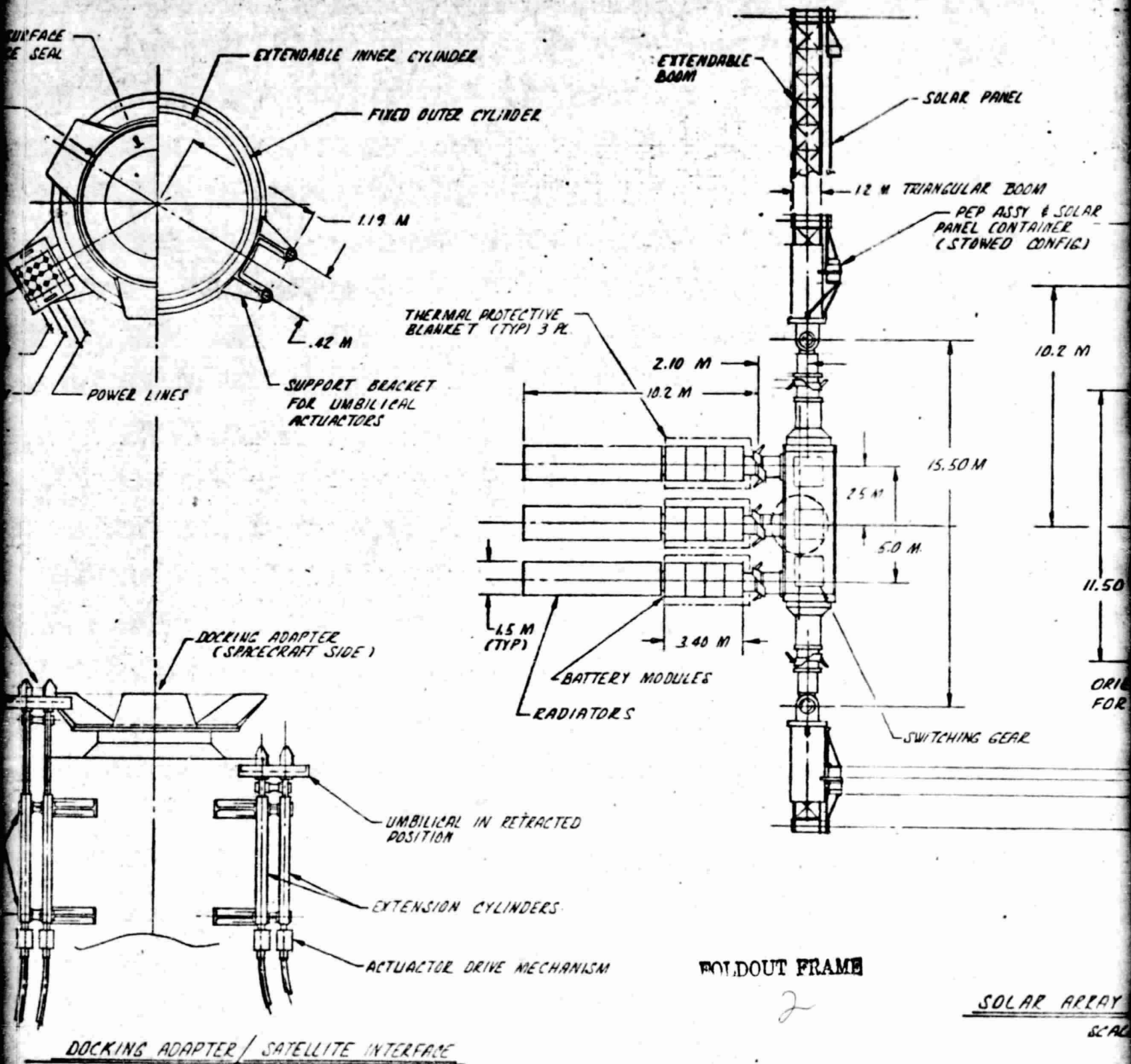
DR BY <i>[Signature]</i> 1-1-79 CHK BY APPROVED BY		Rockwell International Corporation Space Division 12714 Lathrop Avenue - Downey, California 90241	
PAGE A-7		ADVANCED COMMUNICATIONS ANTENNA PLATFORM-ERECTABLE LOW THRUST CHEM. PROPULSION	
SIZE L	CODE IDENT NO 03953	DRAWING NO. 42662-25	
SCALE NOTED		SHEET 1 OF 1	

S-500-52

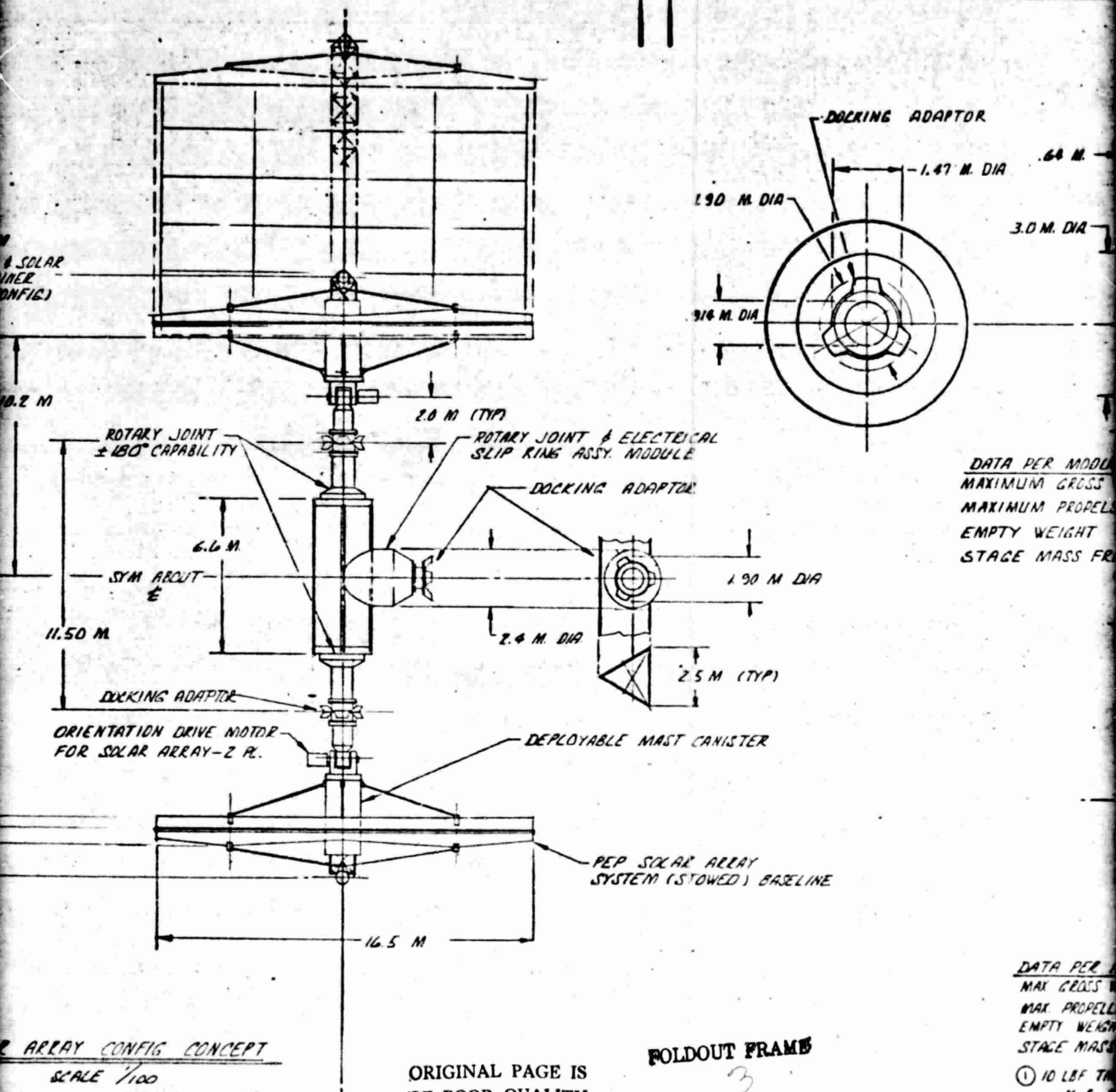


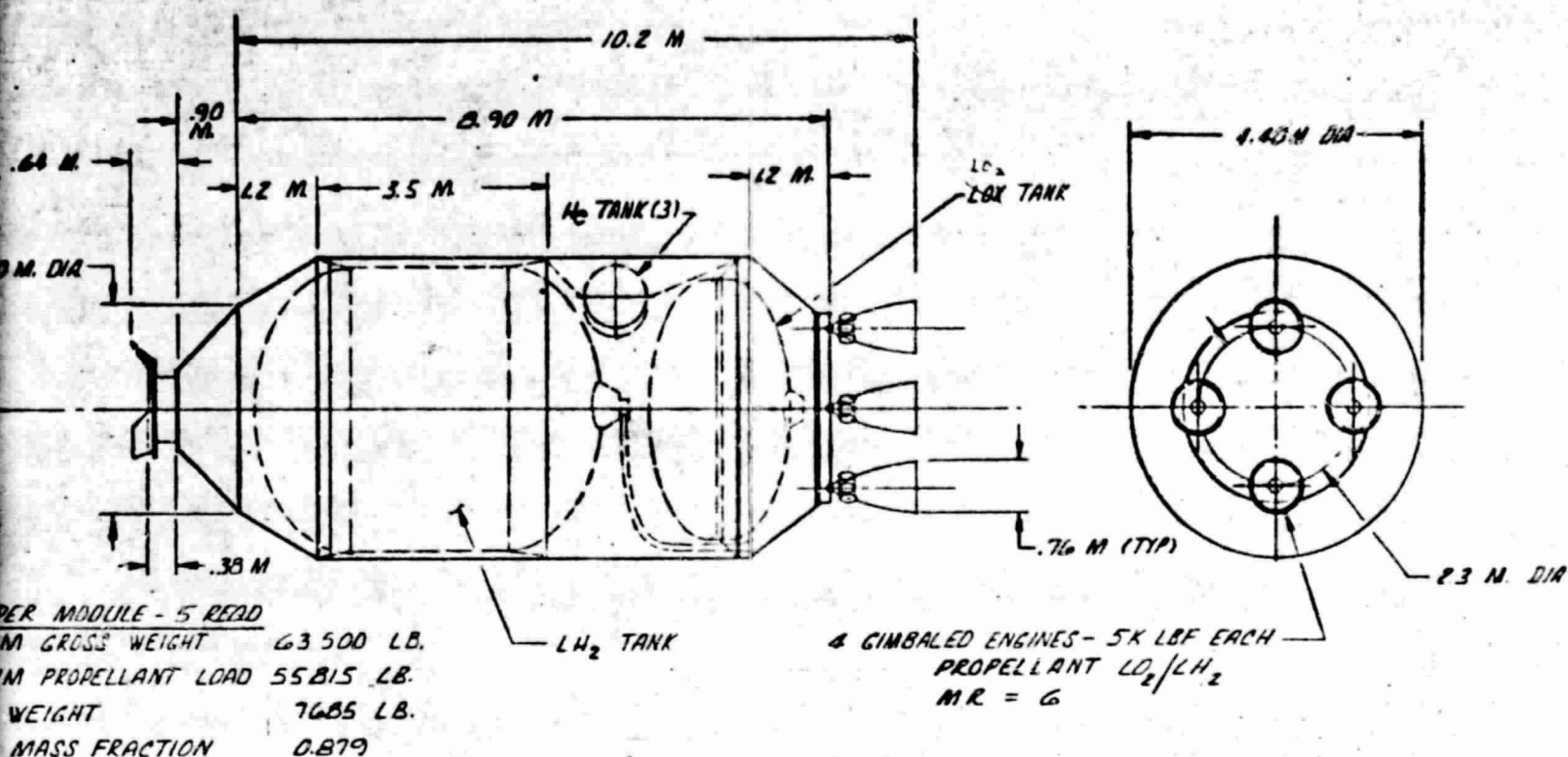
ORIGINAL PAGE IS
OF POOR QUALITY

DOCKING INTERFACE-UTILITIES CONCEPT



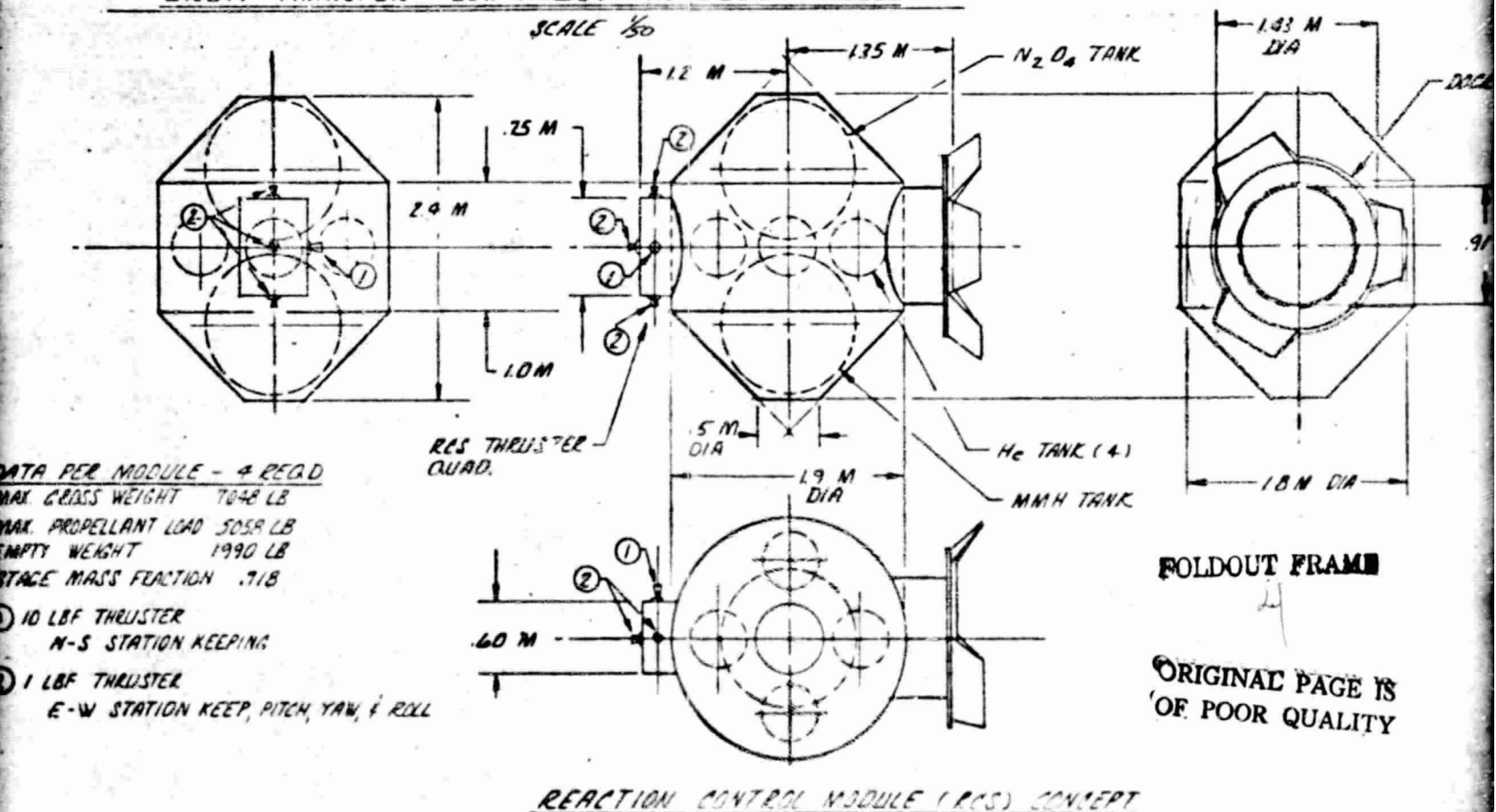
ORIGINAL PAGE IS
 OF POOR QUALITY

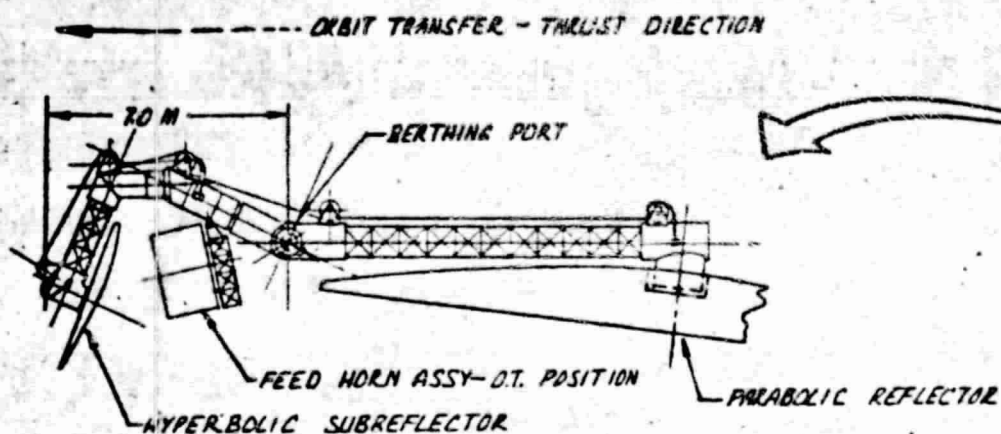




ORBIT TRANSFER - LOW THRUST PROPULSION MODULE

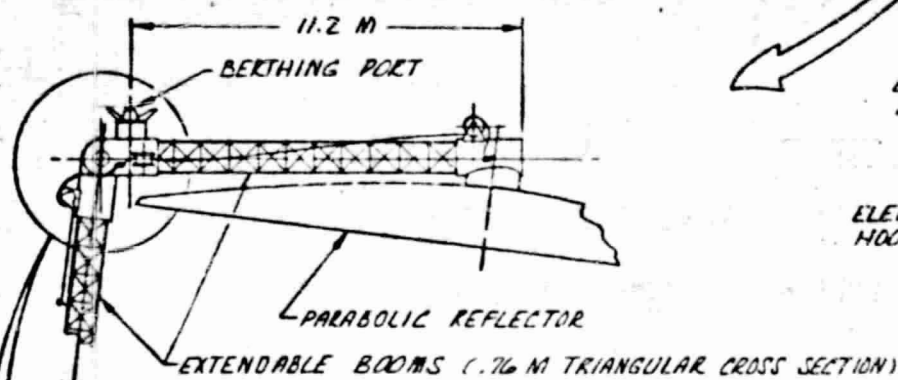
SCALE 1/50





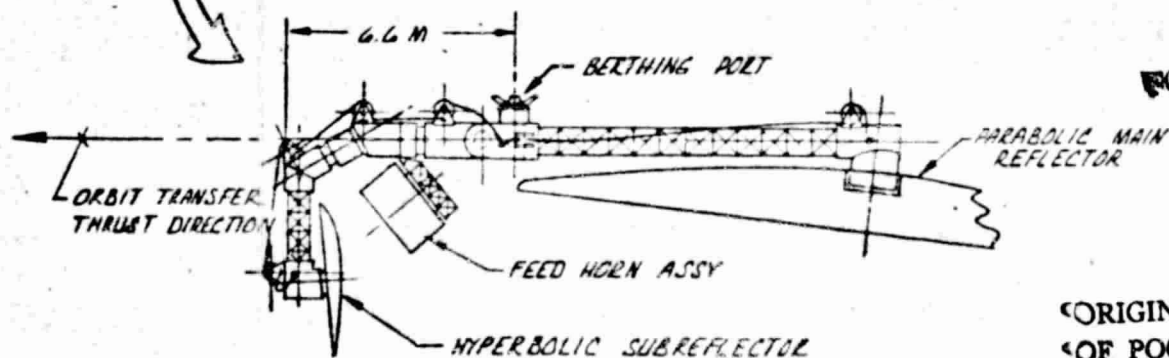
CASSEGRAIN ANTENNA CONFIG - ORBIT TRANSFER MODE

[CONFIG SHOWN ABOVE CAN BE USED ON STRUCTURAL CONCEPT REFLECTED ON DWG 42662-26 SHEET NO.1]



ALTERNATE - ANTENNA BERTHING PORT CONFIG

[CONFIG SHOWN ABOVE CAN BE USED ON STRUCTURAL CONCEPT REFLECTED ON DWG 42662-25 SHEET NO.1]



OPTIONAL CONFIGURATION

SHUTTLE
FOLDOUT FRAME
PAYLOAD

ORIGINAL PAGE IS
OF POOR QUALITY

CASSEGRAIN ANTENNA CONFIG - ORBIT TRANSFER MODE

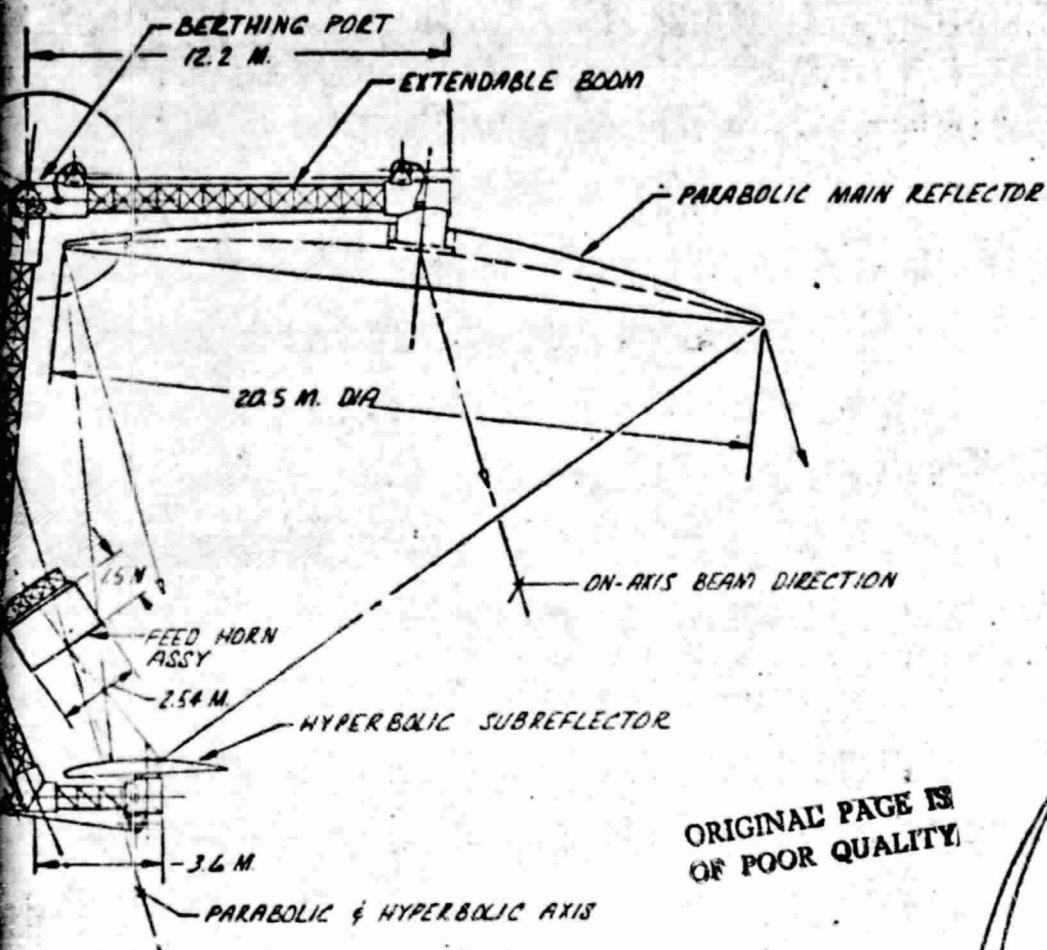
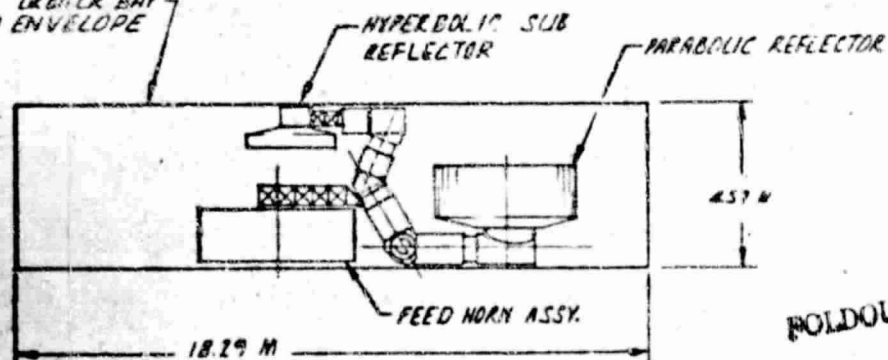


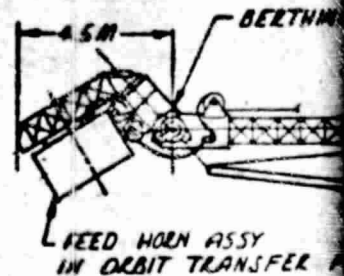
FIGURE 1 - DEPLOYED CASSEGRAIN ANTENNA CONCEPT
SCALE 1/100

SMALL ORBITER BAY
LOAD ENVELOPE

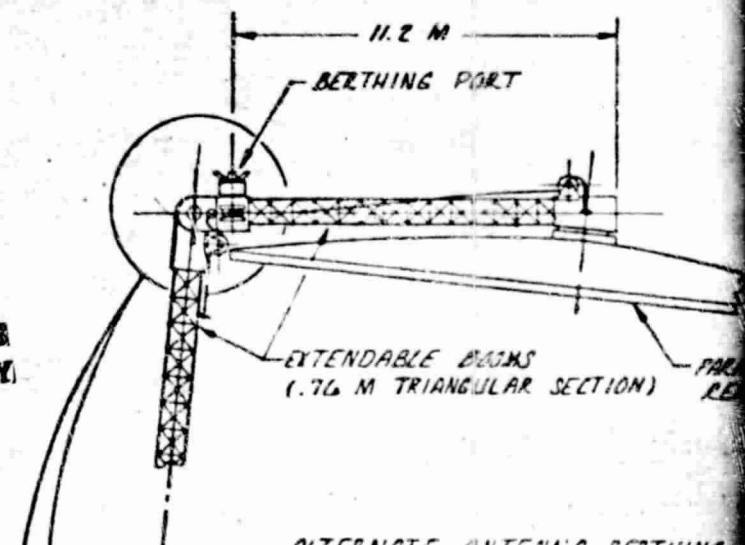


FOLDED & STOWED CASSEGRAIN ANTENNA CONFIG

--- ORBIT TRANSFER

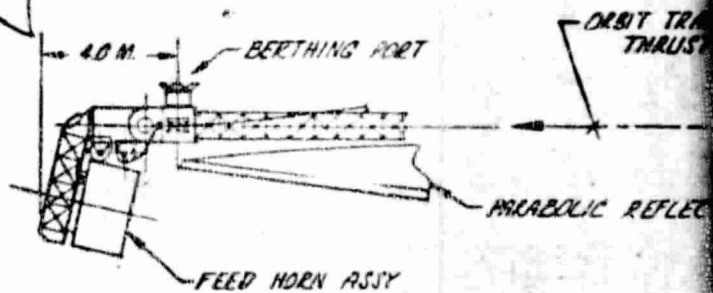


ANTENNA CONFIG-
CONFIG SHOWN ABOVE
CONCEPT REFLECTED ON



ALTERNATE-ANTENNA BERTHING
CONFIG SHOWN ABOVE TO BE USED ON STRUCTURE
REFLECTED ON DWG 42662-25 SHEET 1

FOLDOUT FRAME



ANTENNA CONFIG-ORBIT TRANSFER MODE

TRANSFER - THRUST DIRECTION

BERTHING PORT

REFLECTOR

TRANSFER POSITION

CONFIG - ORBIT TRANSFER MODE

IN ABOVE TO BE USED ON STRUCTURAL
SELECTED ON DWG 42662-26 SH. 1PARABOLIC
REFLECTORBERTHING PORT CONFIG.
IN STRUCTURAL CONCEPT
SHEET 1ORBIT TRANSFER
THRUST DIRECTION

REFLECTOR

ORIGINAL PAGE IS
OF POOR QUALITY

MODE

IDLER REEL

18.2 M.

BERTHING PORT

EXTENDABLE BOOM

REFLECTOR

TAKE-UP REELS
FOR ELECTRICAL
CABLES

20.5 M. DIA

ANTENNA/HORN
ELECTRICAL
CABLE HOOKUP
LEADS

42.7 M

FOLDOUT FRAME

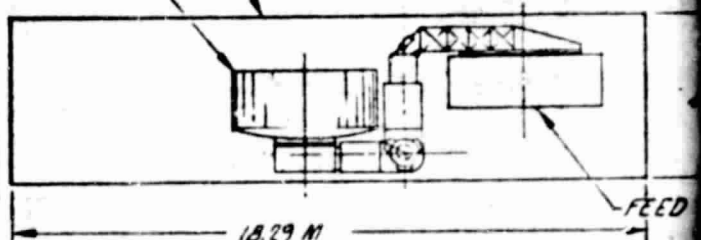
NOTE: FEED HORN & REFLECTOR
ATTACHMENT INTERFACES CONT.
CAPABILITY OF ANTENNA SYS.
ALIGNMENT AND BORE SIGHT
ACCURACY

DEPLOYED OFF-SET FEED REFLECTOR ANTENNA CONCEPT

ANTENNA CONFIG SHOWN IS TYPICAL FOR ALL ANTENNAS REFLECTOR
ON SHEET NO. 1 EXCEPT FOR DIMENSIONAL DIFFERENCES

SHUTTLE ORBITER PAYLOAD BAY ENVELOPE

REFLECTOR

FOLDED & STORED CONFIG
SCALE 1/100

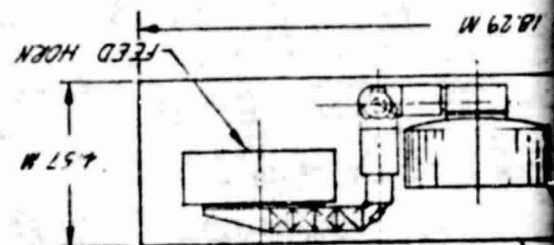
11

SCALE	L	03953	42662-25
DATE	0000	0000	0000

PAGE
A-15,16

POUTOUT FRAME

ORIGINAL PAGE IS
OF POOR QUALITY



SHUTTLE ORBITER PAYLOAD BAY ENVELOPE

IS TYPICAL FOR ALL ANTENNAS REFLECTED
FOR DIMENSIONAL DIFFERENCES

FEED REFLECTOR ANTENNA CONCEPT

NOTE: FEED HORN & REFLECTOR SUPPORT
ATTACHMENT INTERFACES CONTAIN THE
CAPABILITY OF ANTENNA SYSTEM
ALIGNMENT AND BORE SIGHT POINTING
ACCURACY

REFLECTOR

BOOM

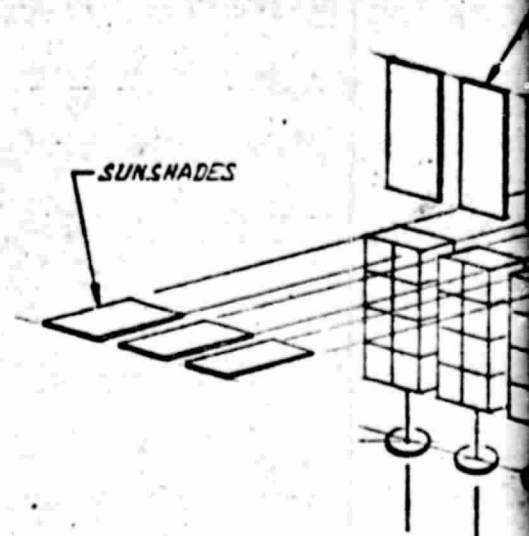
REVISIONS	DATE	APPROVED

72

71

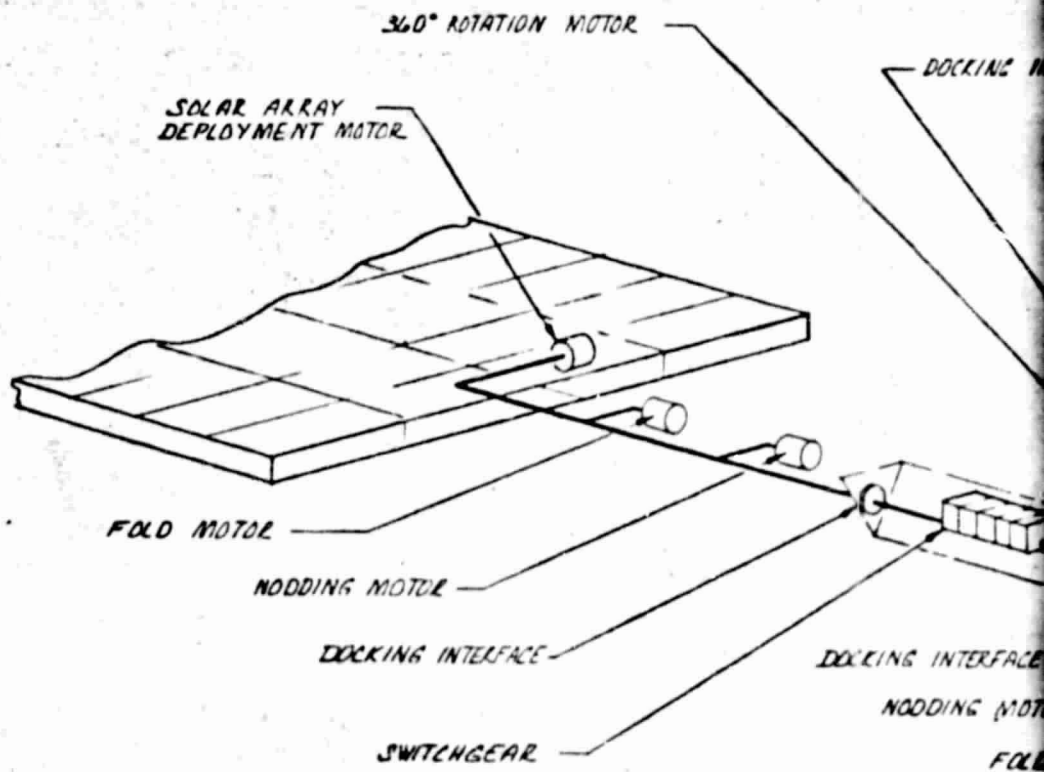
70

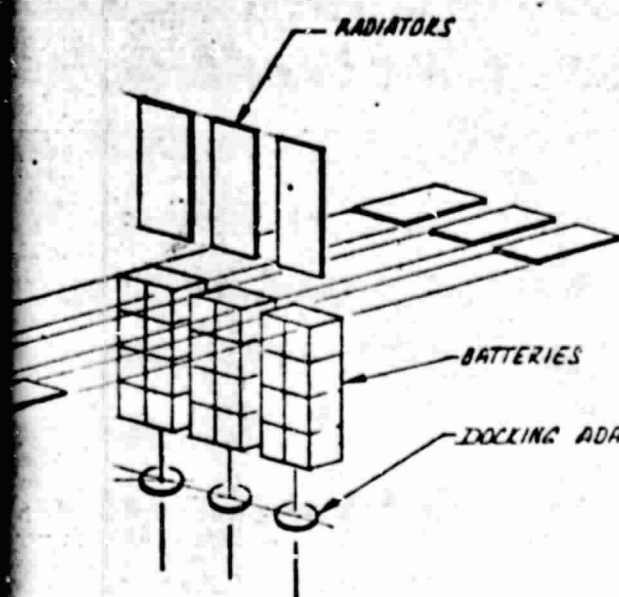
AC-520000



ORIGINAL PAGE IS
OF POOR QUALITY

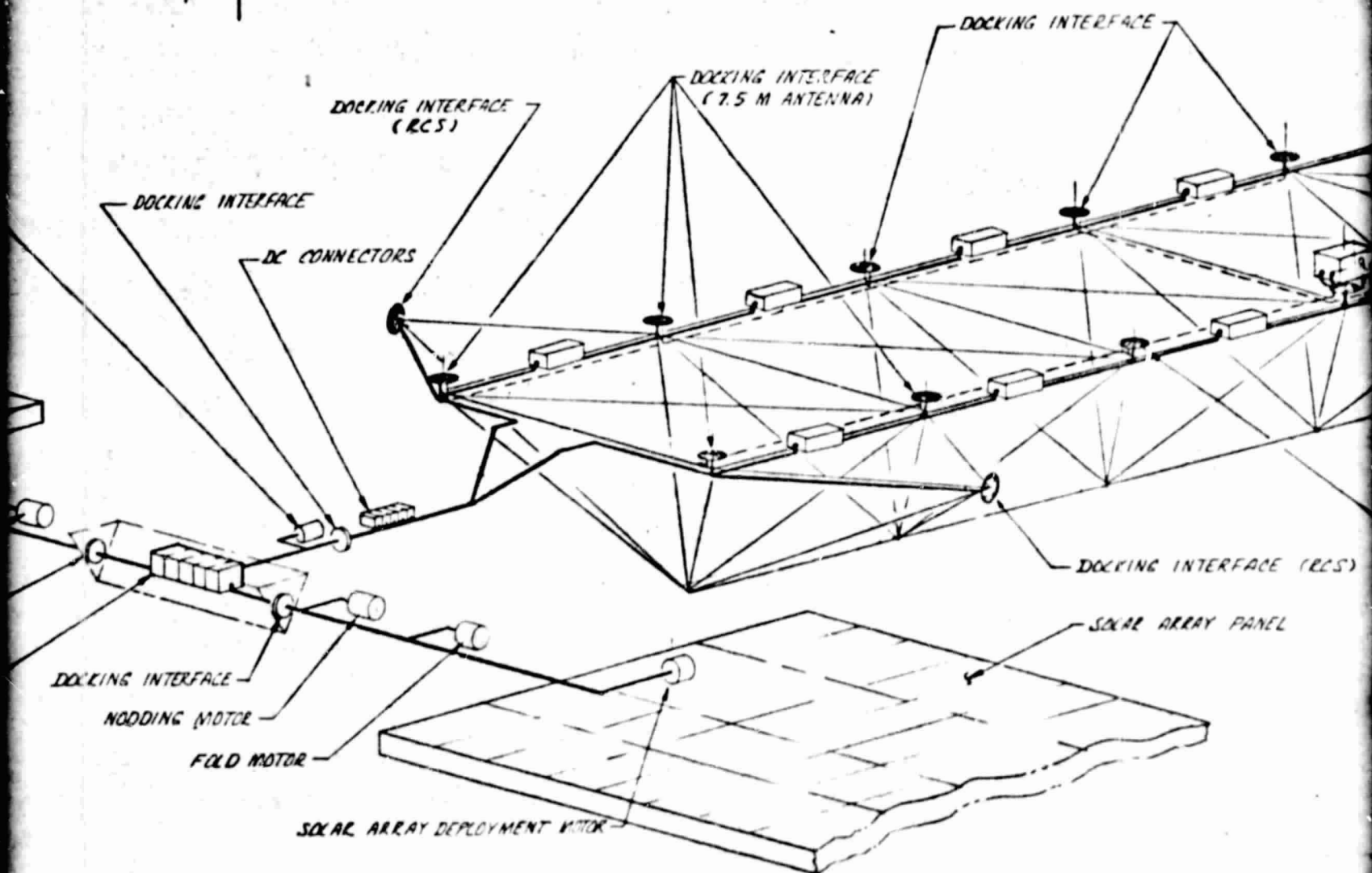
FOLDOUT FRAME

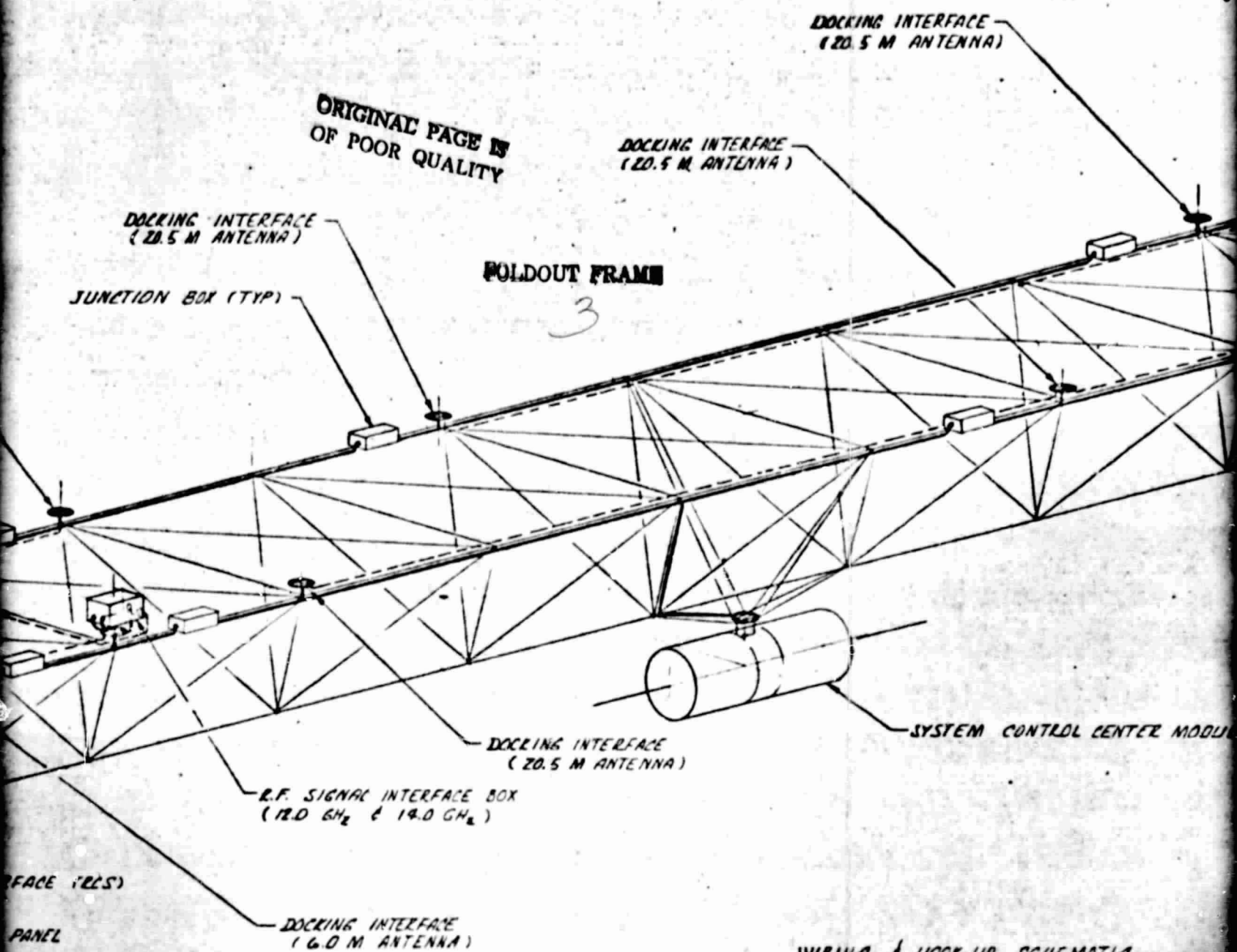




FOLDOUT FRAME

2

ORIGINAL PAGE IS
OF POOR QUALITY



**DOCKING INTERFACE -
(20.5 M ANTENNA)**

ORIGINAL PAGE IS
OF POOR QUALITY

**DOCKING INTERFACE -
(20.5 M ANTENNA)**

**DOCKING INTERFACE
(20.5 M ANTENNA)**

FOLDOUT FRAME

JUNCTION BOX (TYP)

DOCKING INTERFACE
(20.5 M ANTENNA)

-SYSTEM CONTROL CENTER MODUL

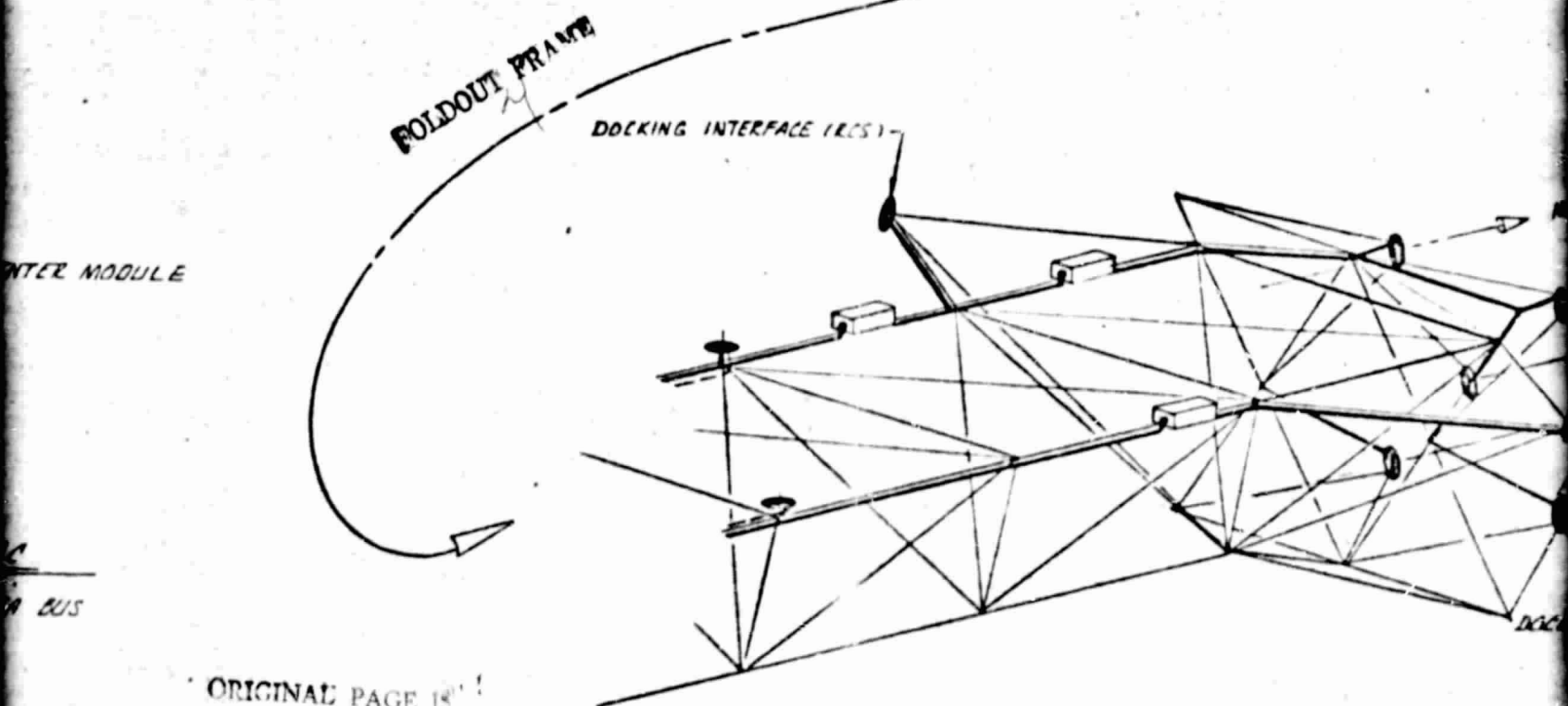
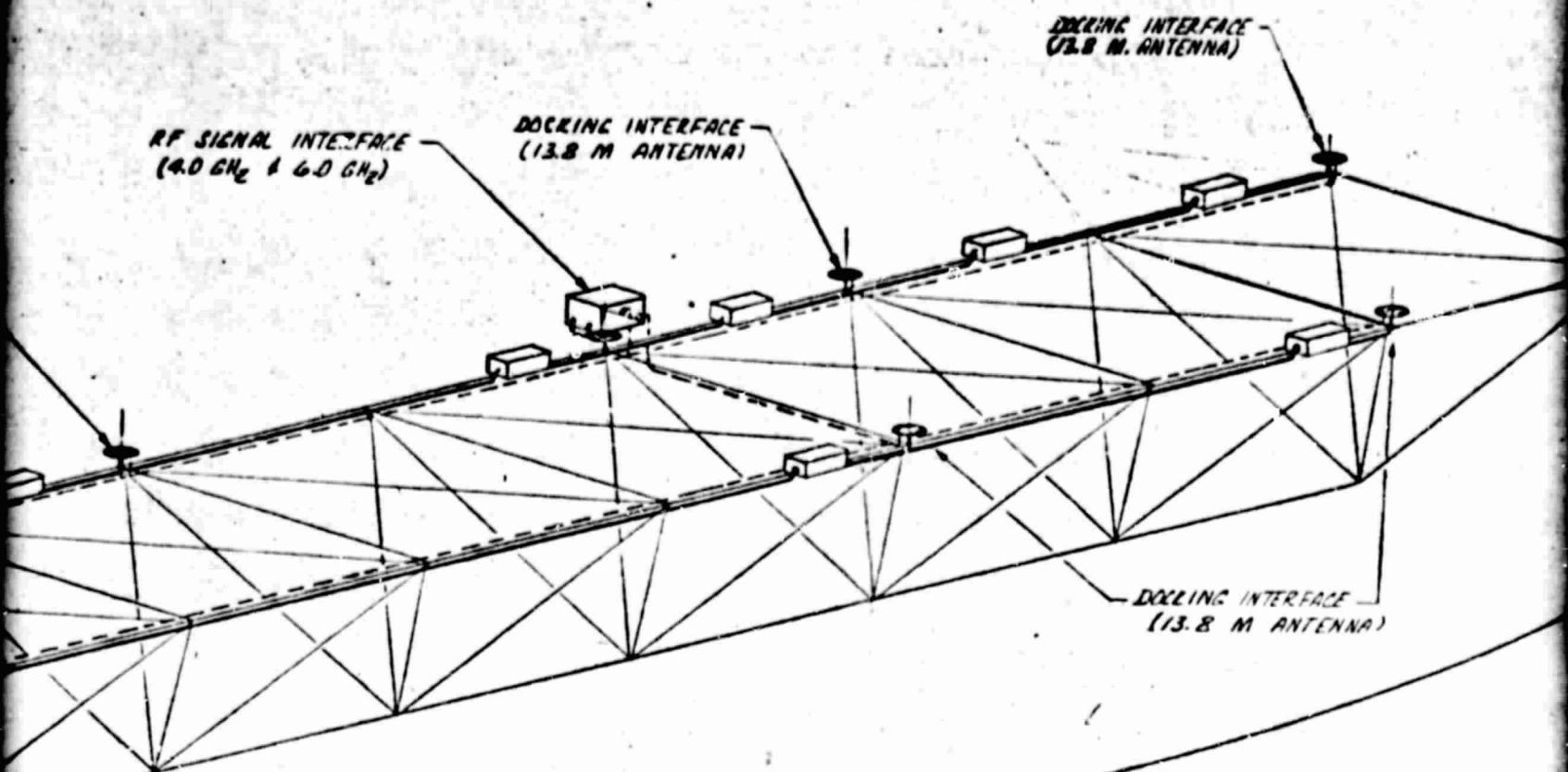
-R.F. SIGNAL INTERFACE BOX
(12.0 GHz & 14.0 GHz)

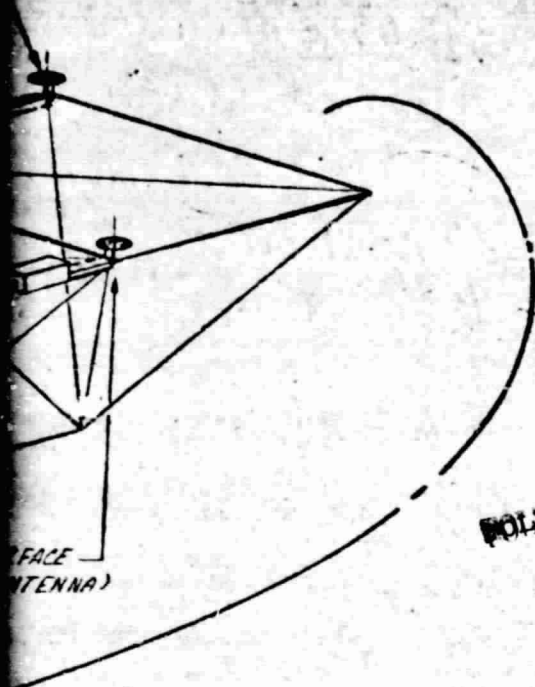
DOCKING INTERFACE
(6.0 M ANTENNA)

WIRING & HOOK-UP SCHEMATIC

POWER LINES & DATA BUS

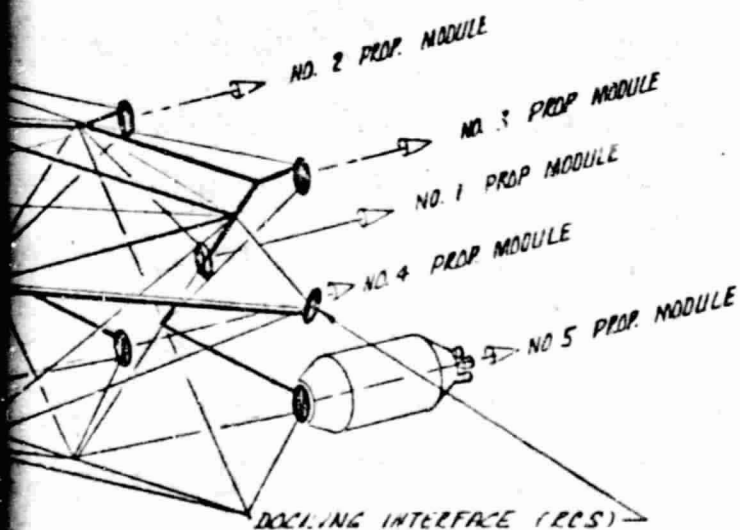
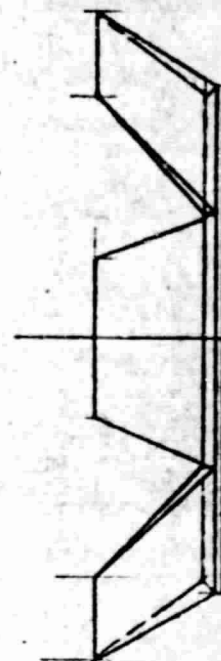
--- R.F. LINES

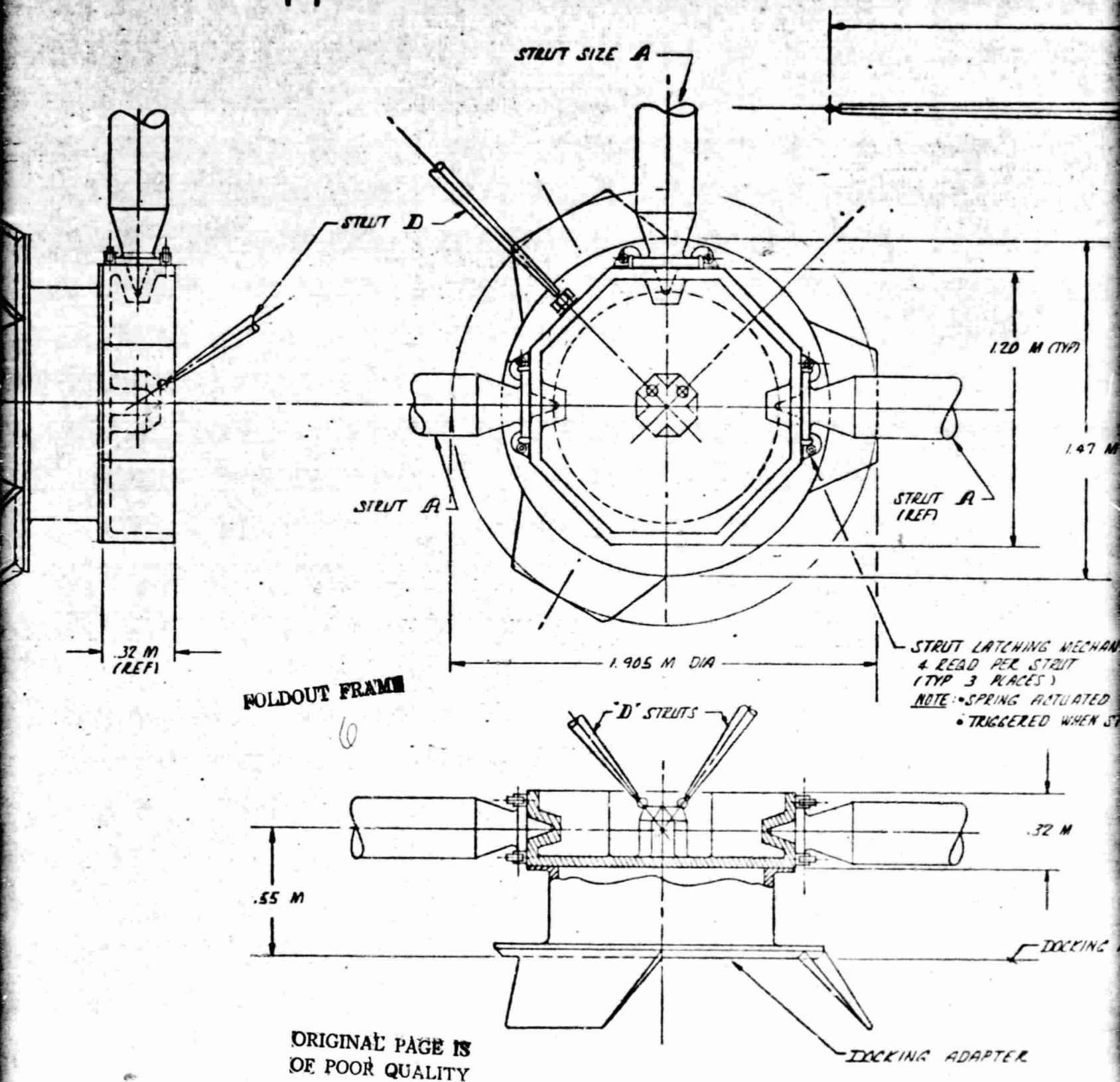




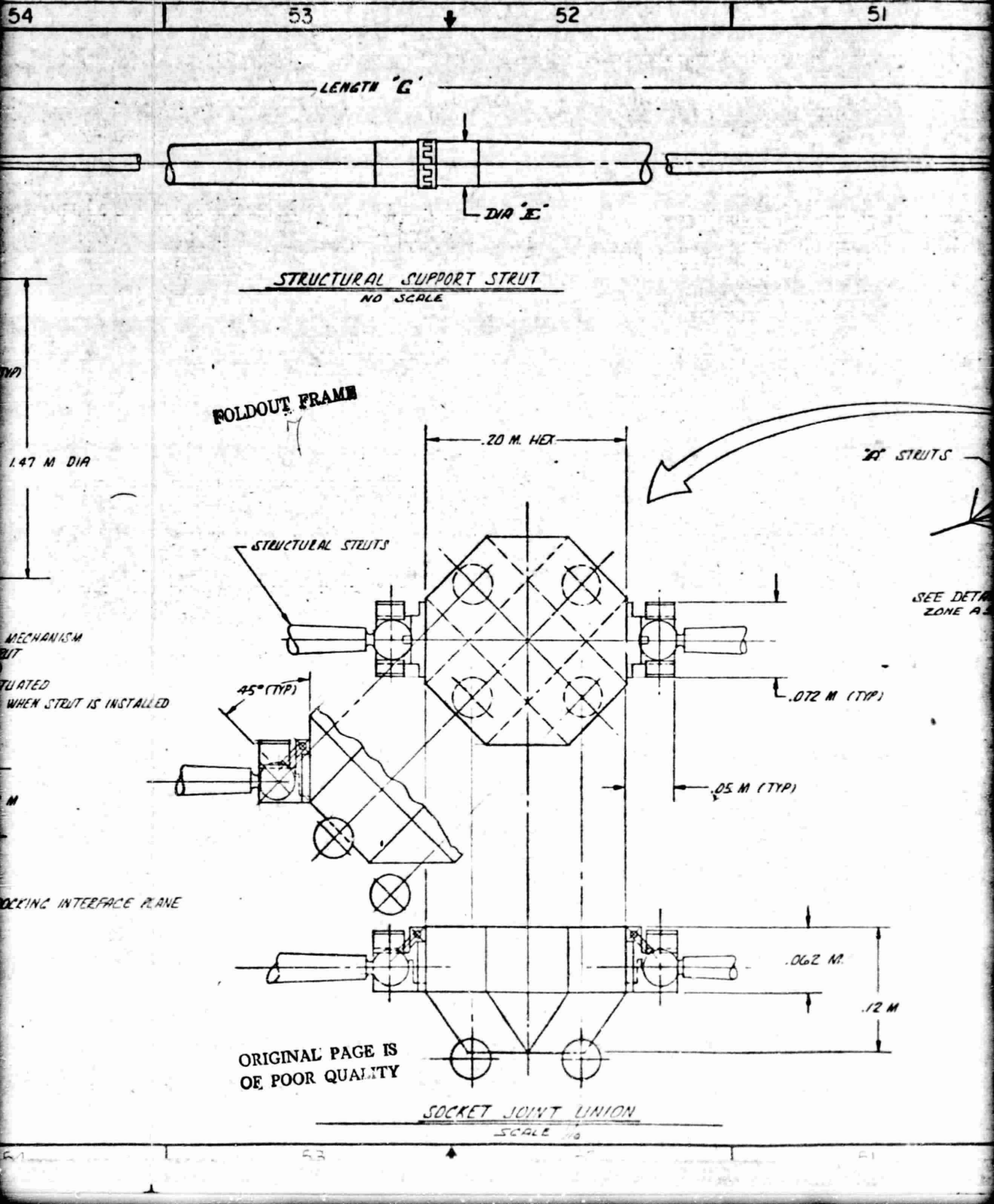
FOLDOUT FRAME
5

ORIGINAL PAGE IS
OF POOR QUALITY





DETAIL B - MOMENT JOINT CONCEPT



51

50

49

REVISIONS

ZONE LTR

DESCRIPTION

DATE

APPROVED

DIA F

C STRUTS

B STRUTS

A STRUTS

D STRUTS

A STRUTS

SEE DETAIL H
ZONE A SE

STRUCTURAL PLATFORM (ISOMETRIC VIEW)

NO SCALE

STRUT	LENGTH G	DIA E	DIA F	WALL THICKNESS
A	120 M	.30 M	.24 M	.0012 M
B	120 M	.44 M	.22 M	.0009 M
C	120 M	.19 M	.098 M	.0006 M
D	16.97 M	.19 M	.098 M	.0006 M

NOTE: STRUT MATL: GRAPHITE EPOXY

FOLDOUT FRAME

8

ORIGINAL PAGE IS
OF POOR QUALITY

PAGE A-17,18

12

BOX	CODE IDENT NO	DRAWING NO
L	03953	42FE2-25
SCALE		

D

C

B

3

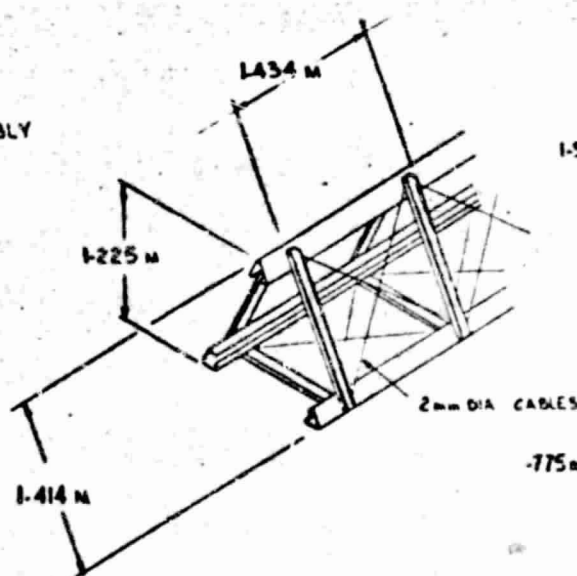
42662-25

A

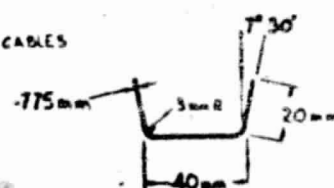
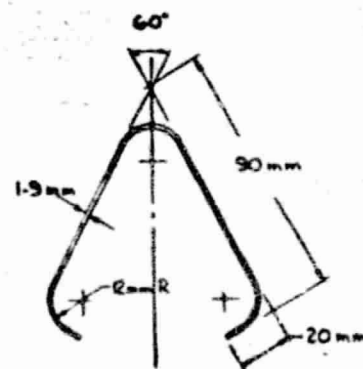
FOLDOUT FRAME

ORIGINAL PAGE IS
OF POOR QUALITY

ASSEMBLY



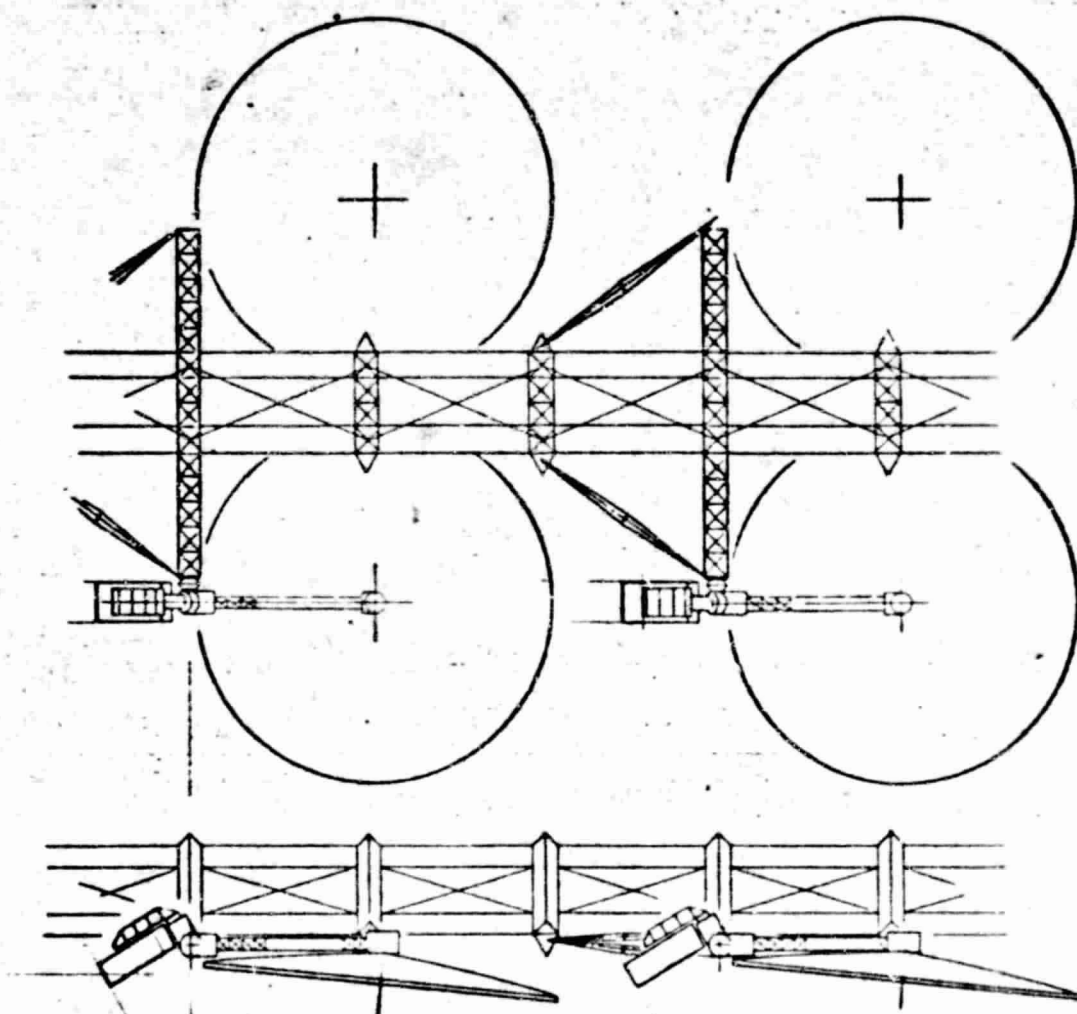
CAP MEMBER



CROSS MEMBER

BEAM GEOMETRY

MATERIAL: GRAPHITE EPOXY



VIEWS SHOWING 20.5 M ANTENNAS
IN ORBIT TRANSFER CONFIGURATION

FOLDOUT FRAME

2

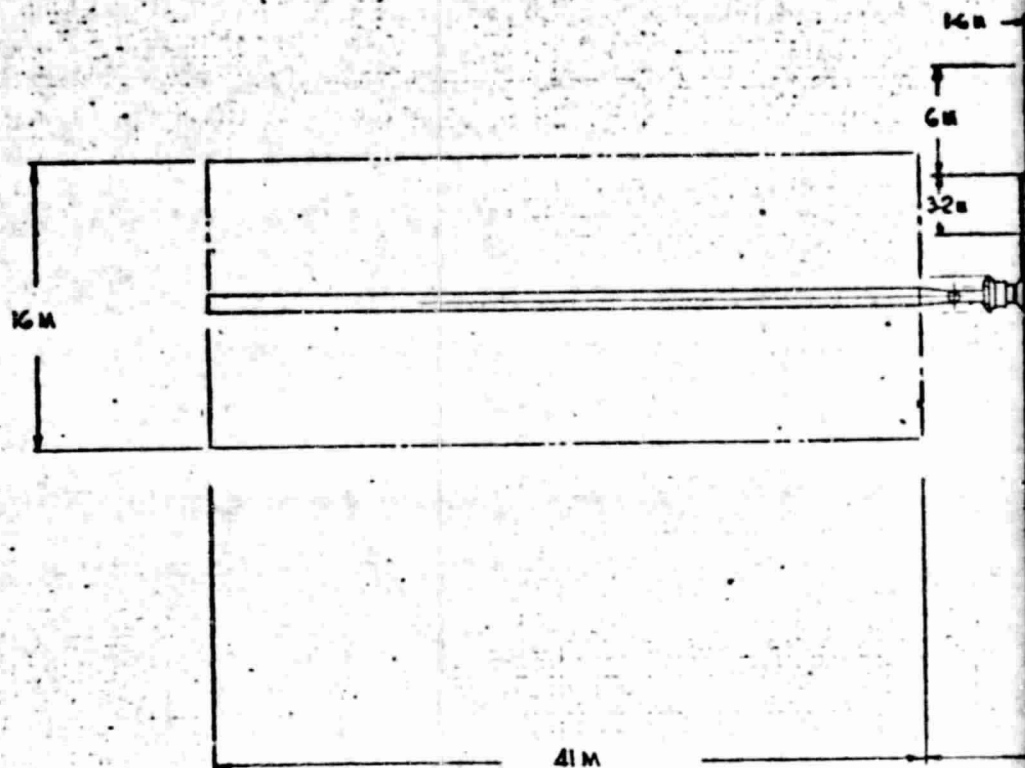
ORIGINAL PAGE IS
OF POOR QUALITY

18

17

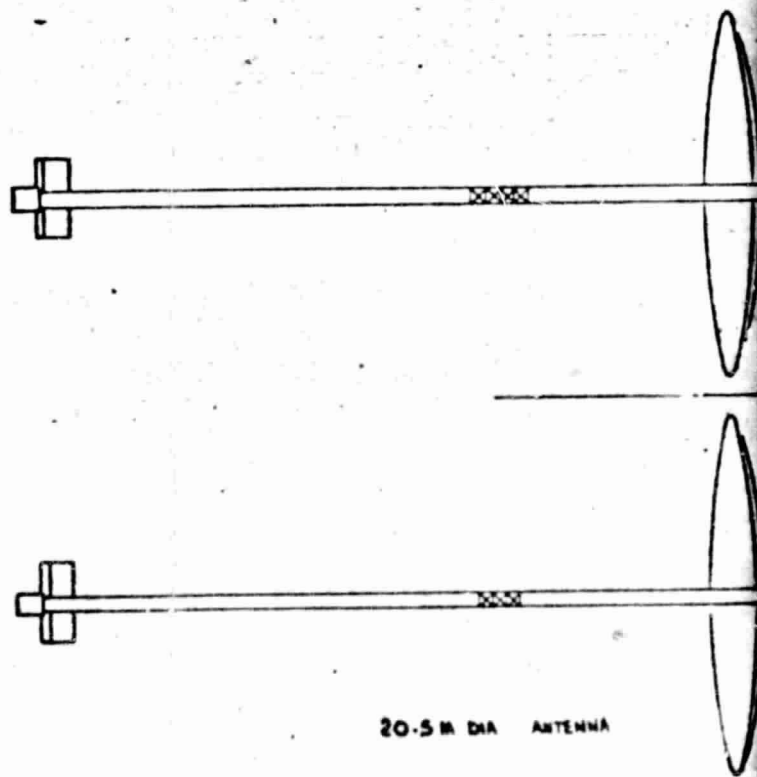
16

15



FOLDOUT FRAME

3

ORIGINAL PAGE IS
OF POOR QUALITY

20.5 M DIA ANTENNA

42662-26

1

15

14

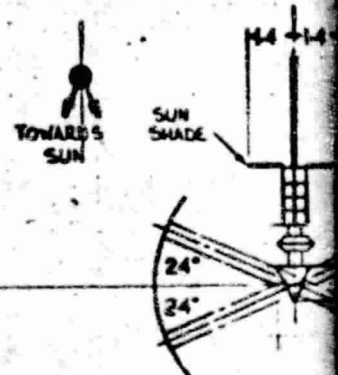
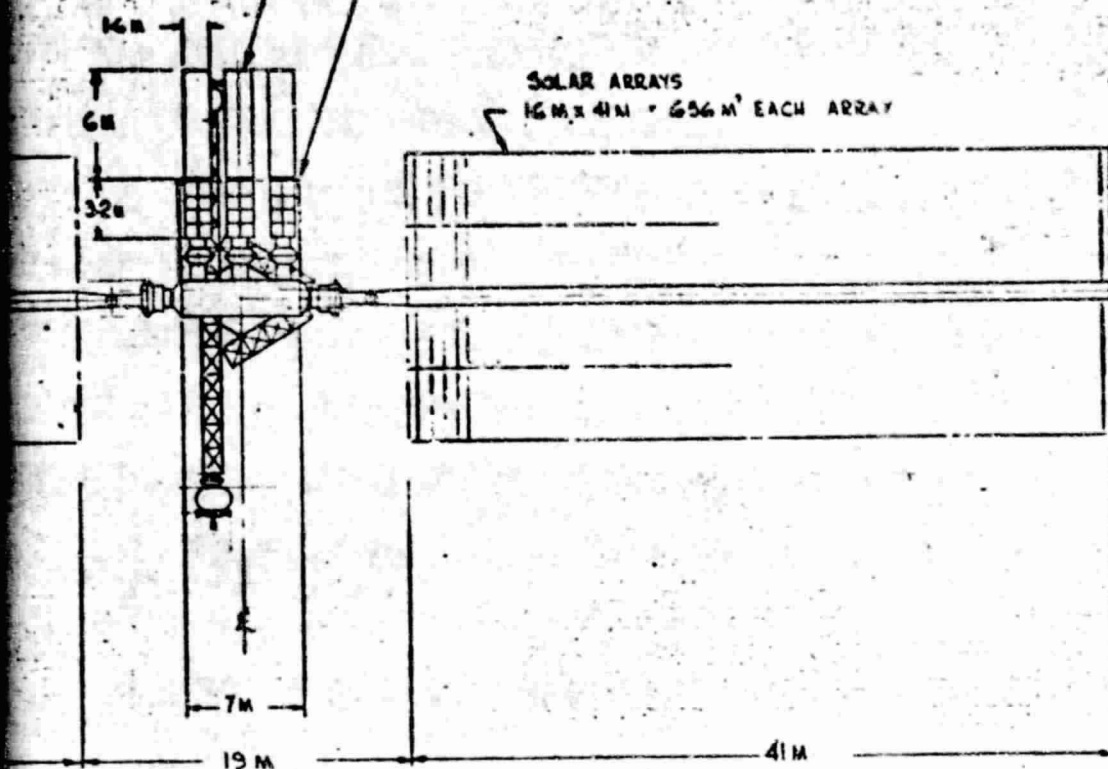
13

12

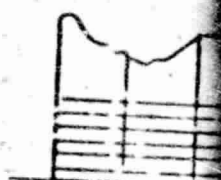
3 MODULES EACH CONTAINING
2 BATTERIES & A RADIATOR

THERMAL INSULATION &
METEORITE PROTECTION

SOLAR ARRAYS
16M x 41M = 656 M² EACH ARRAY



DC CONVERT



South

SOLAR ARRAY
SWITCHGEAR

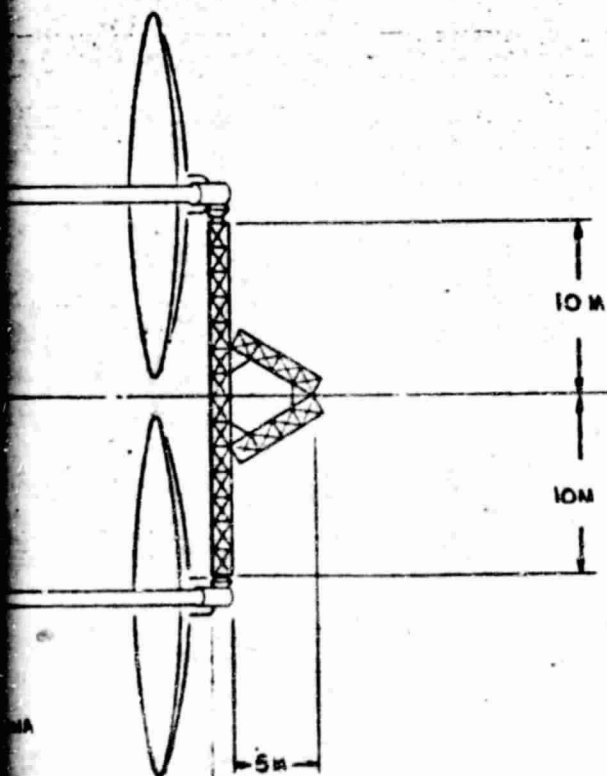
7.5M

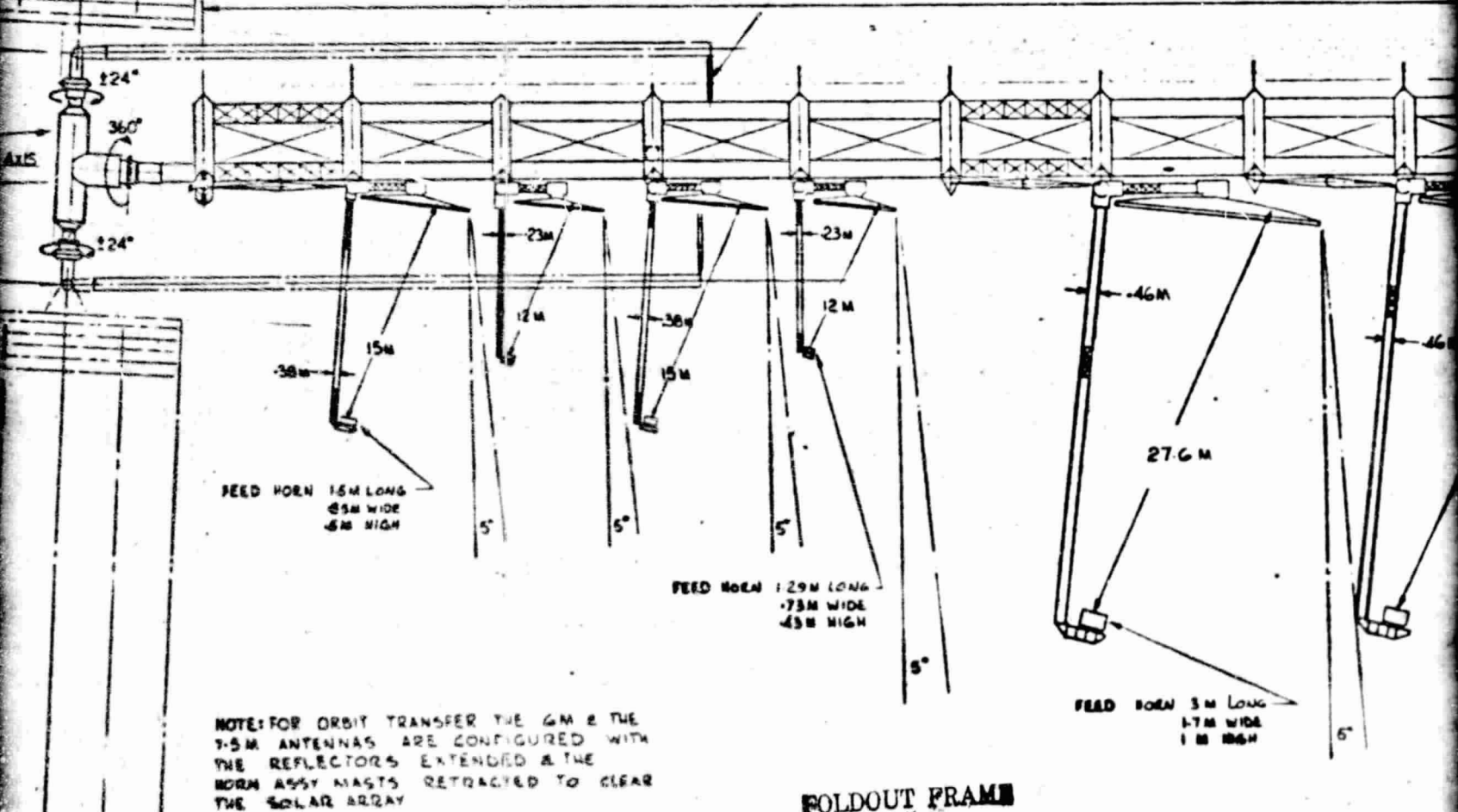
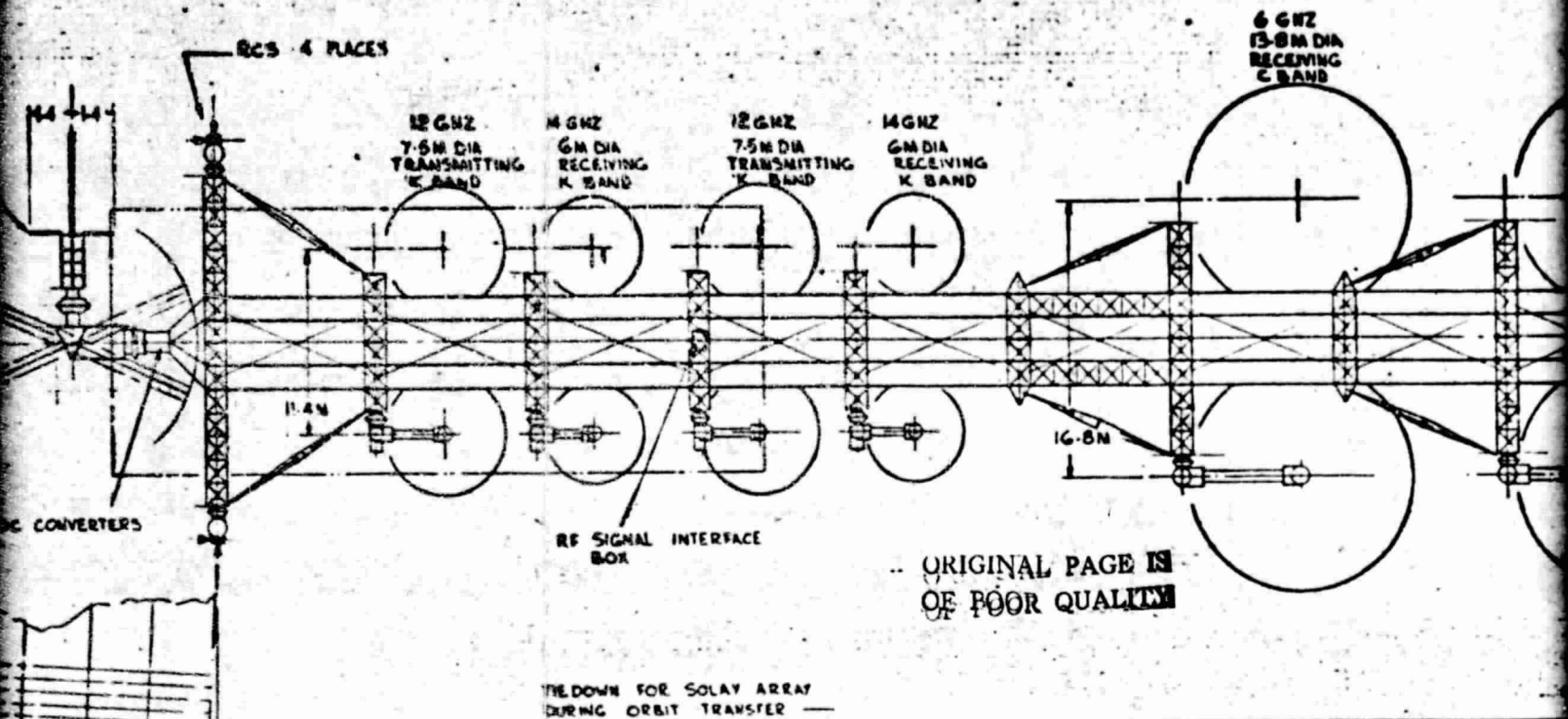
2.5M

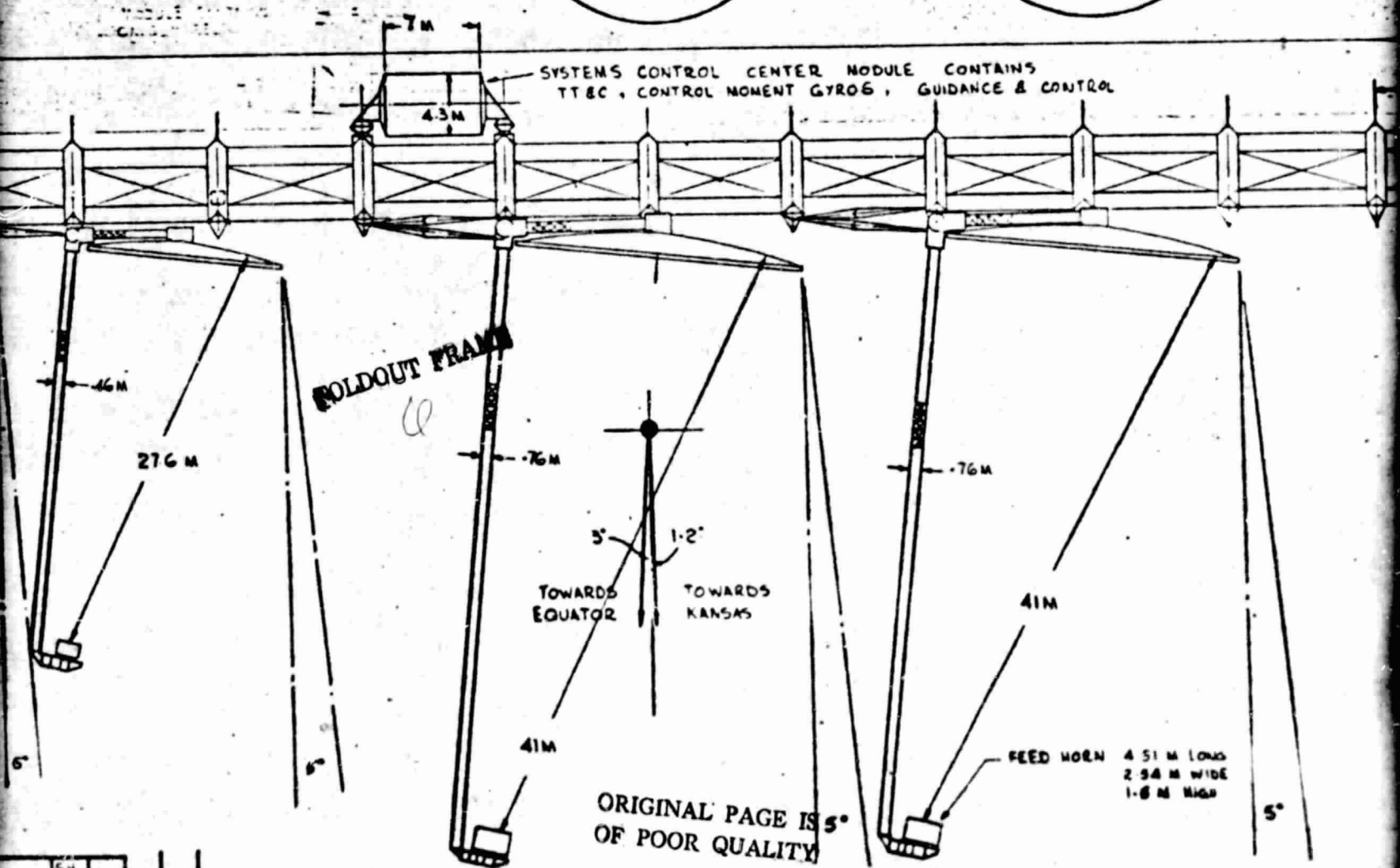
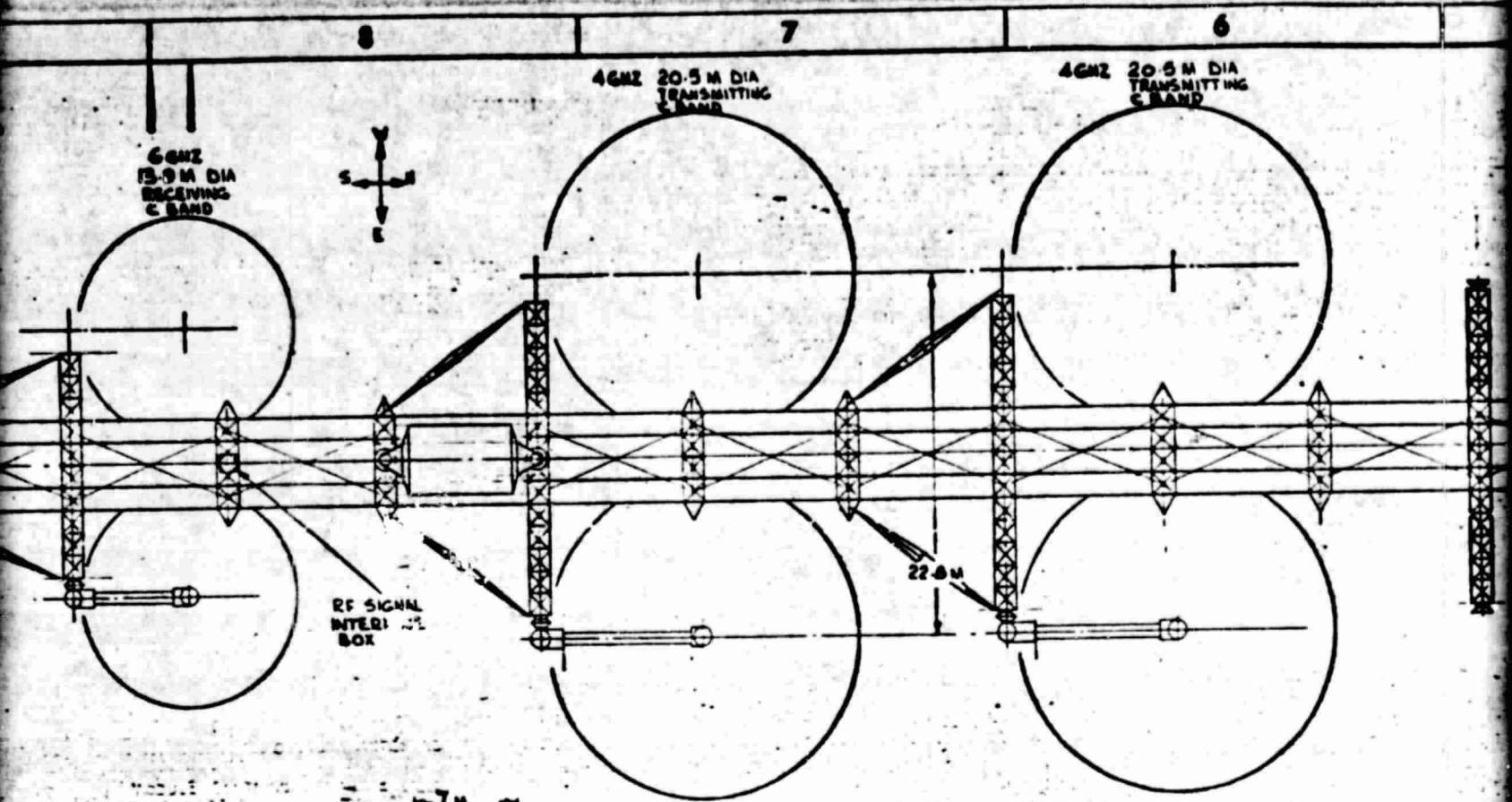
PRINCIPAL AXIS
APPROX

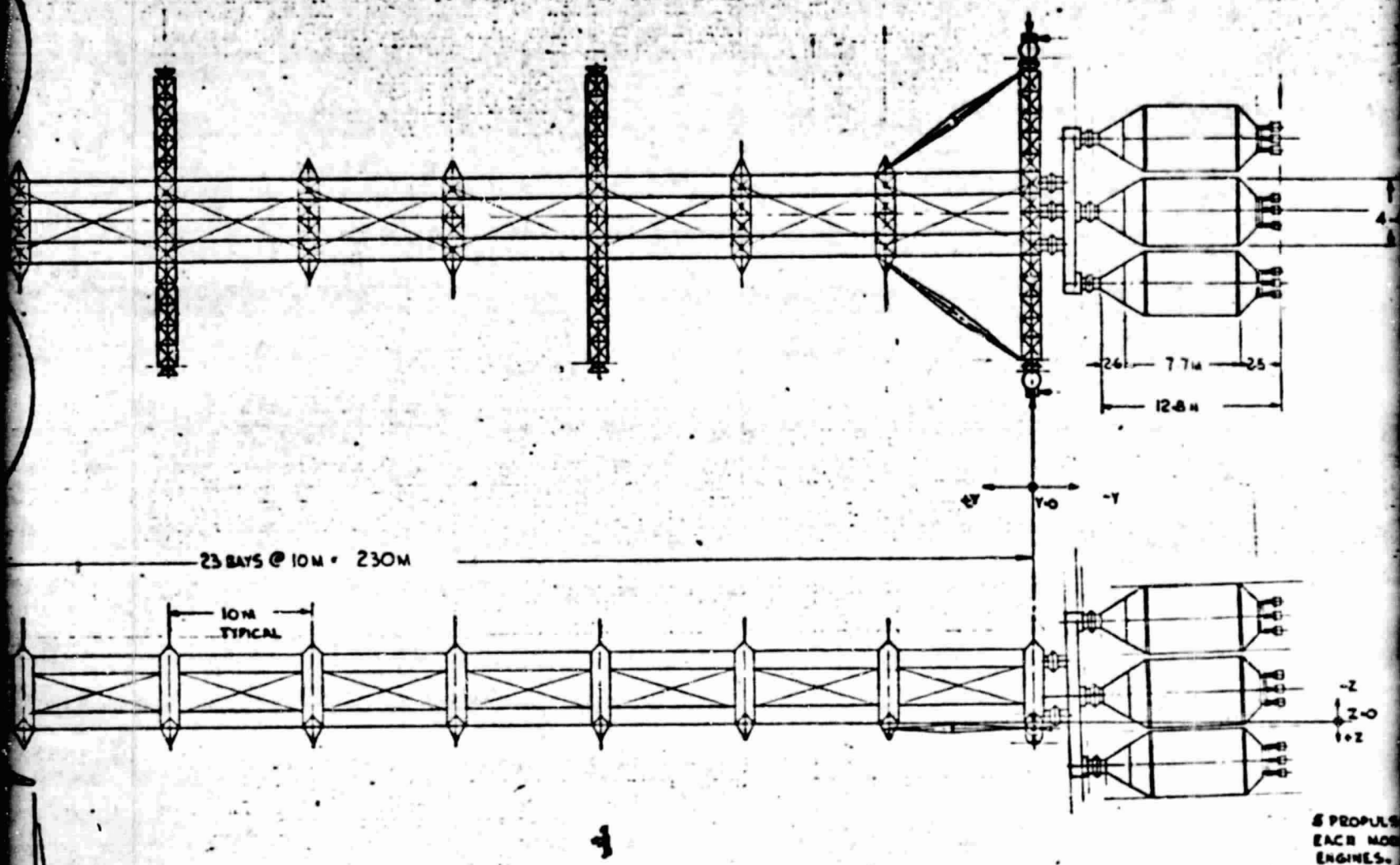
FOLDOUT FRAME
21

ORIGINAL PAGE IS
OF POOR QUALITY









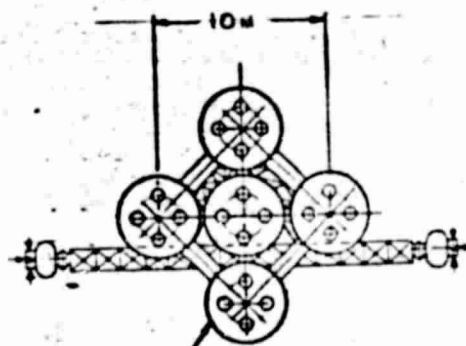
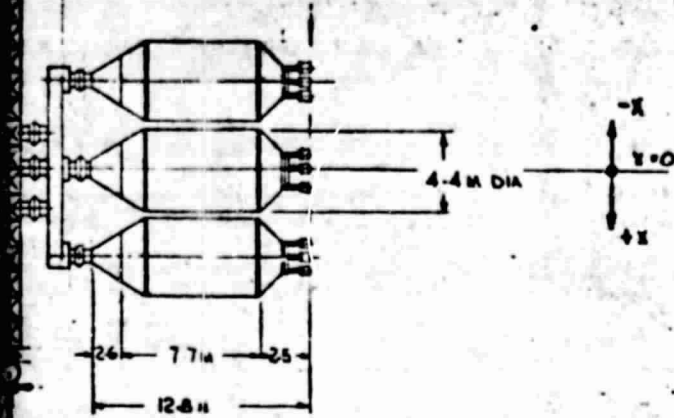
MOLDOUT FRAME

ORIGINAL PAGE IS
OF POOR QUALITY

REFER TO DWG 42662-26 SHEET 2 FOR CABLE ROUTING
REFER TO DWG 42662-25 SHEET 2 FOR THE FOLLOWING:-

OFFSET ANTENNA & STOWAGE.
ALTERNATIVE CASSEGRAIN ANTENNA & STOWAGE.
RCS MODULE.
PROPULSION MODULE.
SOLAR ARRAY.
BATTERY MODULE.
DOCKING ADAPTER.

REVISIONS			
NO.	DATE	DESCRIPTION	APPROVED
1	8-2-79	NO CHANGE DWG	



8 PROPULSION MODULES.
EACH MODULE HAS 4 - 5000 LB FORCE
ENGINES.

OLDOUT FI

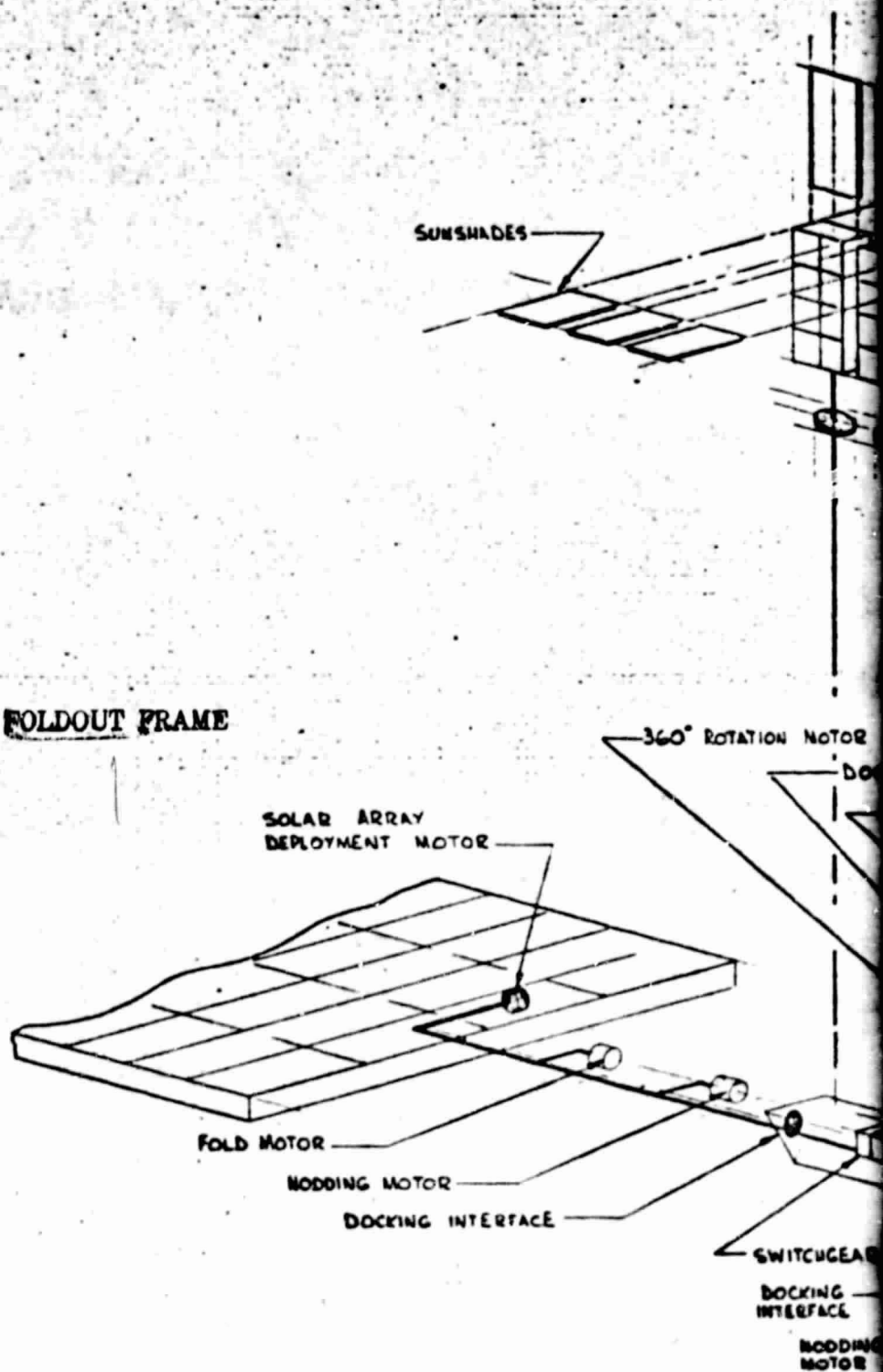
8

ORIGINAL PAGE IS
OF POOR QUALITY

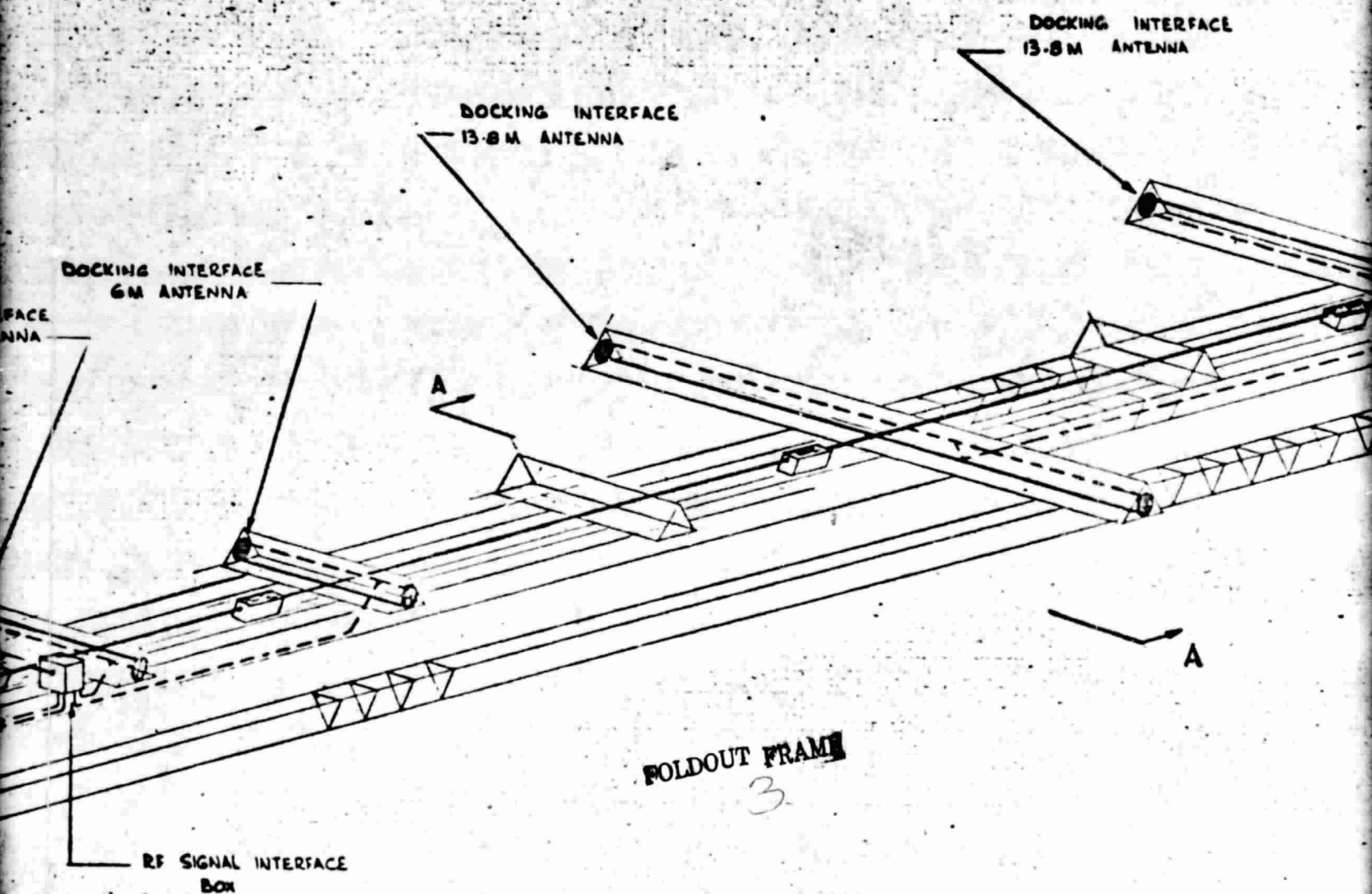
CABLE ROUTING
THE FOLLOWING:
STOWAGE.
RAIN ANTENNA II STOWAGE.
LE.

PAGE
A-19,20

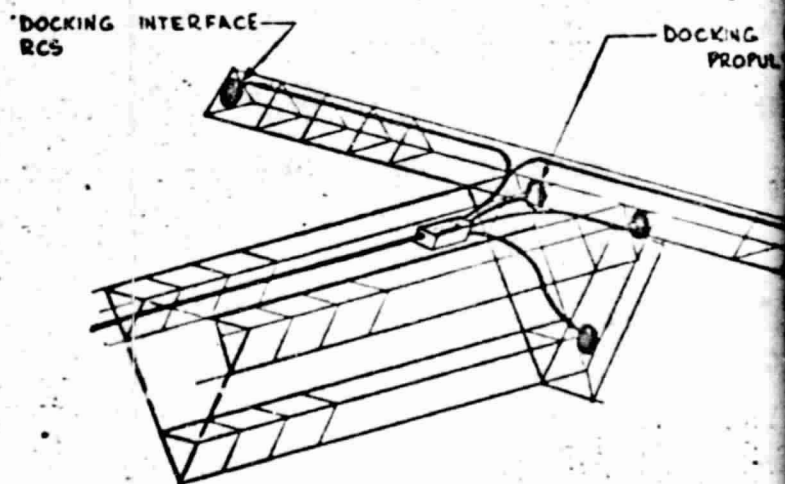
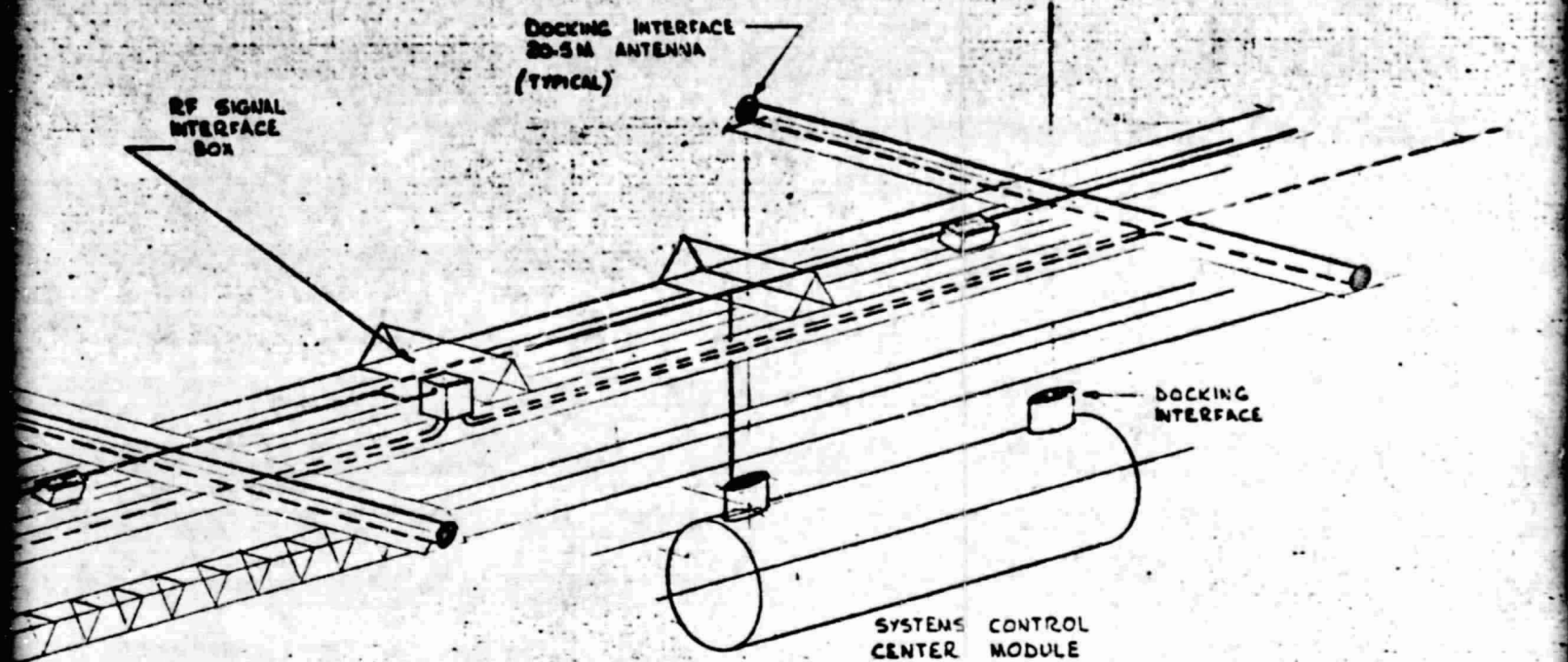
DESIGNED BY R. J. WART JAN 79		RADACOR International Corporation Space Division 18701 Lakeside Boulevard, Torrance, California 90501	
CHECKED BY APPROVED BY		ADVANCED COMM ANTENNA PLATFORM, SPACE FAB, LOW THRUST CHEM PROPULSION.	
SIZE L	LODGE IDENT NO 03953	DRAWING NO 42662-26	
SCALE 1:1000		SHEET	

FOLDOUT FRAME

ORIGINAL PAGE IS
OF POOR QUALITY

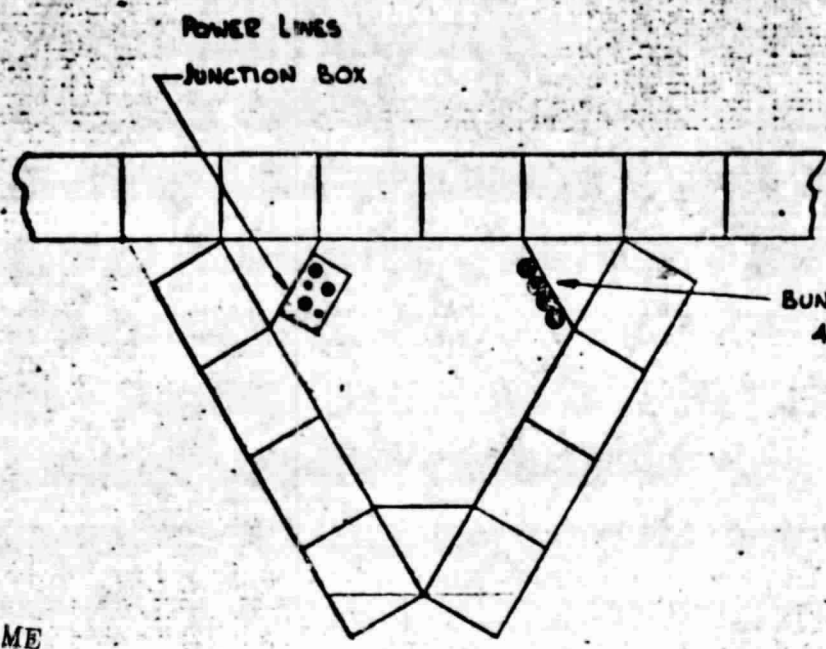


ORIGINAL PAGE IS
OF POOR QUALITY



ORIGINAL PAGE IS
OF POOR QUALITY

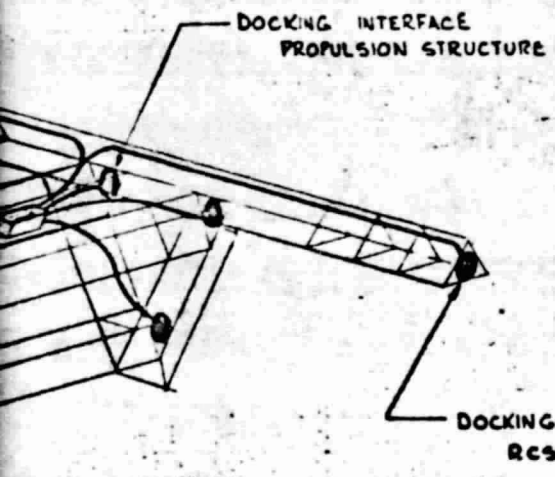
DATE	BY	NO



TYPICAL SECTION
THROUGH TRI-BEAM
SCALE: 1/50

SECTION A-A

FOLDOUT FRAME



- 2. RF LINES
- 1. POWER & DATA LINES

GEN NOTES:

ORIGINAL PAGE IS
OF POOR QUALITY

DES BY	Q. HART	JAN 7
CHK BY		
APPROVED BY		

1

D

C

4

1

L

1

5

9

PAGE
A-21,22

[illegible]

APPENDIX B

CONSTRUCTION TOLERANCES

B.1 INTRODUCTION

The inaccuracies (tolerances) of fabricating piece parts on the ground and the fabrication and assembly of piece parts in space can result in incorrect orientation of functioning systems. Incorrect orientation can, in turn, result in improper spacecraft operation (antenna to ground), excessive weight (RCS propellants), and create spacecraft control problems. Many critical dimensions exist which can potentially add to the misalignment of the systems. Thus, it is necessary to determine the tolerances for each of the critical dimensions to ensure that the worst case misalignment will permit satisfactory operation of the satellite.

The static tolerances associated with the construction process are not the only concern in creating a properly functioning satellite. Thermal deformations can occur during the fabrication and assembly process, and dynamic and thermal distortions will be experienced during operation. While these factors must be considered in the final design of the satellite, they **were not** considered in this investigation. Figure B-1 shows the complete process required for proper design of an operational satellite regarding the subject of construction tolerances and that portion covered herein.

The investigation was made to provide the "first cut" allocations for fabrication and assembly of the parts for each of the three projects;

1. Space-Fabricated Advanced Communications Platform
2. Erectable Advanced Communications Platform
3. SPS Test Article

This effort was a first-cut as the allocated tolerances are to be used by the spacecraft designers as they formulate hardware designs and construction operations. While the allocations are expected to cause no serious design problems or hardware complexity, a reallocation of the tolerances may be required as the design progresses.

B.2 GROUND RULES AND ASSUMPTIONS

1. System module assemblies (ground fabricated) will add no significant inaccuracies (e.g., thruster-to-thruster orientation; antenna dish to feed horn). Dimensions/tolerances will be specified for these items, but their fabrication can be controlled to an accuracy which will not be an additional concern for space assembly.
2. Critical dimensions are those which will affect required operating accuracies of the project systems.

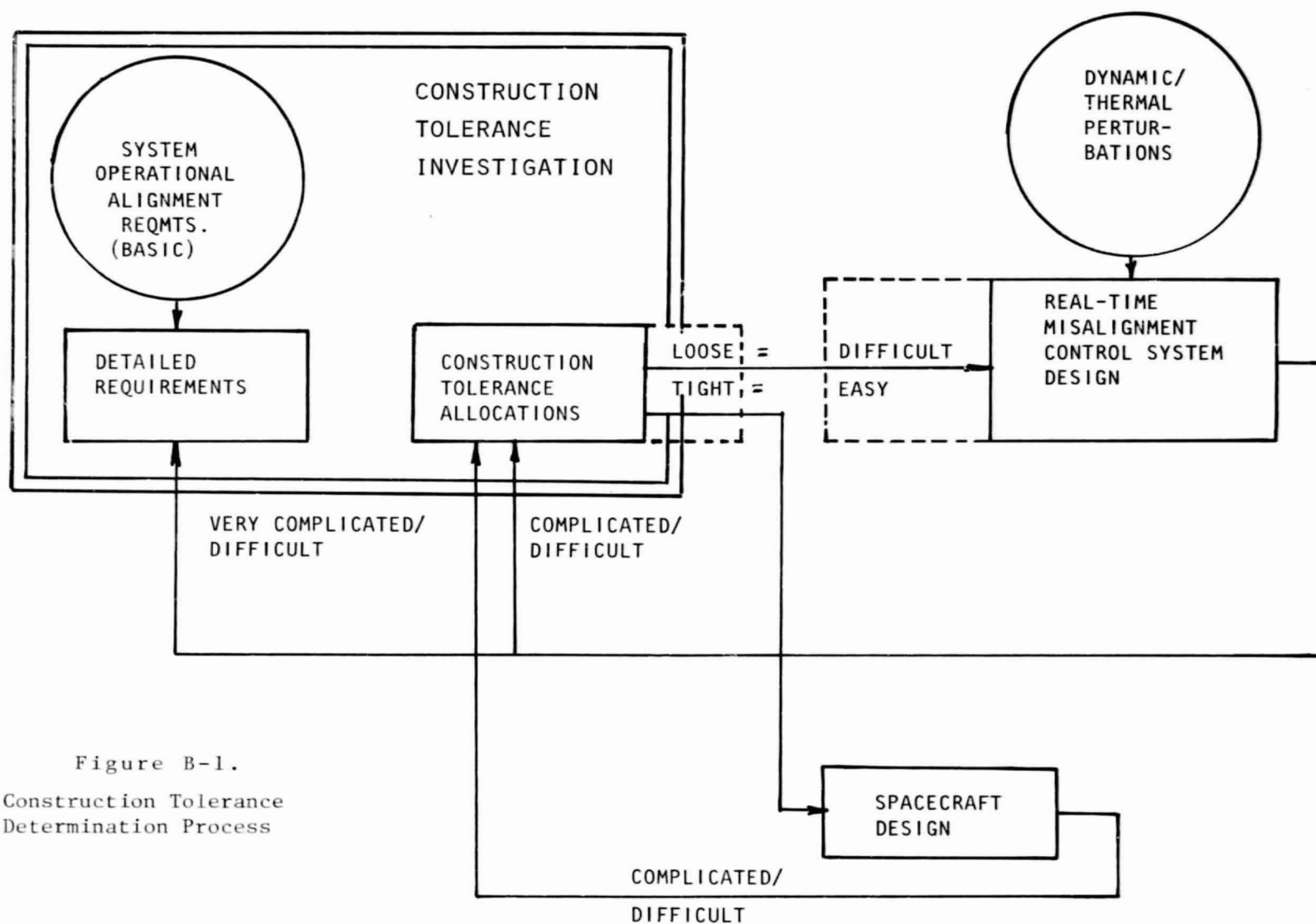


Figure B-1.
Construction Tolerance
Determination Process

3. Structural deformation resulting from thermal exposure or stresses built in during construction have not been included in the determination of the static tolerance allocations.
4. Only those operations/hardware which can have a direct effect on the alignment of the functional systems were considered (e.g., mating of electrical connectors was not considered).

B.3 APPROACH

The investigation was broken into five tasks, as described below.

Task 1—Identify functional systems where installation misalignment would cause undesirable operation.

Task 2—Establish construction tolerance requirements for each system, considering the following:

- Operational alignment
- Propellant usage
- Spacecraft control
- Design complexity
- Environment (dynamic and thermal)

Task 3—Determine contributing sources of inaccuracies (tolerances) resulting from fabrication and assembly operations for each system. Allocate tolerances to each critical dimension considering reasonable fabrication practices for space operations and common fabrication capability for ground operations.

Task 4—Discuss thermal distortion.

Task 5—Summary

B.4 RESULTS

B.4.1 Functional System Identification

Five basic functional systems were identified which could affect the proper operation of the satellite if their final orientation is not controlled during the construction process (including alignment). Table B-1 lists the systems and the projects to which they apply.

Figures B-2, B-3, and B-4 show the current configuration and axis orientation for each of the three projects.

Table B-1. Project Applications for Systems of Concern

System	Space-Fab. Comm. Platform	Project Erect. Comm. Platform	SPS Test Article
ANTENNAS			
Earth target	X	X	-
Space target	-	-	X
RCS	X	X	X
ORBIT TRANSFER PROP.			
Low thrust chemical	X	X	-
SEP	-	-	X
SOLAR ARRAY	X	X	X
SYSTEM CONTROL MODULE	X	X	X

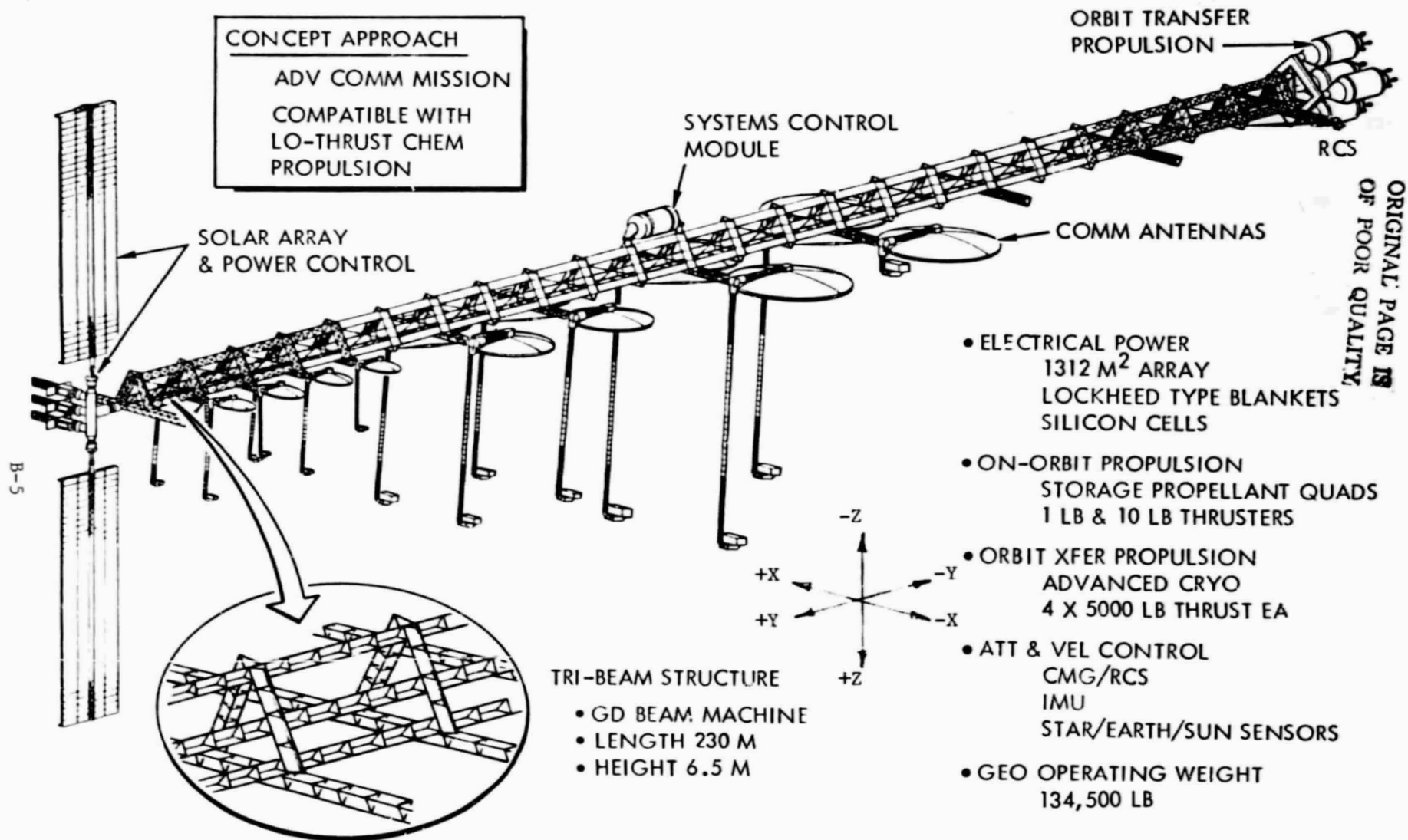


Figure B-2. Space-Fab Communications Platform

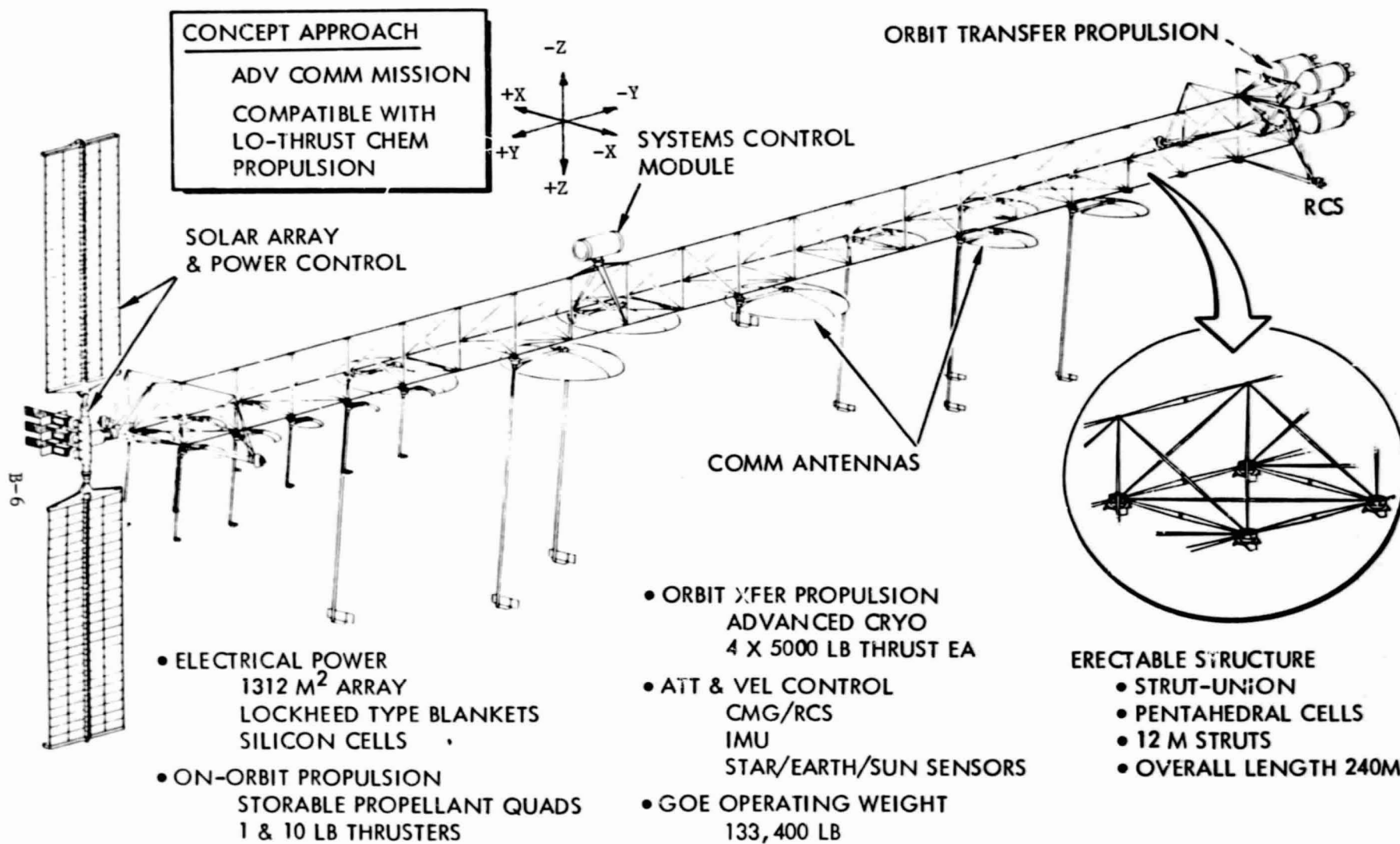
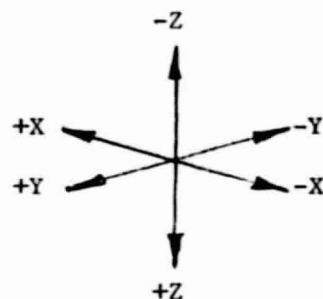


Figure B-3. Erectable Communications Platform

ORIGINAL PAGE IS
OF POOR QUALITY

CONCEPT APPROACH

SPS LEO TEST
COMPATIBLE WITH SEP
ORBIT TRANSFER



- OVERALL DIMENSIONS
LENGTH: 215 M
WIDTH: 20 M

- STRUCTURE
"LADDER"
SPACE FAB
GD BEAM MACHINE

RCS (4 PLACES)

SOLAR ARRAY

M-WAVE
ANTENNA

SYSTEMS CONTROL
MODULE

- ELECTRICAL POWER
3952 M² ARRAY
LOCKHEED TYPE BLANKETS
SILICON CELLS
- PROPULSION
STORABLE PROPELLANT QUADS
25 LB THRUSTERS
PROVISIONS FOR SEP

- ATT & VEL CONTROL
CMG/RCS
IMU
STAR/EARTH/SUN SENSOR
RECTENNA RANGING
- M-WAVE ANTENNA
24 PANELS
3 PANEL TYPES
- TOTAL SYSTEM WEIGHT
83,300 LB

Figure B-4. SPS Test Article

Satellite Systems Division
Space Systems Group



B.4.2 Construction Tolerance Requirements

First-cut translation and angular tolerance requirements were established for each version (seven) of the five basic systems. Figures B-5 through B-11 show the treatment for each of the seven systems. The sketches used to illustrate the system were taken from the project drawings of Appendix A. The requirements are summarized in Table B-2 and are assumed to include an allowance for the thermal inaccuracies which would be experienced during construction.

B.4.3 Construction Tolerance Allocation

Each piece of hardware and/or operation which could potentially add to installed inaccuracy of a system was identified and a tolerance allocated. The allocations were based on current common ground and expected space fabrication practices and capability. Tables B-3 through B-6 itemize the error sources and allocations for each of the systems for the Space-Fabricated Communications Platform project. Table B-7 summarizes the information by piece parts as identified in Section 3.5.2 of the report. Tables B-8 through B-10 present the details for the Erectable Communication Platform project. The data are summarized in Table B-11 and are based on the piece part list from Section 3.5.1. Tables B-12 through B-15 present the details for the SPS Test Article project. The data are summarized in Table B-16 and are based on the list from Section 2.5.4.

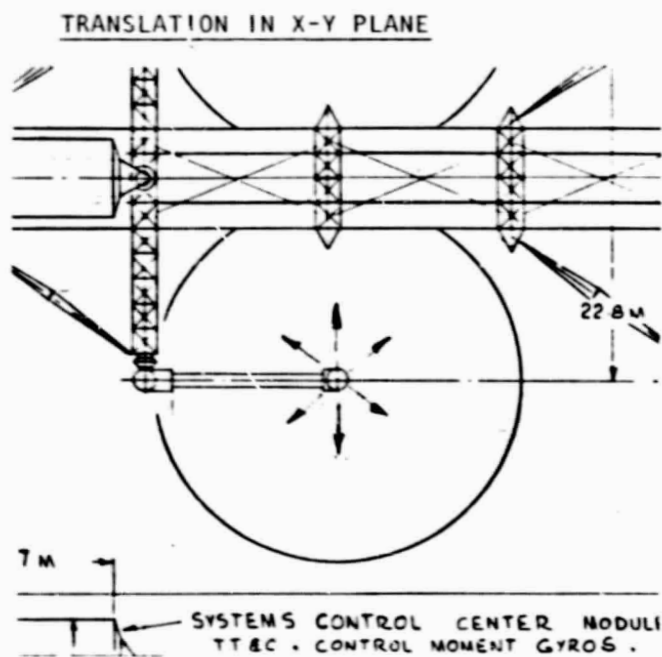
B.4.4 Thermal Distortion

Prior to their use in the construction process, materials will experience distortions due to temperature gradients. The randomness with which the construction process occurs during an orbit will result in additional distortions due to changing environment. These distortions, even though small, may adversely affect the alignment of the systems and since preventing or accounting for thermal distortions during the construction process may be difficult or impractical, it is anticipated they will be removed during the structural alignment process.

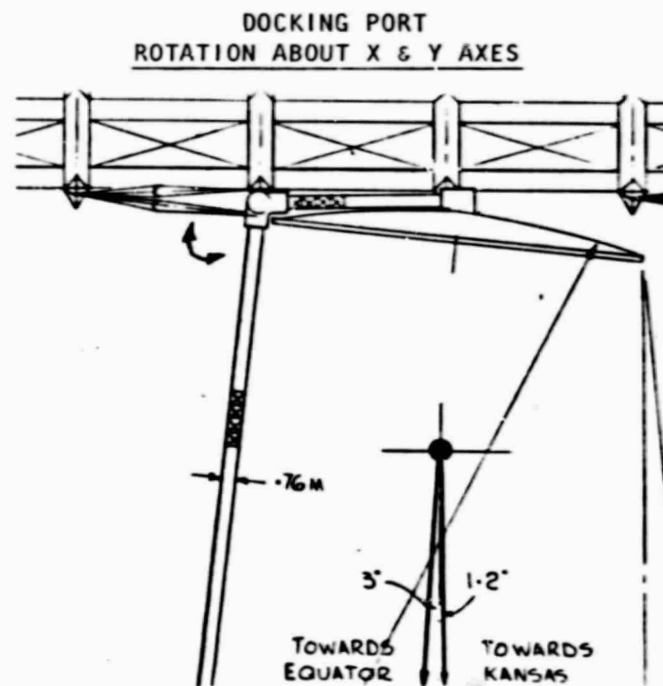
The real concern is the real-time distortions experienced during operation of the spacecraft (thermal and dynamic). Real-time distortions can be accounted for by use of a closed-loop servo-type alignment system to ensure proper operation of the spacecraft under the constantly changing operational environment.

B.4.5 Summary

The results of the investigation are summarized in Table B-17. The impact of the worst case tolerance buildup in the case of the antennas is to provide a post construction angular adjustment capability in the X, Y, and Z axes of $\pm 3^\circ$ to an accuracy of $\pm 0.25^\circ$ for each module. In addition, provide a fine-tuning adjustment of $\pm 0.5^\circ$ for the dish and ± 0.4 m on the feed horn to accuracies of $\pm 0.025^\circ$ and ± 0.02 m, respectively. There is no unacceptable impact on the projects if the RCS, orbit transfer propulsion, solar array, and system control modules/housings systems are installed to the tolerances allocated.



- CONCERN IS OVERLAP WITH ADJACENT ANTENNA PATTERN
- TRANSLATION ERRORS OF ± 0.1 M ARE ACCEPTABLE



- CONCERN IS ANTENNA WILL BE POINTED OUTSIDE OF ITS FINAL ADJUSTMENT CAPABILITY
- $\pm 3^\circ$ OF INSTALLATION ERROR IS ACCEPTABLE (POST CONSTRUCTION ADJUSTMENT CAPABILITY)

Figure B-5. Earth-Pointing Antenna (Both Comm. Platforms)

DOCKING PORT ROTATION ABOUT Y-AXIS

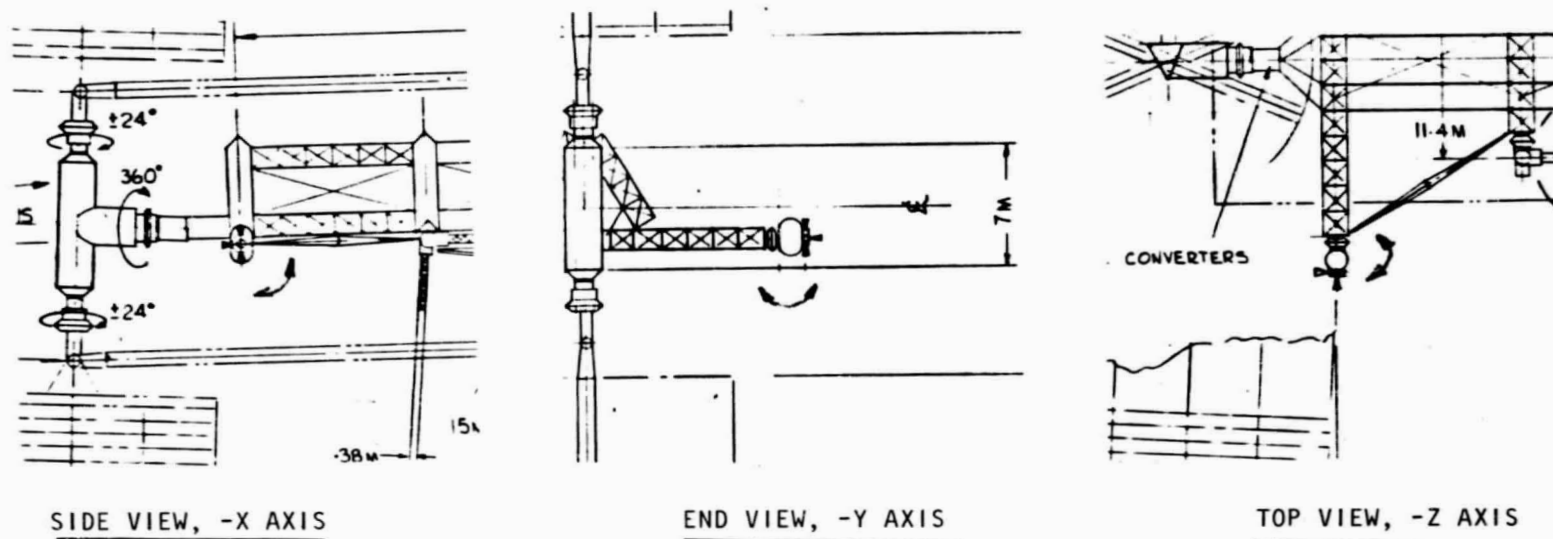
- NO CONCERN AS 360° ROTARY JOINT PROVIDES INFINITE ADJUSTMENT

DOCKING PORT ANGULAR MISALIGNMENT ABOUT Y-AXIS

- ANTENNA/TARGET ALIGNMENT WILL CAUSE SOLAR ARRAY TO BE AT NON-OPTIMUM ANGLE TO SUN
- LOW CRITICALITY OF SOLAR ARRAY ANGLE TO SUN PERMITS A RATHER LARGE ANGULAR MISALIGNMENT OF THE DOCKING PORT.... $\pm 5^\circ$ WILL BE USED

Figure B-6. Space Target Antenna Pointing (SPS Test Article)

DOCKING PORT ANGULARITY ABOUT X, Y, & Z AXES



SIDE VIEW, -X AXIS

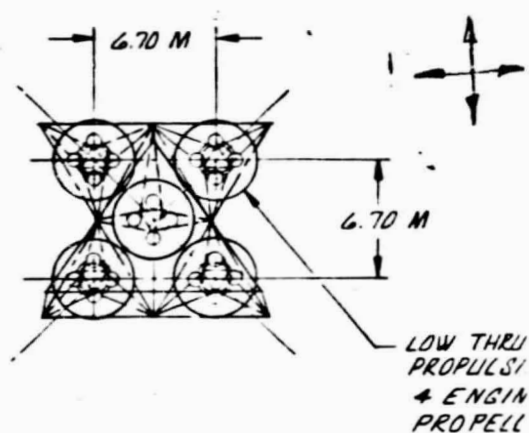
END VIEW, -Y AXIS

TOP VIEW, -Z AXIS

- CONCERN IS EXCESSIVE USE OF PROPELLANT BECAUSE MISALIGNMENT OF INDIVIDUAL THRUSTERS WITH DESIRED AXES WILL CREATE UNDESIRABLE MOMENTS DURING TRANSLATION AND IMPROPER COUPLES DURING ATTITUDE CONTROL OPERATIONS.
- ANGULAR MISALIGNMENT IN ANY AXIS OF 3° (APPROX. 5% PROPELLANT LOSS) OR LESS WILL NOT RESULT IN ADDITIONAL PROPELLANT USAGE BEYOND MARGINS PROVIDED FOR UNKNOWN.
- TRANSLATION MISALIGNMENT IS NOT CRITICAL—USE ± 0.1 M

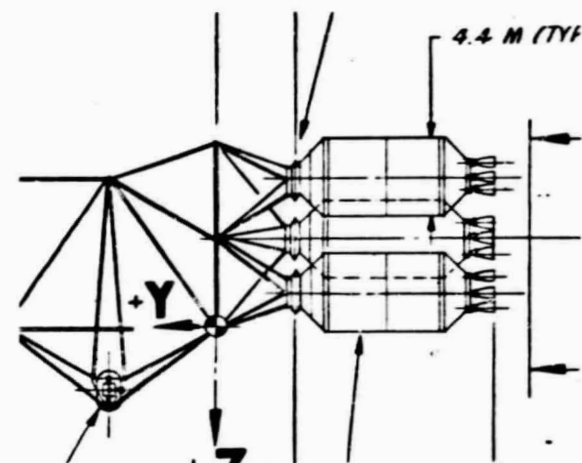
Figure B-7. RCS (All Projects)

TRANSLATION OF MODULE DOCKING PORT
IN X-Z PLANE



- CONCERN IS LINE OF THRUST OF MODULE WILL NOT BE THROUGH C.G. OF PLATFORM
- ± 0.1 M ($\sim 0.03^\circ$) TRANSLATION ERROR IS WELL WITHIN $\pm 7^\circ$ GIMBAL CAPABILITY OF EACH ENGINE OF MODULE

DOCKING PORT ANGULAR MISALIGNMENT
IN X, Y, OR Z AXES



- CONCERN IS LINE OF THRUST OF MODULE WILL NOT BE THROUGH C.G. OF PLATFORM
- $\pm 2^\circ$ IS CHOSEN AND IS WELL WITHIN $\pm 7^\circ$ GIMBAL CAPABILITY OF EACH ENGINE

Figure B-8. Orbit Transfer Propulsion—Low Thrust Chem (Both Comm Platforms)

TRANSLATION OF DOCKING PORT IN X-Z PLANE ON SYSTEM SUPPORT HOUSING

- ERROR WILL CREATE A COUPLE WHEN SEP IS THRUSTING ALONG Y-AXIS
- COUPLE WILL BE INSIGNIFICANT WITH TOLERANCE OF ± 0.1 M

ROTATION OF DOCKING PORT ABOUT Y-AXIS

- NO CONCERN AS BOTH SEP UNITS HAVE 360° ROTATION IN THIS AXIS
- ASSUME $\pm 0.1^\circ$ AS REASONABLE FINAL INSTALLATION MISALIGNMENT

ANGULAR MISALIGNMENT OF DOCKING PORT ABOUT Y-AXIS

- NO CONCERN AS SYMMETRICAL SHAPE AND 360° ROTATIONAL CAPABILITY ABOUT Z-AXIS ELIMINATES ANY UNDESIRABLE EFFECTS OF ASSEMBLY ERRORS
- ASSUME $\pm 3^\circ$ AS REASONABLE FINAL INSTALLATION MISALIGNMENT

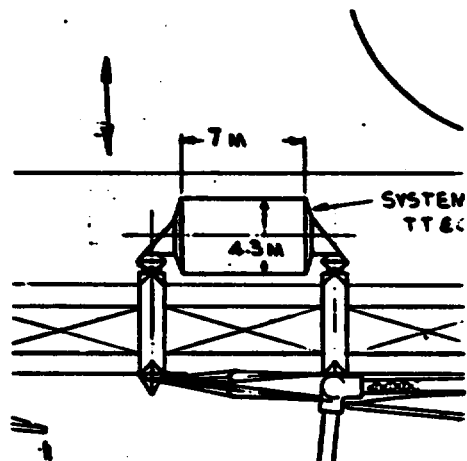
Figure B-9. Orbit Transfer Propulsion—SEP (SPS Test Article)

MISALIGNMENT OF DOCKING PORT IN ANY DIRECTION

- NO CONCERN AS THE DEGREES OF FREEDOM FOR STANDARD OPERATIONS NEGATE ANY INSTALLATION TOLERANCES. IN ADDITION, ANGULAR MISALIGNMENT OF SOLAR ARRAYS OF APPROX. 10 DEG DOES NOT SIGNIFICANTLY AFFECT PERFORMANCE
- ASSUME ± 0.1 M TRANSLATION ERROR AND ± 3 DEG ROTATIONAL ERROR AS REASONABLE DOCKING PORT INSTALLATION TOLERANCE REQUIREMENTS

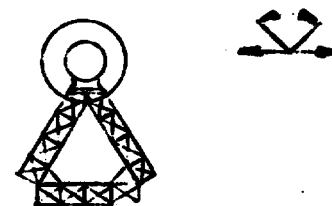
Figure B-10. Solar Arrays (Communication Platforms)

**ONE DOCKING PORT DISPLACEMENT
IN Z-AXIS**



- G&C SYSTEM WILL NOT BE ORIENTED IN CORRECT AXIS
- ASSUME $\pm 1^\circ$ AS MAXIMUM MISALIGNMENT

**DOCKING PORT ANGULARITY IN
X-Z & X-Y PLANES**



- G&C SYSTEM WILL NOT BE ORIENTED IN CORRECT AXES
- ASSUME $\pm 1^\circ$ AS MAXIMUM MISALIGNMENT

Figure B-11. System Control Module (Communication Platforms)



Table B-2. Construction Tolerance Requirements Summary

System	Translation (m)	Angularity (°)
ANTENNA		
Earth target	±0.1	±3
Space target	-	±5
RCS	±0.1	±3
ORBIT TRANSFER PROP.		
Low-thrust chem.	±0.1	±2
SEP	±0.1	±3
SOLAR ARRAY	±0.1	±3
SYSTEM CONTROL MODULE	-	±1

Table B-3. Space-Fab Communications Platform—System Control Module

Source	Allocation
<u>Installation of docking port to structure</u>	
Transverse beams too long at one end of module (±1 cm) (rotation about X-axis)	0.1°
One transverse beam too long at one end of module (±1 cm) (rotation about Y-axis)	0.3° *
Twisted longitudinal beam (1.2°/200 m)	0.6° *
<u>Installation of docking port on module (ground fab)</u>	
Angularity about Y-axis	0.1° *
Both ports not parallel with module centerline in X-Y and Y-Z planes (±0.1 cm)	0.1°
	<hr/>
Worst case total*	1.0°
RSS*	0.7°
Requirement	1.0° max.

Table B-4. Space-Fab Communications Platform—Antenna Pointing—Earth Target

SOURCE	ALLOCATION
INSTALLATION OF DOCKING PORT ON STRUCTURE (± 0.1 CM)	* 0.1°
CROSSBEAM BOWED IN X-Z PLANE (2.5 CM FROM CENTER)	* 0.1°
	
CROSSBEAM TWISTED ALONG ITS LONGITUDINAL AXIS ($1.2^\circ/200\text{M}$)	0.2°
	
ONE LONGITUDINAL BEAM TWISTED ($1.2^\circ/200$ M, ASSUME 1/2 TWISTED)	* 0.6°
INSTALLATION OF DOCKING PORT ON ANTENNA MODULE (GROUND FAB)	* 0.1°
SYSTEM CONTROL MODULE ORIENTED INCORRECTLY ⁽¹⁾	* 1.0°
WORST CASE TOTAL*	<u>1.9°</u>
RSS	1.2°
REQUIREMENT	3.0° MAX.

(1) Additive for determination of post-construction adjustment capability.

Table B-5. Space-Fab Communications Platform—RCS






SOURCE	ALLOCATION
INSTALLATION OF DOCKING PORT ON STRUCTURE (± 0.1 CM)	0.1°
CROSS-BEAM BOWED IN X-Y OR X-Z PLANES (2.5 CM)	0.1°
 	
CROSS-BEAM TWISTED ALONG ITS LONGITUDINAL AXIS ($1.2^\circ/200$ M)	0.2°
 CORRECT  TWISTED  ↓ EARTH	
ONE LONGITUDINAL BEAM TWISTED ($1.2^\circ/200$ M—ASSUME 1/2 TWISTED)	0.6°
INSTALLATION OF DOCKING PORT ON RCS MODULE (GROUND FAB)	0.1°
SYSTEM CONTROL MODULE ORIENTED INCORRECTLY	1.0°
	<hr/>
WORST CASE TOTAL	2.1°
RSS	1.2°
REQUIREMENT	3.0° MAX.

Table B-6. Space-Fab Communications Platform—
Low-Thrust Chem. Orbit Transfer Propulsion

SOURCE	ALLOCATION
THRUST STRUCTURE NOT PERFECT PLANE (± 4 CM ACROSS CORNERS)	0.2°
INSTALLATION OF THRUST STRUCTURE FIXED DOCKING PORT TO PLATFORM STRUCTURE	
LONGITUDINAL BEAM INCORRECT LENGTH (± 1 CM)	0.4°
ATTACHMENT RESULTS IN PORT FACE IN WRONG PLANE (± 0.1 CM)	0.1°
INSTALLATION OF DOCKING PORTS TO THRUST STRUCTURE (GROUND FAB)	
THRUST STRUCTURE PORT OUT OF PLANE (± 0.1 CM)	0.1°
MODULE PORT OUT OF PLANE (± 0.1 CM)	0.1°
SYSTEM CONTROL MODULE ORIENTED INCORRECTLY	<u>1.0°</u>
WORST CASE TOTAL	1.9°
RSS	1.1°
REQUIREMENT	2.0 MAX
NOTE: TWO OF THREE THRUST STRUCTURE DOCKING PORTS MUST BE FLOATING IN X-Z PLANE TO PERMIT CONNECTION TO PORTS ON PLATFORM.	

B-19

satellite Systems Division
Space Systems Group



Table B-7 Critical Construction Tolerance Summary,
Space-Fabricated Comm. Platform

ITEM DESCRIPTION	CRITICAL DIMENSION	TOLERANCE ALLOCATION	SYSTEMS AFFECTED BY CRITICAL DIMENSIONS	CONSTRUCTION OPERATION
LONGITUDINAL BEAM	LENGTH TWISTED	+1 CM $\pm 0.6^\circ$	THRUST STRUCTURE ANTENNA, SCM, RCS	CUTOFF DURING FAB FABRICATION
TRANSVERSE BEAM CROSS BEAM	LENGTH TWISTED BOWED	+1 CM $\pm 0.2^\circ$ ± 2.5 CM	SYS. CONT. MOD (SCM) ANTENNA, RCS ANTENNA, RCS	CUTOFF FABRICATION FABRICATION
DOCKING PORT (STRUCT.)	FACE ALIGN. WITH BEAM END (± 0.1 CM)	$\pm 0.1^\circ$	ANTENNA, RCS, THRUST STRUCTURE (TS)	
THRUST STRUCTURE	OUT OF PLANE (± 4 CM) DOCKING PORT ALIGN.	$\pm 0.2^\circ$ $\pm 0.1^\circ$	ORB. TRANSF. PROP. ORB. TRANSF. PROP.	GROUND FAB GROUND FAB
STRUTS				
RCS MODULE	DOCKING PORT ALIGN.	$\pm 0.1^\circ$	RCS MOD	GROUND FAB
ANTENNA MODULE	↓	↓	ANTENNA MOD	↓
SYST. CONTROL MOD			SYST. CONT. MOD.	
ORBIT TRANSF. PROP. MOD.	DOCKING PORT ALIGN.	$\pm 0.1^\circ$	ORB. TRANSF. PROP. MOD.	GROUND FAB

B-20

Satellite Systems Division
Space Systems Group



Table B-8. Erectable Communications Platform--
System Control Module

SOURCE	ALLOCATION
<p>• INSTALLATION OF DOCKING PORT TO STRUCTURE</p> <p>• STRUTS INCORRECT LENGTH (+0.1 CM) (GND FAB)</p> <p>• INSTALLATION OF DOCKING PORT TO MODULE (GND FAB)</p> <p>• FACE NOT PARALLEL TO MODULE CENTERLINE (+0.1 CM)</p>	<p>0.1°</p> <p>0.1°</p> <hr/> <p>0.2° 0.1° 1.0° MAX</p>

WORST CASE TOTAL
RSS
REQUIREMENT

**Table B-9. Erectable Communications Platform-
Antenna Pointing - Earth Target**

SOURCE	ALLOCATION
•JOINT (WITH DOCKING PORT) NOT INSTALLED WITH PORT IN CORRECT PLANE	0.1°
•STRUCT INCORRECT LENGTH (+0.1 CM) (GND FAB)	
•INSTALLATION OF DOCKING PORT ON JOINT (+0.1 CM) (GND FAB)	0.1°
•INSTALLATION OF DOCKING PORT ON MODULE (+0.1 CM) (GND FAB)	0.1°
•TOTAL STRUCTURE MISALIGNMENT DURING ASSEMBLY (STRUTS INCORRECT LENGTH)	1.0°
•SYSTEM CONTROL MODULE ORIENTED INCORRECTLY	0.2°
	<hr/>
WORST CAST TOTAL	1.5°
RSS	1.0°
REQUIREMENT	3.0° MAX.

B-22

Satellite Systems Division
Space Systems Group





Table B-10. Erectable Communications Platform-
RCS & Orbit Transfer Propulsion

SOURCE	ALLOCATION
<u>RCS</u> • DOCKING PORT INSTALLED IN WRONG PLANE • STRUT(S) INCORRECT LENGTH (+0.1 CM) • INSTALLATION OF DOCKING PORT ON MODULE (+0.1 CM) (GND FAB) • TOTAL STRUCTURE MISALIGNMENT DURING ASSEMBLY • STRUTS INCORRECT LENGTH (STRUCTURE TWISTED OR BOWED) • SYSTEM CONTROL MODULE ORIENTED INCORRECTLY	0.1° 0.1° 1.0° 0.2° — 1.4° 1.0° 3.0° MAX
<u>LOW THRUST CHEN-ORBIT TRANSFER PROPULSION</u> SAME AS RCS	1.4° 2.0° MAX

WORST CASE TOTAL
RSS
REQUIREMENT

TOTAL TOLERANCE
REQUIREMENT

Table B-11. Critical Construction Tolerance Summary,
Erectable Communications Platform

ITEM DESCRIPTION	CRITICAL DIMENSION	TOLERANCE ALLOCATION	SYSTEMS AFFECTED BY CRITICAL DIMENSIONS	CONSTRUCTION OPERATION
RCS MODULE	DOCKING PORT ALIGN	$\pm 0.1^{\circ}$	RCS	GROUND FAB
ANTENNA	DOCKING PORT ALIGN	$\pm 0.1^{\circ}$	ANTENNA MOD	GROUND FAB
SYST. CONTROL MOD	DOCKING PORT ALIGN	$\pm 0.1^{\circ}$	SYS. CONTR. MOD	GROUND FAB
ORBIT TRANSFER PROPULSION MOD	DOCKING PORT ALIGN	$\pm 0.1^{\circ}$	ORBIT TRANSFER PROPULSION MOD	GROUND FAB
STRUTS	LENGTH	± 0.1 CM	ANTENNA, RCS, SYS. CONT. MOD, ORBIT TRANS. PROP.	GROUND FAB
DOCKING PORT (STRUCT.)	FACE ALIGN (± 0.1 CM)	$\pm 0.1^{\circ}$	ALL	ASSEMBLY

Table B-12. SPS Test Article-
System Support Housing

SOURCE	ALLOCATION
•LONGITUDINAL BEAMS INCORRECT LENGTH (<u>±</u> 0.1 CM) (MISALIGNMENT IN "X-Y" PLANE)	* 0.1°
•TOTAL STRUCTURE TWISTED (<u>±</u> 4M) (MISALIGNMENT IN "X-Z" PLANE)	* 1.0°
•TOTAL STRUCTURE BOWED (<u>±</u> 4M) (MISALIGNMENT IN "X-Y" AND "Y-Z" PLANES)	1.0°
•INSTALLATION OF DOCKING PORT TO STRUCTUPE (<u>±</u> 0.1 CM) (GND FAB) (PORT FACES IN DIFFERENT PLANES)	* 0.1°
	—
WORST CASE TOTAL*	1.2°
RSS	1.0°
REQUIREMENT	1.0° MAX

Table B-13. SPS Test Article-
Antenna Pointing - Space Target

SOURCE	ALLOCATION
• INSTALLATION OF DOCKING PORTS (GND FAB)	
• TO SYSTEM SUPPORT HOUSING (ROTARY JOINT) (<u>±</u> 0.1 CM)	0.1°
• TO ROTARY JOINT (SYSTEM SUPPORT HOUSING) (<u>±</u> 0.1 CM)	0.1°
• TO ROTARY JOINT (ANTENNA) (<u>±</u> 0.1 CM)	0.1°
• TO ANTENNA MODULE (<u>±</u> 0.1 CM)	0.1°
• SYSTEM SUPPORT HOUSING ORIENTED INCORRECTLY	1.2°
	—
WORST CASE TOTAL	1.6°
RSS	1.2°
REQUIREMENT	5° MAX
NOTE: LONGITUDINAL BEAM LENGTH NOT CRITICAL - REGARDLESS OF BEAM LENGTH SOLAR ARRAY WILL BE NORMAL TO SUN WITH ANTENNA POINTED AT SPACE TARGET	

Table B-14. SPS Test Article-
RCS

SOURCE	ALLOCATION
•INSTALLATION OF DOCKING PORT ON STRUCTURE (<u>+0.1</u> CM)	* 0.1°
•CROSS BEAM BOWED IN "X-Y" OR "X-Z" PLANE (<u>+2.5</u> CM)	* 0.1°
•CROSS BEAM TWISTED ALONG ITS LONGITUDINAL AXIS (1.2°/200M)	0.2°
•STRUCTURE TWISTED ALONG LONGITUDINAL AXIS	* 1.0°
•INSTALLATION OF DOCKING PORT ON MODULE (GND FAB) (<u>+0.1</u> CM)	* 0.1°
•SYSTEM CONTROL MODULE ORIENTED INCORRECTLY	* 1.2°
	<hr/>
WORST CASE TOTAL*	2.5°
RSS	1.6°
REQUIREMENT	3.0° MAX

Table B-15. SPS Test Article-
Orbit Transfer Propulsion

SOURCE	ALLOCATION
• INSTALLATION OF DOCKING PORTS (GND FAB)	
• SYSTEM SUPPORT HOUSING (ROTARY JOINT) (<u>+0.1</u> CM)	0.1°
• ROTARY JOINT (SYSTEM SUPPORT HOUSING) (<u>+0.1</u> CM)	0.1°
• SYSTEM SUPPORT MODULE ORIENTED INCORRECTLY	1.2°
	<hr/>
WORST CASE TOTAL	1.4°
RSS	1.2°
REQUIREMENT	3.0° MAX

Table B-16. SPS Test Article—Critical Construction Tolerance Summary

ITEM DESCRIPTION	CRITICAL DIMENSION	TOLERANCE ALLOCATION	SYSTEMS AFFECTED BY CRITICAL DIM.	CONSTRUCTION OPERATION
MICROWAVE ANTENNA	DOCKING PORT ALIGN	$\pm 0.1^\circ$	ANTENNA	GROUND FAB
ROTARY JOINT	DOCKING PORT ALIGN	$\pm 0.1^\circ$	ANTENNA & SEP	GROUND FAB
SYSTEM SUPPORT HOUSING	DOCKING PORT ALIGN	$\pm 0.1^\circ$	ANTENNA & SEP	GROUND FAB
DOCKING PORT (STRUCT.)	FACE ALIGN WITH BEAM END (± 0.1 CM)	$\pm 0.1^\circ$	RCS, SYS. SUPPORT HOUSING	ASSEMBLY
LONGITUDINAL BEAM	LENGTH (± 0.1 CM)	$\pm 0.1^\circ$	SYS. SUPP. HOUSING	FABRICATION
CROSS BEAM	TWISTED	$\pm 0.1^\circ$	RCS	FAB/ASSEMBLY
RCS MODULE	DOCKING PORT ALIGN	$\pm 0.1^\circ$	RCS	GROUND FAB

Table B-17. Investigation Summary

	Space Fab Comm Platform		Erectable Comm Platform		SPS Test Article	
	Reqmt	Max Error	Reqmt	Max Error	Reqmt	Max Error
Antenna						
Earth Target	$\pm 3^{\circ}$	$\pm 1.9^{\circ}$	$\pm 3^{\circ}$	$\pm 1.5^{\circ}$	--	--
Space Target	--		--	--	$\pm 5^{\circ}$	$\pm 1.6^{\circ}$
RCS	$\pm 3^{\circ}$	$\pm 2.1^{\circ}$	$\pm 3^{\circ}$	$\pm 1.4^{\circ}$	$\pm 3^{\circ}$	$\pm 2.5^{\circ}$
Orbit Transfer Prop						
Low Thrust Chem	$\pm 2^{\circ}$	$\pm 1.9^{\circ}$	$\pm 2^{\circ}$	$\pm 1.4^{\circ}$	--	--
Sep	--	--	--	--	$\pm 3^{\circ}$	$\pm 1.4^{\circ}$
Solar Array	$\pm 3^{\circ}$		$\pm 3^{\circ}$		--	
System Control Module	$\pm 1^{\circ}$	$\pm 1.0^{\circ}$	$\pm 1^{\circ}$	$\pm 0.2^{\circ}$	$\pm 1^{\circ}$	$\pm 1.2^{\circ}$